Optimizing Performance of Ceramic Pot Filters in Northern Ghana and Modeling Flow through Paraboloid-Shaped Filters

by

Travis Reed Miller

B.S. Environmental Engineering
State University of New York at Buffalo

SUBMITTED TO THE DEPARTMENT OF CIVIL AND ENVIRONMENTAL ENGINEERING IN PARTIAL FULFILLMENT OF THE REQUIREMENTS OF THE DEGREE OF

MASTER OF ENGINEERING IN CIVIL AND ENVIRONMENTAL ENGINEERING
AT THE
MASSACHUSETTS INSTITUTE OF TECHNOLOGY

June 2010

Signature of Author_____
Travis Reed Miller
Department of Civil and Environmental Engineering
May 21, 2010

Certified by_____
Susan Murcott
Senior Lecturer of Civil and Environmental Engineering
Thesis Advisor

Certified by_____
E. Eric Adams
Senior Research Engineer and Lecturer of Civil and Environmental Engineering
Thesis Advisor

Accepted by _____
Daniele Veneziano
Chairman, Departmental Committee for Graduate Students

Optimizing Performance of Ceramic Pot Filters in Northern Ghana and Modeling Flow through Paraboloid-Shaped Filters

by

Travis Reed Miller

Submitted to the Department of Civil and Environmental Engineering on May 21, 2010
in Partial Fulfillment of the Requirements for the Degree of Master of Engineering
in Civil and Environmental Engineering

ABSTRACT

This work aimed to inform the design of ceramic pot filters to be manufactured by the organization Pure Home Water (PHW) in Northern Ghana, and to model the flow through an innovative paraboloid-shaped ceramic pot filter. PHW is an organization dedicated to improving the drinking water quality for residents of Northern Ghana, where waterborne diseases harm many people.

Until 2010, PHW purchased filters manufactured in distant Accra, Ghana for distribution. Recently, the organization decided to establish a factory closer to the point of distribution in Tamale, Ghana. Previous research in other parts of the world had demonstrated that filters could maintain high coliform and turbidity removal performance despite having higher flowrates than typically recommended. 15 types of filters were designed to test the incorporation of grog, type of combustible material, method for processing combustible material, combustible to clay ratio, and shape of the filter. The statistically significant effect of each design variable on *E. coli* removal, total coliform removal, turbidity removal and flowrate was tested. Results from a related durability study were added to make recommendations for PHW. The recommended filter type incorporates hammermilled, unsieved, rice husk in a 4:11 proportion to clay by mass. The incorporation of grog and shape of the filter are left up to the factory's discretion, as they have do not have significant impact on performance.

Previous research described the flow through flower pot shaped filters as a function of Darcy's Law, and this work continued that effort by describing flow through a paraboloid shaped filter. The geometry of the filter was determined experimentally and modeled. A model was developed based on Darcy's Law and the filter geometry which describes flow through the filter.

Additionally, an assumption that the hydraulic conductivity was consistent throughout the height of the filter was tested. Three different methods were used to determine the hydraulic conductivity with height of the filter. The hydraulic conductivity was determined to be consistent throughout its height.

Keywords: ceramic filtration, filter design, coliform removal, paraboloid, hydraulic conductivity
Thesis Supervisor: Susan Murcott, Senior Lecturer of Civil and Environmental Engineering
Thesis Supervisor: E. Eric Adams, Senior Research Engineer and Lecturer of Civil and Environmental Engineering

Acknowledgments

This study has been a journey that I would never have been able to complete without the help of many people. I would like to thank my advisers at MIT, Susan Murcott and E. Eric Adams, for their guidance, patience, and enthusiasm. I would like to thank the other MIT team members, Travis Watters, Tom Hay and Leah Nation, for working hard and sharing a wonderful trip to Ghana with me. I would like to thank Manny Hernandez, for his assistance in building the factory and incredible capacity to design and build things from scratch. I would also like to thank Dr. Jack Germaine for his patience and assistance while characterizing the clay in his lab, as well as Stephen Rudolph for support in his workshop.

I would like to thank our incredible partners in Ghana for their dedication and hard work. Lydia Senanu tirelessly studied the performance of 30 filters over three months, and did an astounding job. Jacob, Ms. Senanu's driver, always knew where to buy that one crucial thing that you are missing. The PHW staff in Taha, including PHW director Mr. Sebani, factory manager John Adams, Awal, Emmanuel, Rubin, Amuda and the construction crew were very helpful in all stages of producing the filters and preparing the experimental setup. They even missed a very important football game to put the finishing touches on the experimental setup! The skilled and graceful potters from Gbalhai, Abiba, Semata, and Selematu were crucial to the success of this project. The powerful women of Taha who ground the clay and grog were invaluable. Zainab and Mildred provided us with incredible food daily, and are great friends. Nurideen protected our lodgings during our stay in Ghana and was always very helpful.

I would also like to thank my friends and family for supporting me as I traveled in Ghana and worked to finish this thesis.

TABLE OF CONTENTS

List of Abbreviations and Acronyms

E. coli	*Escherichia coli*
HTWS	Household Water Treatment and Safe Storage Technologies
LCL	Lower Confidence Level
LRV	Log Removal Values
PHW	Pure Home Water
RDI-C	Resource Development Institute –Cambodia
SODIS	Solar Disinfection
UCL	Upper Confidence Level
UV	Ultraviolet

Part I: Introduction and Objectives
1.0 Introduction

1.1 Ghana Background

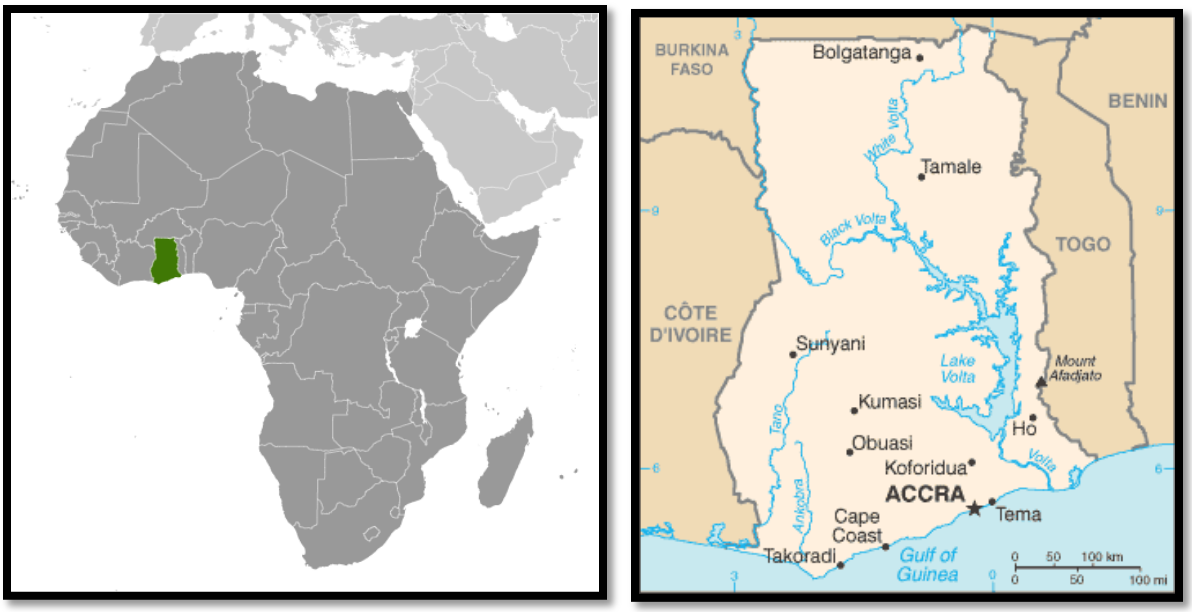

Figure 1-1: Left: Map of Africa Highlighting Ghana; Right: Map of Ghana (CIA, 2010)

Ghana is a West African country slightly smaller in area than the state of Oregon with a tropical climate. 23.8 million people live in Ghana, and 49% of them live in urban areas (WHO, 2010). Ghana gained independence from Britain in 1957, and is currently ruled by an elected president under a multiparty system. English is the official language, though many other languages are also spoken. Amongst its environmental concerns: "recurrent drought in [the] north severely affects agricultural activities; deforestation; overgrazing; soil erosion; poaching and habitat destruction threatens wildlife populations; water pollution; inadequate supplies of potable water"(CIA, 2010).

The estimated per capita income in Ghana as of 2009 is $1,500, which is five times greater than the poorest country in Africa and the world, the Democratic Republic of Congo. In terms of income distribution, Ghana's Gini Index is 39.4, whereas an economy without inequality would be 100. Work is split roughly in thirds between agriculture, industry and services (CIA, 2010).

1.2 Drinking Water in Ghana

Ideally, every home in Ghana would have access to piped, safe drinking water in their home with sufficient quantity to meet all of their basic water needs. Figure 1-2 demonstrates, though, that this is not the present reality for the majority of Ghanaians. The WHO/UNICEF Joint Monitoring Programme estimates that in 2008, 3% of rural households and 30% of urban households have piped connections, and 74% of rural households and 90% of urban households have access to improved drinking water sources. Improved drinking water sources include a public standpipe or outdoor tap, a protected well, a protected spring, or rain water. However, these sources do not always ensure safe water necessary for the prevention of disease.

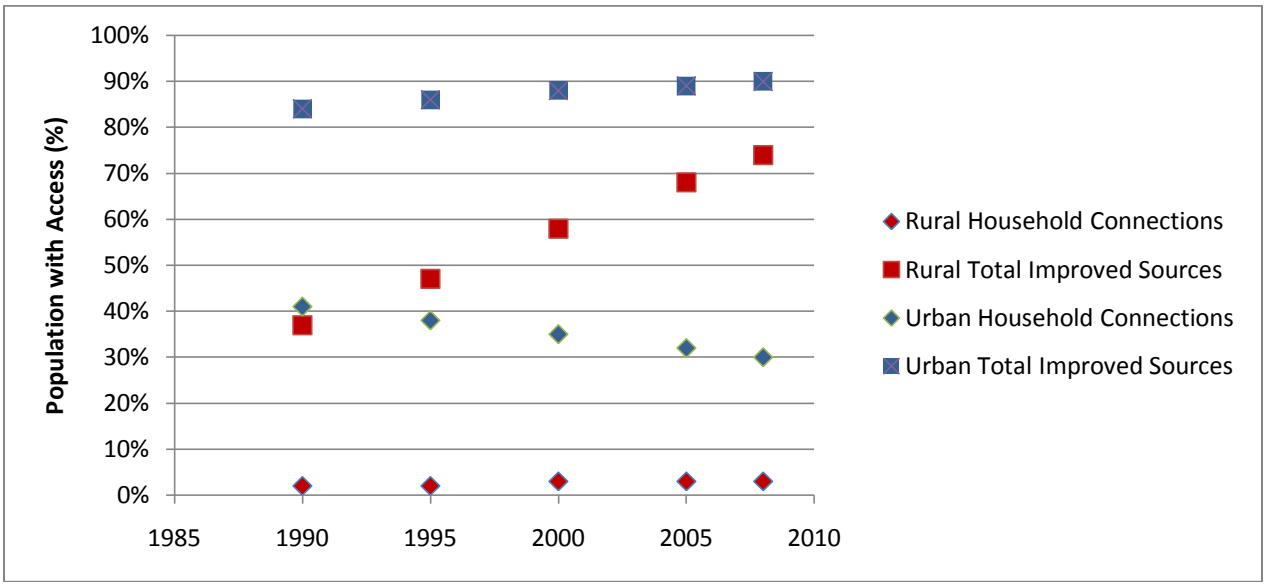

Figure 1-2: Drinking Water Access in Ghana (WHO/UNICEF, 2010)

1.3 Water and Sanitation Related Health Concerns

The lack of safe drinking water and sanitation is a public health concern because people are at risk of contracting disease. In Ghana in 2004, diarrhea was responsible for 10.4% of deaths among children under the age of 5. The death rate amongst children under the age of 5 in Ghana is approximately 12% (WHO, 2010). In addition, guinea worm has been a serious concern in Ghana as one of the five remaining guinea worm endemic countries in the world, and a focus of efforts by the Carter Center. The Carter Center reported 180,000 cases of guinea worm in Ghana in 1987, which were reduced to 501 cases by 2008 as a result of collaborative efforts including the use of drinking water filters (Caldwell, 2009).

1.4 Household Water Treatment and Safe Storage Technologies (HWTS)

HTWS is an effective means of providing safe drinking water sufficient for a family's needs. It can serve as an additional barrier of protection for those who already have an improved water supply, or as a first line of defense for those who use unimproved water supplies. Various HWTS exist, some are better suited for some areas and water conditions than others. These include UV disinfection, solar disinfection (SODIS), chlorine disinfection, coagulation, cloth filters, biosand filters, candle filters, and ceramic water filters, among others.

Vanessa Green (2008) reviewed the applicability of several household treatment options for Northern Ghana. Biosand filters offer higher flowrates than the ceramic water filters, but are more difficult to distribute and maintain. UV disinfection requires energy, which can come from decentralized sources. SODIS only requires clear plastic bottles and sunlight. Chlorine disinfection occurs by the use of liquid chlorine bleach or a solid product called Aquatabs. For UV disinfection, SODIS, and chlorine disinfection to be effective, influent water should have a low turbidity. Water in many of the "dugouts"[1] in Ghana, however, has very high turbidity. The use of coagulants greatly reduces the turbidity and microbes in the water, but does not disinfect

[1] A "dugout" is a surface water body, similar to a man-made pond, which serves as a drinking water source. See Figure 1-3.

pathogens, and therefore needs to be used in conjunction with other technologies. Cloth filtration can remove the microorganism responsible for guinea worm, but not turbidity or smaller microorganisms. Candle filters are effective, but the filter element has very small pore sizes, resulting in very low flowrates when filtering turbid Ghanaian surface waters.

Figure 1-3: Women and Children Gathering Drinking Water from Taha Dugout

Ceramic pot water filters is the technology chosen by the organization Pure Home Water. The filters have been shown to be effective at reducing coliforms and turbidity, and are simple to use and maintain. Colloidal silver is applied to the filter either through painting it on, dipping it in a bath, or adding it to the clay mixture. The organization Potters for Peace originally established a target flowrate of 1 to 2.5 L/hour based on the estimated necessary contact time with the colloidal silver. This flow rate is recommended as a quality control measure for factories; those outside the range are discarded. However, from the perspective of a user, it would seem that a faster flow rate would be desirable. Some studies have demonstrated that it is possible to achieve higher flowrates without compromising removal efficiencies (Bloem, 2008).

Sophie Johnson (2007) determined the average turbidity, total coliform and *E. coli* concentrations of raw urban and rural water sources and water filtered through ceramic pot filters using several different testing techniques. The average membrane filtration test results and turbidity results for six traditional communities in rural areas and two modern communities in urban areas are presented below in Table 1-1.

.

Table 1-1: Average Coliform and Turbidity Test Results for 8 Communities in Northern Ghana

Performance Category	Rural: Source Water	Rural: Filtered Water	Urban: Source Water	Urban: Filtered Water
Average *E. coli* (CFU/100mL)	690	2.5	1.4	0.21
Average Total Coliform (CFU/100mL)	23000	170	1500	150
Average Turbidity (NTU)	190	11	4.5	1.4

1.5 Pure Home Water and Kosim Ceramic Water Filters

In Northern Ghana, Pure Home Water (PHW), a social enterprise, promotes and markets ceramic water filters, targeting low-income households using unimproved sources. Despite the effectiveness of the ceramic water filters, the flow rate is typically low at 1-2 L/hour, and breakage has been reported at 12% "over a three to six month period" (Desmyter et. al., 2008). Improving on those characteristics would allow users to have larger quantities of safe drinking water, and their filter would last longer due to reduced breakage. MIT team member T. R. Watters (2010) completed a study looking at the strength of ceramic pot filters.

1.6 Pure Home Water Plans to Produce Kosim Ceramic Water Filters in Tamale, Ghana

From 2005 until 2010, the Kosim Ceramic Water Filters that are marketed by Pure Home Water were manufactured in the capitol, Accra, and trucked north to Tamale for distribution. They are flower pot shaped, incorporate sawdust into the clay mixture to create pores, and are dipped in a colloidal silver bath. Due to quality control concerns with the filters manufactured in Accra, Pure Home Water has decided to establish its own factory in Tamale, Ghana to produce high quality ceramic filters. Some factories around the world, notably FilterPure in the Dominican Republic, and factories in Nigeria and Tanzania are producing paraboloid filters. Other combustible materials, including rice husk are in use by other factories, notably Resource Development Institute-Cambodia (RDI-C). Pure Home Water is exploring the possibility of producing paraboloid filters made with sawdust or rice husk in its newly established factory outside of Tamale, Ghana.

Figure 1-4: Left: Flower Pot Shaped Filter (upside down)
Right: Paraboloid Shaped Filter (upside down, notch removed for study purposes)

2.0 Study Objectives

2.1 Determine the Optimal Ceramic Filter Type for Coliform Removal, Turbidity Removal and Flowrate in Northern Ghana

The first objective of this study is to demonstrate with statistical significance the impact of several design variables on several performance categories. The design variables to be tested include combustible type, percentage combustible by mass, sifting the combustible, addition of grog to the clay mixture, and the shape of the filter. The performance categories are *E. coli* removal, total coliform removal, turbidity removal, and flowrate. Recommendations for the Pure Home Water factory in Tamale, Ghana are made in this thesis as a result of these study findings.

2.2 Model Flow through the Paraboloid Shape Filter

2.2.1 Derive a Model of Flow through Paraboloid Filter based on Darcy's Law

The second objective of this study is to derive a model of flow through the paraboloid shaped filter using Darcy's law and a description of the geometry of the filter. The derived model is tested against measured data to determine its ability to accurately predict the flowrate at a given height.

2.2.2 Determine if Hydraulic Conductivity is Consistent throughout Filter

The third objective of this study is to determine if the hydraulic conductivity of the paraboloid filter is consistent throughout its height. This is useful to affirm or refute the hypothesis made by paraboloid filter proponents that the method of pressing these filters creates a more even compression and thus more homogenous hydraulic conductivity than the flower pot filters.

Part II: Removal and Flowrate Study
3.0 Removal and Flowrate Prior Research

3.1Mechanism of Filtration

The ceramic water filter removes pathogens through the processes of mechanical screening, sedimentation, adsorption, chemical activity, and biological activity (van Halem D. , 2006). Concerning the mechanical filtration, the untreated water passes through pores in the filter created by combustible material incorporated in the clay that burn off during firing. The size of the pores depends on the size and amount of combustible material, as well as properties of the clay and grog in the mixture. The target pore size is 1.0 micron in order to restrict the passage of small bacteria (Lantagne, 2001). Sedimentation and adsorption of fine particles occurs within tortuous pores, while biological activity occurs through the action of microorganisms living in the filter.

To gather information about the pores of the filter, several methods are used. Scanning Electron Microscope analysis of a piece of a Nicaraguan filter lip showed that the pores were in the range of 0.6-3.0 microns (Lantagne, 2001). van Halem (2006) and Oyanedel-Craver and Smith (2008) both used mercury intrusion porosimetry to gather information about pore size diameters and total pore areas. van Halem (2006) determined that filters from Ghana had 39% porosity, with 1.31 m^2/g total pore area; these were middle values between Nicaraguan and Cambodian filters. Similar experiments showed that the addition of colloidal silver to the filters reduces the porosity and total pore area, suggesting that pores are filled or coated with the silver (van Halem, 2006). Oyanedel-Craver and Smith (2008) used a changing-head flexible wall permeameter test to determine hydraulic conductivity. van Halem (2006) used bubble-point tests to determine the effective pore size of several filters, and concluded that all of the filters had effective pore diameters between 33-52 microns, much higher than the target of 1 micron.

3.2 Improved Filter Flow Rate

The original filter flow rate of 1-2.5 L/hour was designed with the constraint of a 20 minute contact time for the untreated water with the colloidal silver, with a built-in safety factor, based on product directions for residential colloidal silver water treatment (Lantagne, 2001). This slow filtration rate could reduce the quantity of treated water a household has, leading to the use of untreated water as a supplementary drinking water source. There is interest in improving the long-term flow rate of the filters while maintaining its capacity to effectively remove pathogens.

The flow rate of the filter using turbid water decreases with time. van Halem (2009) et. al. conducted trials using chlorine, citric acid, and high pressure backwashing to rejuvenate the flow rate of Nicaraguan filters. It was demonstrated that biomass and particles are mainly responsible for clogging the pores in the filters, as compared to inorganic fouling due to calcium carbonate precipitation. Interestingly, households surveyed in Cambodia did not want the filter flow rate to be increased because they associated a slow filter with better purification (Bloem, 2008). Klarman (2009) noted the discrepancy between the public health community's desire to increase the flow rate and users apparent satisfaction with the flow rate, and suspects the interview process and customary water usage differences between developed and developing countries as possible explanations.

Adjusting some of the properties of the filter can lead to an increase in the flowrate. Increasing the ratio of combustible material to clay will produce more pores, and thus increase

the flow rate. However, as the ratio and thus density of the combustible material is increased, there is increased probability that pores may become connected, and larger than desired (Klarman, 2009). The clay type will also affect the filter's hydraulic conductivity and removal (Oyandel-Craver, 2008).

3.3 Previous Removal and Flow Rate Studies

3.3.1 Investigation of the Potters for Peace Colloidal Silver Impregnated Ceramic Filter: Report 1 Intrinsic Effectiveness; Daniele S. Lantagne, Alethia Environmental, December 2001

Lantange (2001) studied several properties of the filters, including techniques for rejuvenating flow rate and finished water quality at different flow rates. To test the effectiveness of rejuvenating a filter in use in a home in Nicaragua, the flow rate of the filter was tested after various situations: at the home with well water, in a laboratory using city water, after scrubbing with a toothbrush to remove large particles blocking the flow, and after baking. The results suggested that scrubbing the filter regularly was the best mechanism to improve flow, leading Lantange (2001) to state that "the filtration rate of the PFP filter can be maintained indefinitely provided that users scrub the filter regularly to prevent build-up of particulate matter…".

To demonstrate the effect of flow rate on bacteria removal, four filters with different flow rates between 1-3 L/hour from the same factory in Nicaragua were filled with water from a contaminated well. The filters had not been coated with colloidal silver yet. Tests were performed to determine the presence of hydrogen sulfide bacteria, total coliforms, and *E. coli.* The results showed that all of filters tested positive for hydrogen sulfide bacteria and total coliforms, while three tested negative for *E. coli;* the second slowest filter tested positive for *E. coli* so it is not clear that the flow rate is related to removal efficiency from this study.

3.3.2 Ceramic Silver Impregnated Pot Filters for Household Drinking Water Treatment In Developing Countries; Doris van Halem, Delft University, November 2006

In a 12-week study, van Halem (2006) tested removal of three indicator organisms in 24 filters from Nicaragua, Ghana and Cambodia. The complete water system, meaning the filter, bucket and tap as a whole, were tested for removal of sulphite-reducing *Clostridium* spores to indicate oocysts and protozoa, *E. coli* K12 to indicate pathogenic bacteria, and MS2 bacteriophages to indicate viruses.

Filters were loaded with 6 liters of canal water daily, due to limitations in the ability to load filters with different discharges equally daily because of different flowrates. The water was spiked with high concentrations of *E. coli*, 266 CFU/100 mL to1.39 x10^7 CFU/100mL, every other week. Eleven filters from Ghana were tested, with the log reduction values from 4 to 7. The filters from Ghana performed slightly worse than those from Nicaragua, but better than those from Cambodia. Filter discharge decreased over the study, while scrubbing the filters resulted in temporary increases in the flow rates.

3.3.3 Sustainable Colloidal-Silver-Impregnated Ceramic Filter for Point-of-Use Water Treatment; Vinka A. Oyanedel-Craver and James A Smith, University of Virginia, 2008

Ceramic filters were created by Oyanedel-Craver and Smith (2008) using three different types of clay, grog and flour. The clay types included one commercially available and two natural clays, the commercial grog was used to reduce shrinkage and increase flow, and the flour was used as a combustible. "The two natural soil samples were dried, ground in a jar mill for 24 h, and passed through a 60-mesh sieve." The mixture of the filters was 40% clay, 10% flour and 50% grog, which is not representative of a common factory mixture for filter production. Filters were tested for *E. coli* removal without colloidal silver, with colloidal silver painted on the filters and with the filters submerged in colloidal silver. The study concluded that filters submerged in colloidal silver reduced bacterial transport more than those painted with colloidal silver. Importantly, bacterial removal was improved with increasing clay content and specific surface area of the clay, as well as pore size distribution and hydrodynamic dispersion. The authors predict that filters using clay with relatively uniform and fine-grained particle distributions will have smaller pores and better removal efficiency.

3.3.4 Silver Impregnated Ceramic Pot Filter: Flow Rate versus Removal Efficiency of Pathogens; Sophie C. Bloem, Delft University, May 2008

Bloem (2008) studied flower pot shaped filters made in Cambodia with rice husk as the combustible, and laterite added in an attempt to enhance virus removal. The ratio of rice husk to laterite to clay was varied, as shown in Table 3-1; R2L is representative of the standard factory ratio used by the Resource Development Institute-Cambodia (RDI-C) factory in Cambodia. Two sets of the seven filters presented in the table were made; one set was painted with a silver nitrate solution, while the other was not. The Filter ID notation has the first letter represent the factor being changed, R for Rice Husk or LA for laterite, while the number followed by L represented the targeted filter flow rate.

Table 3-1: Filter Types used by Bloem (2008), with and without Silver Nitrate

Filter ID	Rice Husk Percent	Laterite Percent	Grog Percent
R2L	21.6%	4.9%	73.5%
R4L	23.8%	4.8%	71.4%
R5L	25.6%	4.7%	69.8%
R6L	27.3%	4.5%	68.2%
LA4L	20.6%	9.3%	70.1%
LA5L	19.6%	13.4%	67.0%
LA6L	18.8%	17.1%	64.1%

Bloem (2008) and partners filled all 14 filters with 10L of river water treated to remove large particles twice daily for 6 months. This amount was chosen after a brief survey of households using filters suggested that most filled the filter twice daily. After every 30L of water added to the filters, 10L of water spiked with *E.coli* and M2S were added to the filters to simulate polluted waters. Filters and receptacles were cleaned after every 150L of water, roughly weekly.

Bacteria removal was measured by log reduction of *E.coli* using membrane filtration, virus removal was measured by log reduction of MS2, and flow rate was measured by filling the filter to the brim, and measuring how much water is captured in a clean, empty receptacle after 30 minutes; receptacles of filters with silver were wiped with paper first to remove silver from the receptacle walls. During the first month of the study, indicator organism removal was measured every other day, and every 10 days for the remainder to the study. Flow rate was measured every 5 days during the first month of the study, and every 10 days for the remainder of the study.

The flow rate of the water filters increased by increasing the rice husk or laterite added. Bloem (2008) observed that a threshold of increased material was needed to dramatically increase the flow rate. During the first 20 days of the study, the flow rate increased in all of the filters, with flow rates nearly 10 L/ hour in the R6L filter.

Bloem (2008) observed a long-term trend of reduced flow rate over the course of the study in the filters, which is attributed to clogging. As a group, filters without silver had a larger decrease in flow rate than those with silver, which is attributed to biofilm inhibition caused by the silver. It was not clear that cleaning the filters had an impact on the flow rate.

During the first 20 days, the filters with silver consistently removed more *E. coli*, achieving log reduction of 5 to 8, while those without silver achieved log reduction of 2 to 4.5. There was no clear indication that the flowrate impacted *E. coli* removal throughout the six month period of study. Also, the filters without silver and their receptacles developed noticeably smelly, green biofilm, while the filters with silver did not. The results for virus removal were much worse than for *E. coli*, with log reduction below 0.4 during the first month of testing regardless of the silver application. Laterite proportions also did not correlate to increased virus removal.

3.3.5 Investigation of Ceramic Pot Filter Design Variables; Molly Klarman, Emory University, May 2009

Klarman (2009) studied eight different filter types, shown in Table 3-2, at the FilterPure factory in the Dominican Republic.

Table 3-2: Filter Types Studied By Klarman (2009) with Three Replicates

Filter ID	Combustible Volume	Clay Volume	Combustible Type	Screen Size, µm^2
53C:47S	47%	53%	Pine sawdust	0.30
50C:50S	50%	50%	Pine sawdust	0.30
55C:45S	45%	55%	Pine sawdust	0.30
60C:40S	40%	60%	Pine sawdust	0.30
45C:55S	55%	45%	Pine sawdust	0.30
40C:60S	60%	40%	Pine sawdust	0.30
0.45µm	47%	53%	Pine sawdust	0.45
Coffee husks	47%	53%	Coffee husks	0.30
Rice husks	47%	53%	Rice husks	0.30

The main combustible used was pine sawdust, though rice husk and coffee husk were also tried. The ratio of combustible to clay by volume was varied; 53C:47S is the standard used by the FilterPure factory. A larger screen size for the sawdust also was tried. The filters have a

paraboloid shape, unlike the standard flowerpot shape. Also, unlike other filter factories, FilterPure incorporates silver into the water that the dry clay and combustible material is mixed with, intentionally incorporating the silver throughout the clay before it is fired.

For five weeks, the filters were filled twice daily six days per week with either 6L or 12L of water depending on the flow rate. The water was from a nearby river, and stored in a plastic holding tank. The filters and receptacles were cleaned according to FilterPure instructions, once a week. The water quality parameters *E. coli* and total coliforms were quantified using IDEXX Quanti-Tray®, and turbidity, pH and conductivity were determined weekly. Flow rate was measured by filling the filter to the rim and collecting the effluent in a cup for ten minutes.

The flow rate of most of the filters increased over time, demonstrating a different trend than other studies. Unlike other studies, the turbidity of the influent water was very low, under 5 NTUs. Initial flow rates of the sawdust filters ranged from 0.25 L/hour to 4.24 L/hour. Results support the hypothesis that increased ratio of combustible to clay reduces bacteria removal. A strong correlation was demonstrated between total coliform reduction and initial flow rate of all the filters for the first week; the relationships for data across the five weeks including outliers are much weaker, however. Klarman (2009) determined that 1.7 L/hour was the maximum flow rate in order to maintain 99% total coliform removal. It is also suspected that the other combustible materials, rice husks and coffee husks, do not mix as homogenously as saw dust resulting in higher flow rates and worse removal. Screen size change from 0.30 μm^2 to 0.45 μm^2 did not seem to have a large affect on flow rate or removal.

4.0 Optimal Removal and Flowrate Study Research Methodology

4.1 Description of Factory in Taha village, Tamale, Ghana

Pure Home Water is in the process of constructing a ceramic water filter and brick factory. The organization owns a plot of land adjacent to the Taha village off of a major dirt road a few miles outside of the city of Tamale. As of January 2010, the plot is being prepared for a finished factory building. When the MIT team arrived on 3 January 2010, the plot simply had a layer of compacted gravel, a storage container, and an enclosed shelter made of poles and grass mats.

Figure 4-1: Travis Watters Posing with Sign Marking Taha Village

Figure 4-2: Manny Hernandez atop Kiln, along with Pure Home Water Staff

During the MIT team's field study in January 2010, most of the materials processing was done on plastic tarps laid on the gravel. A downdraft "Mani" kiln, shown in Figure 4-2, was built during this time under the supervision of Manny Hernandez, international kiln expert and recently retired faculty in the Ceramic Arts Department of the University of Northern Illinois. This enabled the author, with assistance from other members of the MIT team, Manny Hernandez, the Pure Home Water staff, the women potters of Gbalhai, to produce the factory's first 30 filters for performance testing.

4.2 Design and Fabrication of Filters for Study

4.2.1 Selection of Design Variables

Pure Home Water has several important factors to consider when deciding upon the final design of its future filters, listed below:

List 4-1: Major Factors Consider in the Design of Ceramic Filters for This Study

Incorporation of grog
Type of combustible
Method for processing combustible
Percentage Combustible by Mass
Shape of filter

The final design of each filter is summarized in Table 4-1, and can be found in APPENDIX B. Pure Home Water (PHW) has two potential sources of clay: a clay pit used by local potters in the village of Gbalhai, located about 1km from the PHW factory in Taha, and clay located near the edge of another property owned by the organization about 5km north of Tamale. For this study, the clay from Gbalhai was the only accessible source at the time, so it was used exclusively. Grog is ground, fired ceramic material that acts as a filler in ceramics and is said to prevent shrinkage, increase durability and increase filter flow rates. Depending on the plasticity of the clay used, local potters often combine grog with clay. In this study, one set of filters contained grog at a fixed ratio to clay, while one set contained no grog.

Clay and combustible properties are not consistent from one location to the next, therefore it is important for Pure Home Water to test filters prepared with different combustible materials in different ratios. In other words, recipes used in Nicaragua, or even Southern Ghana, may not be optimal for Tamale, Ghana. This consideration constitutes the main purpose of this author's research for this project.

Ceramic pot water filter manufacturers around the world utilize several types of combustible materials, the most common being sawdust and rice husk; flour and coffee grounds are others. Locally available sawdust and rice husk were used in this study. All of the combustible materials were passed through a hammermill. The combustible material which blew out of the "fine" chute as well as that which passed through the "waste" chute were utilized in equal amounts for resource and energy efficiency, with the exception of two filter pairs which included "fine", sifted material exclusively.

To arrive at a desirable combustible to clay ratio, three different ratios were prepared. The RDI-C standard ratio for filters made without laterite uses 8.9 kg rice husk to 30 kg clay; rich husk is 22.9% of the total by mass. This ratio was roughly used as a starting point in this

study. Two higher ratios were chosen in addition, based roughly on those chosen by Bloem (2008) in Cambodia.

Although ratios are prepared by finding the mass of the input materials, the pore size and porosity of a filter is based on the volume of a combustible particle, not its mass. Since volume is related to mass by density, estimated dry densities of milled rice husk and sawdust in were determined on site. The estimated dry densities were considerably different, so combustibles were added to the dry mix in roughly equivalent volumes based on the calculated masses. For production, mass measurements are preferable to volume measurements because they are easier and more reproducible by using a scale than by leveling a container of fixed volume.

Pure Home Water has obtained or built its own molds and presses for both flower pot and paraboloid shaped filters. In Accra, Ghana and many factories around the world, flower pot filters are the most common type of pot filter produced and distributed, having been promoted by Ron Rivera and the Potters for Peace (PFP) organization. In some other factories, including the FilterPure factory in the Dominican Republic as well as factories in Nigeria and Tanzania, paraboloid filters are produced, based on design modifications by Manny Hernandez. All filters except for one pair produced for the study were made in the flower pot shape because of time constraints and the time of completion of the paraboloid mold and press towards the end of this field study.

Table 4-1: Filter Design Characteristics

Filter Pair Number	Combustible Type	Hammermill Product	Combustible Percentage of Total Mass		Grog Added	Shape
1	Rice Husk	Fine and Waste	Low	21.4%	No	Flower Pot
2	Rice Husk	Fine and Waste	Low	20.0%	Yes	Flower Pot
3	Rice Husk	Fine and Waste	Medium	26.7%	No	Flower Pot
4	Rice Husk	Fine and Waste	Medium	25.0%	Yes	Flower Pot
5	Rice Husk	Fine and Waste	High	31.3%	No	Flower Pot
6	Rice Husk	Fine and Waste	High	29.4%	Yes	Flower Pot
7	Sawdust	Fine and Waste	Low	16.6%	No	Flower Pot
8	Sawdust	Fine and Waste	Low	15.4%	Yes	Flower Pot
9	Sawdust	Fine and Waste	Medium	20.9%	No	Flower Pot
10	Sawdust	Fine and Waste	Medium	19.5%	Yes	Flower Pot
11	Sawdust	Fine and Waste	High	24.9%	No	Flower Pot
12	Sawdust	Fine and Waste	High	23.3%	Yes	Flower Pot
13	Sawdust	Fine, Sifted	Low	14.2%	No	Flower Pot
14	Rice Husk	Fine, Sifted	Low	18.8%	No	Flower Pot
15	Rice Husk	Fine and Waste	Low	20.0%	Yes	Paraboloid

4.2.2 Input Material Processing

The combustible materials were all processed through a hammermill. The hammermill, generously provided by MIT Senior Lecturer Amy Smith and shipped from Kumasi to Tamale in January 2010, was equipped with a 220V, 50 Hz, 1.5 kW, 2 HP single-phase motor. Approximately 2,000 cubic centimeters of raw combustible material were added to the

hammermill at a time. The material was milled for one minute, at which point the waste chute was opened. Grain sacks were used to collect the material.

Filters 1 through 12 and 15 utilized both the material that was processed through the fine chute and the waste chute; filters 13 and 14 utilized only material processed through the fine chute and then was sifted. Sawdust that was gathered through the fine chute and sifted was done by a special attachment: a plastic funnel was cut to fit the fine chute, and taped with duct tape to a flour sifter, with approximately 1mm x 1mm mesh. The rice husk, unfortunately, clogged the sifter too quickly, and was thus sifted by hand after being collected from the fine chute.

Figure 4-3: Pure Home Water Staffer Reuben with MIT Team Member Leah Nation Adding Combustible to the Hammermill

Figure 4-4: Hammermill with Sifter Attachment

Figure 4-5: Inside of Hammermill

The clay was dried in the sun and then pounded with mortar and pestle. Tarps were laid on the ground, and clay which was dug from the ground in the neighboring village of Gbalhai was broken into clods about the size of a small fist and allowed to dry for one to three days in the sun. Local women from the Taha and Gbalhai villages were hired to pound the clay into powder using large wooden mortar and pestles. The clay was then passed through a sieve with 18x14 aluminum mesh which has a 1.12mm opening, manufactured in the USA but available locally. The wooden sieve box was propped on a make-shift tarp-lined brick pit.

Figure 4-6: Women Pounding Clay with Large Wooden Mortar and Pestles

The grog was made using broken ceramic filters. During the 14-hour transit from Accra to Tamale, some ceramic water filters manufactured in Accra had broken. These chards were also

pounded by the local women using mortar and pestle. The ground grog was passed through a sieve with a locally available mosquito screen, with approximately 1mm x 2mm openings.

Figure 4-7: Initial breaking of ceramic pot chards, Travis Reed Miller with Leah Nation

4.2.3 Filter Input Material Characterization

4.2.3.1 Filter Input Material Densities

At the factory site in Ghana, input material characterization was limited by equipment availability. To roughly determine the density of the clay and combustible materials, a plastic beaker was filled to the 1 L mark with each dry material, tapped slightly to level the material, and weighed on a Camry Dial Spring Scale, with a capacity of 20 kg and demarcations at 50 g.

At MIT, the density of each material was determined using a more accurate scale. Samples of each material were collected in 200mL Whirl-Pak® bags at the site in Ghana and brought back to MIT. A Fischer Scientific 08-732-5C 53mm x 17.5mm aluminum pan was used as the container for weighing the materials. To determine the volume of the container, it was filled with water, which was then measured in a standard graduated cylinder. The volume was determined to be 55 cm^3. An Ohaus Corp. Scout Pro SP202 scale was used, with a capacity of 200 g and a readability of 0.01g.

Figure 4-8: Scout Pro SP202 Scale and Container

Each material was added to the container and weighed three times, and an average value was found. The combustible materials were poured from the Whirl-Pak® bags into the container to be weighed, while clay and grog were "scooped" out using the container to prevent sorting by grain size. Tapping the materials to level them, as was done in Ghana, would be difficult to replicate properly. Therefore, a straight edge was used to scrape off the material to be level with the container. This resulted in the laboratory measurements producing slightly less dense results than the field measurements. Still, the results are linearly related with an R^2 value of 0.9853.

To find a density that better represents the combustibles when they are in a clay mixture, and thus not exposed to air and instead surrounded by wet, kneaded clay, a similar procedure as above was followed using more compacted combustibles. This procedure still does not entirely represent the combustible in the clay mixture. The volume of a standard metal tare was found to be 40 cm^3 using water and a standard graduated cylinder. Each combustible was pressed firmly into the metal tare with two fingers as material was added. A Mettler Toledo PB3002-S electronic scale was used to measure the sample.

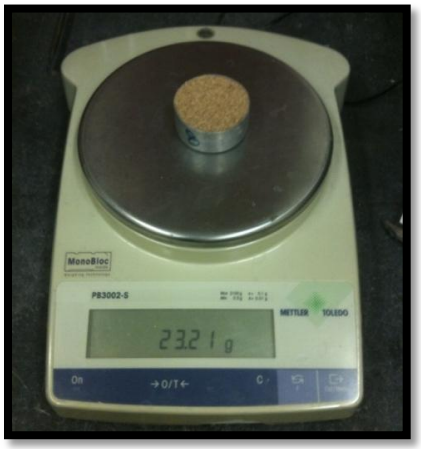

Figure 4-9: Mettler Toledo PB3002-S Scale and Metal Tare at MIT

4.2.3.2 Filter Input Material Images

An Epson Stylus CX4400 flatbed scanner, set to 1200 DPI, was used to take close-up images of the filter input materials, shown in Figures 5-1 through 5-8. A piece of ¼" graph paper was set next to the material for size reference. The proportion of particles of different sizes should not be taken as a proxy for particle size distribution at it is a very small sample. Instead, it is a useful demonstration of the range of particles present.

4.2.3.3 Filter Input Material Particle Size Distribution

Particle size distribution analyses were performed on samples of clay and grog in accordance with ASTM Standard D 6913 – 04, using the set of sieves listed in Table 4-2. The material was air dried and hand-shaken. The median diameter was considered to be the interpolated sieve opening for 50% of material passing.

Table 4-2: Set of Sieves Used in Particle Size Distribution Analyses

Sieve Number	Sieve Opening (mm)
10	2
20	0.85
40	0.42
70	0.212
120	0.125
200	0.074
Pan	

Similar analyses were performed on the combustible material, even though ASTM Standard D 6913 – 04 does not allow fibrous materials to be tested. The procedure worked well for sawdust, however a problem arose with rice husk. The hammermill processed many of the rice husk particles into very fine pieces, which plugged the holes in the #40 sieve. Had less than 50% of the material passed through preceding sieves, the diameter still could be determined. However, a majority of the material in each test passed through preceding sieves. Therefore, the particle size distribution analysis for rice husk is not useful.

Figure 4-10: Sieve #40 Partially Plugged with Fine Rice Husk, for Demonstration

The median particle sizes (D50) corresponding to 50% passing on the cumulative particle-size distribution curves were calculated for all materials. The D10, D30, and D60, corresponding to 10%, 30%, and 60%, respectively, passing on the cumulative particle-size distribution curves, were calculated for all materials and were interpolated for clay as they are useful for soil classification

The coefficient of uniformity, Cu, and coefficient of curvature, Cc, were calculated for the clay.

$$Cu = \frac{D_{60}}{D_{10}} \tag{4-1}$$

$$Cc = \frac{(D_{30})^2}{D_{10} D_{60}} \tag{4-2}$$

4.2.3.4 Clay Characterization

4.2.3.4.1 Atterberg Limit Tests: Liquid and Plastic Limit and Plasticity Index

The Atterberg Limits, including liquid and plastic limit and plasticity index of the clay were found according to ASTM Standard D4318 - 10. The Casagrande Cup was used for the Liquid Limit. The Casagrande Cup is a metal cup attached to a device which taps it on a solid surface, disturbing the contents; each tap is counted as a "blow". The bottom of the cup is filled with the clay, and a groove of standard size is carved to separate the clay into two sides. The "blow count" is recorded as the number of blows required to make the clay rejoin along ½" of length of the groove. The water content of several clay samples is adjusted to record different blow counts. The liquid limit is the water content at when the blow count is 25. The plastic limit is the water content when a 1/8" diameter strand of clay begins to crumble. The plasticity index is the difference between the liquid limit and the plastic limit.

4.2.3.4.2 Specific Gravity

The specific gravity of the clay was found according to ASTM Standard D854 - 10.

4.2.3.4.3 Classification

The clay was classified according to the Unified Soil Classification System, ASTM Standard D2487 – 10.

4.2.4 Production of Filters

4.2.4.1 Preparing Materials and Pressing Filters

The materials for the filter were mixed together by hand. To prepare the materials for the filters, a tarp was laid on the compacted gravel surface at the PHW Taha factory site. Each component, including clay, combustible, and sometimes grog, was measured on a Camry dial spring scale, and then added to a pile. For each production batch, enough of each material was added to make two filters, so that each filter in a pair came from the same mixture. The pile of dry materials was first mixed by hand, and then after a homogenous mix was achieved by inspection, the local potters gradually added water to the mixture, and began to wedge the clay. Wedging, or kneading, the clay is a technique used by potters to "homogenize the clay and get rid of air pockets".[2] The local potters were employed in this task because of their expert knowledge.

Figure 4-11: Camry Spring Scale at the Factory Site in Ghana (Safety Glasses in Pan)

Figure 4-12: Travis Reed Miller with Local Potters Semata, Selematu, Abiba and their Children

[2]"The Wedging Bat." Ceramics Today. Accessed 24 February 2010. http://www.ceramicstoday.com/articles/081500.htm

After the clay was wedged, the clay was added to the mold in the press. For the flower pot shaped filters, a serviceable but cumbersome portable press[3] was used, as well as a custom-made nylon mold[4]. This press can be more easily transported and assembled than a permanent press which requires on-site welding. The portable press utilized a 20 ton hydraulic jack, and the male mold pressed the clay from above. 8.5 kg of the clay and combustible mixture was formed into roughly a cube and used for each filter, allowing for excess.

The process to produce a flower pot filter was more cumbersome and tedious than that for the paraboloid shaped filter. The following list outlines the steps in producing a flower pot shaped filter using the portable press:

List 4-2: Steps to Press a Flower Pot Filter on a Portable Press

1. Raise the male mold out of the female mold by turning the bar; lock it into position by fitting the gear onto the welded nut.
2. Remove the female mold from the press.
3. Fix wetted plastic bags over the female and male molds.
4. Place the 8.5 kg cube of clay mixture into the female mold.
5. Using a fist, create an evenly-distributed depression several inches deep in the cube of clay. This is necessary to allow for the male mold to fit into the female mold so that there is enough clearance for the hydraulic jack to fit into the press.
6. The bar is turned to lower the male mold into the female mold.
7. The hydraulic jack is fitted into the press above the male mold.
8. The hydraulic jack is pumped approximately 200 times, until the excess clay emerges from all sides and the male and female mold are nearly touching on all sides. Care is taken to ensure that the gear is no longer fixed on the nut preventing the mold from moving down; if it accidently is, the cable snaps.
9. The hydraulic jack is released and removed from the press, and the piston is pressed down by standing on it.
10. The bar is turned to raise the male mold from the female mold.
11. If the male and female molds do not separate easily, a rubber hammer is used to hit the female mold on all sides until it falls down.
12. A plywood bat cut to be larger than the outer diameter of the filter element lip, but smaller than the inside dimension of the press, is placed on top of the newly formed filter, and the female mold is removed from the press.
13. Two people hold the female mold containing the newly pressed filter, which together weigh approximately 60 pounds, and flip it over, and then place it down with the bat on the ground, as in Figure 4-15.
14. The female mold is lifted straight off the filter.
15. The edges of the filter element are trimmed using a sharp object.

[3] The portable press was provided by Peter Chartrand, US Director of Potters for Peace, and Joseph O'Connell of Creative Machines, both of Bisbee, Arizona.

[4] The custom-made nylon mold was provided by Alex Bernabo, W. Design Inc., 5 John Walsh Blvd., Peekskill, NY 10566.

Figure 4-13: Portable Press and Nylon Male and Female Molds Used For Flower Pot Filters

Figure 4-14: Portable Pressed Used For Flower Pot Filter, Male Mold Being Lowered

Figure 4-15: Local Potters Flipping Over Female Mold with Plywood Bat

The process for producing a paraboloid filter with the full-size permanent press, shown in Figure 4-16, custom built on site, is considerably less cumbersome than the portable press as its design has been refined for ease of use. Male and female cement molds were also made on site for the press. This press utilized an 8 ton hydraulic jack, and the female mold pressed the clay over the male mold from above. Approximately 7.5 kg of clay and combustible mixture was formed into a cube used for each filter. The following list outlines the steps involved in producing a paraboloid filter:

List 4-3: Steps to Press a Paraboloid Filter on a Permanent Press

1. The table with the male mold affixed is slid out from under the female mold.
2. A plastic bag is fitted over the male and female molds.
3. A donut-shaped plywood bat is set over the plastic bag on the male mold.
4. The 7.5 kg cube of clay mixture is set on top of the male mold, and patted down to roughly match the shape of the top portion of the male mold.
5. The table is slid under the female mold.
6. The hand crank is used to lower the female mold on top of the male mold.
7. The metal bar is moved from its resting position hanging on the left side of the press to the middle of the press, centered above the hydraulic jack.
8. The hydraulic jack is pumped approximately 40 times, until the bottom edge of the female mold reaches the plywood bat around the male mold.
9. The hydraulic jack is released, and springs press the piston back into starting position.
10. The metal bar is slid back into resting position.
11. The hand crank is used to lift the female mold off of the male mold.
12. The table with the male mold and filter is slid out from under the female mold.
13. The pressed filter is lifted by the bat off of the male mold.
14. The plastic bag is removed from the inside of the filter.

Figure 4-16: Left: Permanent Press Used For Paraboloid Filters with Welder, Red Right: Male Mold on Table, Slid Out with Recently Pressed Filter

4.2.4.2 Drying Filters

Once pressed, the filters were set on plywood bats to dry. The identification number of the filter was pressed into the underside of the lip using a standard numerical rubber stamp. For the first day of drying, the filters were kept out of direct sunlight by placing them inside the grass mat shelter. Afterwards, they were turned right-side up so that the interior of the pot could dry; paraboloid filters were set on their sides. Once the interior of the pot appeared to be dry, the filters were set on bats or tables in the sun, and were rotated 90 degrees every hour or half hour. When the filters developed cracks, they were wetted and patched with excess clay and combustible mixture.

Figure 4-17: Filters Drying Upside Down in Sunlight on Table with Slats

Figure 4-18: Filters Drying in Sun on Plywood Bats, Turned by MIT Team Member Leah Nation

4.2.4.3 Firing Filters

Once all of the filters were sufficiently dry, they were fired in the "Mani"[5] downdraft kiln. All 28 flower pot filters were able to fit into the kiln in one firing; four paraboloid filters were fired separately along with sample bricks used in the durability study by Watters (2010). The filters were randomly stacked four or five high in the kiln, separated by custom-made ceramic spacers to allow heat flow. The spacers, shown in Figure 4-19, were designed by Manny Hernandez and produced by the Gbalhai women potters. Later, notches were cut along the bottom for increased air flow.

Figure 4-19: Ceramic Spacers before Notches Added Along Bottom

[5] The "Mani" kiln is named after Manny Hernandez, PHW factory consultant. .

The filters were fired based on guidance from the director of the FilterPure factory in the Dominican Republic. After throughly drying the filters during the initial part of the firing which lasted nearly four hours, the temperature was raised to the target temperature is 877 degrees Celsius, as described below. Two methods were used to measure the temperature inside the kiln as checks against each other. For the first method, a pyrometer was inserted into the side of the kiln. For the second method, several cone packs were placed around the kiln strategically. Each cone pack contained Shimpo[6] cones 013, 012, and 011 which reportedly melted and bent at 844, 871 and 883 degrees Celsius respectively. When the temperature of the kiln is between 844 and 883 degrees Celsius, the temperature can be determined fairly accurately by observing the state of the cone packs through spy holes.

Early in the morning, a "candle fire", a small fire with a few sticks, was lit on the floor of the openings of the fireboxes with small pieces of wood. At this point, the side door of the kiln was still partially open to allow moisture from the filters to escape. While more moisture escaped, bigger pieces of wood were burned toward the middle the floor of the firebox. When black smoke arose out of the chimney, it signalled that the combustible was burning. At approximately 250 degrees Celsius as determined by the pyrometer, the side door was closed with bricks and mortar made of clay and sand sealed the cracks. At around 400 degrees Celsius, the filters were assumed to be dry, and the heat was rapidly increased by adding wood toward the middle and back of the firebox. Earlier, wood was only added to the floor of the firebox. At this stage, wood was added on top of a grate made of loosely spaced bricks to allow embers to fall and provide additional heat. Later, the pyrocones were checked through a spy hole to determine with certainty that the optimal temperature had been reached.

Figure 4-20: Pure Home Water Staffer Tending the Candle Fire

[6] NIDEC-SHIMPO America Corporation. http://www.shimpoceramics.com/

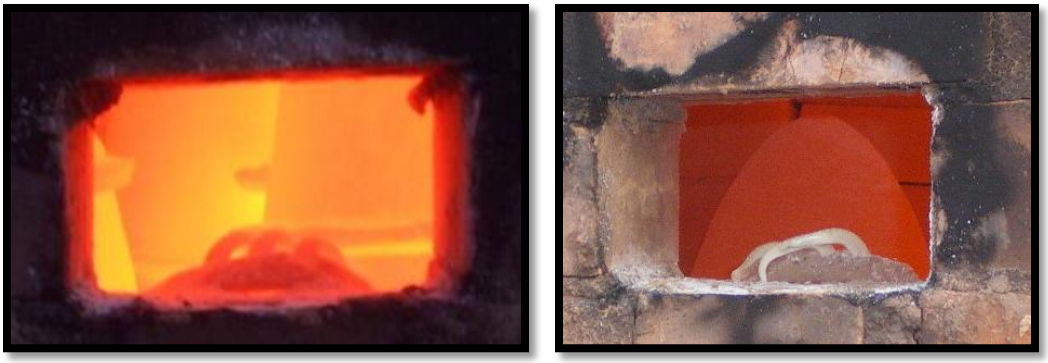

Figure 4-21: Melted Pyrocones As Seen Through Spyhole
Left: Flower Pot Filters, Right: Paraboloid Filters

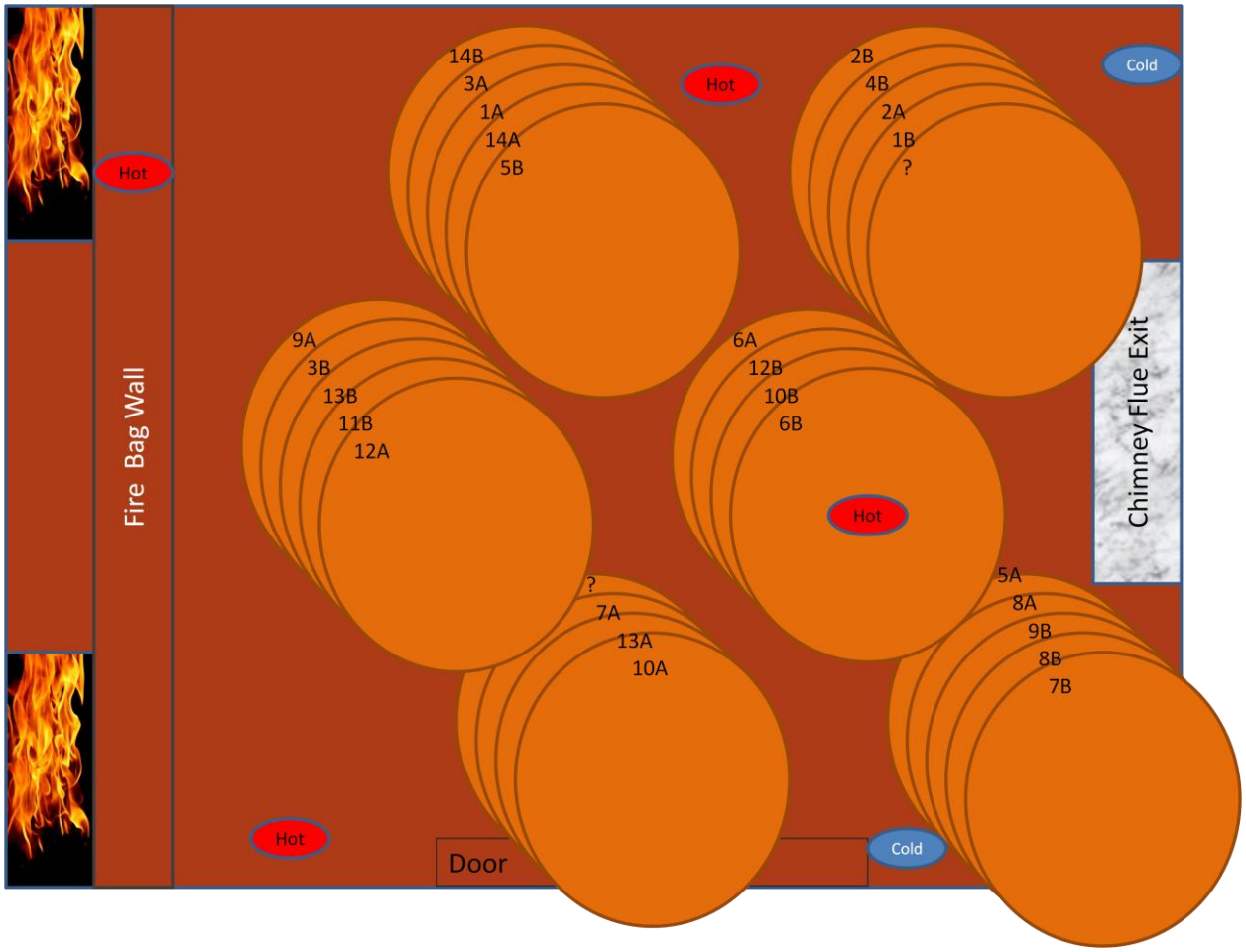

Figure 4-22: Position of Flower Pot Filters in the Kiln with Hot and Cold Spots (Top View)

Figure 4-23: Left: Flower Pot Filters after Firing, Right: Paraboloid Filters after Firing

4.2.4.4 Patching the Filters

As these were the first filters produced by the PHW factory, many of the flower-pot filters emerged from the kiln with cracks, some minor and some severe; none of the paraboloid filters had cracks. It was necessary to patch the cracks in order for them to be included in the study. Upon recommendation from the local potters, the filters were patched with a mixture of cement and egg yolks which dried quickly in the sun. Images of the filters after patching can be seen in APPENDIX B. At this point, patching filters to be used in residences is not recommended because there may be cause for public health concerns about chemicals leaching from the cement-egg yolk mixture. Limits on time necessitated that these cracked filters be used instead of creating a set without cracks. There was not enough time to complete an additional initial flow rate test with the patched filters.

Figure 4-24: Left: Potter Patching a Filter, Right: Example of Dried Filter Patch

4.2.4.6 Colloidal Silver Application

Pure Home Water has decided to continue the practice of most ceramic pot filter factories which dip the filters in colloidal silver. Based on conversations between the Spanish colloidal silver company, Argenol, and other filter producers, Manny Hernandez determined that 0.245 g/L of silver would equate to the recommended concentration of colloidal silver painted on filters. The most accurate scale available was a spring scale which weighed up to 500 g in 10 g intervals. Therefore, several Whirl-Pak® bags were filled with 10 g of 70% pure Argenol colloidal silver powder each.

Each Whirl-Pak® bag containing 7g of pure silver was mixed with 28.6 L of clean municipal tanker truck water to reach the desired concentration of 0.245 g pure silver/L. According to methods by Oyanedel-Craver and Smith (2008), each filter was submerged for 45 seconds. Note that Oyanedel-Craver and Smith (2008) used a concentration of 0.800 g/L silver, which is much higher than what was used in this study.

Unfortunately, on the first attempt, only one Whirl-Pak® bag was brought to the site, and an insufficient volume of colloidal silver solution was prepared; the reality that each filter absorbs approximately 1 L of solution was not anticipated. Some of the filters were thoroughly soaked, while others were merely splashed repeatedly with the remaining solution. Therefore, the following morning, three buckets with 28.6 L of colloidal silver solution each were prepared, and each filter was soaked completely for 45 seconds.

4.3 Filter Testing

The filters have been loaded with local surface water used in Taha as drinking water supply and tested for twelve weeks, from 1 February 2010 to 23 April 23, in Ghana in order to determine the coliform and turbidity removal efficiencies and flowrates of the 15 filter types. The intent is to roughly mimic a typical residential usage pattern by filtering water from an actual source at a similar frequency to a resident user.

Bloem (2008) tested a set of filters in Cambodia for six months, while Klarman (2009) tested a set of filters in Dominican Republic for five weeks using different methodologies, as described in Section 3.3 above. In this study, each filter was tested for coliform and turbidity removal efficiencies as well as flowrate once per week. Lydia Senanu, a skilled laboratory technician who worked for PHW for the past several years, was hired to complete the loading, sampling and testing of the filters.

4.3.1 Filter Testing Setup

Thirty filters, two pots of each of the 15 filter types, were set up for testing in a grass mat enclosure in such a way that water could be put through the filters each weekday with flowrate tested and samples collected once per week for twelve weeks. Filters were arranged in five groups of six to accommodate testing 30 filters in a five-day work week. Plastic tarps were laid on the ground to prevent dust contamination; only one-half of a wall remained open as an entrance. Apart from the plastic tarps, such a shelter is not very unlike village households where Kosim filters are already in use.

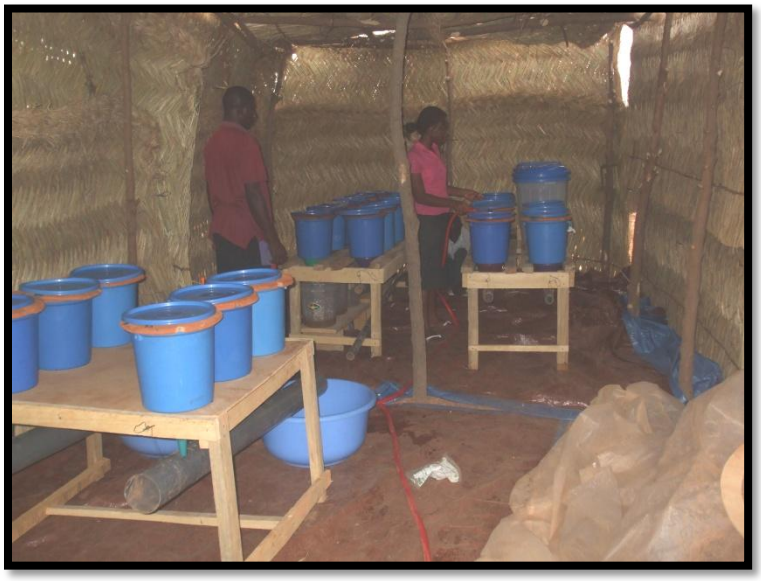

Figure 4-25: Filters in Testing Setup in Grass Mat Enclosure

In normal use, the filters sit in safe storage buckets and collect water in the bottom of the bucket, with a tap on the side for users to decant the water. In the testing set-up, to make best use of the laboratory technician's time, the flowrate testing and sampling occurred simultaneously by using a clean collection container under the bucket. Therefore, it was necessary to cut a hole in the bottom of the bucket and through the table. However, in most plastic buckets, the bottom is raised towards the center; if only a small hole was cut in the middle of the raised section, not all of the water would pass through the hole as it would pool around the

bottom edge and the flowrate would be measured inaccurately. Therefore, the hole was cut with a jig saw wide enough to accommodate a 15cm funnel. Epoxy was used to secure the bottom of the funnel lip to the inside of the bucket. A table that held six filters was made with a piece of plywood and holes were cut out with a jig saw, while two other tables holding 12 filters each were made with lengths of wood supporting the buckets on the two edges.

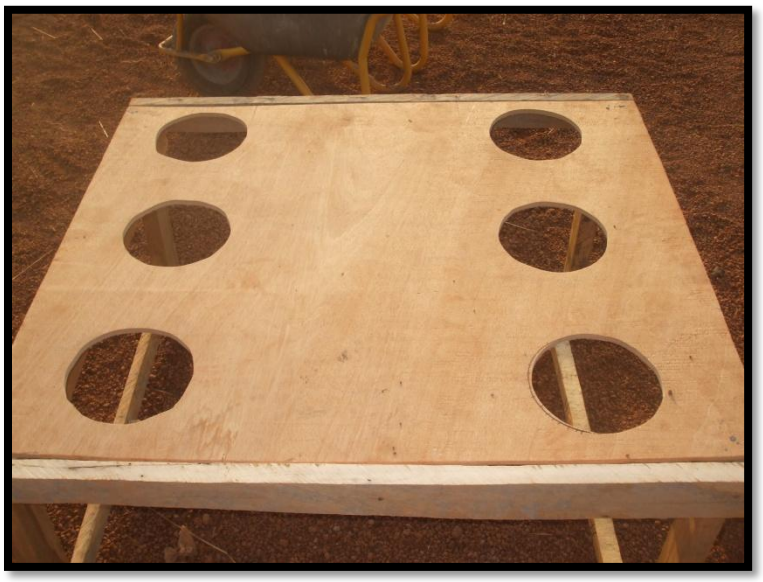

Figure 4-26: Table with Holes Cut for 6 Filters

Buckets for flower-pot shaped filters were smaller than those for paraboloid shaped filters due to the smaller diameter of the filter elements. The paraboloid-shaped filter elements fit well into the standard Pure Home Water buckets currently in use with filters produced in Accra, Ghana. The flower pot filter elements required smaller buckets.

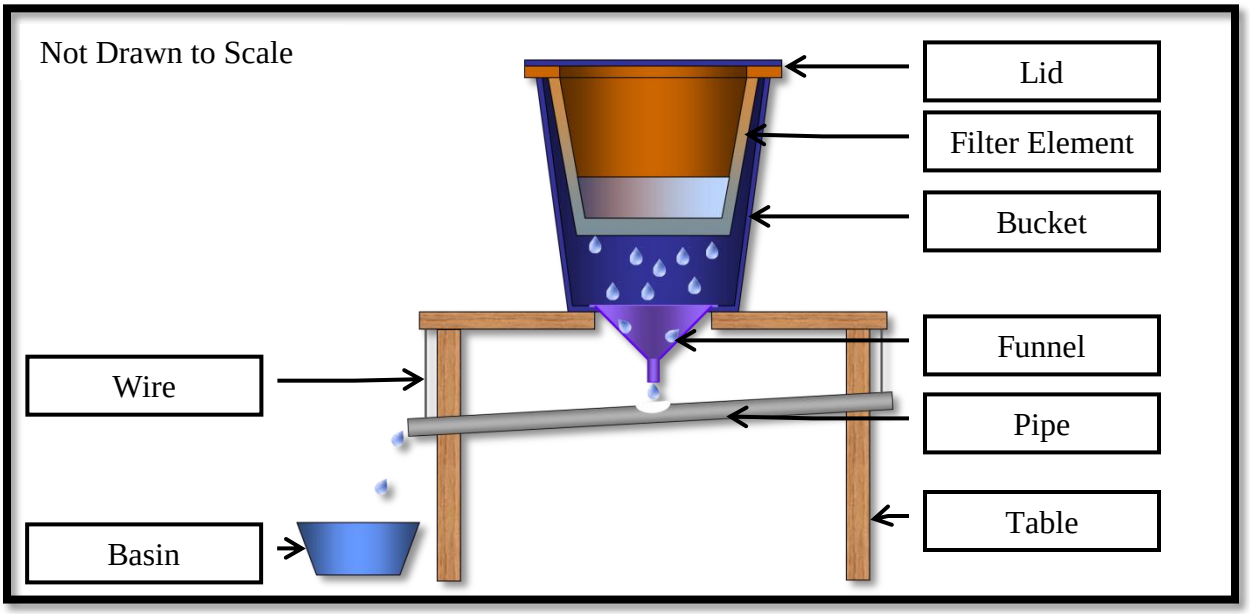

Figure 4-27: Diagram of Flower Pot Filter in Filter Testing Setup during Non-Testing Days

The setup for days when a set of filters is not being tested is seen above in Figure 4-27. A PVC pipe was hung below a row of filters at a slope. Wire is wrapped around the pipe, and loosely around nails in the sides of the table for easy removal. The pipe has openings roughly cut with a jigsaw that loosely align with the position of the funnel under the bucket.

On the non-testing days, the majority of the water is directed outside of the grass mat enclosure into a collection basin, while some is retained for cleaning purposes. The water is directed outside to avoid the burden of carrying full basins of water daily. The two tables holding 12 filters direct filtered water in pipes through holes made in the grass mat walls, as seen in Figure 4-28. The table holding 6 filters directs water in two separate pipes into two separate temporary storage basins, as seen in Figure 4-29. One basin is designated as a wash basin, and the other a rinse basin.

Figure 4-28: Pipes Carrying Water From 24 Filters Through Grass Mat Walls

Figure 4-29: Pipes Carrying Water From 6 Filters Into Temporary Storage Basins

Water for the study is collected from a nearby water source, a surface dam locally referred to as a "dugout", and stored in a tank. Local women from Taha are hired to carry approximately 20 L of water in metal cans on their head from the local "dugout", and deposit the water to fill a 700 L storage tank, purchased from the Ghanaian company Polytank. A hose conveys the water from the tank to the filters.

Figure 4-30: Women Collecting Water in Metal Cans from Taha "Dugout"

Figure 4-31: Left: Small, 700L Polytank at Factory Site
Right: Women Pouring "Dugout" Water from Metal Cans into 700L Polytank

4.4 Filter Testing Procedure

Every weekday, the laboratory technician followed the procedures described below. She arrived at the worksite in the morning to load the filters, measured flowrates and collected samples which were then stored in a laboratory refrigerator during the day. In the afternoon, the water samples were tested, and the previous day's test results were recorded.

4.4.1 Loading, Flowrate Testing Procedure and Sampling Procedure

List 4-4: Daily Filter Loading, Flowrate Testing Procedure and Sampling Procedure

1. The 700L tank containing "dugout" water is stirred with a long wooden pole.
2. The hose is connected to the tank; any water remaining in the hose from the previous day is flushed out.
3. The wash and rinse basins are filled with approximately 30L of filtered water from the previous day's filter experiments. Omo, a Ghanaian all purpose soap, is added to the wash basin.
4. Three chlorine "Aquatabs" are added to the rinse basin, one tab for each 10 L of filtered water. The "Aquatabs" dissolve for thirty minutes before the rinse water is used.
5. Clean flowrate measuring containers are placed on small benches underneath the six filters to be tested that day, for example 1A-3B.
6. The six filters being tested are filled with "dugout" water from the hose, and the time is noted.
7. The remaining filters are filled with "dugout" water from the hose, with the exception of the six filters to be tested the following day, for example 4A-6B.
8. After 30 minutes, the volume of water collected in the flowrate measuring containers is recorded.
9. 200mL Stand-up Whirl-Pak® bags are labeled with the date and filter number, or "hose" for influent water.
10. Approximately 250 mL of water are collected in Whirl-Pak® bags from each of the filters being tested, as well as the influent water from the end of the hose. The samples are held in a cooler with ice packs until they reach the laboratory refrigerator.
11. The contents of the flowrate measuring containers are discarded, and they are cleaned by briefly washing them in the wash basin, then the rinse basin.
12. It would be desirable for lids with holes in them to be placed on top of the flowrate measuring containers to preserve their cleanliness for the following day by preventing dust entry, but also allowing any residual chlorine vapors from the rinse water to escape. However, in this study, the flowrate measuring containers were placed upside down on top of lids overnight to encourage residue to drip to the top of the container.
13. The filter elements to be tested the following day are lifted with their lids and buckets from their holes and placed upside down on their lids.
14. The buckets, with attached funnel, are briefly washed and rinsed in the basins.
15. The buckets are replaced in their holes in the tables, and the filters with their lids are replaced inside of the buckets.
16. These filter elements are filled with "dugout" water from the hose. The intent of this sequence is that the water passing through the filter element will flush out any residual soap or chlorine on the bucket or funnel so that it will not affect the following day's sample.

17. The water in wash and rinse basins are discarded, allowing for more filtered water to fill them.
18. Periodically, the interior of the filter element is cleaned. It occurred during the week 4, 6, 8, and 10. This is done as routine maintenance to remove large particles hindering the flow of the water through the filters. To do so, the flower pot filter is set on the inside face of the lid, and a small amount of filtered water is poured inside. A small brush with short, sturdy plastic bristles is used to scrub only the interior surface of the filter. The dirty water from inside the filter element is discarded, and the filter element and lid are replaced in the bucket.

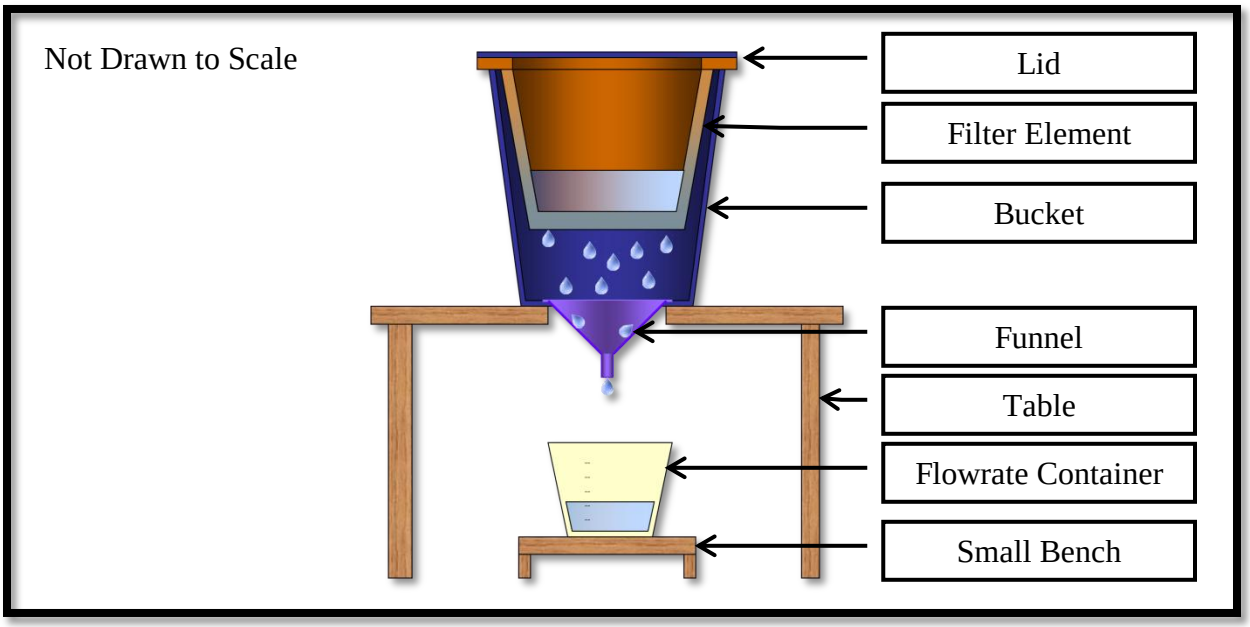

Figure 4-32: Diagram of Flower Pot Filter in Filter Testing Setup during Testing Days

Figure 4-33: Flower Pot Filters 1A-3B in Filter Testing Setup during Testing Days

To measure the collected water, 6 clear containers were turned into measuring containers. To do so, a standard glass 100 mL graduated cylinder was filled to the 100 mL mark, and poured into the bucket repeatedly until 8 L, making a mark on the bucket with a ruler each time. The marks were extrapolated onto strips of paper, which were coated with clear plastic tape, and taped onto the collection containers in line with a 1 L measurement mark, as can be seen below in Figure 4-34.

Figures 4-34: Left: Flowrate Testing Bucket, Right: Enlarged Image of Measurement Strip

4.4.2 Comparison of Sampling Methods

In order to determine if any residual inside the flowrate containter from water treated with "Aquatabs" affected the apparent total coliform and *E. coli* removal rates, a comparison test was undertaken for five days. During these five days, filtered water samples were collected both directly into Whirl-Pak® bags, and into flowrate containers. The results of these two samples were tested for statistical difference.

4.4.3 Membrane Filtration Testing Procedure

The membrane filtration testing procedure followed a modified form of USEPA Membrane Filtration Method 10029 for Simultaneous total coliform and *E. coli* screening[7]. The apparatus used was a Millipore Membrane Filtration Field Unit. The petri dishes were prepared with m-ColiBlue24 Broth® (Hach). Stainless steel, reusable petri dishes were used instead of disposable petri dishes; the petri dishes were submerged in boiling water, allowed to dry on and under paper towels, and stored in a clean container. Voltic brand bottled water was used instead of sterile buffer. A "blank" using Voltic brand bottled water was prepared each day Membrane Filtration testing was performed.

[7]"Coliforms—Total and E. coli DOC316.53.001213." Hach Company. Updated February 2008, Edition 5. http://www.hach.com/fmmimghach?/CODE%3ADOC316.53.0121315750|1

List 4-5: Membrane Filtration Procedure[8]:

1. Sterilization of the portable Millipore MF stainless steel filter holder
    a. Sterilize the filter holder between each water sampling. The procedure is to:
        i. Remove the stainless steel receiver flask from the funnel base assembly
        ii. Soak the ceramic ring around the holder base with one half capful of methanol using a dispenser bottle, and subsequently ignite the methanol with a match
        iii. Close the filtering cup over the funnel and the burning wick
        iv. Leave the filter unit scaled in place for 15 minutes. Remove cup and rinse funnel thoroughly with approximately 100mL of sterile water
2. Petri dish label and selective growth medium
    a. The petri dish is labeled and absorbent pad is placed aseptically in the dish with the use of sterile tweezers
    b. The m-ColiBlue24® culture medium pre-packaged in 2mL plastic ampoule is poured into the petri dish and the excess medium remaining in the petri dish is decanted.
    c. When medium is poured, special attention is paid to ensure that every surface of the absorbent pad is uniformly soaked and the excess is poured away, leaving behind about one drop at the bottom
3. Sample volume selection and dilution
    a. According to the m-ColiBlue24® manufacturer, the technique for determining maximum sample size is:
        i. "Select a maximum sample size to give 20 to 200 colony-forming units (CFU) per filter. The ideal sample volume of nonpotable water or wastewater for coliform testing yields 20–80 coliform colonies per filter. Generally, for finished, potable water, the volume to be filtered will be 100 mL." ("Coliforms" 2008)
    b. When possible, 100 mL of the water sample was tested.
        i. However, the high turbidity encountered in many of the samples made it difficult and time consuming to pass 100 mL of the sample through the filtration unit.
            1. Therefore, typical sample volumes of the influent (hose) water were 10 mL, 1 mL and 0.1mL.
                a. The 10 mL sample was measured with a standard sterilized glass graduated cylinder.
                b. The 1 mL samples was measured using a disposable, sterile plastic 1 mL pipette.
                c. The 0.1 mL sample was measured by taking a 1 mL sample from a dilution of 1mL of sample in 9 mL Voltic brand bottled water.

[8] Mattelet, C. (2006). Household Ceramic Water Filter Evaluation Using Three Simple Low-cost Methods: Membrane Filtration, 3M Petrifilm And Hydrogen Sulfide Bacteria In Northern Region, Ghana. Department of Civil and Environmental Engineering. Cambridge MA, USA, Massachusetts Institute of Technology. Master of Engineering.

2. Typical sample volumes of the effluent (filtered) water were 100 mL, 50 mL and 10 mL, depending on the turbidity, and were measured with a standard sterilized glass graduated cylinder.

c. In addition, the plate counts of the influent (hose) were often too numerous to count (TNTC). Based on expectations from the experience of previous filtering events, sample sizes were selected in an attempt to achieve coliform counts within the desired range.

4. Sample pouring and filtration
   a. 30mL of boiled, cooled water is then flushed in the assembled filter
   b. 0.45μm filter paper is then placed on the filter support base using sterile tweezers
   c. If the sample volume is 100 mL or 50 mL, then it is poured directly into the filter funnel.
   d. If the sample volume is 10 mL or 1 mL, then approximately 30 mL of boiled, cooled water is poured into the funnel right before funneling to ensure even distribution of the sample across the filter paper.
   e. Approximately 30 mL of boiled, cooled water are added to rinse the side walls of the funnel.
5. Funnel rinsing
   a. The interior walls of the funnel are rinsed with about 30mL of boiled, cooled water.
6. Filter paper removing
   a. Filter paper is removed carefully with sterilized tweezers and placed into the labeled petri dish in a rolling motion to prevent trapping of air bubbles. The air bubbles may prevent the absorbing of media on the top of the filter paper, therefore resulting in the uneven growth of colonies
7. Incubation
   a. The petri dishes are placed in the incubator at 35°C for 24 hours. The petri dishes are inverted to avoid condensation drops forming on the filter paper.
8. Colony forming unit (CFU) estimation
   a. The number of CFUs are counted.
      i. Blue CFUs indicate *E. coli*.
      ii. Red and blue CFUs sum to equal total coliforms.
   b. The indicator organisms level in water sample are expressed as the number per 100mL
   c. The concentration of indicator organisms in the water tested is found by (4-1):

$$CFU\ Concentration = \frac{Number\ of\ CFUs\ Counted \times 100}{Volume\ of\ Sample\ (mL)} = \frac{CFUs}{100\ mL} \quad (4\text{-}1)$$

4.5.4 Turbidity Testing Procedure

A Hach 2100P turbidimeter was used to analyze samples of the influent and filtered water.

4.5 Determination of Filter Lip Total Porosity

4.5.1 Removing Filter Lip Pieces

It is useful to know how similar or dissimilar the total porosity of two filters made from the same mix of clay, grog and combustible material are. Similar total porosities demonstrate that the mix of one batch used for two filters was more homogenous throughout; all portions of the mix contained the same amounts of clay, grog and combustible materials. Additionally, the measured total porosity can be compared to the total porosity calculated from the material densities and filter mix recipes.

Two small triangular pieces were cut from with a hack saw from the lip of each filter and transported back to MIT. The pieces were approximately 2 cm wide, and were on opposite sides of the filter to provide for variation. In this way, samples of the filter could be taken back to MIT without impacting the filters' ability to function.

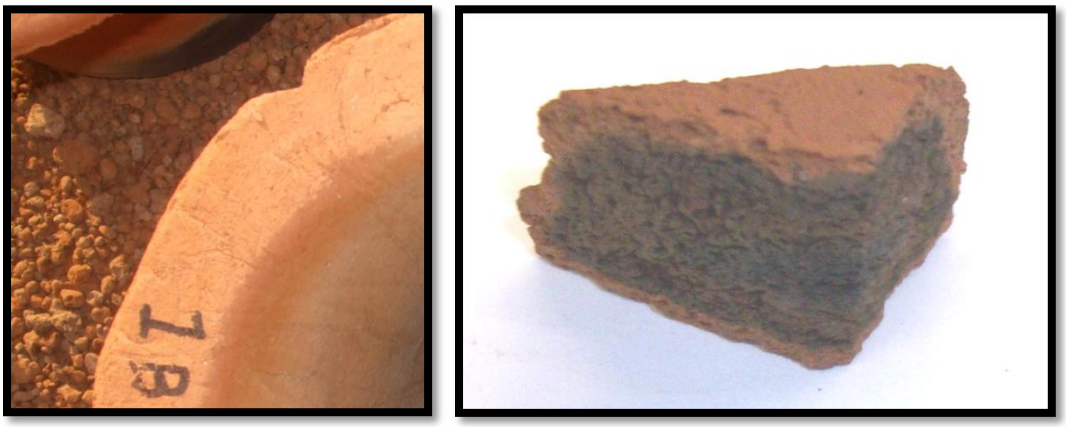

Figure 4-35: Left: Triangular Notch Cut from Filter 1B, Right: Filter Lip Piece from Filter 1B

4.5.2 Lab Methods for Determining Filter Lip Total Porosity

The total porosity is a ratio between the volume of the voids and the total volume. Two simple methods were used to determine the total porosity of the filter lip pieces; ideally, the total porosity would have been found using a mercury porosimeter, but the instrument at MIT was out of service. The first method measured volumetric displacement of the filter pieces directly, and the second method measured volumetric displacement indirectly by measuring the mass of the water displaced.

4.5.2.1 Lab Method to Directly Determine Volume for Filter Lip Total Porosity

The volume of the saturated solid, $V_{SS,}$ is determined by volumetric displacement of water at a known temperature and density. The pore water does not increase the volumetric displacement because there is no net flow of water with the saturated solid; the saturated solid is assumed to represent the total volume.

$$Total\ Porosity = \frac{V_W}{V_{SS}} = \frac{\frac{M_W}{\rho_W}}{V_{SS}} = \frac{\frac{M_{SS} - M_{DS}}{\rho_W}}{V_{SS}} \quad (4\text{-}2)$$

where:

V_w is volume of water in saturated solid
V_{ss} is volume of saturated solid
M_w is mass of pore water
P_w is density of pore water
M_{ss} is mass of saturated solid
M_{ds} is mass of dry solid

List 4-6: Steps to Determine Values for Equation 4-1 for Filter Lip Total Porosity

1. Find the mass of filter lip piece when dry, M_{DS}
2. Saturate the filter lip piece in water for at least 24 hours to ensure full saturation
3. Fill a 500 mL volumetric flask to its mark with water
4. Place on scale and tare-out the scale
5. Add saturated sample to the flask, mass reported is M_{SS}
6. Use a graduated 5 mL pipette to draw out the water that was displaced down to the mark, volume of water in pipette is V_{SS}
7. Measure the temperature of the water using a standard electronic thermometer

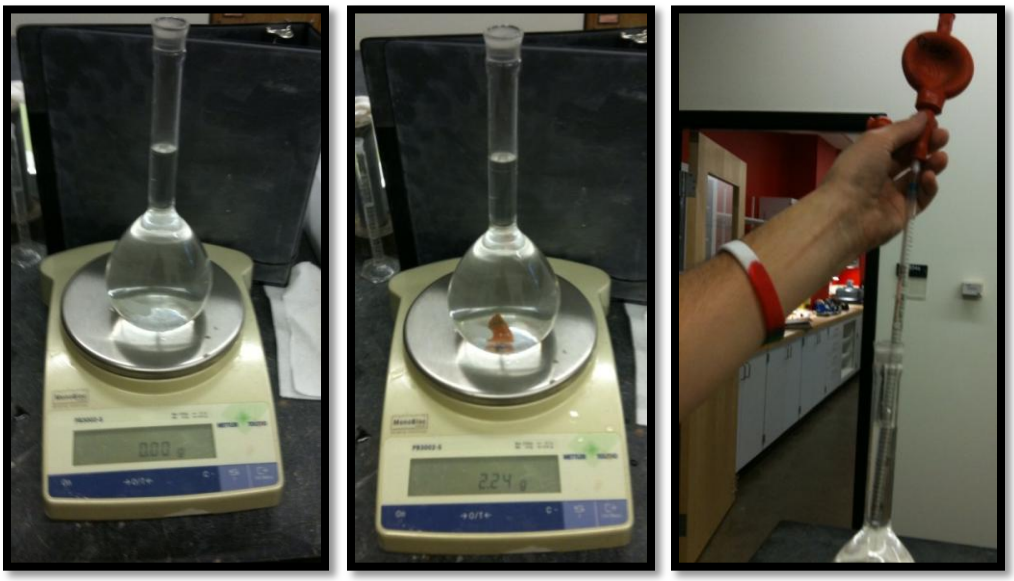

Figure 4-36: Left: 500 mL Volumetric Flask on Scale, Filled to Mark with Water
Middle: 500 mL Volumetric Flask on Scale, Filled to Mark with Water and Piece
Right: Water Being Drawn Down to Mark on Volumetric Flask with 5mL Pipette

4.5.2.2 Lab Method to Indirectly Determine Volume for Filter Lip Total Porosity

van Halem (2006) proposed the second method, where the volume of the saturated solid is determined by finding the mass when the filter piece is submerged. This method is consistent with the ASTM Standard C 373-88. A description of the experimental set-up can be found for a similar test in Section 8.5. The mass of the oven-dry and saturated pieces are found directly using a digital scale.

$$V_{filter} = \frac{m_{saturated} - m_{underwater}}{\rho_{water}}$$

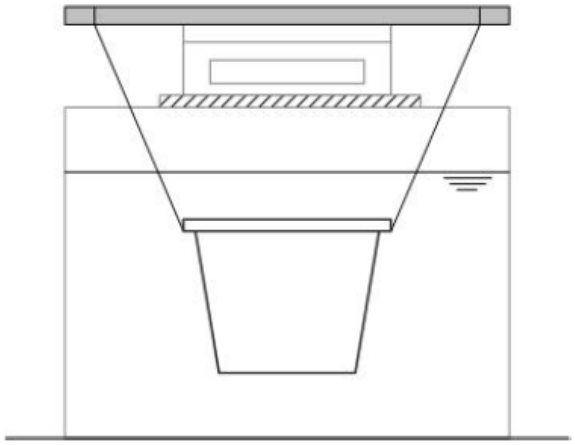

Figure 4-37: van Halem (2006) Method to Determine Volume of Filter

$$Total\ Porosity = \frac{V_W}{V_{SS}} = \frac{M_{SS} - M_{DS}}{M_{SS} - M_{US}} \quad (4\text{-}3)$$

where:

V_W	is volume of water in saturated solid
V_{SS}	is volume of saturated solid
M_{SS}	is mass of saturated solid
M_{DS}	is mass of dry solid
M_{US}	is the mass of saturated solid when underwater

4.6 Statistical Analysis of Filter Testing Results

The following methods for statistical analysis were adapted from Mendenhall and Sincich (2006). Throughout the section, the symbolic representations below are utilized.

H_0	Null hypothesis
H_a	Alternative hypothesis
μ	Population mean
$\bar{y}$	Sample mean
s	Sample standard deviation
n	Sample size
T	Test statistic
t_α	T-value
v	Degrees of freedom
σ	Population variance
$z_{\alpha/2}$	Normal curve area,1.96 when α=0.05
d	Matched pair sample difference
$\bar{d}$	Mean of the n sample differences
σ_d	Population variance of the differences
s_d	Sample standard deviation of differences

4.6.1 One-Tailed Test of Hypothesis about a Population Mean μ: Independent Samples

If the result falls within the rejection region, the null hypothesis is rejected and the alternative hypothesis is accepted; the population means are unequal. If the result does not fall within the rejection region, then there is not enough evidence to reject the null hypothesis; the population means are equal.

4.6.1.1 Small-Sample Test of Hypothesis about a Population Mean μ

This test was used to determine the tiered ranking of filters based on performance categories, including total coliform log removal, turbidity removal and flowrate. It was also used to determine whether the percent combustible by mass had a statistical impact on the performance of filters in each category.

Null Hypothesis:

$H_0: \mu = \mu_0$

Alternative Hypothesis:

$H_a: \mu > \mu_0$

Test Statistic:

$$T = \frac{\bar{y} - \mu_0}{s/\sqrt{n}}$$

Rejection Region:

$T > t_\alpha$ where the distribution is based on (n-1) degrees of freedom.

Assumption: The relative frequency distribution of the population from which the sample was selected is approximately normal.

In Microsoft Excel 2007, the Analysis ToolPak was used to complete these tests. The "t-test: Two-Sample Assuming Unequal Variances" was performed. The Analysis ToolPak makes the modifications below to the degrees of freedom, v, used in the T distribution and the estimated standard error. These are the same modifications suggested by Mendenhall and Sincich (2006) similar circumstances for estimation of the differences between means, as in Section 4.7.2.2.

$$v = \frac{(s_1^2/n_1 + s_2^2/n_2)^2}{\frac{(s_1^2/n_1)^2}{n_1 - 1} + \frac{(s_2^2/n_2)^2}{n_2 - 1}}$$

$$\hat{\sigma}_{(\overline{y_1} - \overline{y_2})} = \sqrt{\frac{s_1^2}{n_1} + \frac{s_2^2}{n_2}}$$

4.6.2 Estimation of the Difference between Two Population Means: Independent Samples

Practical Interpretation of a Confidence Interval for (θ_1- θ_2)

Let (LCL, UCL) represent a (1-α)100% confidence interval for (θ_1- θ_2)
If LCL>0 and UCL>0, conclude $\theta_1 > \theta_2$
If LCL<0 and UCL<0, conclude $\theta_1 < \theta_2$
If LCL<0 and UCL>0 (i.e. the interval includes 0), conclude no evidence of a difference between θ_1 and θ_2.

4.6.2.1 Large Sample (1-α)100% Confidence

This test was used to determine the confidence interval for the difference between combustible types and the addition or absence of grog in filters for each performance category.

Interval for (μ_1- μ_2):

$$(\overline{y_1} - \overline{y_2}) \pm z_{\alpha/2}\sigma_{(\overline{y_1} - \overline{y_2})} = (\overline{y_1} - \overline{y_2}) \pm z_{\alpha/2}\sqrt{\frac{\sigma_1^2}{n_1} + \frac{\sigma_2^2}{n_2}} \approx (\overline{y_1} - \overline{y_2}) \pm z_{\alpha/2}\sqrt{\frac{s_1^2}{n_1} + \frac{s_2^2}{n_2}}$$

Assumptions:

1. The two random samples are selected in an independent manner from the target populations. That is, the choice of elements in one sample does not affect, and is not affected by, the choice of elements in the other sample.
2. The sample sizes n_1 and n_2 are sufficiently large for the central limit theorem to apply. (We recommend $n_1 \geq 30$ and $n_2 \geq 30$).

4.6.2.2 Small Sample (1-α)100% Confidence

This test was used to determine the confidence interval for the difference between filters in the set 1 though 12, and those with additional variables of sifted combustible and paraboloid shape.

Approximate Small-Sample Inferences for (μ_1- μ_2) for $\sigma_1^2 \neq \sigma_2^2$ and $n_1 \neq n_2$
Interval for (μ_1- μ_2):

$$(\overline{y_1} - \overline{y_2}) \pm t_{\alpha/2}\hat{\sigma}_{(\overline{y_1} - \overline{y_2})}$$

Modifications to the degrees of freedom, v, used in the T distribution and the estimated standard error.

$$v = \frac{(s_1^2/n_1 + s_2^2/n_2)^2}{\frac{(s_1^2/n_1)^2}{n_1 - 1} + \frac{(s_2^2/n_2)^2}{n_2 - 1}}$$

$$\hat{\sigma}_{(\overline{y_1} - \overline{y_2})} = \sqrt{\frac{s_1^2}{n_1} + \frac{s_2^2}{n_2}}$$

Assumptions:

1. Both of the populations from which the samples are selected have relative frequency distributions that are approximately normal.
2. The random samples are selected in an independent manner form the two populations.

4.6.3 Testing the Difference between Two Population Means (μ_1- μ_2): Matched Pairs

4.6.3.1 Small Sample (1-α)100% Confidence

This test was used to determine the difference between the population means of each filter within a pair for each performance category of total coliform log removal, *E. coli*, turbidity removal and flowrate.

Null Hypothesis:

$H_0: (\mu_1 - \mu_2) = D_0$

Alternative Hypothesis:

$H_a: (\mu_1 - \mu_2) \neq D_0$

Test Statistic:

$$T = \frac{\bar{d} - D_0}{s_d/\sqrt{n}}$$

Rejection Region:

$|T| > t_\alpha$ where the distribution is based on (n-1) degrees of freedom.

Assumptions:

1. The relative frequency distribution of the population of differences is approximately normal.
2. The paired differences are randomly selected form the population of differences.

5.0 Optimal Removal and Flowrate Study Results

All statistical analyses used methods described in Section 4.7.

5.1 Characterization of Filter Inputs

5.1.1 Filter Input Material Densities

Table 5-1 displays the filter input material densities found using methods described in Section 4.2.3.1.

Table 5-1: Filter Input Material Densities, Field and Lab

Material	Processing Procedures	Field Density, Uncompacted (g/cm^3)	Lab Density, Uncompacted (g/cm^3)	Lab Density, Compacted (g/cm^3)
Rice Husk	Hammermill, waste	0.50	0.40	0.62
Rice Husk	Hammermill, fine	0.35	0.28	0.63
Rice Husk	Hammermill, fine and sifted	0.35	0.27	0.65
Sawdust	Hammermill, waste	0.30	0.27	0.39
Sawdust	Hammermill, fine	0.30	0.23	0.35
Sawdust	Hammermill, fine and sifted	0.25	0.19	0.35
Clay	Sieved, 18 x 14 mesh	1.50	1.07	2.75*
Grog	Sieved, 1mm x 2mm mesh	(N/A)	0.83	1.11

*Value calculated from specific gravity test (Section 5.1.4.2)

5.1.2 Scanned Images of Filter Input Materials

Figures 5-1 through 5-8 show the images found using methods described in Section 4.3.2.2.

Figure 5-1: Scanned Image of Rice Husk through Hammermill Waste Chute

Figure 5-2: Scanned Image of Rice Husk through Hammermill Fine Chute

Figure 5-3: Scanned Image of Rice Husk through Hammermill Fine Chute and 1mm x 1mm Sieve

Figure 5-4: Scanned Image of Sawdust through Hammermill Waste Chute

Figure 5-5: Scanned Image of Sawdust through Hammermill Fine Chute

Figure 5-6: Scanned Image of Sawdust through Hammermill Fine Chute and 1mm x 1mm Sieve

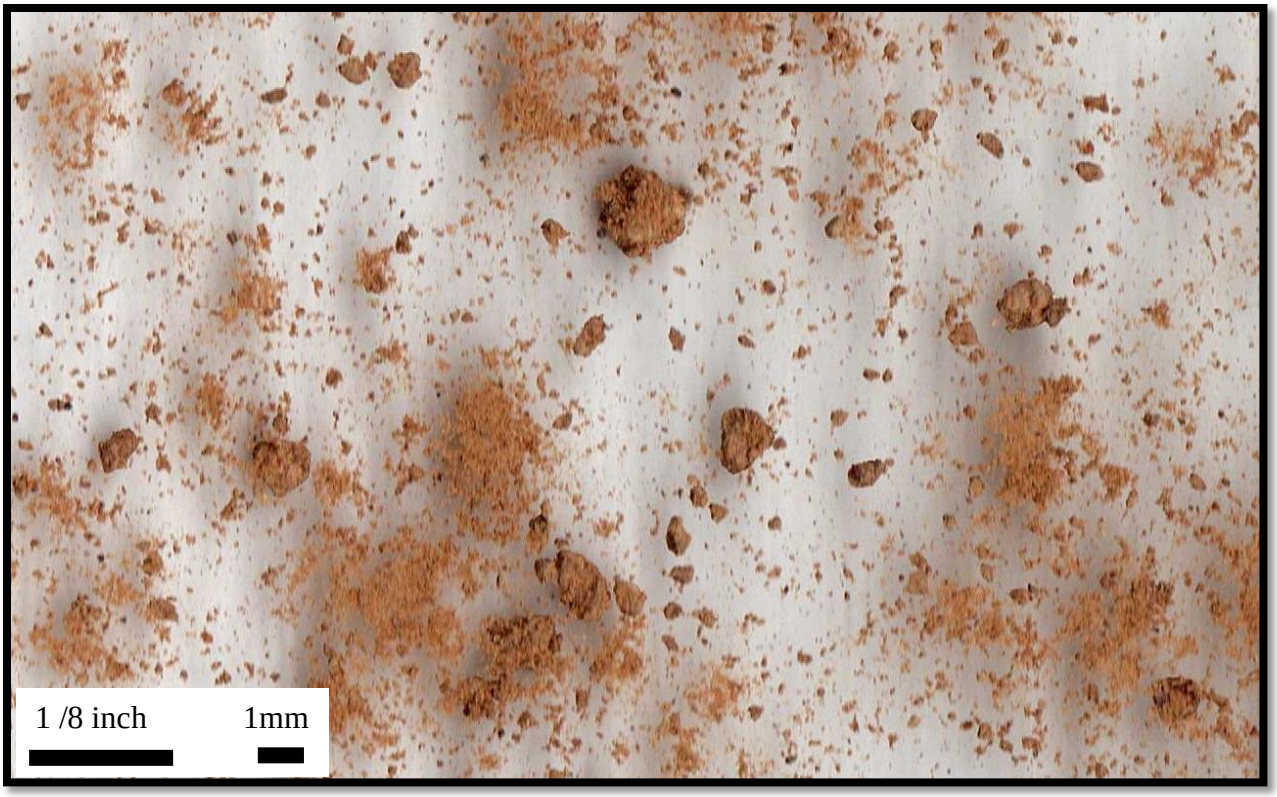

Figure 5-7: Scanned Image of Clay, Sieved through 18 x 14 Mesh with 1.12mm Openings

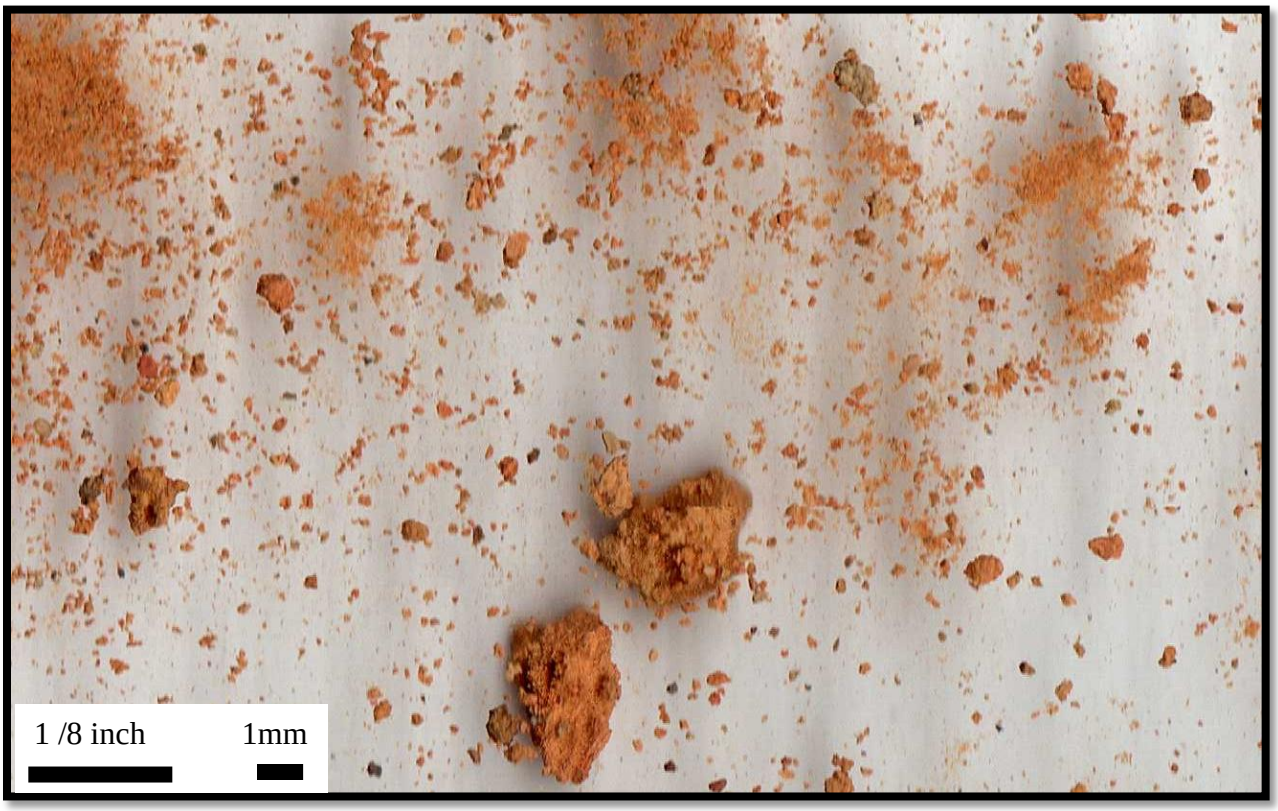

Figure 5-8: Scanned Image of Grog, Sieved through 1mm x 2mm Mesh Sieve

5.1.3 Filter Input Material Particle Size Distribution

The particle size distributions, described in Section 4.2.3.3, of combustibles processed by all three processing procedures as well as clay and grog are presented in Figures 5-9 through 5-11, and Table 5-2 presents the median particle sizes. "1 Water: 1 Fine" is included because filters 1 through 12 had "waste" and "fine" combustible material added on an equal, or 1:1, mass basis. The fine rice husk materials were not able to be tested because they plugged the holes in the #40 sieve. Table 5-3 presents useful parameters for clay characterization, also described in Section 4.2.3.3.

Table 5-2: Median Particle Sizes

Material	Processing Procedures	Median Particle Size, d50, mm
Rice Husk	Hammermill, waste	0.482
Rice Husk	Hammermill, fine	N/A
Rice Husk	Hammermill, fine and sifted	N/A
Rice Husk	Hammermill, 1 waste: 1 fine	N/A
Sawdust	Hammermill, waste	0.389
Sawdust	Hammermill, fine	0.363
Sawdust	Hammermill, fine and sifted	0.323
Sawdust	Hammermill, 1 waste: 1 fine	0.378
Clay	Sieved, 18 x 14 mesh	0.471
Grog	Sieved, 1mm x 2mm mesh	0.205

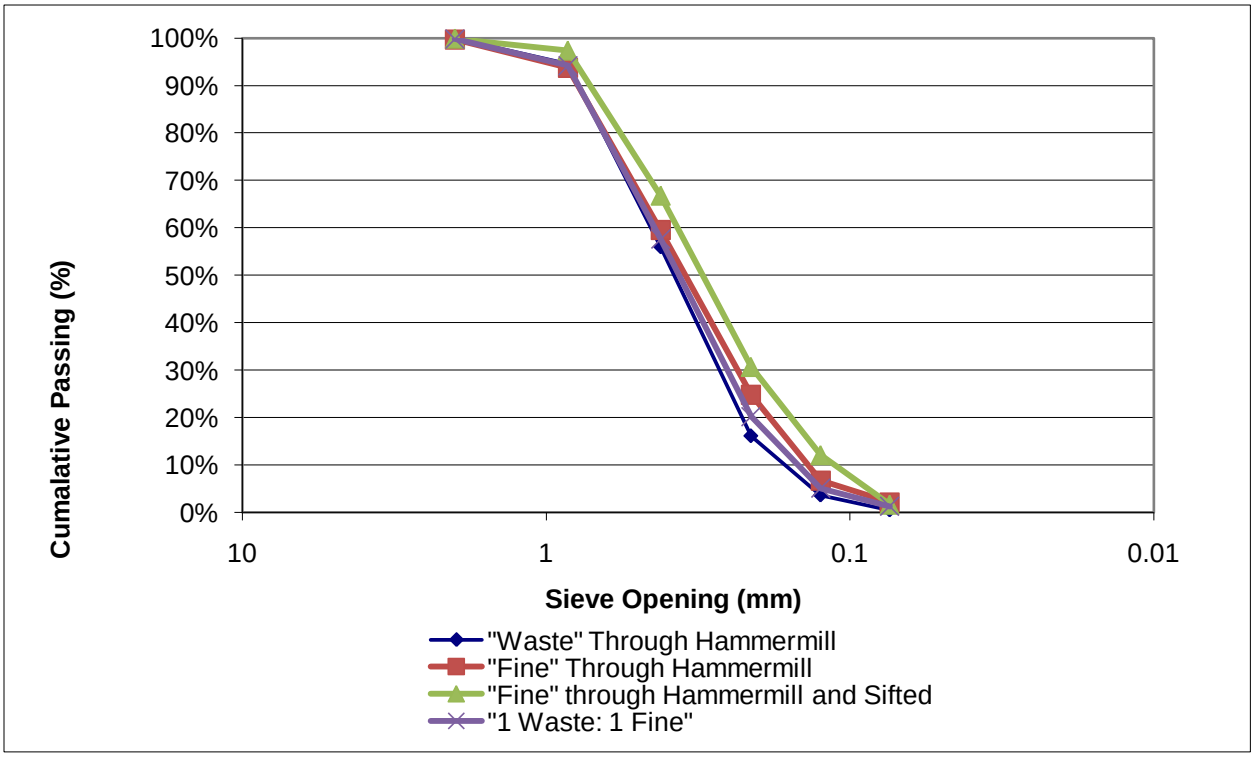

Figure 5-9: Particle Size Distribution of Sawdust, All Processing Procedures

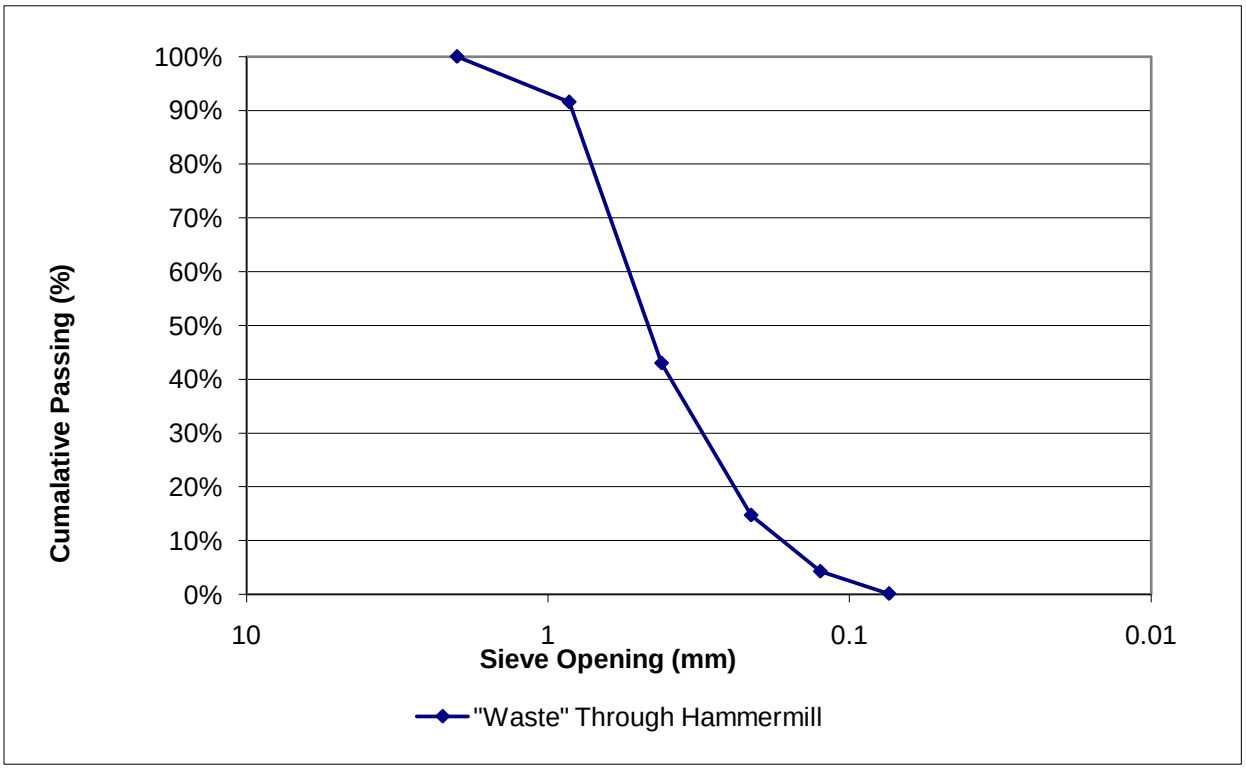

Figure 5-10: Particle Size Distribution of Rice Husk, "Waste" Through Hammermill

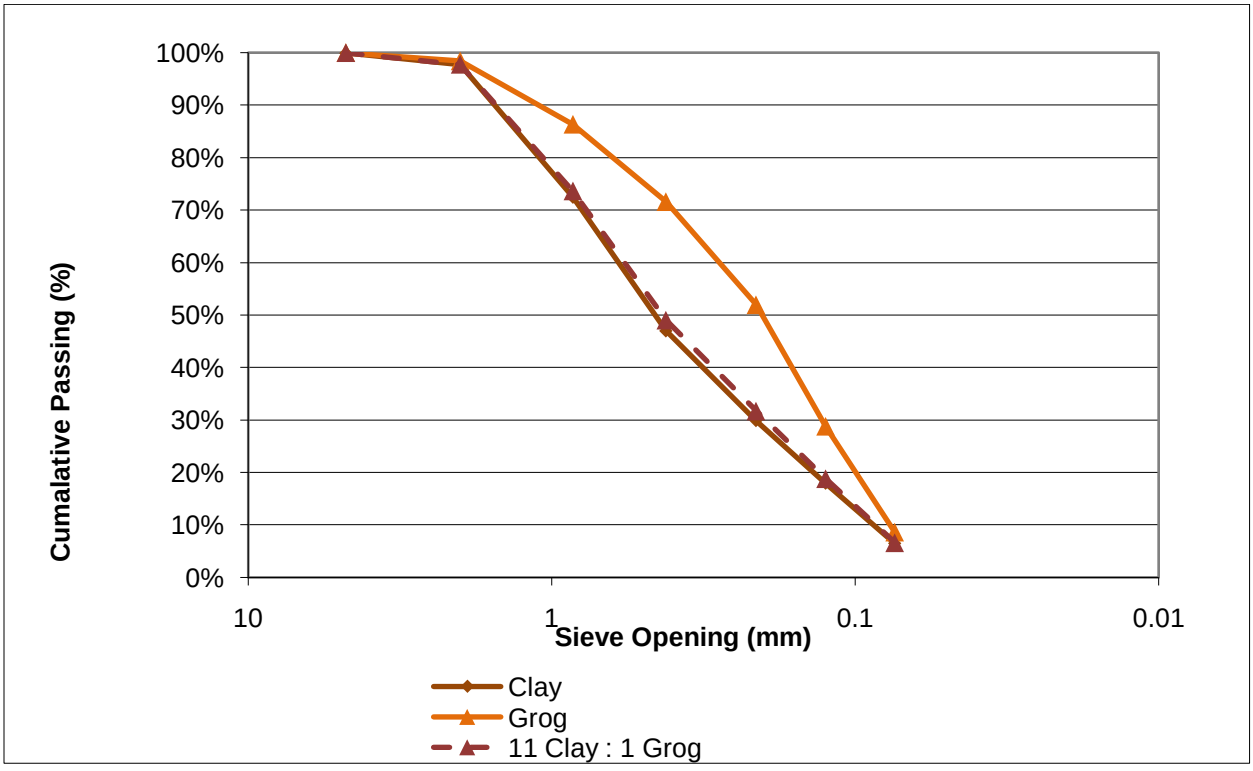

Figure 5-11: Particle Size Distributions of Clay and Grog

Table 5-3: Diameters and Coefficients of Clay Useful for Soil Classification

Clay Diameters and Coefficients	Value
D10	0.090 mm
D30	0.214 mm
D60	0.640 mm
Cu, Coefficient of Uniformity	7.123
Cc, Coefficent of Curvature	0.795

5.1.4 Clay Characterization

5.1.4.1 Atterberg Limit Tests: Liquid and Plastic Limit and Plasticity Index

The methods of the Atterberg Limit Tests are described in Section 4.2.3.4.1. Figure 5-12 presents the results of the liquid limit test; the liquid limit is the water content at 25 blow counts, and is 35.43%.

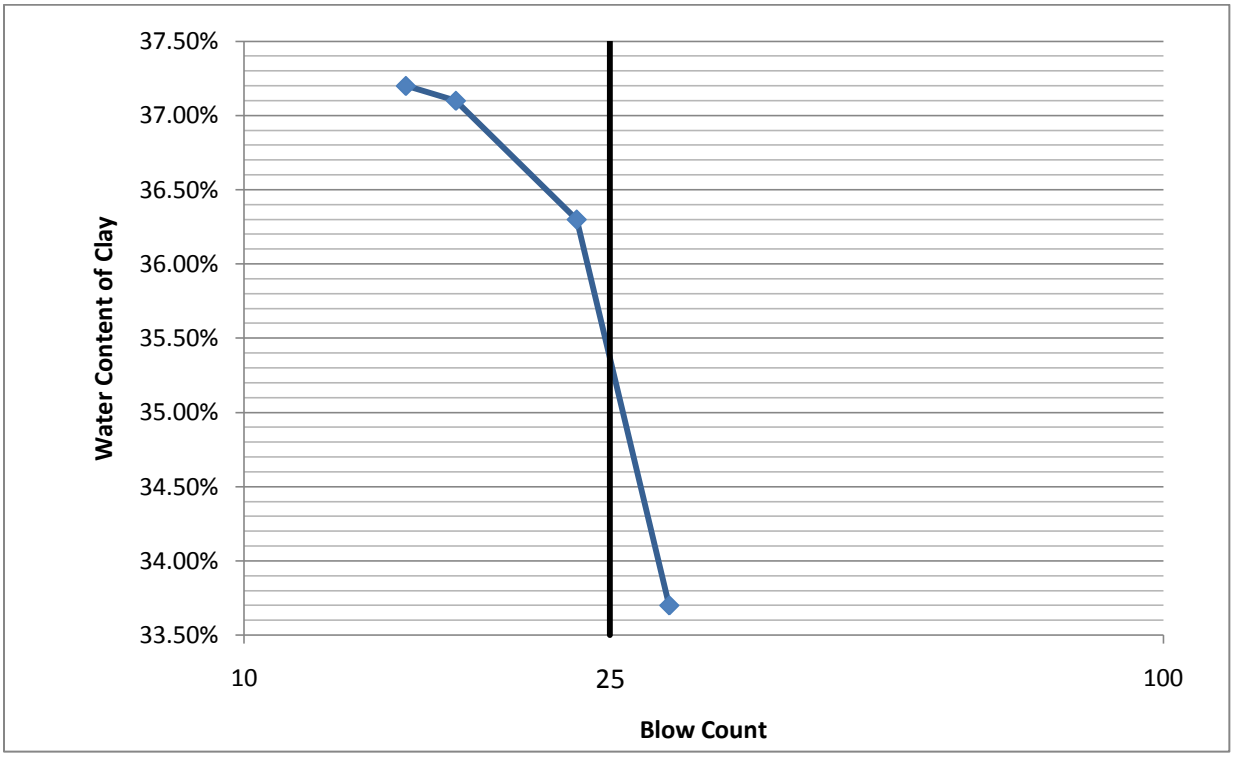

Figure 5-12: Liquid Limit Blow Count Results from Test with Casagrande Cup

The plastic limit is the water content when a 1/8" diameter strand of clay begins to crumble. The average of three sample, in Table 5-4, is 22.13%. The plasticity index, therefore, is 13.30%.

Table 5-4: Water Contents of Plastic Limit Test Samples

Sample 1	Sample 2	Sample 3	Average
21.10%	22.40%	22.90%	22.13%

5.1.4.2 Specific Gravity

The methods for the Specific Gravity test are described in Section 4.2.3.4.2. The results of three samples and the average are presented in Table 5-5.

Table 5-5: Specific Gravity of Test Samples

Sample 1	Sample 2	Sample 3	Average
2.73737	2.75159	2.74500	2.74465

5.1.4.3 Classification

The "clay" is classified as poorly graded sand with clay, SP-SC. The classification methods are described in Section 4.2.3.4.3.

5.2 Filter Lip Total Porosity

The total porosity of each filter pair calculated from filter lip measurements using two different methods is compared with three different calculations of total porosity based on different densities for the input materials in Figure 5-13. "Measured, Underwater Method, 1 Standard Deviation Error Bars" represents the total porosity calculated using methods described in Section 4.5.2.2. "Measured, Pipette Method, 1 Standard Deviation Error Bars" represents the total porosity calculated using methods described in Section 4.5.2.1. "Uncompacted Materials, Lab" represents calculations based upon densities of materials determined in the lab at MIT without actively compacting them. "Uncompacted Materials, Field" represents similar calculations with densities determined on site in Ghana. "Compacted Materials and Specific Gravity of Clay" represents calculations based on the density of clay determined from specific gravity measurements, and densities of the other input materials based on manual compaction.

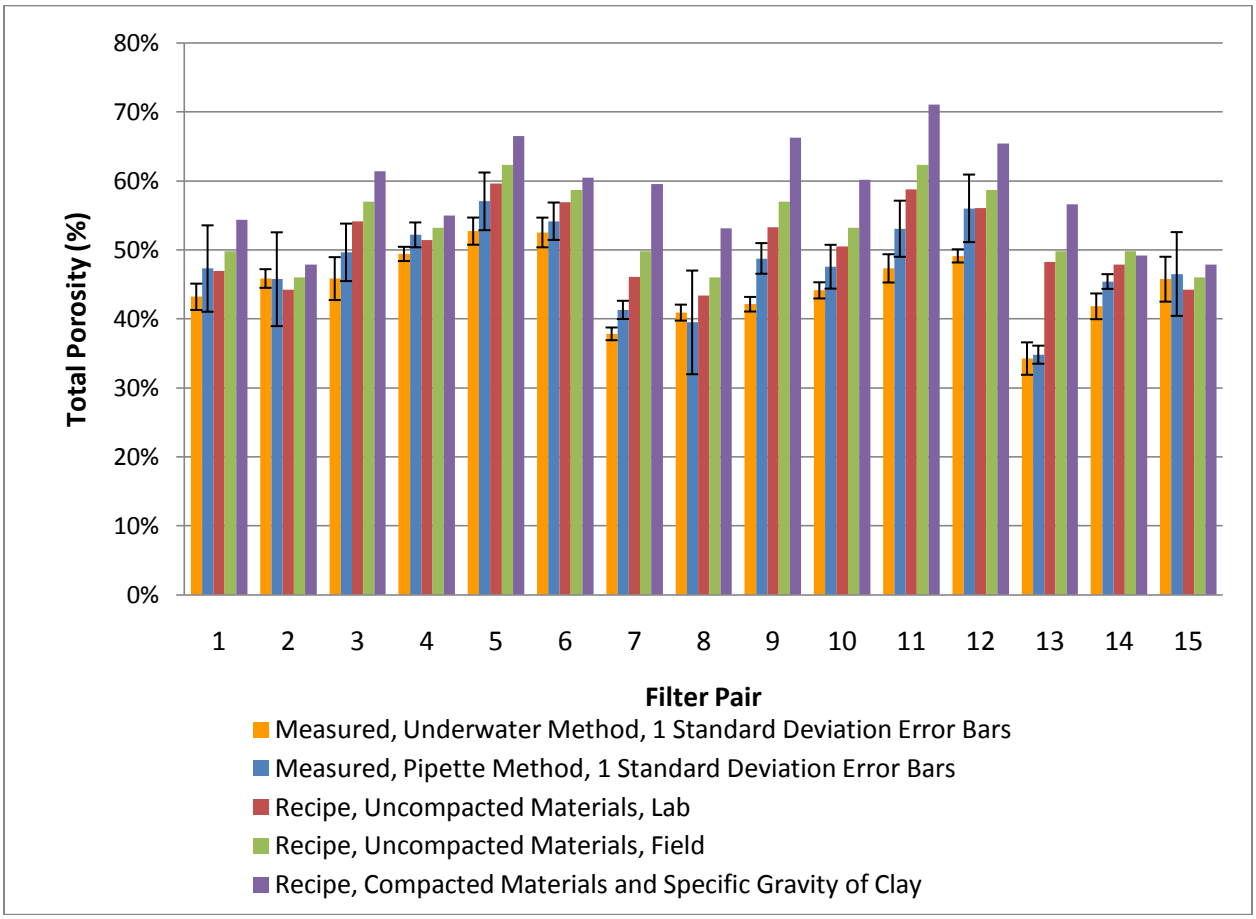

Figure 5-13: Comparison of Measured Total Porosity and Recipe Total Porosity

5.3 Total Coliform Removal

Total coliform removal was found according to methods described in Section 4.4.3. In order to calculate the Log Removal Values (LRVs) of total coliform performed by the filters, it was necessary to make a conservative adjustment to the data. Results from membrane filtration testing Too Numerous To Count (26 events, 8%) were adjusted by assuming the count was the maximum in the acceptable counting range, 200. Results from membrane filtration testing that were zero (184 events, 58%) were adjusted to be equal to one.

Table 5-6 presents data about the total coliform in influent water, and Table 5-7 ranks the filters in statistical tiers according to their performance. Figures 5-14 through 5-19 are box and whisker charts of the total coliform log removal of individual filters, as well as the averages of a pair of filters.

Table 5-6: Total coliform in Influent Water across 12-Week Study

Median (CFU/100mL)	3500
Mean (CFU/100mL)	6860.2
Standard Deviation (CFU/100mL)	7223.8

Table 5-7: Total Coliform Log Removal Tiered Ranking of Filter Pairs based on Series of Two-Sample T-Tests assuming Unequal Variances with 95% Confidence, 1=Best to 5=Worst

Tier	Filter Pairs
1	15
2	2
3	1,3,5
4	4, 10, 12
5	6, 7, 8, 9, 11, 14

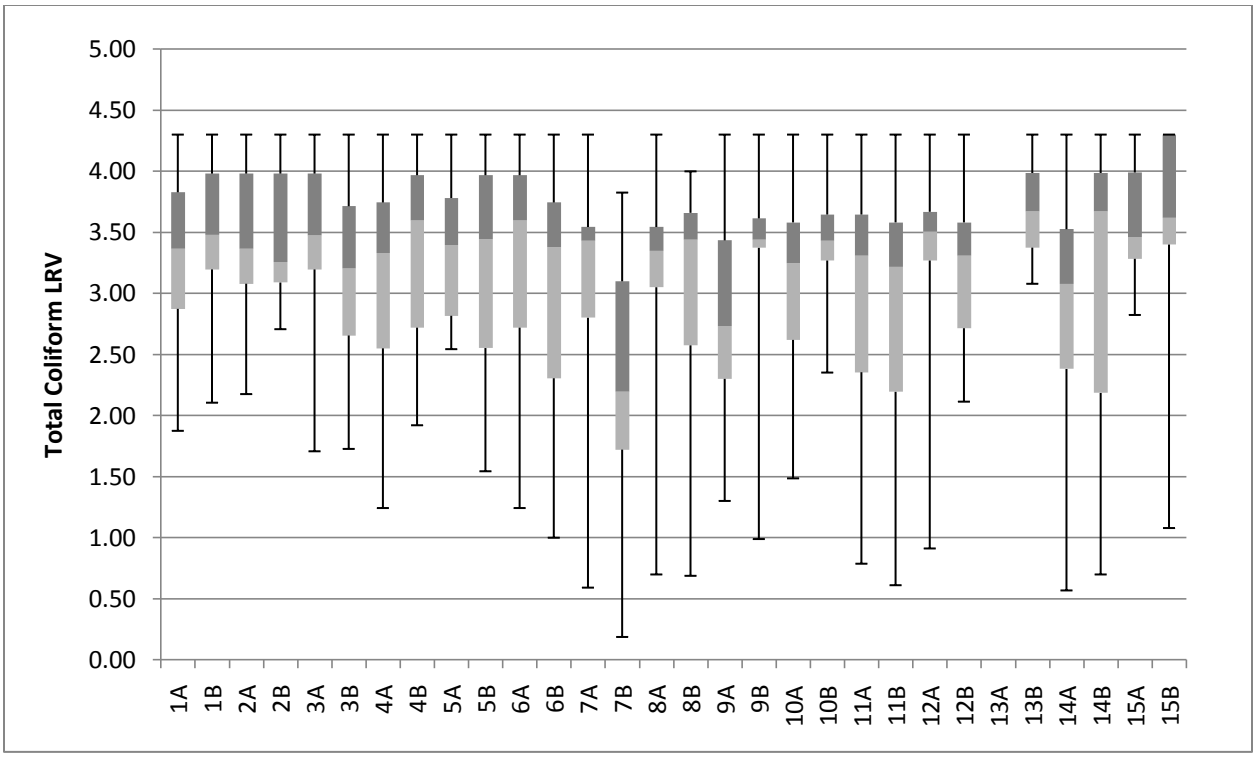

Figure 5-14: Total Coliform Log Removal of Filters 1-15

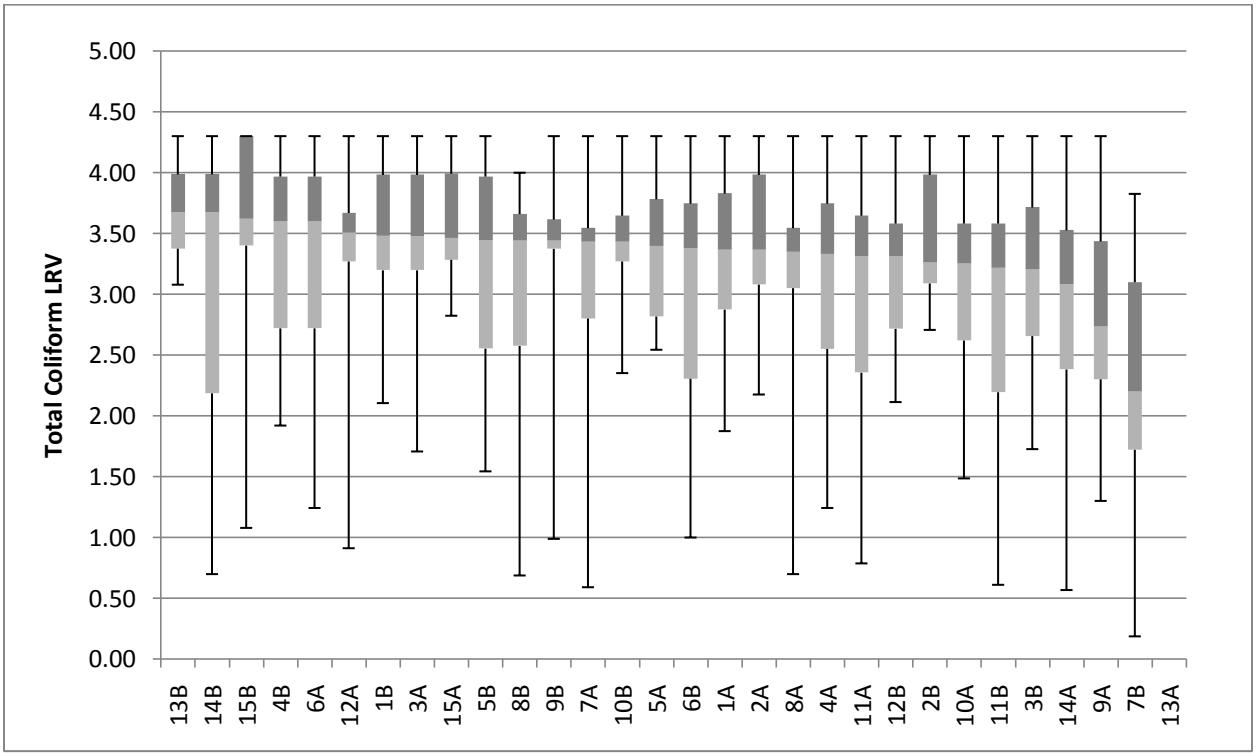

Figure 5-15: Total Coliform Log Removal of Filters 1-15, Largest to Smallest Median

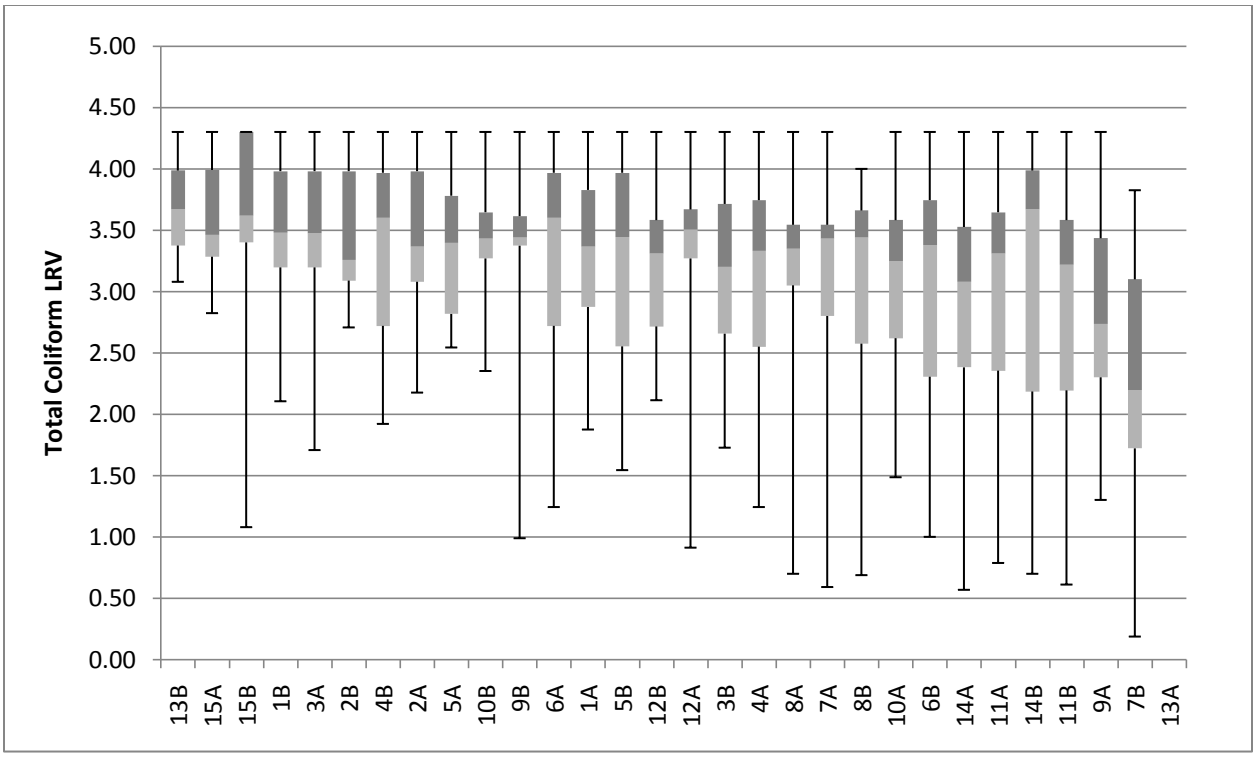

Figure 5-16: Total Coliform Log Removal of Filters 1-15, Largest to Smallest Mean

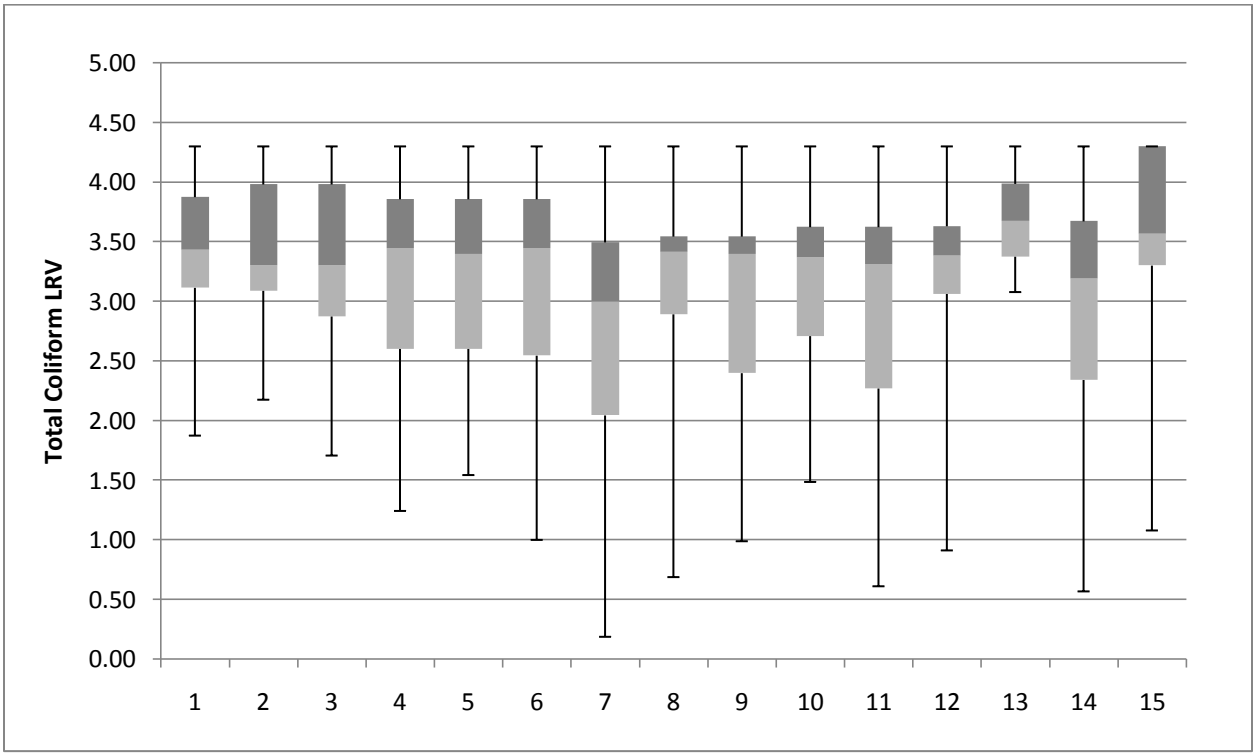

Figure 5-17: Total Coliform Log Removal of Filter Pairs 1-15

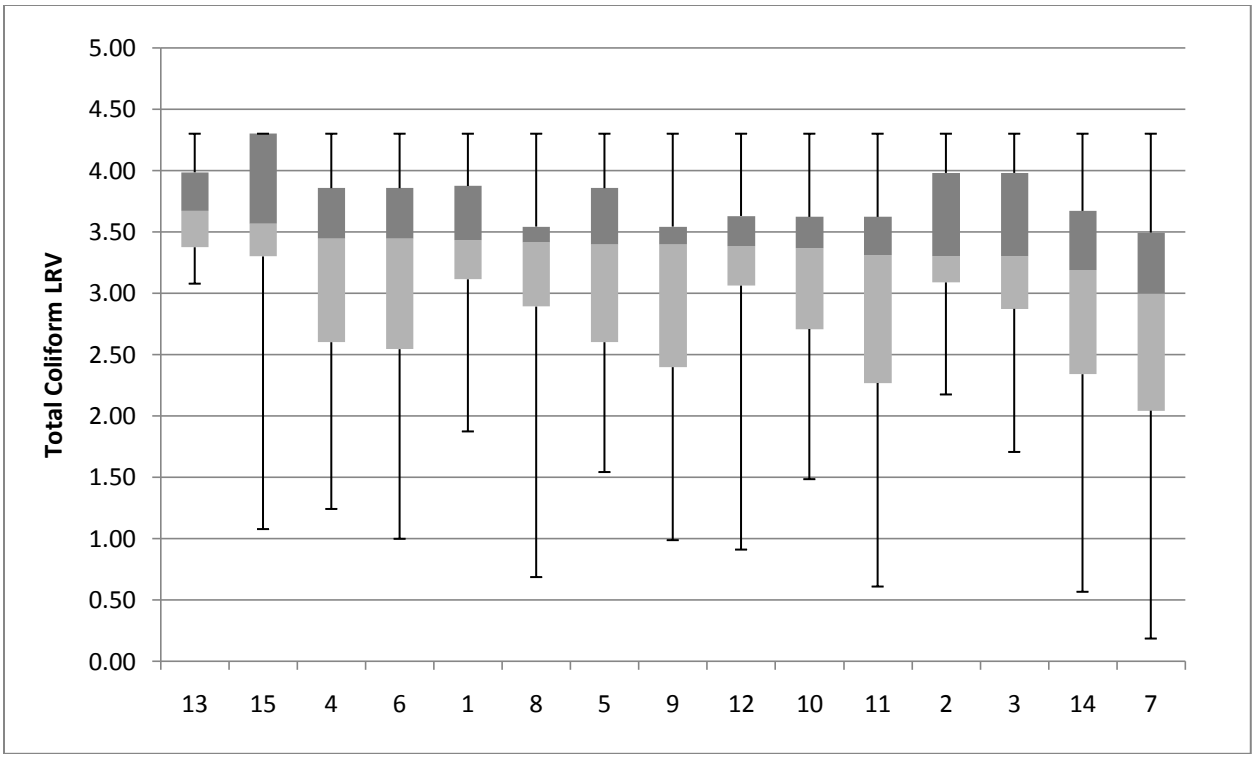

Figure 5-18: Total Coliform Log Removal of Filter Pairs 1-15, Largest to Smallest Median

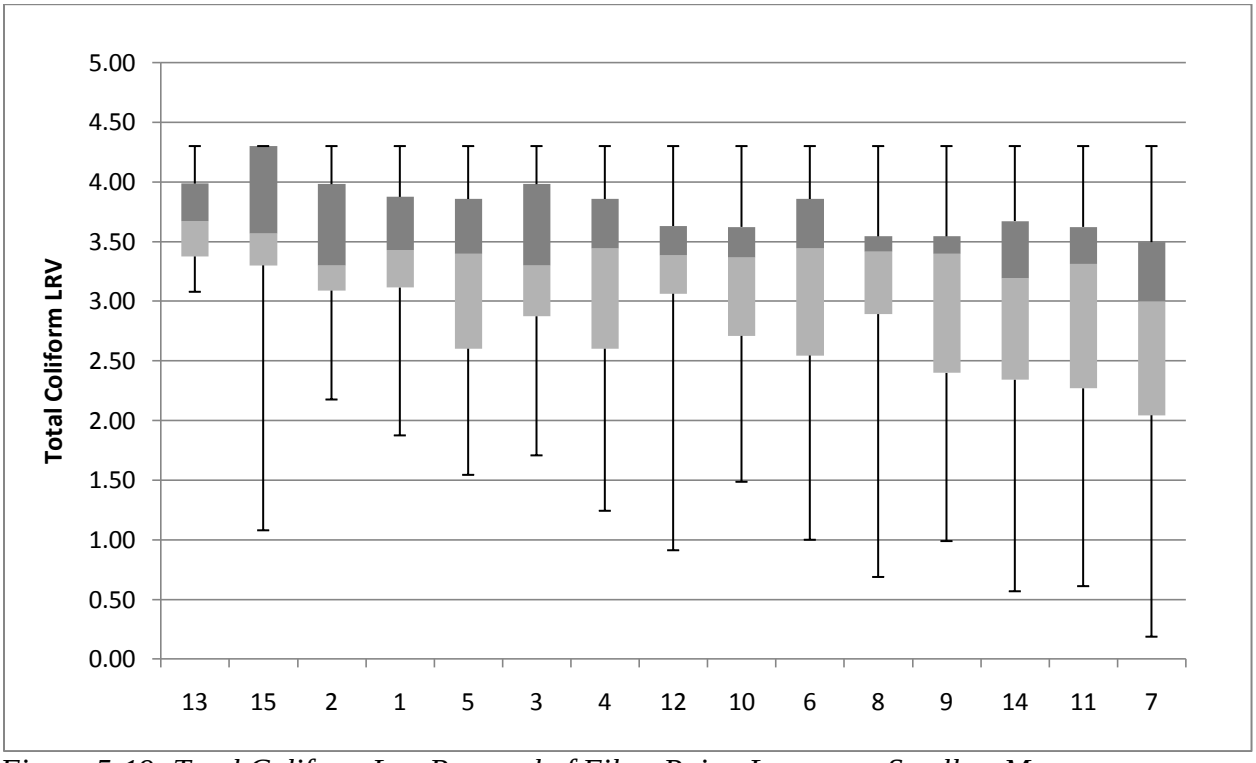

Figure 5-19: Total Coliform Log Removal of Filter Pairs, Largest to Smallest Mean

5.3.1 Effect of Combustible Type on Total Coliform Log Removal

Figure 5-20 presents the total coliform log removal and average influent total coliform over time. Figure 5-21 presents box and whisker charts comparing combustible types. Results of an estimation of the difference of the two means of the populations of the Total Coliform Removal data for rice husk filters 1 through 6, normalized for total combustible volume, and sawdust filters 7-12 with a 95% confidence interval:

Lower Confidence Level (LCL): -.01852, Upper Confidence Level (UCL): 0.374261
No evidence of a difference between means.

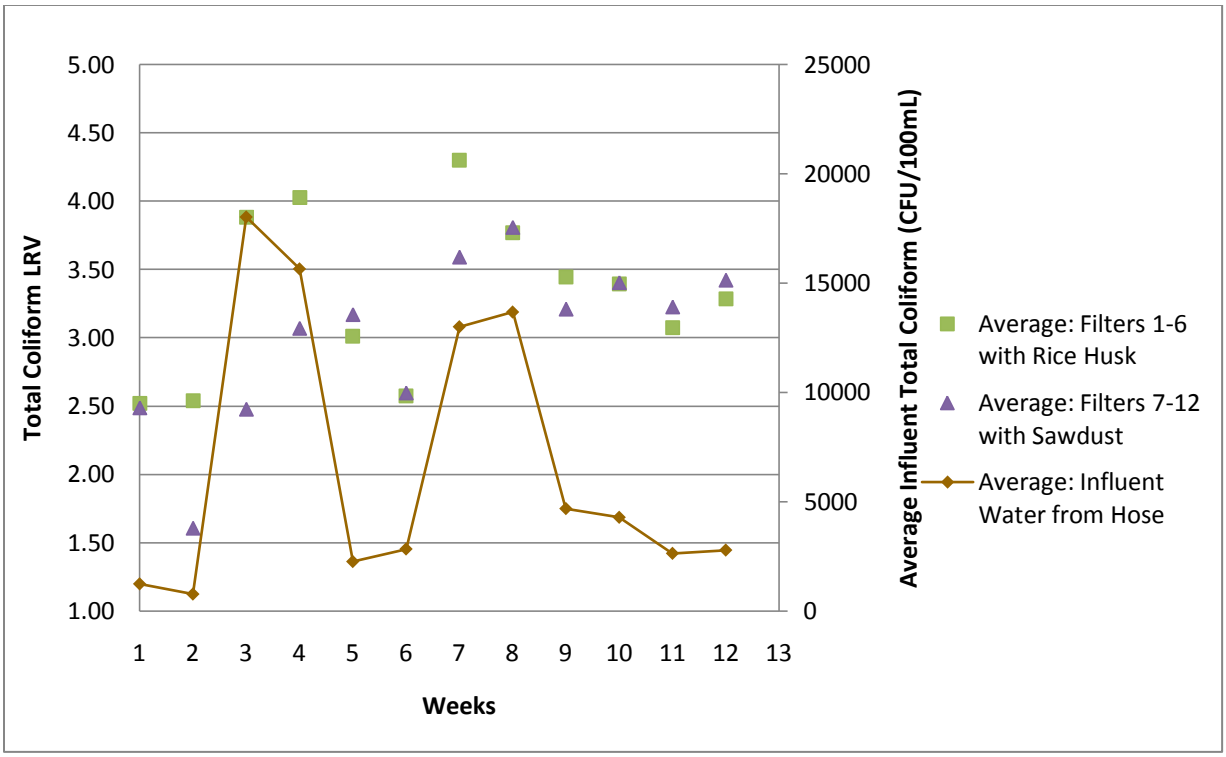

Figure 5-20: Total Coliform Log Removal over Time by Combustible Type, Filters 1-12

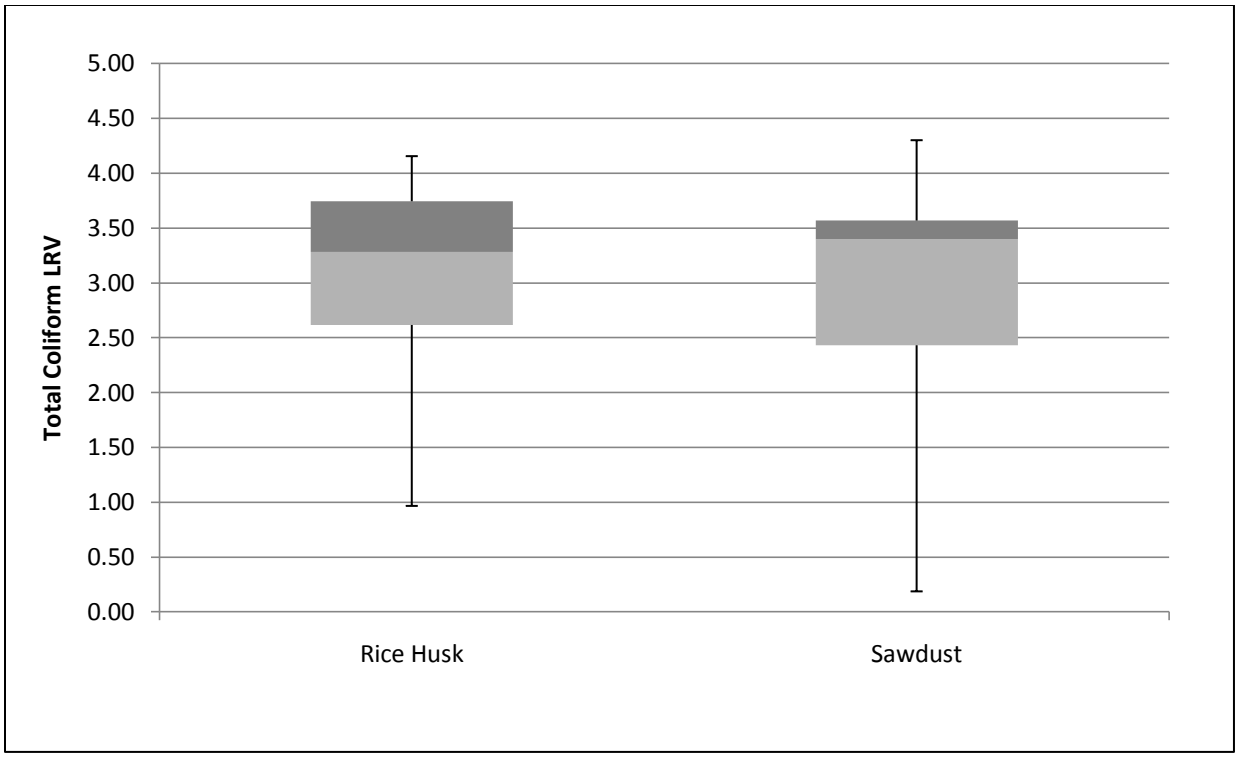

Figure 5-21: Total Coliform Log Removal by Combustible Type, Filters 1-12, Normalized

When comparing filters with rice husk as a group to filters with saw dust, the rice husk data was normalized to account for slight differences in the anticipated total volume of combustible, calculated using uncompacted lab densities, added based on material density determined in the field and material density determined in the laboratory. The sum of the volume of rice husk added to filters 1 through 6 is 72,857 cm^3, while the sum of the volume of saw dust added to filters 7 through 12 is 70,393 cm^3. Therefore, the rice husk data used in Figure 5-21 was multiplied by a factor of 70,393/72,857, or 0.9662, to provide roughly equal comparison.

5.3.2 Effect of Combustible Percentage by Mass on Total Coliform Log Removal

A series of two-sample T-tests assuming unequal variances with 95% confidence showed no evidence of a trend in total coliform log removal due to percent combustible by mass sorted by combustible type for either rice husk or sawdust filters. Figure 5-22 presents box and whisker charts of the filters with increasing combustible mass sorted by combustible type.

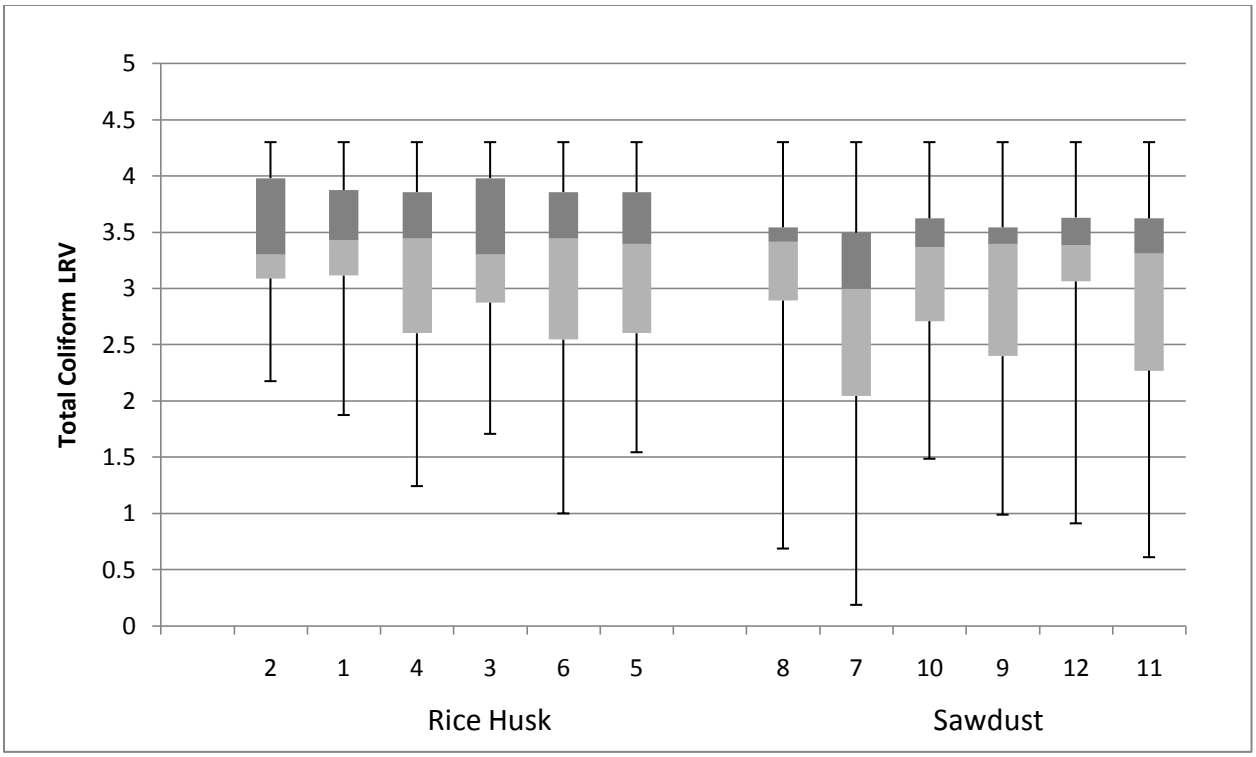

Figure 5-22: Total Coliform Removal of Filter Pairs 1-12, Smallest to Largest Percent Combustible by Mass, Sorted by Combustible Type

5.3.3 Effect of Addition of Grog on Total Coliform Log Removal

Figure 5-23 shows total coliform log removal with or without grog over time, and Figure 5-24 presents box and whisker charts comparing filters with and without grog. Results of an estimation of the difference of the two means of the populations of the Total Coliform Removal data for odd-numbered filters 1 through 12 without grog and even-numbered filters 1 through 12 with grog a 95% confidence interval:

LCL: -0.32333848, UCL: 0.079270702
No evidence of a difference between the means.

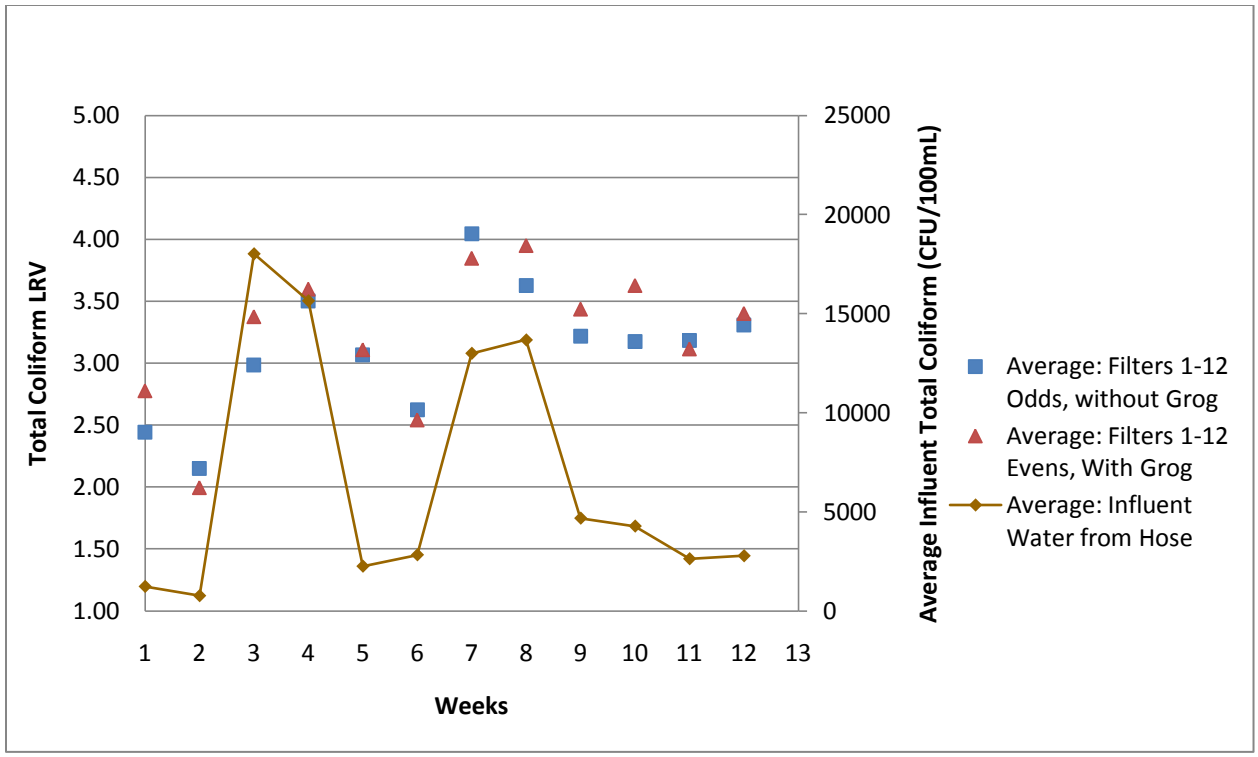

Figure 5-23: Total Coliform Removal over Time With or Without Grog, Filters 1-12

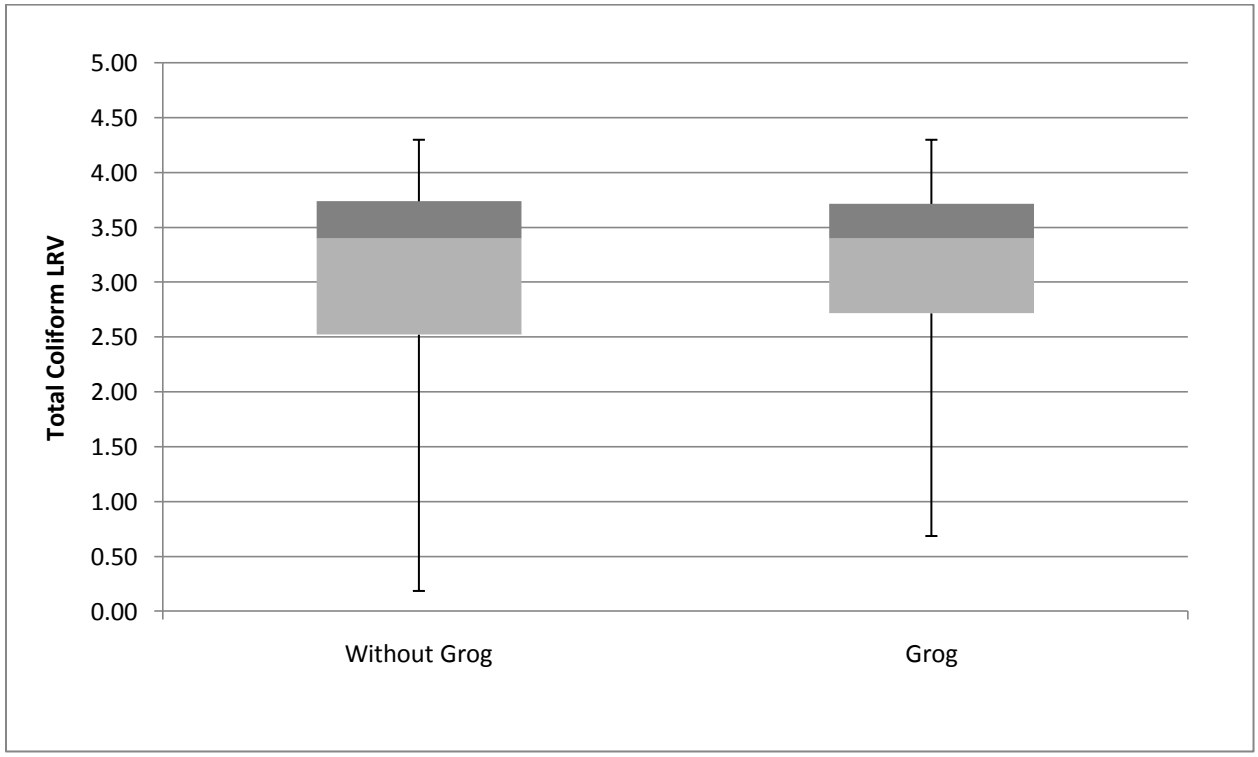

Figure 5-24: Total Coliform Removal With or Without Grog, Filters 1-12

5.3.4 Effect of Additional Variables: Sifted Combustible and Shape on Total Coliform Log Removal

Method of Preparation of Rice Husk Filters:
Results of an estimation of the difference with independent samples of the two means of the populations of the Total Coliform Removal data for filter pair 1 and filter pair 14 with the following confidence intervals:

95% Confidence Interval	No evidence of a difference between the means.
90% Confidence Interval	No evidence of a difference between the means.
80% Confidence Interval	No evidence of a difference between the means.

Method of Preparation of Sawdust Filters:
Due to the small sample size of filter pair 13 (3 events), no conclusions can reasonably be drawn.

Shape of Filters:
Results of an estimation of the difference with independent samples of the two means of the populations of the Total Coliform Removal data for filter pair 2 and filter pair 15 with the following confidence intervals:

95% Confidence Interval	No evidence of a difference between the means.
90% Confidence Interval	No evidence of a difference between the means.
80% Confidence Interval	No evidence of a difference between the means.

5.3.5 Comparison of Sampling Methods for Total Coliform Log Removal

Methods for the comparison are described in Section 4.4.2. Results of a two-tailed estimation between the difference of two populations with matched pairs with a 95% confidence interval, comparing the Total Coliform CFU per 100mL measured when sampling filtered water directly with a Whirl-Pak® bag and indirectly with a flowrate container:

LCL: -4.34627324, UCL: 3.53145843
No evidence of a difference between the means.

5.4 *E. coli* Removal

E. coli removal was found using methods described in Section 4.4.3. Due to the infrequent occurrences of non-zero *E.Coli* events, the effects on *E. Coli* observed in filtered water were only compared by combustible type, and not by combustible percentage by mass, addition of grog, or the additional variables, sifted combustible and shape.

Table 5-8 presents data about the *E.coli* in influent water, and Table 5-9 ranks the filters in tiers according to their performance. Figures 5-25 through 5-27 present the concentration and frequency of non-zero *E. coli* events in filtered water.

Table 5-8: E. coli in Influent Water across 12-Week Study

Median (CFU/100mL)	0
Mean (CFU/100mL)	53.8
Standard Deviation (CFU/100mL)	155.3

Table 5-9: E. coli Removal Tiered Ranking of Filter Pairs based WHO 1997 Risk Levels, 1=Best to 3=Worst

Tier	Filter Pairs
1	2,3,4,5,6,9,12,14,15
2	1,8,11
3	7,10

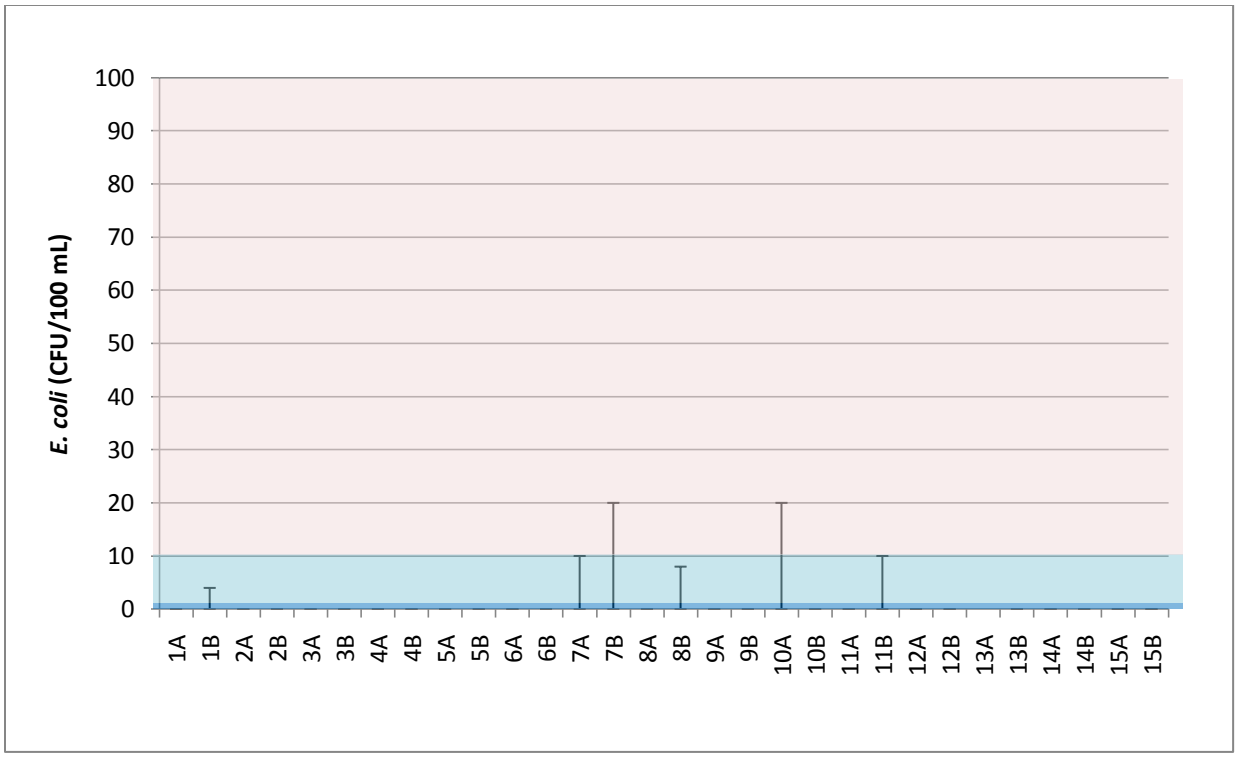

Key: WHO 1997 Risk Levels

Conformity	Low	Intermediate
<1	1-10	10-100

Figure 5-25: E. coli CFU per 100mL, Filters 1-15

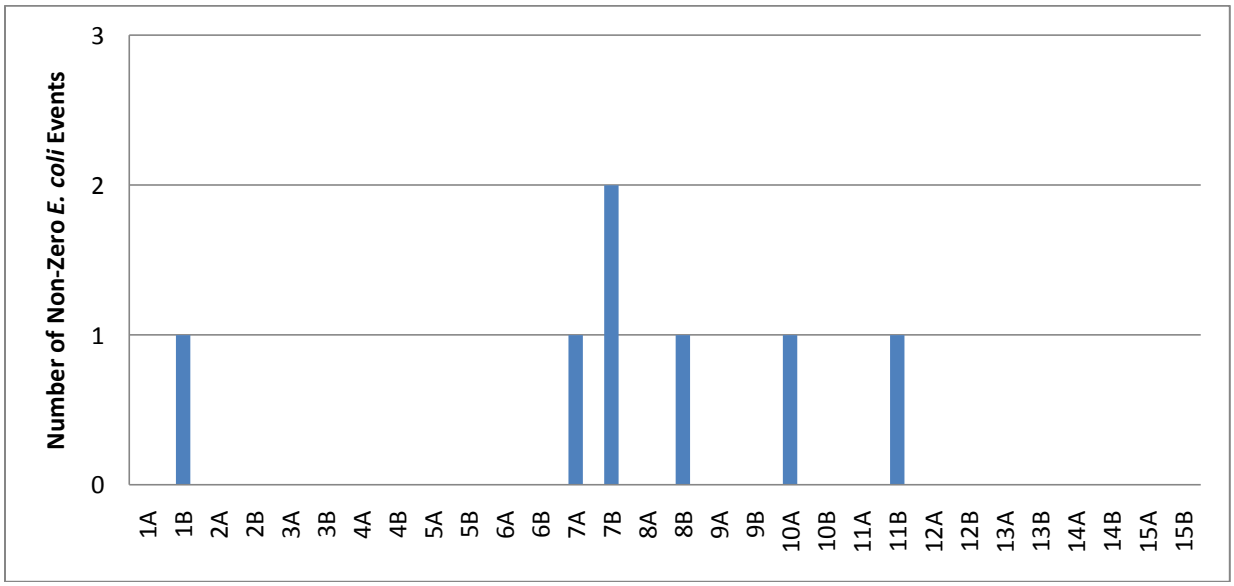

Figure 5-26: Frequency of Non-Zero E. coli Events, Filters 1-15

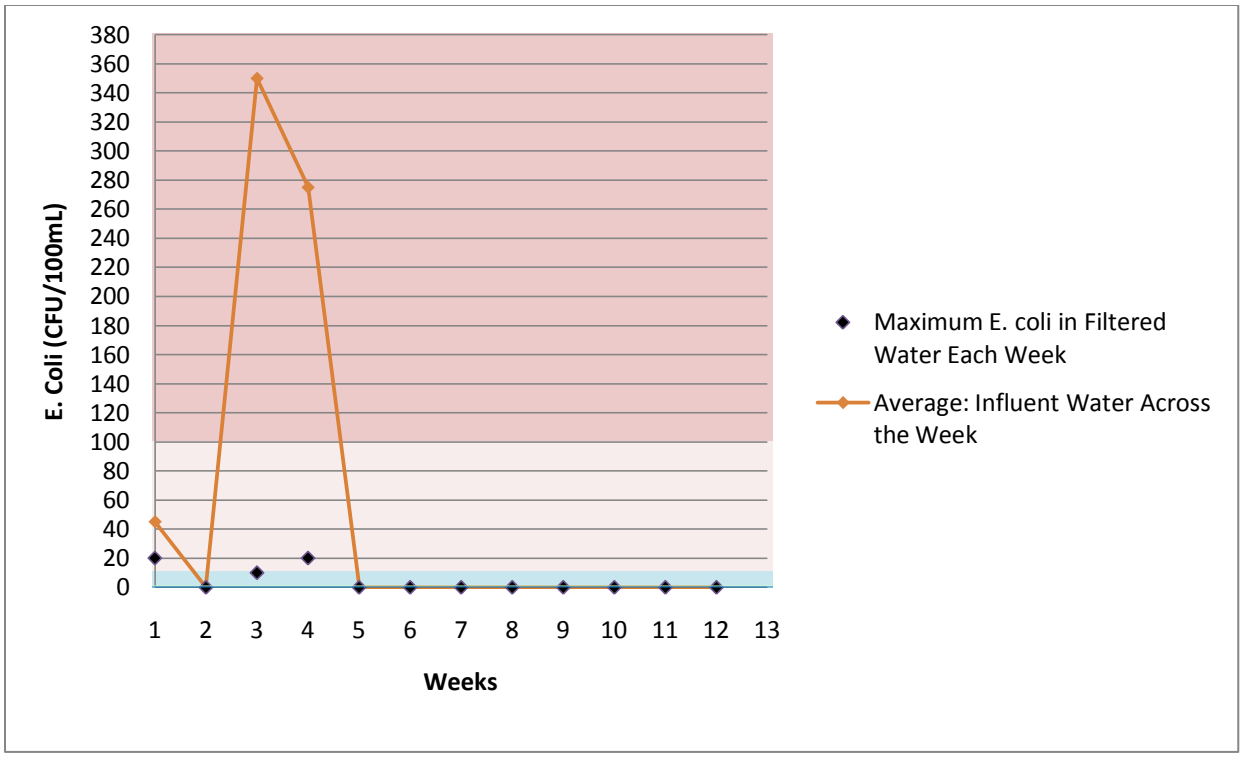

Key: WHO 1997 Risk Levels

Conformity	Low	Intermediate	High
<1	1-10	10-100	100-1000

Figure 5-27: Average Influent E. coli CFU per 100mL compared to Maximum E. Coli CFU per 100mL in Filtered Water from Filters 1-12

5.4.1 Effect of Combustible Type on *E. coli* Removal

Results of an estimation of the difference of the two means of the populations of the *E. Coli* CFU per 100mL measured data for rice husk filters 1 through 6 and sawdust filters 7-12 with a 95% confidence interval:

LCL: -0.99562, UCL: -0.05521
Mean of the sawdust filters *E. Coli* CFU per 100mL is greater than the mean of the rice husk filters *E. Coli* CFU per 100mL by 0.055 to 0.996 *E. Coli* CFU per 100mL.

5.4.2 Effect of Combustible Percentage by Mass on *E. coli* Removal

Not tested.

5.4.3 Effect of Addition of Grog on *E. coli* Removal

Not tested.

5.4.4 Effect of Additional Variables: Sifted Combustible and Shape on *E. coli* Removal

Not tested.

5.4.5 Comparison of Sampling Methods for *E. coli* Removal

All of the samples tested using both sampling methods resulted in zero *E. coli* CFU per 100 mL. This does not provide evidence of a difference between the means.

5.5 Turbidity Removal

Table 5-10 presents data about the turbidity in influent water, found using methods described in Section 4.5.4. The filters were not ranked in statistical tiers according to their performance because the overall results were so poor that none of the filters was considered to have satisfactory turbidity removal performance. Figures 5-28 through 5-33 are box and whisker charts of the total coliform log removal of individual filters, as well as the averages of a pair of filters.

Table 5-10: Turbidity of Influent Water across 12-Week Study

Median (NTU)	153
Mean (NTU)	157.4
Standard Deviation (NTU)	40.2

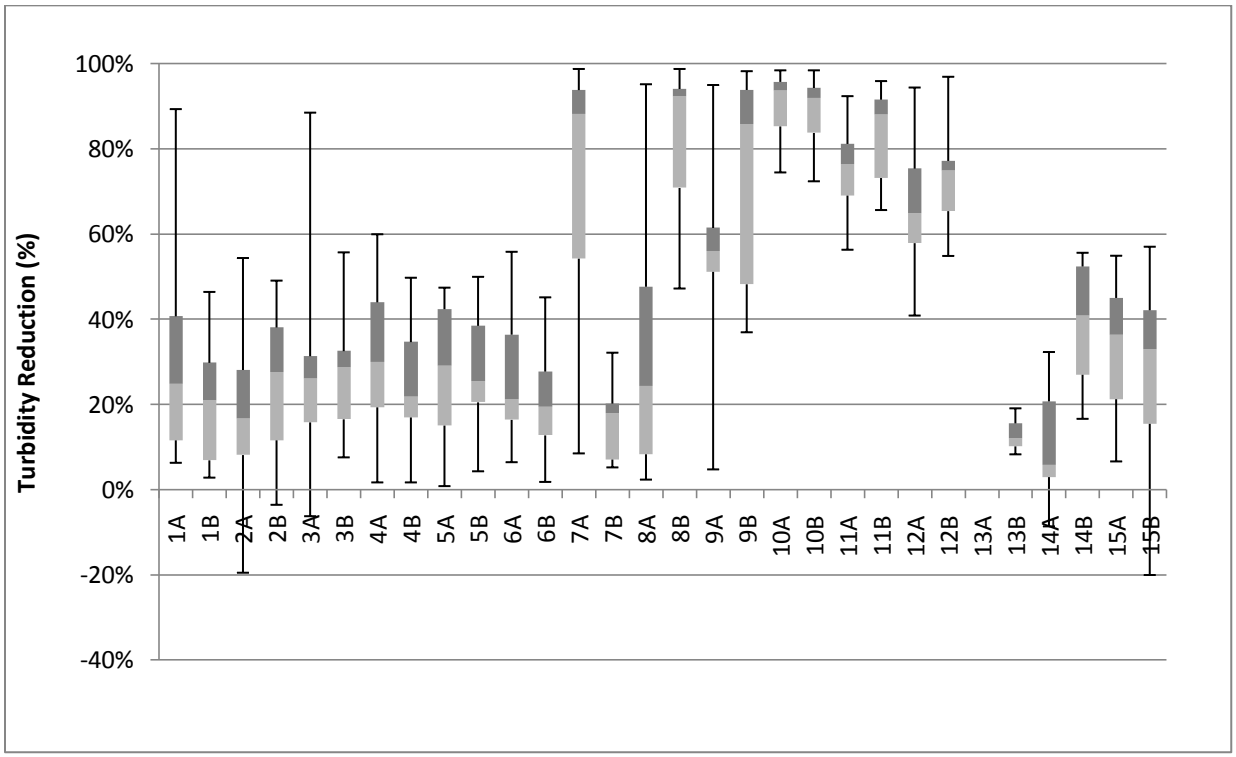

Figure 5-28: Turbidity Removal, Filters 1-15

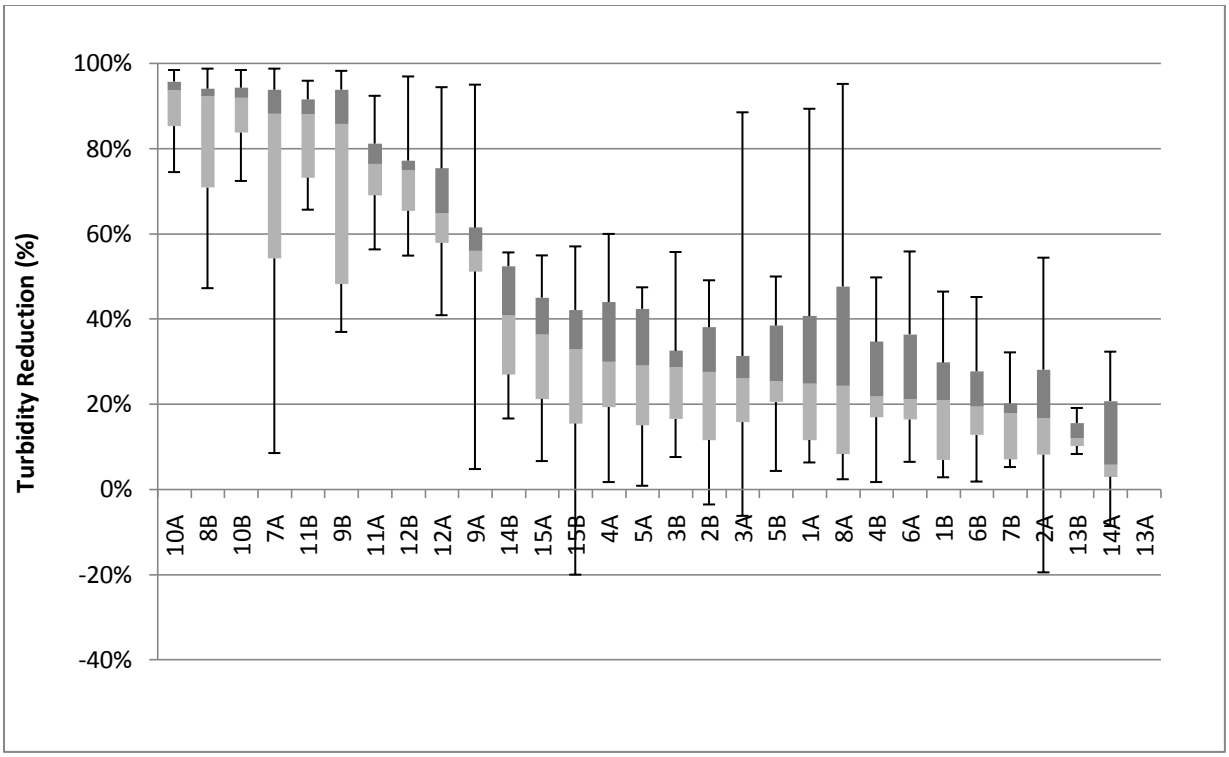

Figure 5-29: Turbidity Removal, Largest to Smallest Median, Filters 1-15

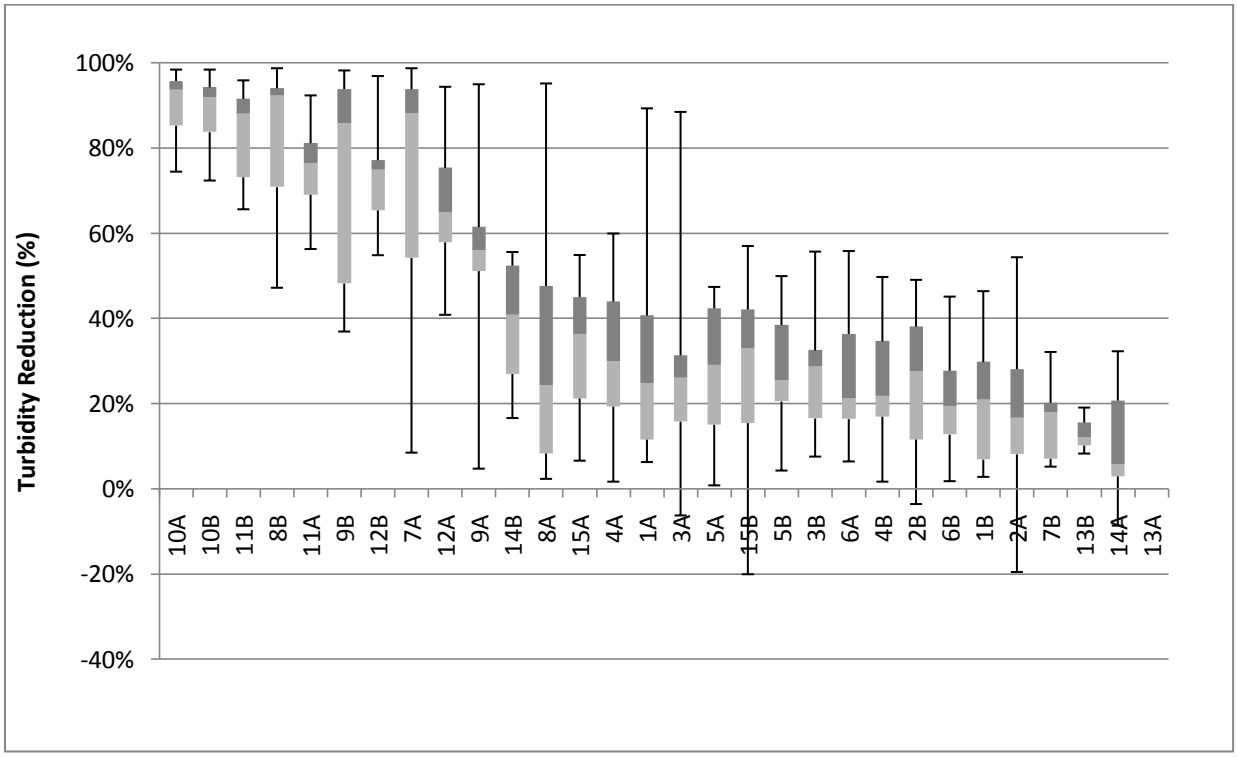

Figure 5-30: Turbidity Removal, Largest to Smallest Mean, Filters 1-15

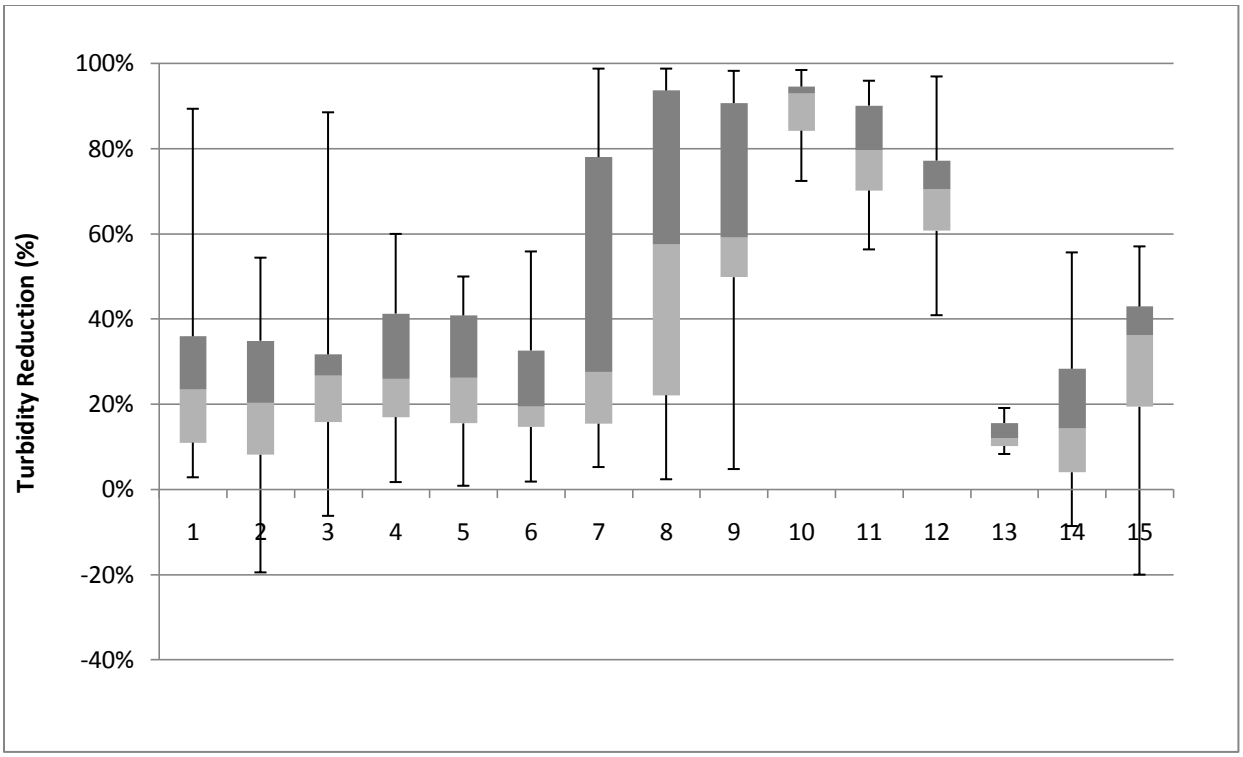

Figure 5-31: Turbidity Removal of Pairs, Filters 1-15

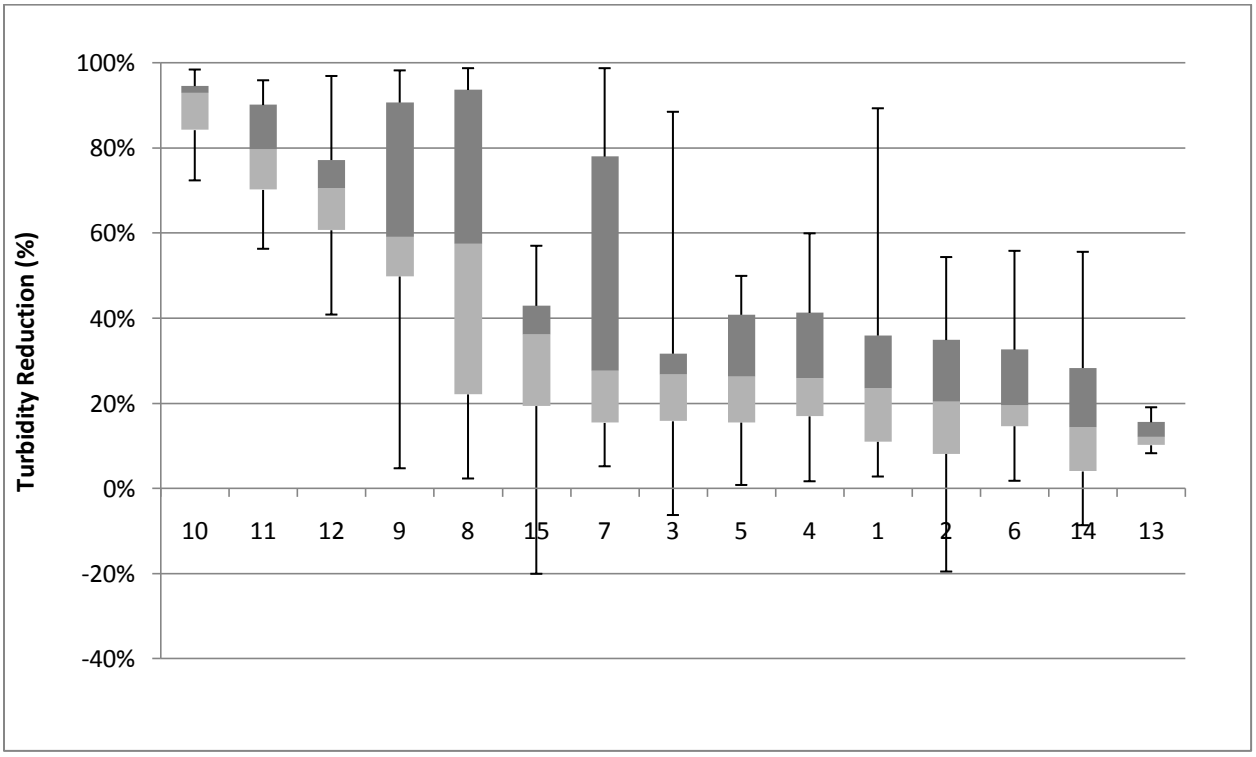

Figure 5-32: Turbidity Removal of Pairs, Largest to Smallest Median, Filters 1-15

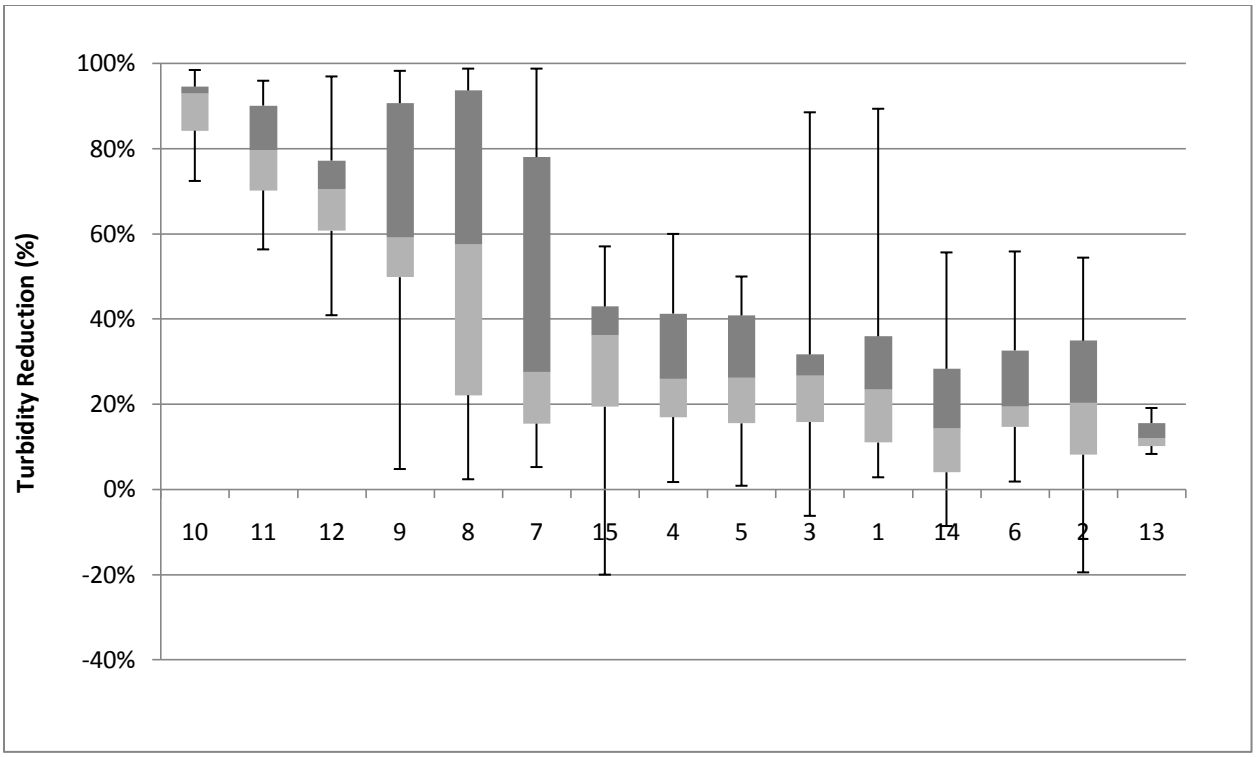

Figure 5-33: Turbidity Removal of Pairs, Largest to Smallest Mean, Filters 1-15

5.5.1 Effect of Combustible Type on Turbidity Removal

Figure 5-34 compares the turbidity of influent and filtered water over time. Figure 5-35 compares influent turbidity and turbidity reduction over time, while Figure 5-36 compares turbidity reduction directly to influent turbidity. Figure 5-37 presents box and whisker charts of turbidity removal sorted by combustible type. Results of an estimation of the difference of the two means of the populations of the turbidity removal data for rice husk filters 1 through 6, normalized for total combustible volume, and sawdust filters 7-12 with a 95% confidence interval:

> LCL: -47.70%, UCL: -36.90%
> Mean of the sawdust filters' turbidity removal is greater than the mean of the rice husk filters' turbidity removal by 36.90% to 47.70%.

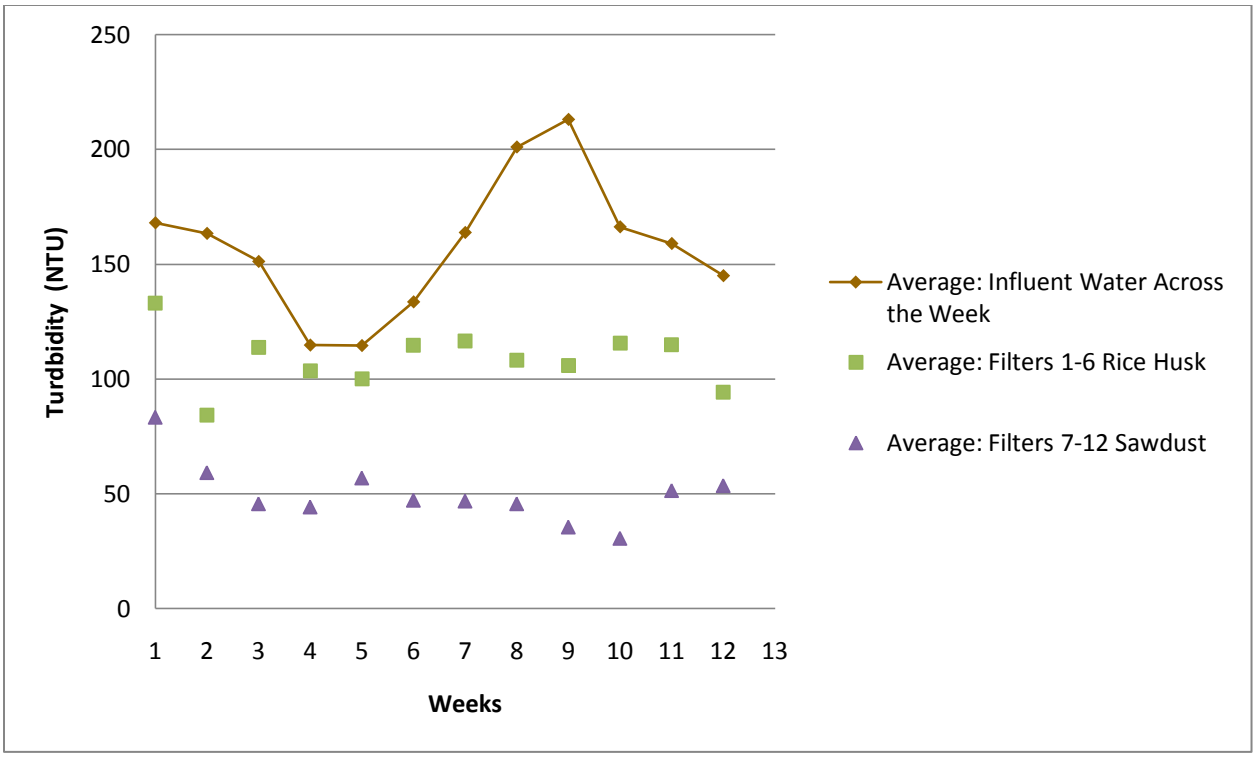

Figure 5-34: Turbidity Measured over Time by Combustible Type, Filters 1-12

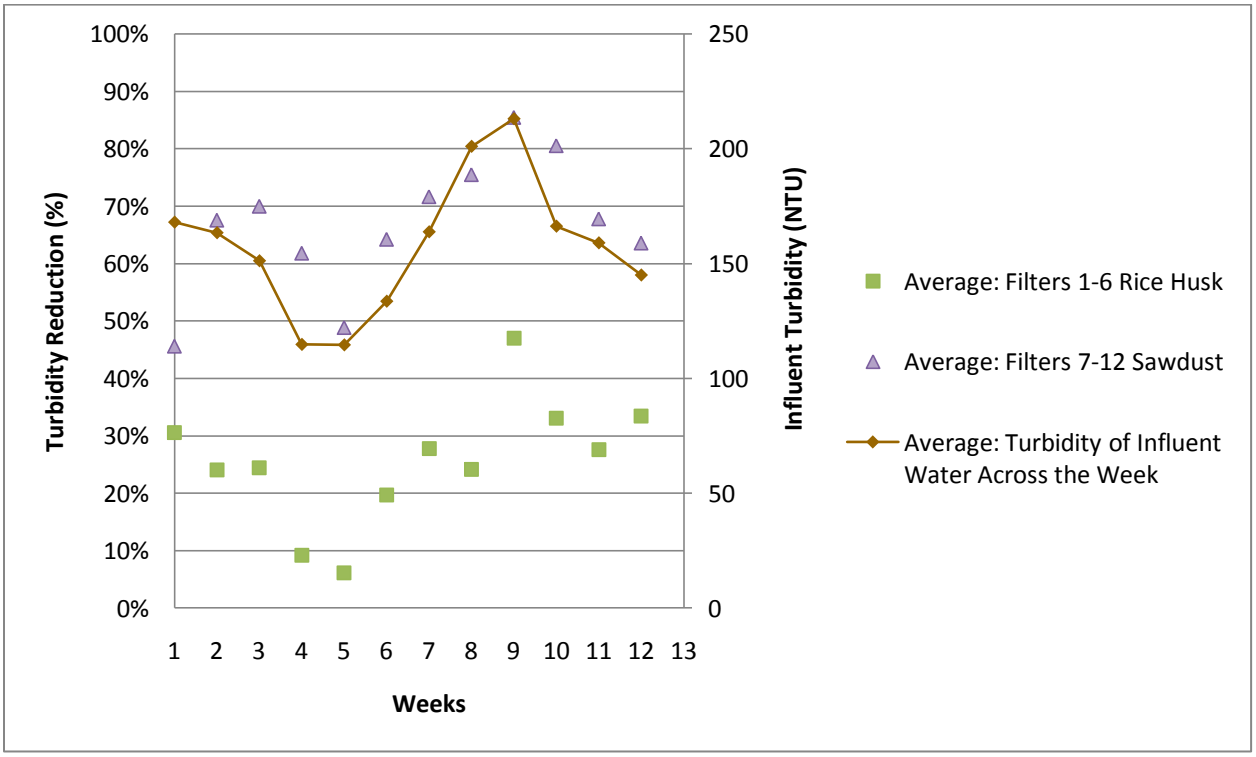

Figure 5-35: Average Turbidity Removal over Time Compared to Influent Turbidity, Filters 1-12 by Combustible Type

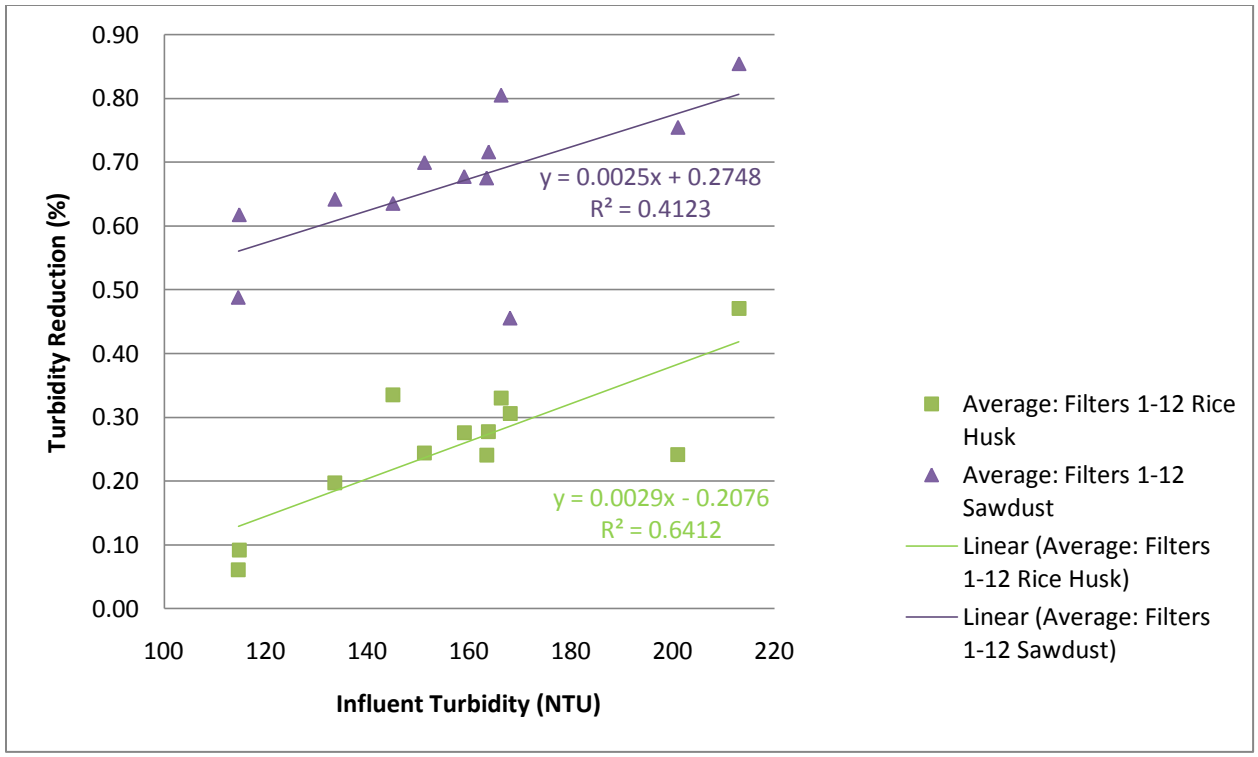

Figure 5-36: Average Turbidity Removal over Time Compared to Influent Turbidity

As with Total Coliform Removal data above in Section 5.3.1, the rice husk data used in Figure 5.5.1d was multiplied by a factor of 70,393/72,857 to provide equal comparison based on total volume of combustible added to filters 1 through 12.

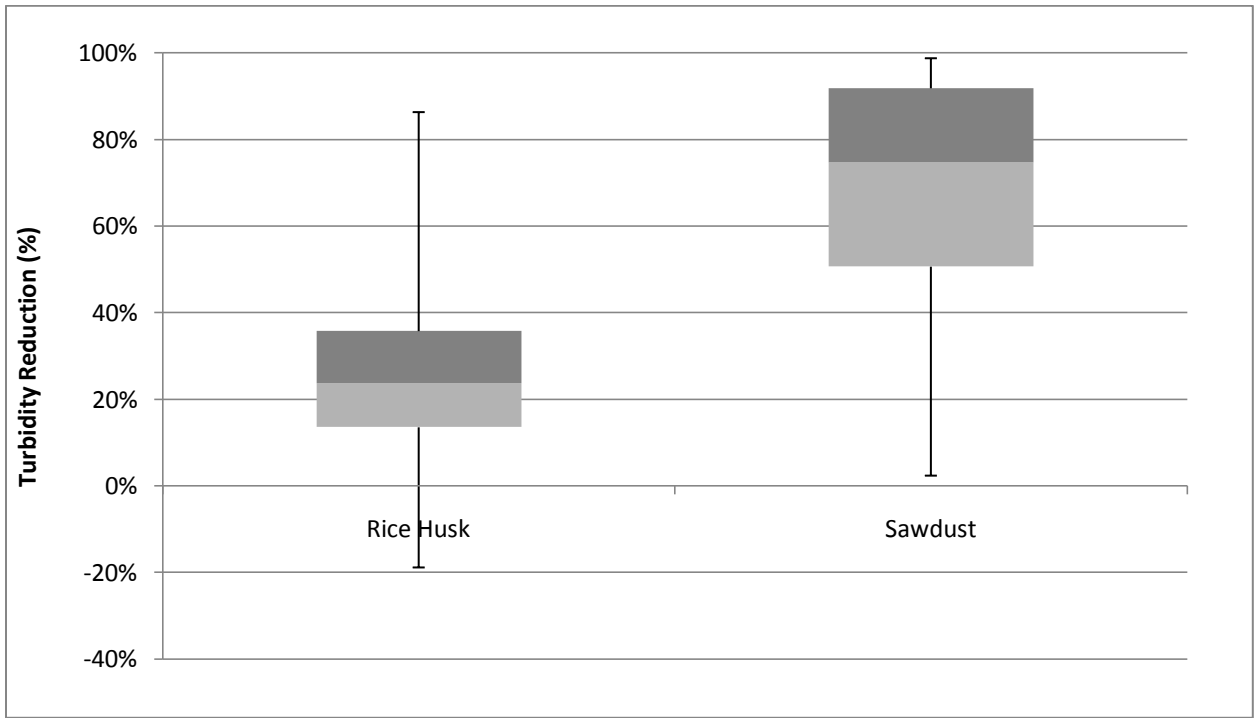

Figure 5-37: Turbidity Removal by Combustible Type, Filters 1-12, Normalized

5.5.2 Effect of Combustible Percentage by Mass on Turbidity Removal

Figure 5-38 presents box and whisker charts of turbidity removal by increasing mass of combustible sorted by combustible type. A series of two-sample t-tests assuming unequal variances with 95% confidence showed no evidence of a trend in turbidity removal due to percent combustible by mass sorted by combustible type for either rice husk or sawdust filters.

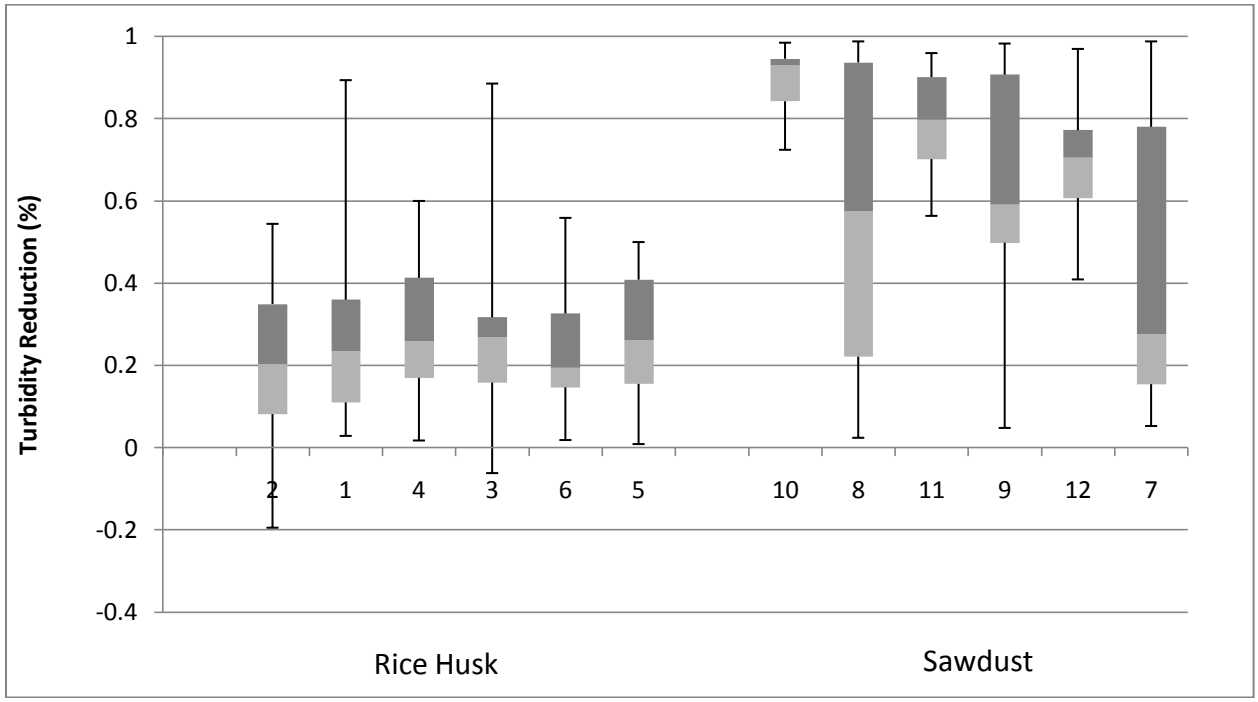

Figure 5-38: Turbidity Removal of Filter Pairs 1-12, Increasing Percent Combustible by Volume, Sorted by Combustible Type

5.5.3 Effect of Addition of Grog on Turbidity Removal

Figure 5-38 presents average turbidity over time for filtered water from filters with and without grog compared to influent water, while Figure 5-40 shows average turbidity reduction. Figure 5-41 plots turbidity reduction compared to influent turbidity. Figure 5-41 presents box and whisker charts of turbidity removal sorted by filters with and without grog. Results of an estimation of the difference of the two means of the populations of the turbidity removal data for odd-numbered filters 1 through 12 without grog and even-numbered filters 1 through 12 with grog a 95% confidence interval:

LCL: -0.10597, 0.039037
No evidence of a difference between the means.

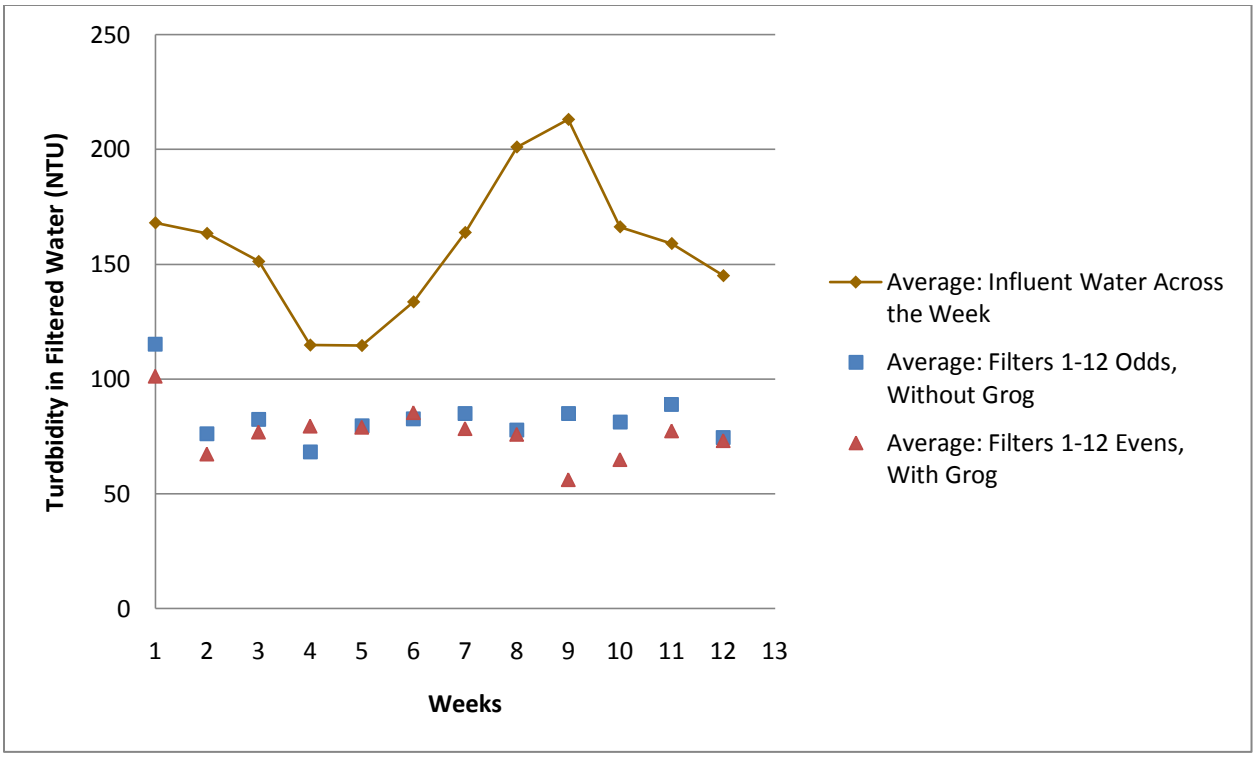

Figure 5-39: Average Turbidity Measured over Time Compared to Influent Turbidity, Filters 1-12 With or Without Grog

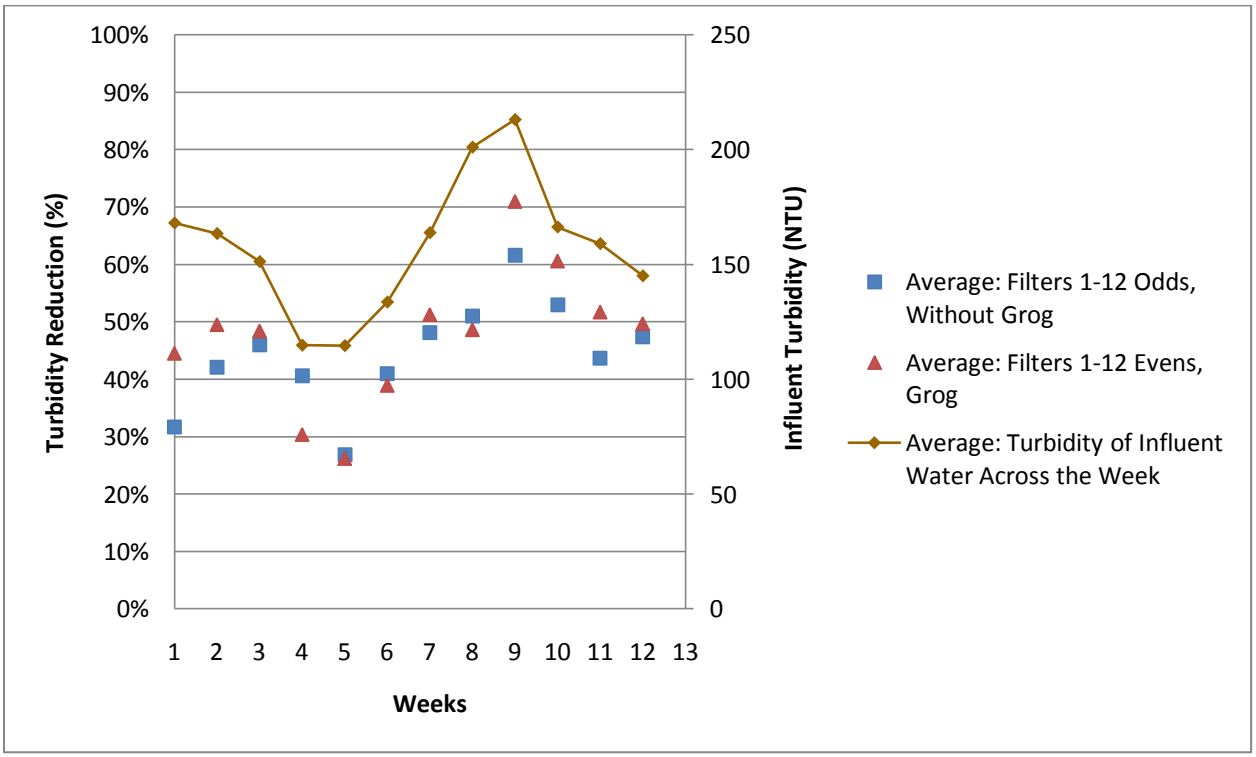

Figure 5-40: Average Turbidity Removal over Time Compared to Influent Turbidity, Filters 1-12 With or Without Grog

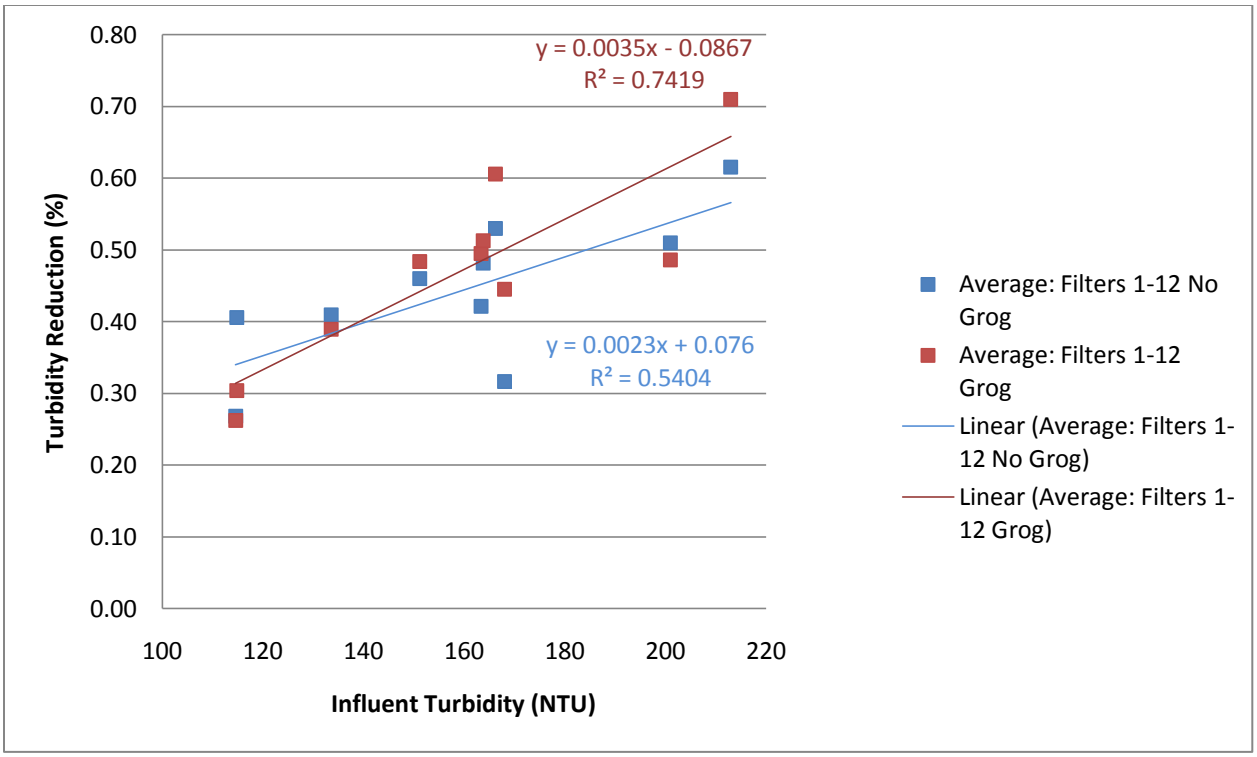

Figure 5-41: Average Turbidity Removal Compared to Influent Turbidity

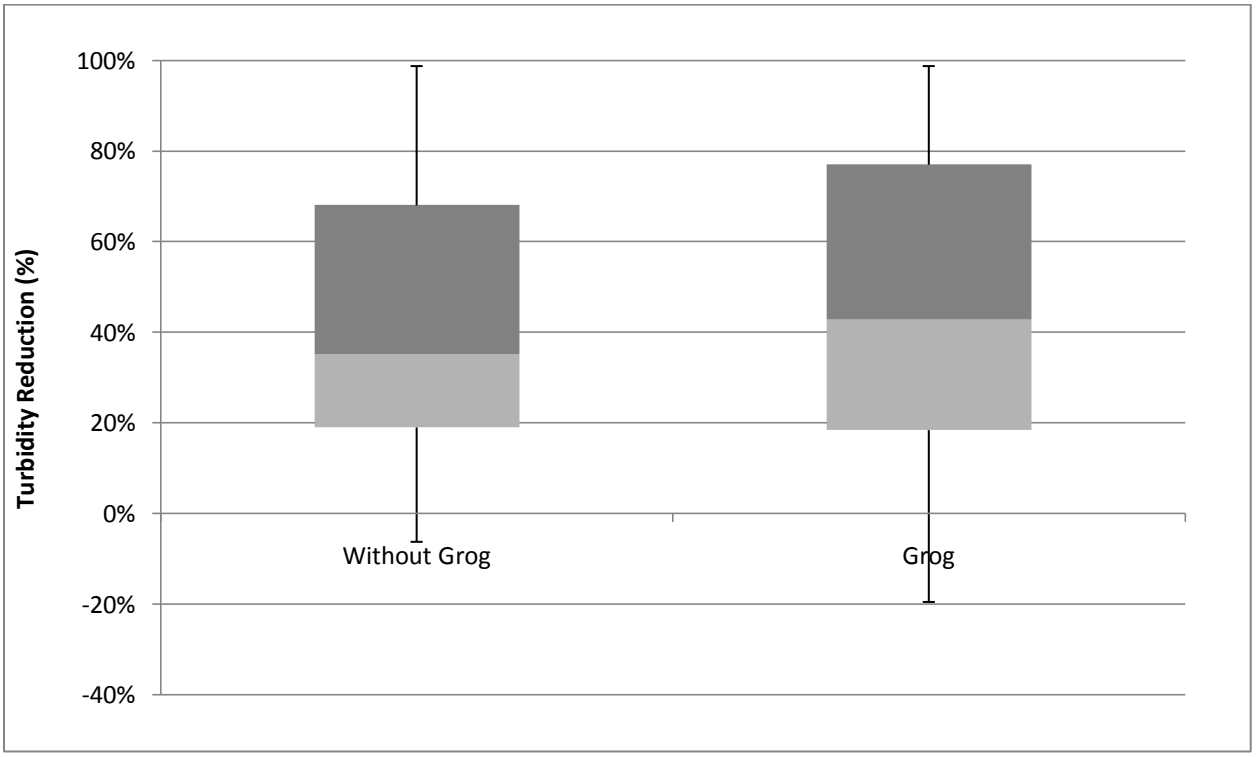

Figure 5-42: Turbidity Removal With or Without Grog, Filters 1-12

5.5.4 Effect of Additional Variables: Sifted Combustible and Shape on Turbidity Removal

Method of Preparation of Rice Husk Filters:

Results of an estimation of the difference with independent samples of the two means of the populations of the turbidity removal data for filter pair 1 and filter pair 14 with the following confidence intervals:

95% Confidence Interval	No confidence of a difference between the means.
90% Confidence Interval	No confidence of a difference between the means.
80% Confidence Interval	The mean of filter 1 is greater than the mean of filter 14 by 0.1% to 16.2%.

Method of Preparation of Sawdust Filters:

Due to the small sample size of filter pair 13 (3 events), no conclusions can reasonably be drawn.

Shape of Filters:

Results of an estimation of the difference with independent samples of the two means of the populations of the turbidity removal data for filter pair 2 and filter pair 15 with the following confidence intervals:

95% Confidence Interval	No confidence of a difference between the means.
90% Confidence Interval	The mean of filter 15 is greater than the mean of filter 2 by 0.1% to 19.1%.
80% Confidence Interval	The mean of filter 15 is greater than the mean of filter 2 by 2.2% to 17.0%.

5.6 Flowrate

The flowrates of the filters were found using methods described in Section 4.4.1. Table 5-11 ranks the filters in statistical tiers according to their performance. Figures 5-14 through 5-19 are box and whisker charts of the total coliform log removal of individual filters, as well as the averages of a pair of filters.

Table 5-11: Flowrate Tiered Ranking of Filter Pairs based on Series of Two-Sample t-tests assuming Unequal Variances with 95% Confidence, 1=Best to 7=Worst

Tier	Filter Pairs
1	6
2	5
3	3,4
4	1,12
5	2,11,14
6	15
7	7,8,9,10

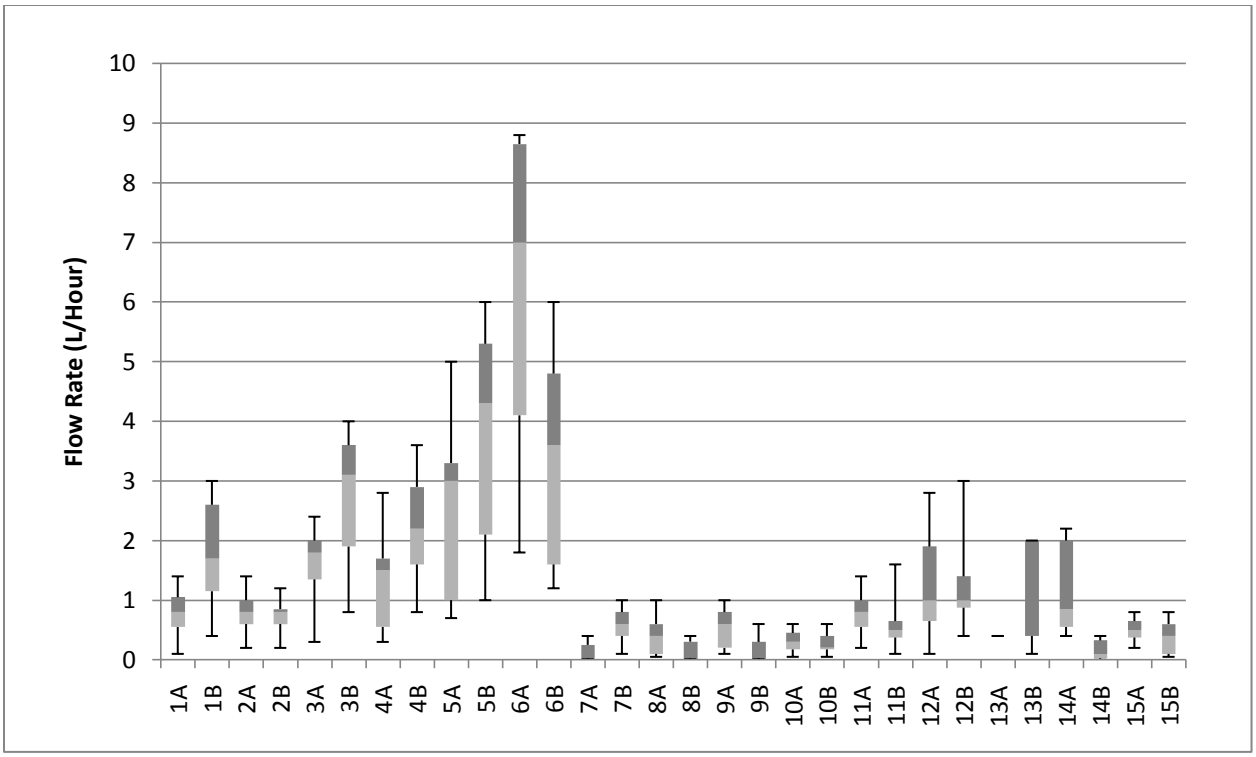

Figure 5-43: Flowrate of Filters 1-15

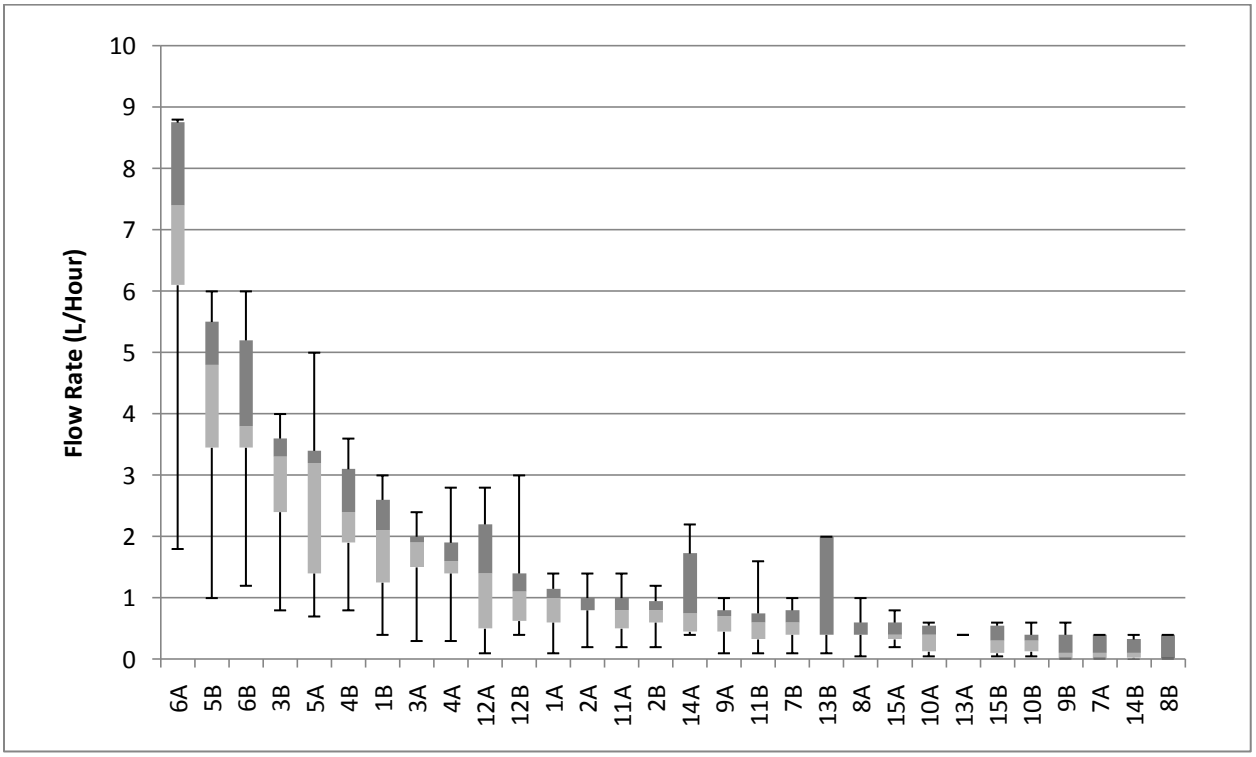

Figure 5-44: Flowrate of Filters 1-15, Largest to Smallest Median

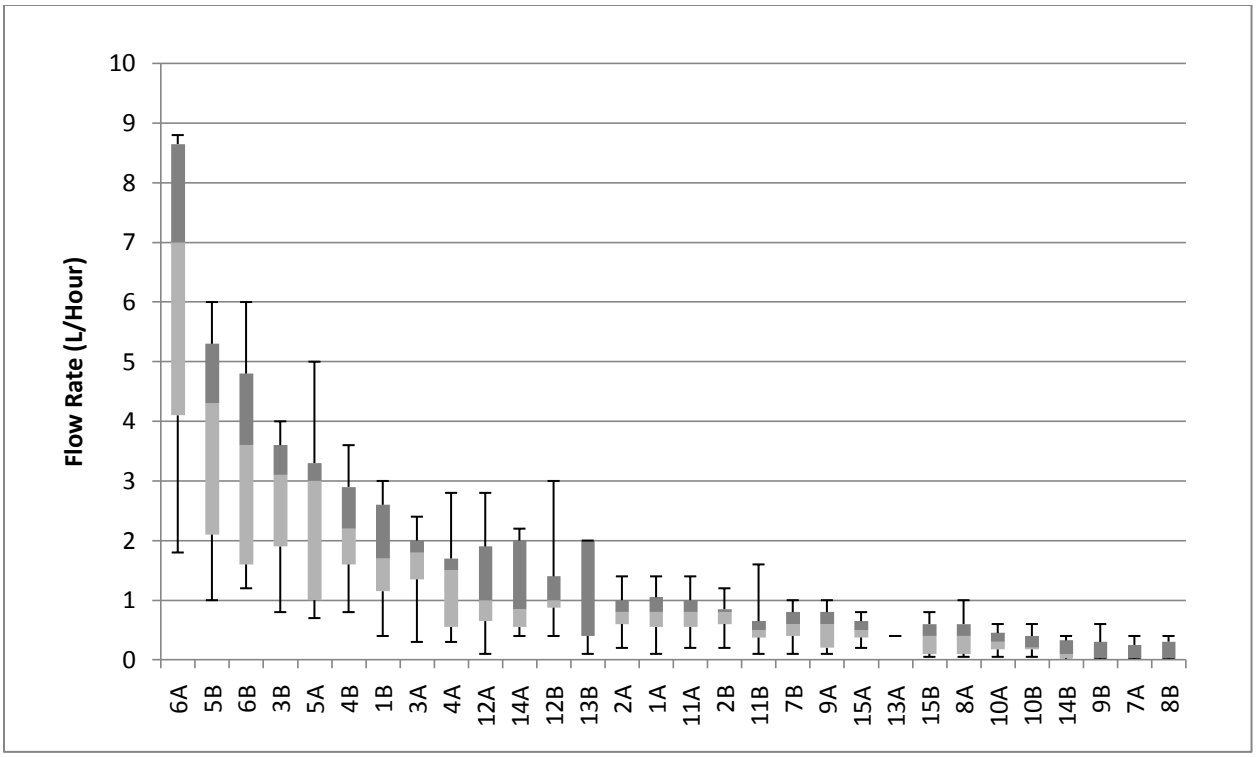

Figure 5-45: Flowrate of Filters 1-15, Largest to Smallest Mean

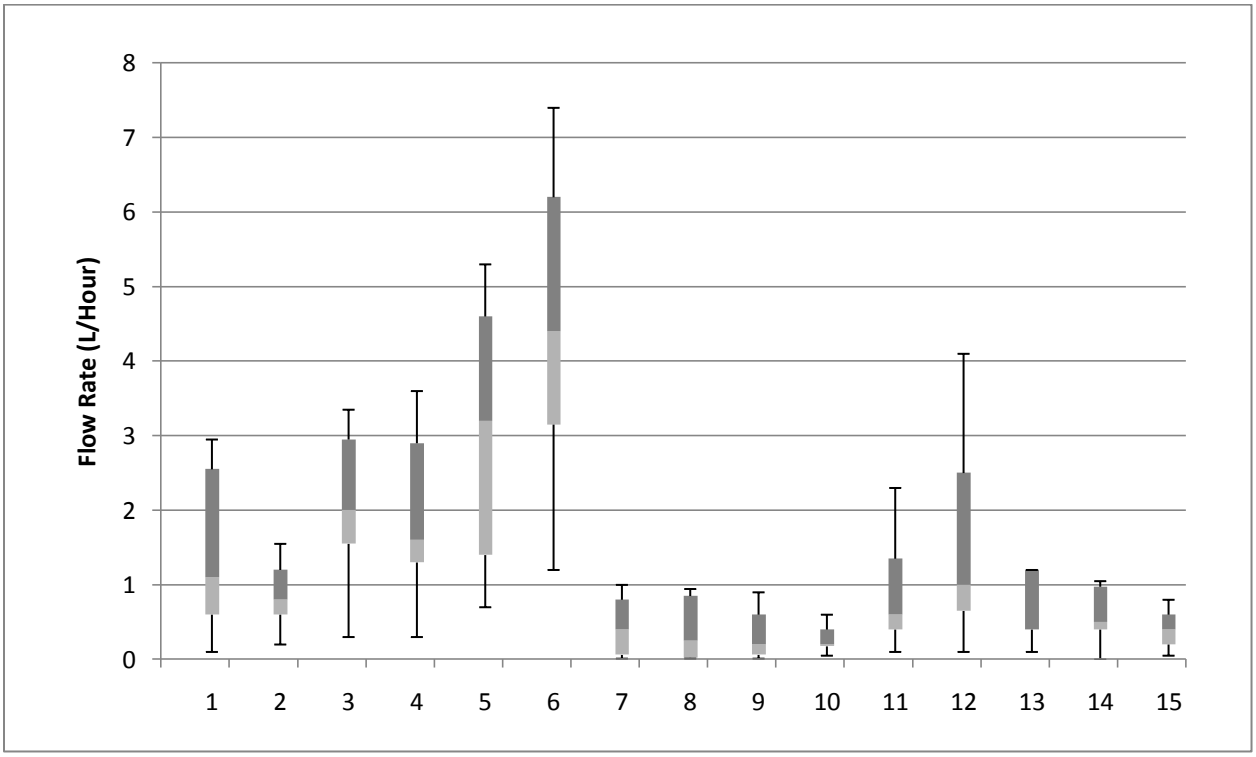

Figure 5-46: Flowrate of Filter Pairs 1-15

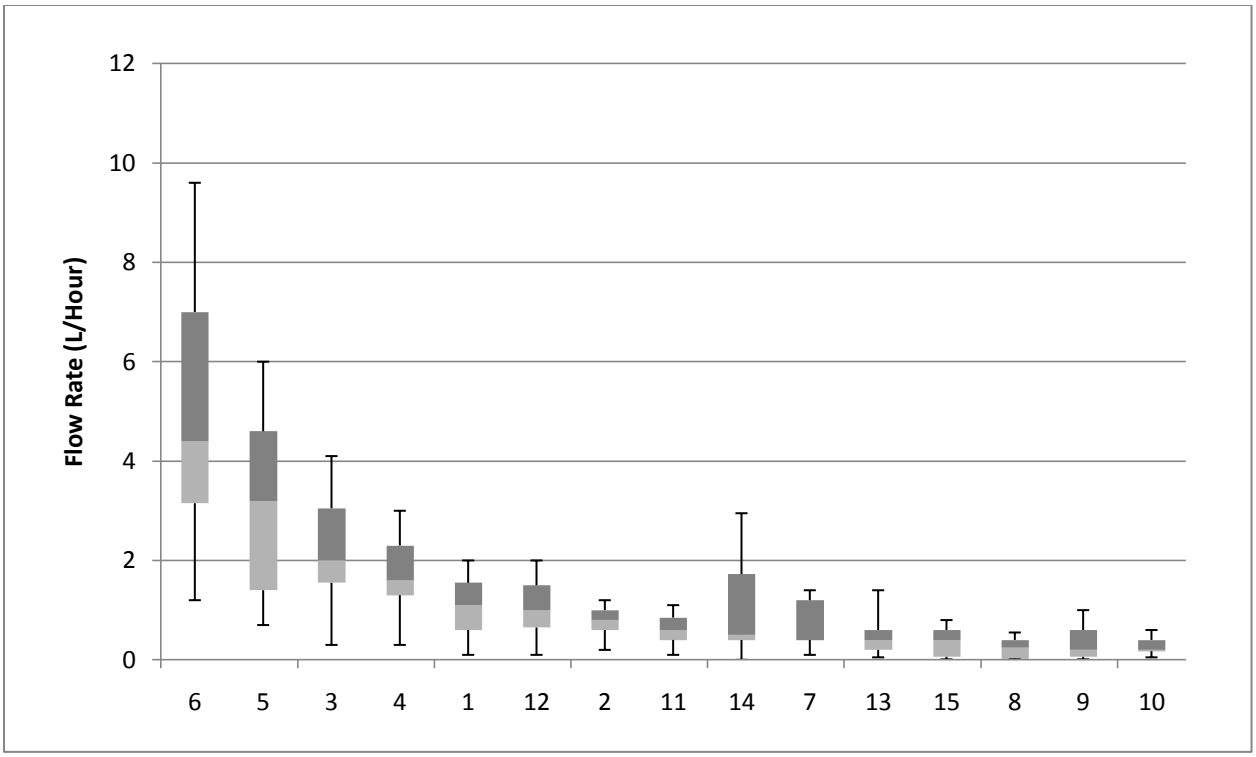

Figure 5-47: Flowrate of Filter Pairs 1-15, Largest to Smallest Median

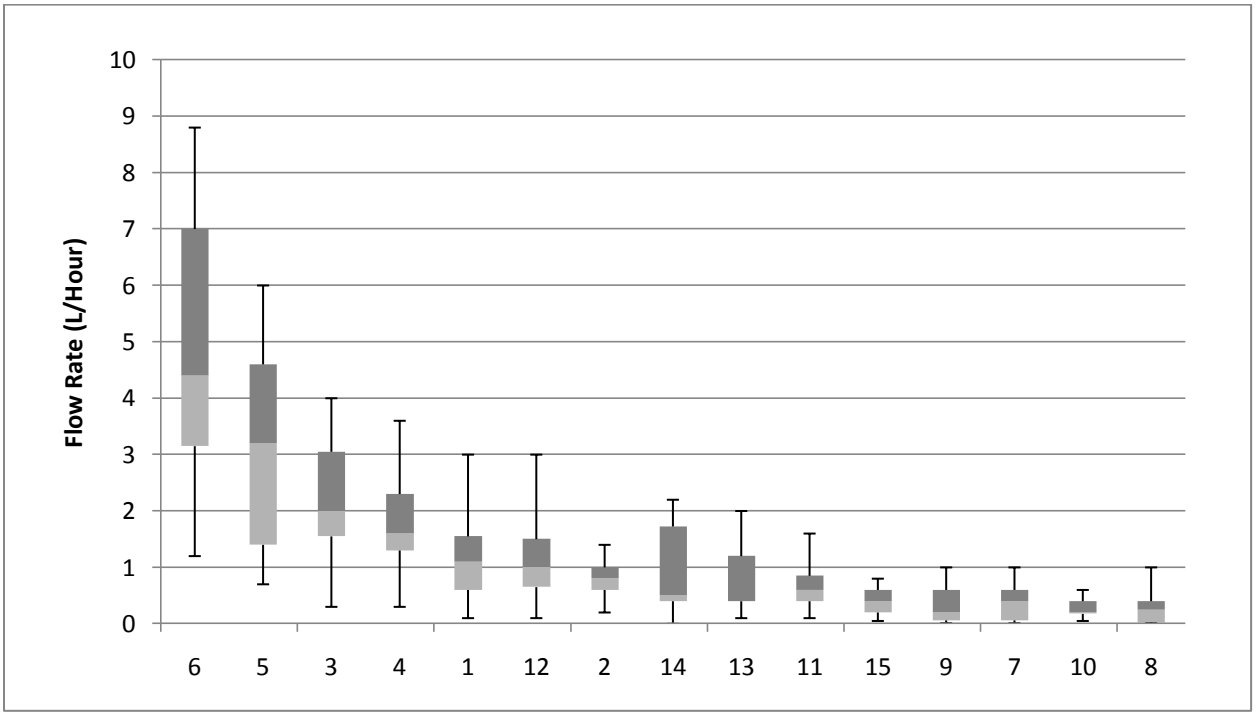

Figure 5-48: Flowrate of Filter Pairs 1-15, Largest to Smallest Mean

5.6.1 Effect of Combustible Type on Flowrate

Figure 5-49 presents average flowrate compared to influent turbidity over time, while Figure 5-50 compares average flowrate to influent turbidity directly. Figure 5-51 presents a box and whisker chart comparing flowrate sorted by combustible type. As with Total Coliform Removal data above in Section 5.1.1 and Turbidity Removal data in Section 5.3.1, the rice husk data used in Figure 5-51 was multiplied by a factor of 70,393/72,857 to provide equal comparison based on total volume of combustible, calculated using uncompacted lab densities, added to filters 1 through 12. Results of an estimation of the difference of the two means of the populations of the flowrate data for rice husk filters 1 through 6, normalized for total combustible volume, and sawdust filters 7 through 12 with a 95% confidence interval:

> LCL: 1.314643, UCL: 1.962045
> Mean of the rice husk filters' flowrates is greater than the mean of the sawdust filters' flowrates by1.31 to 1.96 L/ hour.

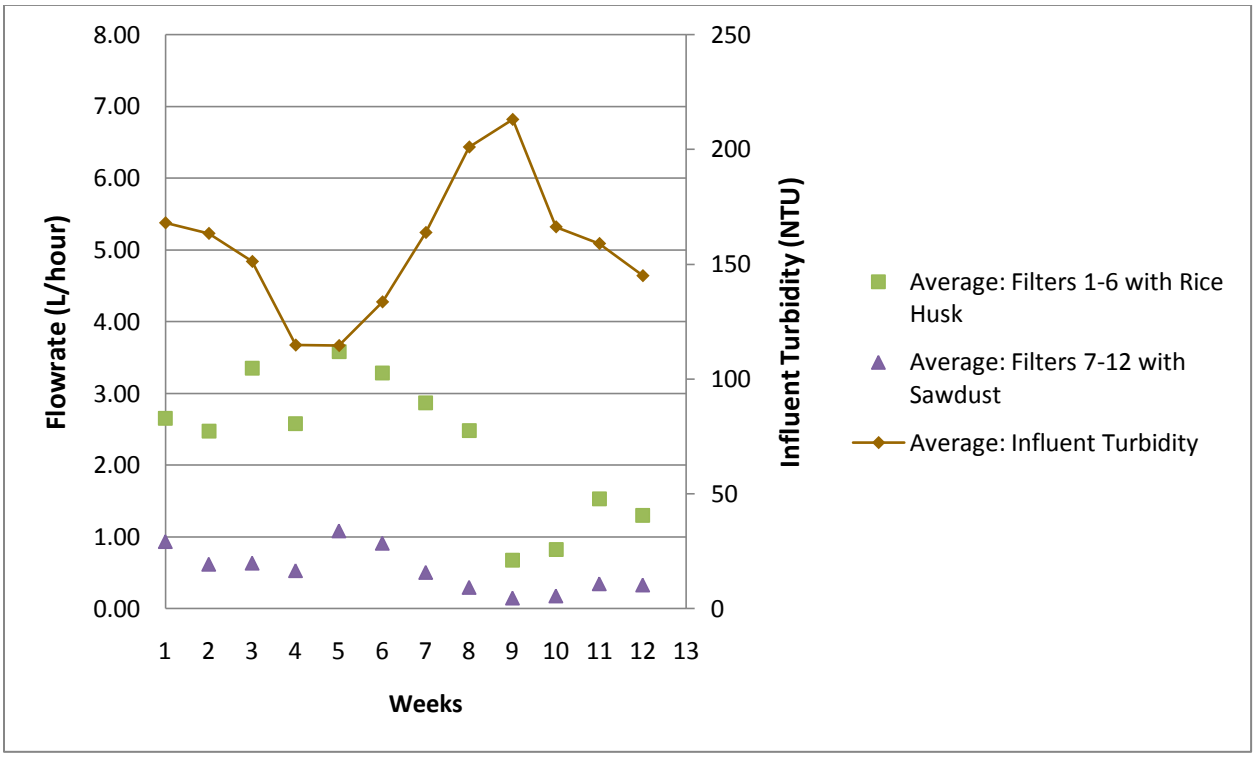

Figure 5-49: Average Flowrate over Time Compared to Influent Turbidity, Filters 1-12 by Combustible Type

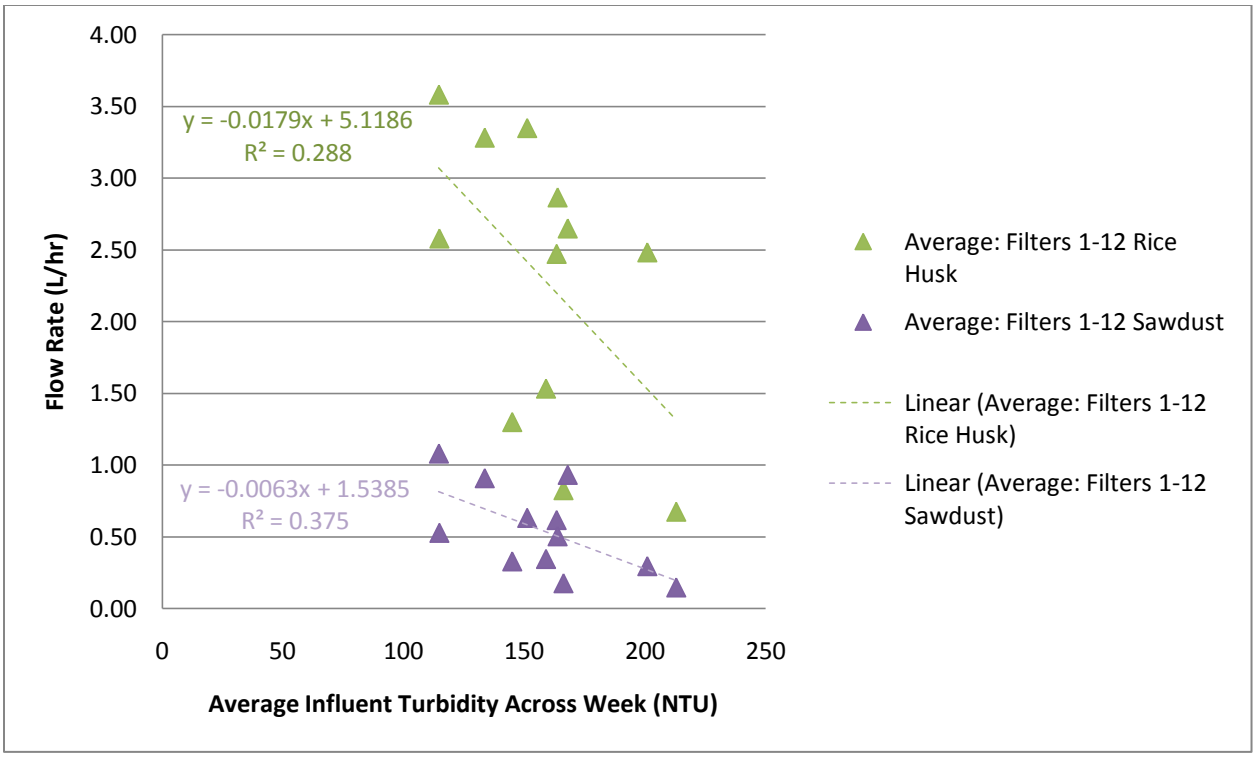

Figure 5-50: Average Flowrate Compared to Influent Turbidity

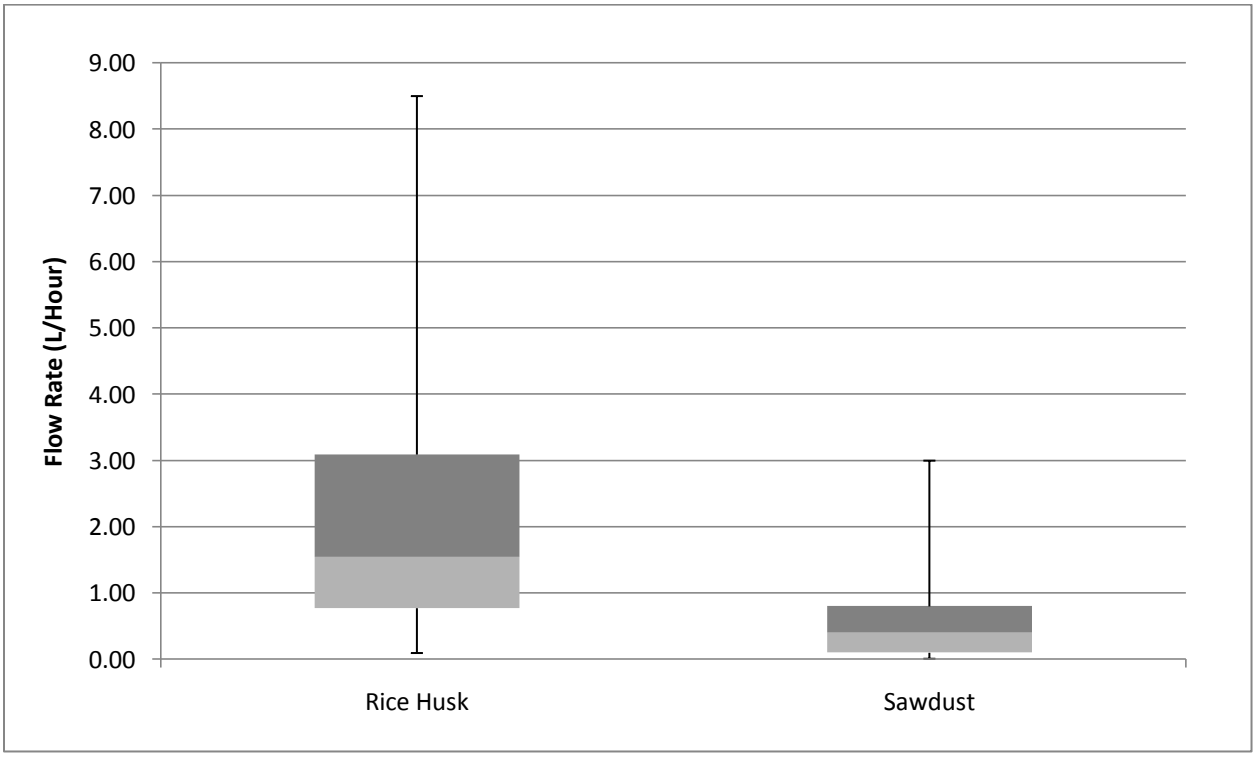

Figure 5-51: Flowrate, Filters 1-12 by Combustible Type, Normalized

5.6.2 Effect of Combustible Percentage by Mass on Flowrate

Figure 5-32 presents a box and whisker chart of filter flowrates by increasing mass, sorted by combustible type. A series of two-sample T-tests assuming unequal variances with 95% confidence showed a direct relationship between increasing flowrate and increasing percent combustible by mass for filters 1 through 6 with rice husk. A similar relationship was not found for filters 7 through 12 with sawdust, however, the two filters with the highest percent combustible by mass, 11 and 12, had statistically higher flowrates than the other four filters with lower percent combustible by mass.

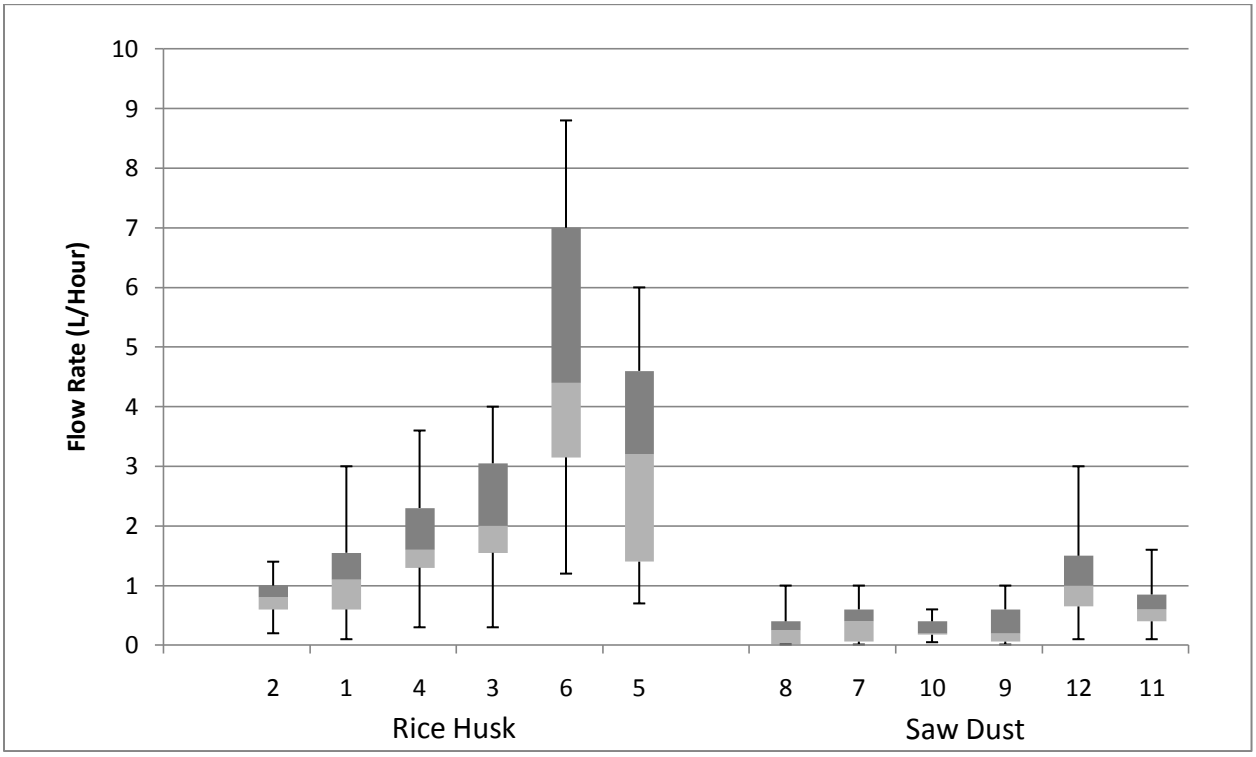

Figure 5-52: Flowrate of Filter Pairs 1-12, Increasing Percent combustible by mass, Sorted by Combustible Type

5.6.3 Effect of Addition of Grog on Flowrate

Figure 5-53 compares flowrate and influent turbidity over time, while Figure 5-54 compares flowrate directly to influent turbidity. Figure 5-55 presents box and whisker charts of flowrate sorted by filters with and without grog. Results of an estimation of the difference of the two means of the populations of the flowrate data for odd-numbered filters 1 through 12 without grog, and even-numbered filters 1 through 12 with grog a 95% confidence interval:

LCL: -0.6581, 0.129083
No confidence of a difference between the means.

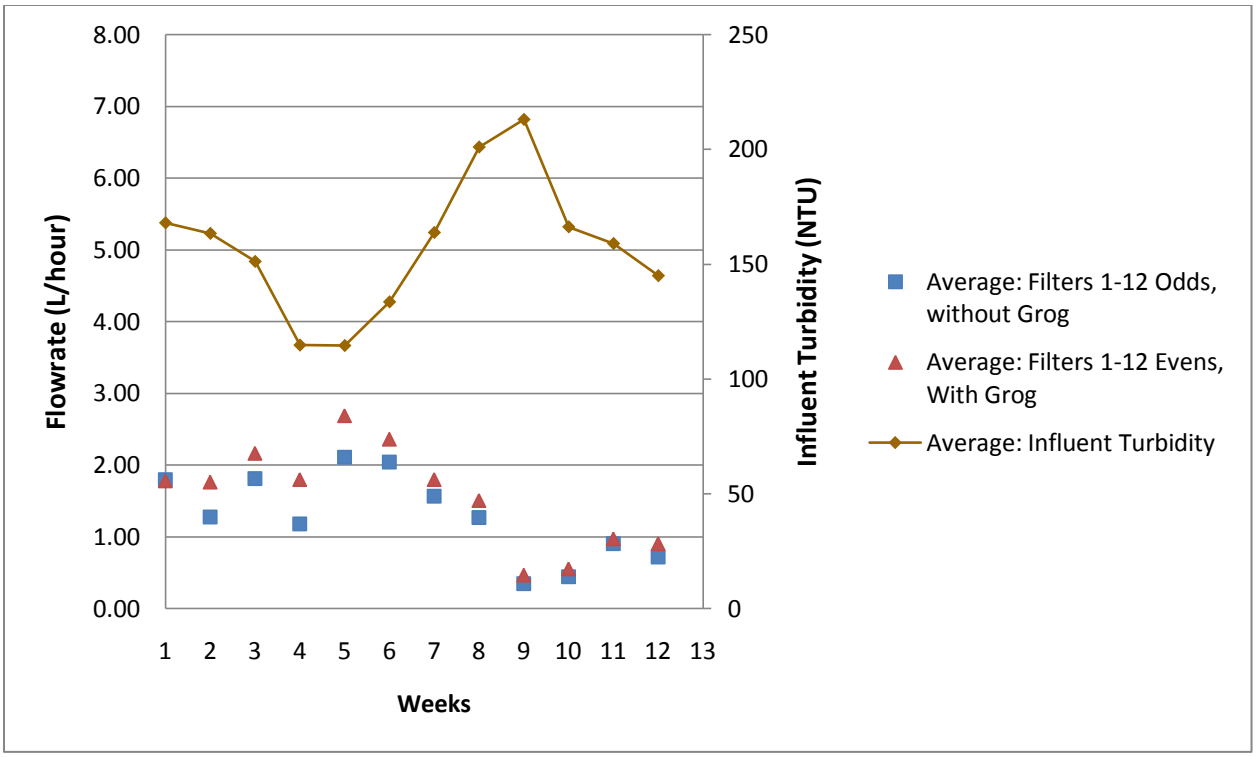

Figure 5-53: Average Flowrate over Time Compared to Influent Turbidity, Filters 1-12 With or Without Grog

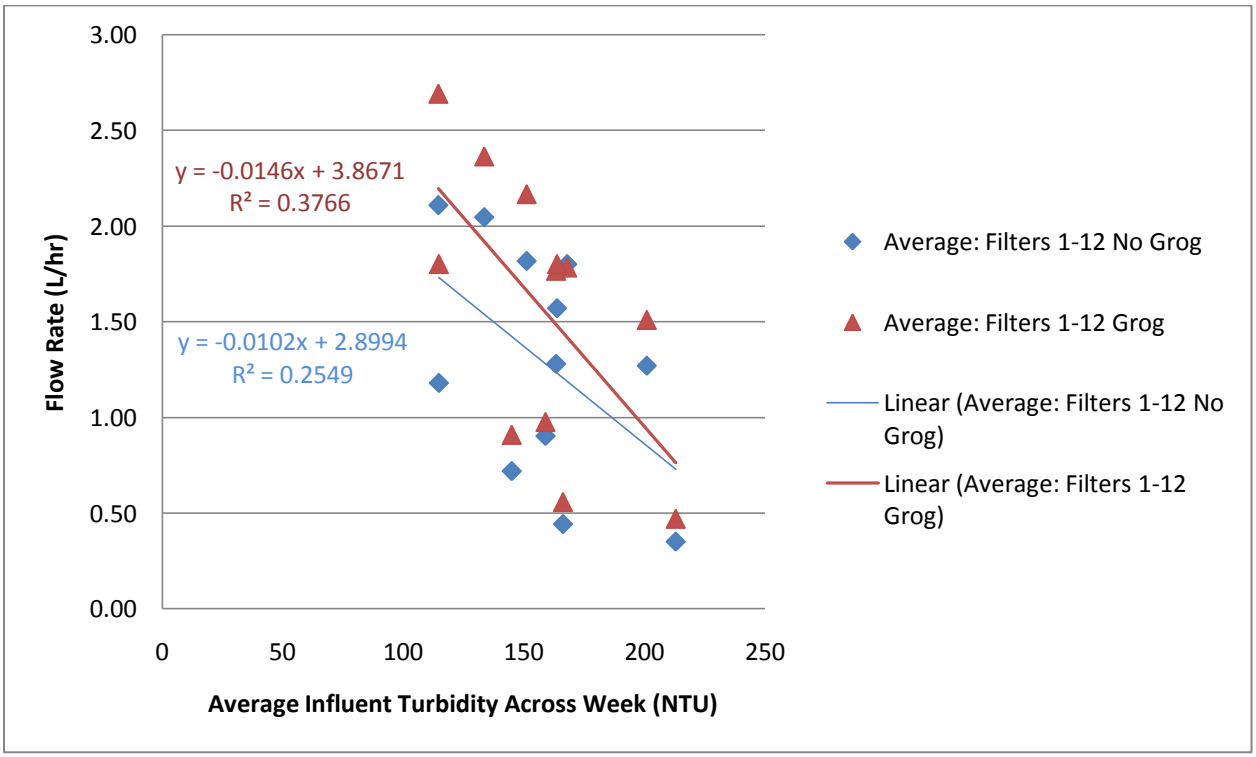

Figure 5-54: Average Flowrate Compared to Influent Turbidity, By Combustible Type

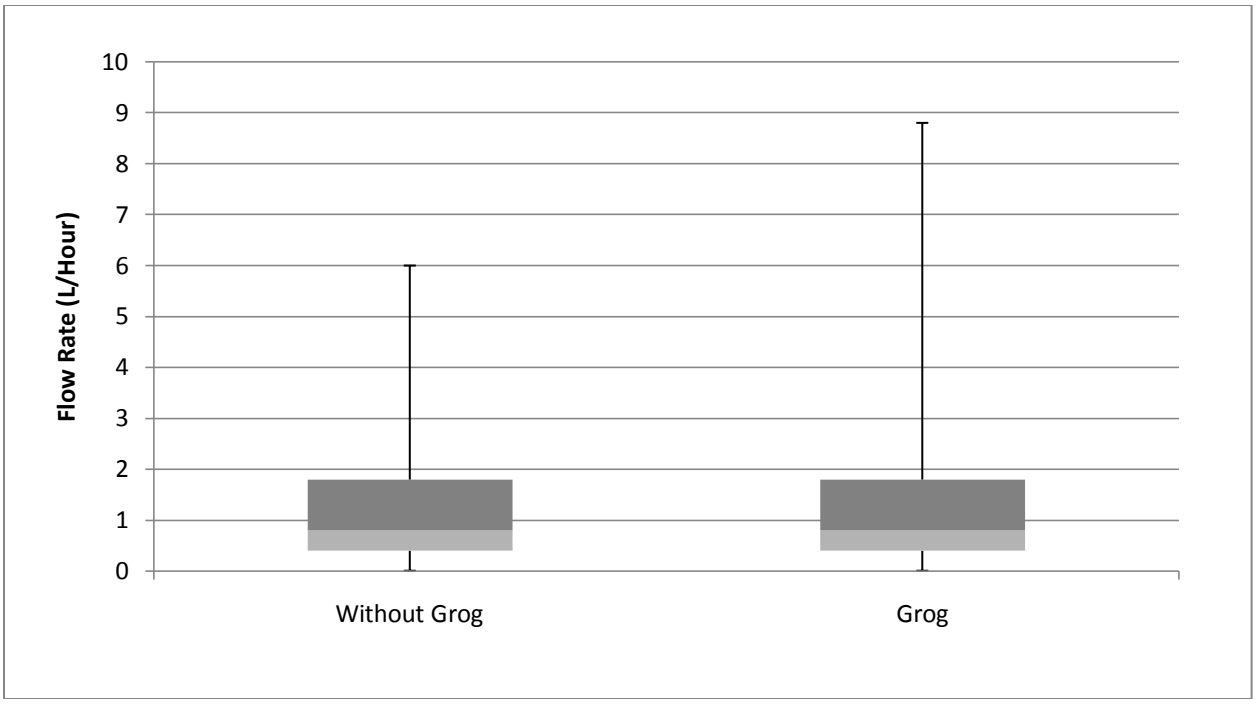

Figure 5-55: Flowrate of Filters 1-12, With or Without Grog

5.6.4 Effect of Additional Variables: Sifted Combustible and Shape

Method of Preparation of Rice Husk Filters:

Results of an estimation of the difference with independent samples of the two means of the populations of the flowrate data for filter pair 1 and filter pair 14 with the following confidence intervals:

95% Confidence Interval	No evidence in a difference of means.
90% Confidence Interval	No evidence in a difference of means.
80% Confidence Interval	The mean of filter pair 1 is greater than the mean of filter pair 14 by 0.049 to 0.726 L/hour.

Method of Preparation of Sawdust Filters:

Due to the small sample size of filter pair 13 (3 events), no conclusions can reasonably be drawn.

Shape of Filters:

Results of an estimation of the difference with independent samples of the two means of the populations of the Total Coliform Removal data for filter pair 2 and filter pair 15 with the following confidence intervals:

95% Confidence Interval	The mean of filter pair 2 is greater than the mean of filter pair 15 by 0.13 to 0.30 L/hour.
90% Confidence Interval	The mean of filter pair 2 is greater than the mean of filter pair 15 by 0.16 to 0.44 L/hour.
80% Confidence Interval	The mean of filter pair 2 is greater than the mean of filter pair 15 by 0.19 to 0.41L/hour.

5.7 Comparison of Filters within Filter Pairs

Table 5-12 presents the results of two-tailed tests of the differences between the population means of matched events of filters A and B in a pair with a 95% confidence interval. "Equal Means" demonstrates that there is not enough evidence to reject the null hypothesis that the population means are equal. "Unequal Means" demonstrates that there is enough evidence to reject the null hypothesis that the population means are equal.

Table 5-12: Comparison of Means of Performance Measurements for Filters within a Filter Pair

Pair	Total Coliform LRV	E. Coli CFU/100mL	Turbidity Removal	Flowrate
1	Equal Means	Equal Means	Equal Means	Unequal Means
2	Equal Means	Equal Means	Equal Means	Equal Means
3	Equal Means	Equal Means	Equal Means	Unequal Means
4	Equal Means	Equal Means	Equal Means	Unequal Means
5	Equal Means	Equal Means	Equal Means	Unequal Means
6	Equal Means	Equal Means	Equal Means	Unequal Means
7	Unequal Means	Equal Means	Unequal Means	Unequal Means
8	Equal Means	Equal Means	Unequal Means	Unequal Means
9	Equal Means	Equal Means	Equal Means	Unequal Means
10	Equal Means	Equal Means	Equal Means	Equal Means
11	Equal Means	Equal Means	Unequal Means	Equal Means
12	Equal Means	Equal Means	Unequal Means	Equal Means
14	Equal Means		Unequal Means	Equal Means
15	Equal Means	Unequal Means	Equal Means	Unequal Means

6.0 Discussion of Optimal Removal and Flowrate Study Results

6.1 Characterization of Filter Inputs

6.1.1 Filter Input Material Densities

The calculated densities of materials in Section 5.1.1 depended on the method of compacting the materials prior to mass measurement. There are two practical purposes for calculating these densities. The first is so that people making batches of filters at factories can consistently achieve the desired percent combustible by volume, because volume of the voides and therefore volume of the combustible dictates porosity, by determining the mass of the combustible to be added through a density calculation. Mass is much easier and more accurate to find repeatedly as compared to volume. For this purpose, an uncompacted, dry density determined by accurate scales and standardized equipment for measuring volumes is useful. The difference in equipment, and degree of settling due to tapping changes the calculated dry density. A standard technique could remove some of this variation.

The second practical purpose is so that the total porosity of a filter can be predicted based on the mass on input materials. When the materials are mixed together dry, then kneaded together when saturated with water, there is little to no air space left between the particles; the dry, uncompacted method does not represent the volume occupied by a mass of these wet, kneaded particles. The manual compaction method was imperfect in that the amount of pressure applied to the materials was inconsistent, and the sawdust did not compact easily.

For clay, the specific gravity test is very accurate in determining the density of saturated clay particles. This method could be modified for use with grog and other combustible materials. Distilled water was used as the medium for dissolution in the clay specific gravity tests; in order for the combustibles to be tested in this manner, a much less dense liquid must be substituted for water so that the combustibles do not float. Kerosene is another liquid typically used in specific gravity tests; kerosene should be tried, and if it does not work, another low-hazard low-density liquid should be substituted.

6.1.2 Scanned Images of Filter Input Materials

The method of scanning images of filter input materials, Figures 5-1 through 5-8 in Section 5.1.2, proved to be powerful in demonstrating the range of particle sizes present in each type of combustible materials. The size of the combustible material predicts the size of the pores that will be created in the filter. Lantange (2001) describes results of scanning electron microscope analysis of pores in a filter as having isolated cracks and spaces measuring 0.15mm x 0.50mm, with connected pores in the 0.0006mm to 0.003mm range. A goal of a 0.001mm pore size was set by the organization Potters for Peace for purposes of bacteria screening.

Perhaps the larger particles created isolated pores that did not contribute to the flow. However, when the combustibles combust, the gases produced must either escape from the filter body or remain compressed in the isolated space. If the gases escape, they create a pore in their wake; whether or not this pore is interconnected from the interior to exterior of the filter is important.

Most of the material created by the hammermill appears to be much greater in size than the goal of 0.001mm pores. The rice husk material from the waste chute, Figure 5-1, all appears to be on the order of 1mm, 10^3 times greater than the goal. The rice husk material from the fine chute, Figure 5-2, includes smaller material, whose size is unknown. The fine rice husk tends to

stick to itself; the particles may agglomerate in the clay and combustible mix. The sawdust material from the waste chute, Figure 5-4, appears to include particles on the order of 2mm, $2x10^3$ times greater than the goal. The sawdust material from the fine chute, Figure 5-5, also includes smaller materials, but includes longer pieces as well. Even the fine, sifted sawdust material includes longer pieces. The initial rice husk particles are wider than the angular initial sawdust pieces, so the rice husk particles are more likely to be retained when sifted through a screen of mesh size comparable to their width.

6.1.3 Filter Input Material Particle Size Distribution

The particle size distributions of clay, grog, and most combustible materials can be found in Section 5.1.3. It is unfortunate that the fine rice husk material was not able to be tested due to the fines plugging the holes in the #40 sieve; another method would be useful. The waste sawdust appears to have a smaller median diameter than the rice husk. The ability of some angular sawdust pieces to pass through sieves smaller than their longer dimension probably contributed to the apparent smaller median diameter.

The clay has a larger median diameter than grog. This is likely due to the presence of small pebbles in the natural clay that were not present in the grog. The small pebble-like grog particles are due to incomplete grinding by mortar and pestle.

6.1.4 Clay Characterization

The characterization of the clay can be found in Section 5.1.4. Clay with higher plasticity, described by the plasticity index (PI) may be useful for creating filters (Oyanedel-Craver and Smith, 2008). Ideally, clay for a filter would hold together with a lower water content, represented by a lower plastic limit, and not slump once pressed due to a high water content, represented by higher liquid limit. A high liquid limit is especially useful when attempting to improve the flowrate by increasing the percentage of combustible, because the amount of water added to the mixture must also increase with more combustible. The high amount of combustible, and therefore large amounts of water, added to filters 5, 6, 11 and 12 made it difficult for the pots to keep their shape; the potters did not like to make filters 11 and 12 especially. The highest plasticity index (PI) described by the Unified Soil Classification System, ASTM Standard D2487 – 10, is 60 whereas the clay from Gbalhai has a PI of 13.3.
If other clay sources are proven to have a higher plasticity index, they will likely be preferable to the clay currently being sourced at Gbalhai.

6.2 Filter Lip Total Porosity

The indirect method of determining volume for calculating total porosity of the filter lip pieces described in Section 4.5.2.2 is simple and more accurate than the direct method of determining volume, demonstrated by smaller standard deviations. The use of an accurate scale versus the use a flask and pipette with an imprecise location of the bottom of the meniscus accounts for the better accuracy. Ideally, more pieces from more locations on the filter would be tested for precision. It is reasonable to assume that the volume of the pore water does not contribute to the volumetric displacement of the saturated filter piece in an appreciable way; any water that hypothetically was to flow out of the pore would create a vacuum in the absence of air, which is physically nearly impossible under the open air conditions. Therefore, the formula used is likely accurate.

The calculations of total porosity based on the mass of input materials and their densities, found in Section 5.2, are very similar to the calculations of total porosity based on measurements. All of the former calculations report higher total porosities than the latter calculations. Surprisingly, the calculations based on densities determined in the field with uncompacted material agree with the measured total porosities the best. Since the total porosity can be considered a ratio of combustible volume to total filter volume, the better agreement between uncompacted density data may be due to consistent volume and mass measurement techniques for all input materials. Perhaps if densities of the combustibles were also determined using specific gravity techniques, the total porosities calculated from those densities would agree better with the measured data.

It is also interesting to note that total porosities measured with the indirect volume method did not follow the same trend of those measured with the direct volume method with regards to the incorporation of grog, or the recipes calculated with material densities. The total porosities measured with the indirect volume method showed that the porosity of a filter increased with grog, while the other methods showed a decrease in porosity with grog, with few exceptions. This suggests that grog creates different pore structures or larger pores when added.

6.3 Total Coliform Removal

Total coliform removal is a measure of a water treatment technology's microbial removal performance. In comparison to other studies, the filters in this study, whose results are in Section 5.3, performed similarly. The range of conservative total coliform log removal values found in this study was from 0.19 LRV to 4.30 LRV. Klarman (2009) reported total coliform log removal values (LRVs) for filters manufactured in the Dominican Republic in the range of 0.5 LRV to 3.8 LRV, with influent total coliform counts of 535 CFU/100mL to 11,567 CFU/100mL. van Halem (2006) reports that filter from Ghana, Nicaragua and Cambodia had total coliform log removal values in the range of 1 LRV to 4 LRV using canal water, with influent total coliform counts of 7 CFU/100mL and 2100 CFU/100mL. Bloem et al. (2008) did not present results for total coliform log removal.

6.3.1 Effect of Combustible Type on Total Coliform Log Removal

Although as a group filters with rice husk were not found to have statistically better in total coliform log removal than filters with sawdust in Section 5.3.1, all of the filter pairs in the highest three tiers contained rice husk. Filter pair 6, which also contains rice husk, was an exception in that it was in the lowest tier. It could be implied that the rice husk produces pores that are better able to screen coliform from the filtered water. Perhaps the angular nature of the larger sawdust pieces which were present in all of the sawdust types created opportunistic flow pathways that permitted more coliform to pass through than pathways created in rice husk filters.

6.3.2 Effect of Combustible Percentage by Mass on Total Coliform Log Removal

Surprisingly, the mass of combustible in the filter recipe did not statistically impact the total coliform log removal in Section 5.3.2; one would expect that a lower percentage of combustible by mass would lead to a smaller effective pore size and thus higher total coliform log removal. When combustible is present in the filter in higher concentrations, the likelihood that particles will be touching is increased. In such a scenario, the resulting pore space would be larger than an isolated particle, which could impact the ability of the pore to screen coliforms. This result suggests either that the percentage of combustible by mass is not great enough for the

particles to be touching and creating larger pores, or that the larger pores created are still small enough to remove coliforms.

6.3.3 Effect of Addition of Grog on Total Coliform Log Removal

The addition of one part grog to eleven parts clay was shown not to statistically influence total coliform log removal in Section 5.3.3. This is a low proportion of fine grog, however, and a higher proportion that is more coarsely ground might prove influential. The theoretical background to this suggestion is that the addition of grog changes the pore structure of the filter in such away as to allow for enhanced flow while retaining removal. The fines in the grog likely did not affect the pore structure in a meaningful way. The larger grog particles present may have changed pore structures, but not in an appreciable way.

6.3.4 Effect of Additional Variables: Sifted Combustible and Shape on Total Coliform Log Removal

Neither of the additional variables, sifting hammermilled rice husk or paraboloid shape impacted the total coliform removal in Section 5.3.4. Although the particle size distribution of the fine rice husk material is not known, the scanned images demonstrate that the fine and sifted materials have similar compositions, though the waste rice husk material is quite different and was expected to influence results. The paraboloid shape is not expected to influence removal.

6.3.5 Comparison of Sampling Methods for Total Coliform Log Removal

The potential impact of chlorine residual on coliform count inside the flowrate container used to collect the filtered water was tested, as described in Section 5.3.5. Had the results of membrane filtration testing on samples of filtered water collected in sterile Whirl-Pak® bags shown higher counts of total coliforms than results of membrane filtration testing on samples of the same filtered water collected in the flowrate container, it could be concluded that the chlorine residual impacted the coliform count. However, the majority of the coliform counts from both the flowrate container and the Whrilpak® bags were negative. There is no evidence of a statistical difference in the means of the filtered water total coliform counts for one week of filtering. Still, the result would be more robust had there been total coliform counts within the acceptable range for counting (20 to 200) and the two methods produced equivalent counts.

6.4 *E. coli* Removal

The *E. coli* removal results can be found in Section 5.4. The low influent *E. coli* concentrations for most of the study make it difficult to comment on the ability of the filters to remove *E. coli.* Out of 323 filtered water membrane tests for *E. coli*, only 7 tests produced non-zero results. Of those 7, only two tests produced *E. coli* counts that entered into the WHO intermediate risk level of 10 CFU/100mL to 100 mL/100mL, though influent water was in the intermediate risk category for 72 out of 323 filter tests. Therefore, only the effect of combustible type was tested because there was an opportunity to test statistical difference because all but one of the non-zero filtered water membrane tests was from water filtered through filter created with rice husk.

It is difficult to compare the performance of these filters at reducing *E. coli* due to the very low influent *E. coli* concentrations. Klarman (2009) excluded *E. coli* removal data from her report due to influent *E. coli* concentrations consistently below 5 CFU/100mL. Several other researchers spiked their influent water to demonstrate the potential removal capacity of the filters

in extremely contaminated waters. Bloem (2008) found that the raw influent water contained 5 to 26 CFU/100mL, and thus spiked the influent water periodically with *E. coli* in the range of 10^3 to 10^6 CFU/mL. Filters with colloidal silver achieved *E. coli* log removal between 4 LRV and 8 LRV. van Halem (2006) spiked the influent water with *E. coli* such that it had concentrations in the range of >266 CFU/100mL to 1.39×10^7 CFU/100mL. *E. coli* log removal between was achieved by a set of filters between 2LRV and 7.99LRV.

6.4.1 Effect of Combustible Type on *E. coli* Removal

The statistical observation that the rice husk filters outperform sawdust filters in *E. coli* removal in Section 5.4.1 is consistent with the observation for rice husk filters aside from filter 6 for total coliform removal.

6.4.2 Comparison of Sampling Methods for *E. coli* Removal

The results of the comparison can be found in Section 5.4.5. The *E .coli* count during the week of comparison sampling was found to be 0 CFU/100mL. The result that all of the samples from either sampling method had counts of 0 CFU/100mL as well supports the notion that there is a lack of contamination in the sampling methods, but does not confirm that the flowrate container method does not reduce the *E. coli* count as a result of chlorine residual in the container.

6.5 Turbidity Removal

Results in Section 5.5 demonstrate that the filters performed very poorly at removing turbidity from the influent water. The WHO (2004) reports that water with turbidity below 5 NTU is generally acceptable, but it should be below 0.1NTU for effective disinfection. None of the filtered water samples met drinking water secondary standards. Also, it seems that the turbidity removal of the filters correlates well with the influent turbidity.

The "dugout" from which the influent water came is consistently very turbid, implying that the water contains fines which are not easily settled. It would have been preferable to use a hydrometer analysis to determine the particle size distribution of the fines suspended in the water. The effective particle size from the analysis could be compared to the filter pore size.

Johnson (2007) reported that ceramic water filters manufactured in Accra and sold by Pure Home Water in Northern Ghana from 2005-2007 were capable of reducing on average 92% of turbidity, with a resulting average filtered water turbidity of 11NTU. The filters studied by Johnson (2007) greatly outperform the turbidity removal of filters in this study, though they have similar total coliform removal. Klarman (2009) found that all of the influent water in the Dominican Republic had turbidity below 5 NTU, which is quite a different scenario from the Ghanain dugout water. Bloem (2008) did not report turbidity removal, as influent turbidity was less than 13 NTU in Cambodia. van Halem (2006) demonstrated that for influent turbidity of canal water between 8 NTU and 31 NTU, the average effluent turbidity for all filters was less than 2 NTU.

6.5.1 Effect of Combustible Type on Turbidity Removal

It is an interesting phenomena that the filters with sawdust outperform the filters with rice husk in turbidity removal, but not in total coliform removal, as shown in Section 5.5.1. One would anticipate that pore size screening is mainly responsible for removal of both turbidity and total coliform, though the colloidal silver also has an effect on the total coliform removal.

Across the 12 week study, the average turbidity of the filters with sawdust was 25NTU to 85NTU lower than the average turbidity of the filters with rice husk.

One possible explanation is that the less turbid water produced by sawdust filters results in a lower presence of fines on the membrane filtration filter paper. The turbidity of the diluted filtered water samples[9], of rice husk filters across the 12 week study had an average of 25NTU with a standard deviation of 23NTU. For sawdust filters, the average was 13NTU with a standard deviation of 13NTU. Particles present on the filter paper may interfere with the growth of colonies, and thus result in a false representation of actual coliform counts. Still, the turbid influent water resulted in very high total coliform counts on many occasions, suggesting that turbidity does not necessarily interfere with colony growth. It is possible though that those counts underestimate the total coliform count for the same water had the water been clear. Another possibility is that indeed the pores are smaller in the sawdust filters and are thus able to screen particles more effectively, but some property of the rice husk filters makes the colloidal silver more effective at inactivating total coliforms.

6.5.2 Effect of Combustible Percentage by Mass on Turbidity Removal

The combustible percentage by mass does not appear to have an effect on the turbidity removal in Section 5.5.2. Considering again that the pore size screening method removes both total coliform and turbidity, then this result is consistent with the absence of an effect of combustible percentage by mass for the total coliform removal as well.

6.5.3 Effect of Addition of Grog on Turbidity Removal

The addition of grog was not shown to have a statistical influence on turbidity removal in Section 5.5.3. As with total coliform removal, it is important to consider that in this study the 1:11 mass ratio of grog to clay is low, and a higher proportion might prove influential.

6.5.4 Effect of Additional Variables: Sifted Combustible and Shape on Turbidity Removal

Neither of the additional variables, sifting hammermilled rice husk or paraboloid shape impacted the turbidity removal in Section 5.5.4. The same reasoning in Section 6.3.4 regarding total coliform removal applies.

6.6 Flowrate

The flowrate of water through the filter is expected to be directly proportional to the size and quantity of the pores. The flowrates of the filters in this study can be found in Section 5.6.

6.6.1 Effect of Combustible Type on Flowrate

The rice husk filters flow significantly faster than the sawdust filters, suggesting that for the same volume of combustible added, the rice husk produces larger or more pores in Section 5.6.1. If that is indeed the case, then it supports the finding of poor turbidity removal by the rice husk filters. It does not support the better total coliform removal by rice husk filters.

6.6.2 Effect of Combustible Percentage by Mass on Flowrate

As expected, the flowrate results in Section 5.6.2 generally demonstrate an increase in flowrate with increasing combustible percentage by mass. This result may imply that percentages of combustible by mass in the range studied, 14.2% to 31.3% of total mass, do not

[9] Samples of water with high turbidity were diluted before being tested with the membrane filtration.

result in many particles touching each other creating larger pores because the removal results do not change with increasing combustible percentage by mass. Instead, the combination of these results suggests that increasing combustible percentage by mass in the range studied largely results in more small pores and few if any larger, overlapping pores.

6.6.3 Effect of Addition of Grog on Flowrate

Though proponents of the addition of grog suggest that the flowrate is increased due to the addition of grog, it was not shown to be the case at this proportion, as shown in Section 5.6.3. If the proportion of grog was increased or if it were ground more coarsely, it may have an effect

6.6.4 Effect of Additional Variables: Sifted Combustible and Shape on Flowrate

The lack of a statistically significant difference in Section 5.6.4 between the mean flowrates of rice husk filters with sifted and unsifted combustibles suggests that the particle size distributions of the two material types are similar, leading to similar pore sizes. The range of particle sizes appears to similar upon inspection of Figures 5-2 and 5-3. The higher flowrate of the flower pot shaped filter, filter 2, compared to the paraboloid shaped filter, filter 15, can be likely explained by differences in geometry; a comparison of two similar filters in low turbidity water showed the flower pot shaped filter to have a higher flowrate in Section 9.3.

6.7 Comparison of Filters within Filter Pairs

The differences between filters within filter pairs in Section 5.7 follow the trend of differences between groups of filters for each performance category. There was little statistically significant difference between groups of filters for total coliform log removal and *E. coli* counts; the filters within pairs were found to have equal means. There was statistically significant variation between groups of filters for turbidity removal and flowrate; several filters within filter pairs had different means for these performance categories. It would have been desirable to have a triplicate filter for more robust statistical conclusions. Still, it seems that the filters within a filter pair more or less perform similarly.

Part III: Flow Through the Paraboloid Shaped Filter
7.0 Previous Mathematical Models of Flow through Ceramic Filters

Several authors have modeled flow through ceramic filters utilizing Darcy's Law (7-1). Darcy's law considers flow through a cross-sectional area of a porous medium of a given thickness and hydraulic conductivity subject to a head of water.

$$Q = \frac{KAh}{t} \tag{7-1}$$

where:

- Q is the flow through the filter
- K is hydraulic conductivity of the side walls and bottom
- A is the cross-sectional area through which water flows
- t is thickness of the filter
- h is the head

Lantange (2001) presents a model, (7-2) and (7-3), created by Sten Eriksen in 2001 which considers the flower pot filter as a cylinder with a disk on the bottom. The variables used were adjusted from the original format to be consistent between all equations presented from multiple authors.

$$Q_S = \frac{K\pi D H_W^2}{2t_S} \tag{7-2}$$

$$Q_B = \frac{K\pi D^2 H_W}{4t_B} \tag{7-3}$$

where:

- Q_S is flow through the sides wall
- Q_B is flow through the bottom
- K is hydraulic conductivity of the side walls and bottom
- D is filter diameter
- t_S is thickness of the side walls
- H_W is height of the water
- t_B is thickness of the bottom

Lantagne (2001) observed that the majority of the treated water flows through the sides of the filters. This was done by painting a filter with impermeable paint on the sides and measuring the flow rate, and painting another filter with impermeable paint on the bottom and measuring the flow rate. The sum of the two flow rates did not sum to the flow through an unpainted filter, however. It is likely that storage in the filter walls affected this result. If the sides of the filter were painted and the filter was not saturated prior to the flow test, some of the water would have moved up into the unsaturated filter side walls; the volume of water collected would have then underrepresented saturated flow. Similarly, if the bottom of the filter was painted and the filter was not saturated prior to the flow test, some of the water would have moved into the bottom of the filter, again under-representing saturated flow.

Fahlin (2003) improved upon the model derived by Eriksen by allowing for a non-uniform head distribution for the side flow through the filter, and different hydraulic conductivities for the side walls and bottom as seen in (7-4). Fahlin (2003) comments that Darcy's Law may not reflect side flow as accurately as bottom flow without considering the difference in angle of the side wall versus the bottom (7-5).

$$Q_T = \frac{K_B A_B h}{t_B} + \frac{K_S A_S h_S}{t_S} \tag{7-4}$$

$$h_s = Fh \tag{7-5}$$

where:

- Q_T is total filter discharge
- K_B is hydraulic conductivity of the bottom
- K_S is hydraulic conductivity of the side walls
- A_B is surface area of the bottom
- A_S is surface area of the side walls
- t_B is thickness of the bottom
- t_S is thickness of the side walls
- h_S is the side head
- F is a factor from 0 to 1 representing the fraction of vertical head experienced at the side of the filter
- h is the vertical head

van Halem (2006) considered, like Fahlin (2003), that the flower pot filter was shaped like a truncated cone with a disk on the bottom and not a cylinder (7-6).

$$Q_T = \frac{K}{t_S} 2\pi \left(\frac{(r_T - r_B)}{6L} {H_w}^3 + \frac{r_B {H_w}^2}{2} \right) + \frac{K}{t_B} \pi {r_B}^2 H_w \tag{7-6}$$

where:

- Q_T is total filter discharge
- K is hydraulic conductivity of the side walls and bottom
- t_S is thickness of the side walls
- r_T is radius at the top of the filter
- r_B is radius at the bottom of the filter
- L is slant height along the exterior side wall
- t_B is thickness of the bottom
- t_S is thickness of the side walls
- H_W is height of the water

This equation (7-6) was used to model the flow of the filter at different heights and compare the model to experimental results. van Halem (2006) demonstrated that the material is "more or less homogenous" throughout the height of the filter using mercury intrusion porosimetry. This was confirmed because the model matched data from measurements of the flow rate at decreasing water level heights with filters from Ghana and Nicaragua.

Leftwich et. al. (2009) derived another equation for flow through a flower pot filter allowing for variation in the angle of the side wall with respect to the bottom (7-7). The approach is very similar to that of van Halem (2006), except that the change in radius with respect to height is expressed in an angle. Leftwich et. al. (2009) described a mass flowrate; for consistency with other authors an equation adjusted for volumetric flowrate is presented below. The original version (7-7) contains a mathematical error. The corrected version is presented below (7-8).

$$Q_T = K\pi H_W(t)\left[\frac{{r_B}^2}{t_B} + \frac{r_B H_W(t)}{t_S} - \frac{2(H_W(t))^2}{3t_S}\tan\theta\right] \quad (7\text{-}7)$$

$$Q_T = K\pi H_W(t)\left[\frac{{r_B}^2}{t_B} + \frac{r_B H_W(t)}{t_S} + \frac{(H_W(t))^2}{3t_S}\tan\theta\right] \quad (7\text{-}8)$$

where:

Q_T	is total filter discharge
K	is hydraulic conductivity of the side walls and bottom
$H_W(t)$	is the height of the water with time
r_B	is radius at the bottom of the filter
t_B	is thickness of the bottom
t_S	is thickness of the side walls
H_W	is height of the water
θ	is angle of deviation of the sidewall from the normal to the bottom

Leftwich et. al (2009) anticipated that this would be useful for analysis and optimization of the filter shape and material properties, including clay to sawdust ratios and suitable types of clay.

8.0 Model and Testing of Flow through Paraboloid Filter Methodology

8.1 Paraboloid Filter Geometry

8.1.1 Parabola

According to Wolfram Mathworld, a paraboloid is the "surface of revolution obtained by rotating a parabola about its axis of symmetry," and a parabola is "the set of all points in the plane equidistant from a given line L (the conic section directrix) and a given point F not on the line (the focus)."

8.1.2 Paraboloid

Wolfram Mathworld describes a paraboloid with the equations below. Note, though Wolfram Mathworld denotes radius as "a", here radius is denoted by "r" for consistency.

Quadratic surface of a paraboloid:

$$z = br^2 \tag{8-1}$$

$$r = \sqrt{x^2 + y^2} \tag{8-2}$$

$$r = \sqrt{z/b} \tag{8-3}$$

$$r = c\sqrt{z} \tag{8-4}$$

where:

z	is the height from the vertex
b	is a coefficient
x	is an x-coordinate
y	is a y-coordinate
r	is the radius
c	is $\sqrt{1/b}$

Surface area of a paraboloid:

$$A = \frac{\pi r}{6h^2}\left[(r^2 + 4h^2)^{3/2} - r^3\right] \tag{8-5}$$

where:

A	is the surface area
h	is the height along the z-axis from the vertex
r	is the radius at the height h

Volume of a paraboloid:

$$V = \frac{1}{2}\pi r^2 h \tag{8-6}$$

where:

V	is the volume
h	is the height along the z-axis from the vertex
r	is the radius at the height h

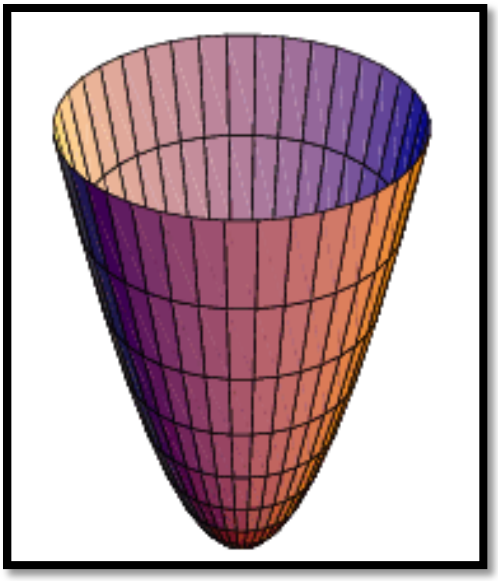

Figure 8-1: Paraboloid

8.1.3 Determination of Ghanain Paraboloid Filter Geometry

In order to use Darcy's law, it is useful to understand how the radius changes with height. The potter who made the cast for the mold for the paraboloid filter threw it on a potter's wheel; it was not made with equipment to ensure a precisely parabolic shape. To confirm that the shape is indeed that of a paraboloid, two simple laboratory studies were undertaken.

8.1.3.1 Determination of Radius Change with Height Using Water

Considering that the paraboloid filter actually has a paraboloid shape, and thus that the equation for volume applies, the radius at a known height and volume can be determined, as seen below.

$$r = \sqrt{\frac{2V}{\pi h}} \tag{8-7}$$

where:

V	is the volume
h	is the height along the z-axis from the vertex
r	is the radius at the height h

To determine the volume and the height, water of measured volume was poured inside the filter and the height of the water level was recorded. Up until 12cm from the bottom of the inside of the filter, 100mL of water was poured from a standard 100mL graduated cylinder into the lined filter, and the height of water was read from a steel ruler positioned vertically in the center. From 12cm to 22.3 cm, water was added in 200mL increments between readings due the difficulty in reading smaller changes in height on the ruler.

The filter was lined to prevent water from entering the pores of the filter and giving false volume measurements. It was first lined with Parafilm®[10], a thin waxy material often used to cover laboratory glassware. Afterwards, a plastic bag tested for leaks was placed into the filter.

[10] Parafilm ® is a "unique self-sealing, moldable and flexible film for numerous uses in the typical laboratory." SPI Supplies. http://www.2spi.com/catalog/supp/parafilm.php

The Parafilm® lining was necessary to reduce the roughness of the filter and prevent tears in the plastic bag.

Figure 8-2: Paraboloid Filter Lined with Parafilm®

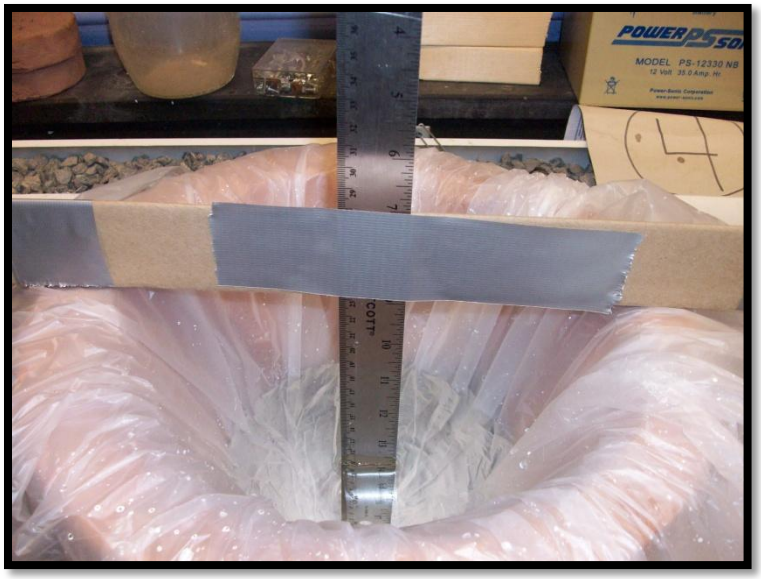

Figure 8-3: Filter lined with Parafilm® and Plastic Bag, Water Inside Measured by Ruler

The results were plotted, and fitted with a curve such that $r = c\sqrt{z}$ (Equation 8-4).

8.1.3.2 Determination of Radius Change with Height Using Cardboard Rings

The results in the previous section relied on the assumption that the filter had a paraboloid shape. To confirm those results, an additional approach was undertaken using circles of known radius placed at measured heights. Concentric circles were drawn on corrugated cardboard of measured thickness, and a slit for the steel ruler was drawn in the center. The circle with the largest radius was cut first, slid onto the ruler, placed inside the filter, and slid down the

ruler until it met with the interior of the filter. The height at the top of the cardboard was measured, and later adjusted downward to account for the thickness of the cardboard. The results were plotted, and fitted with a curve such that $r = c\sqrt{z}$ (Equation 8-4).

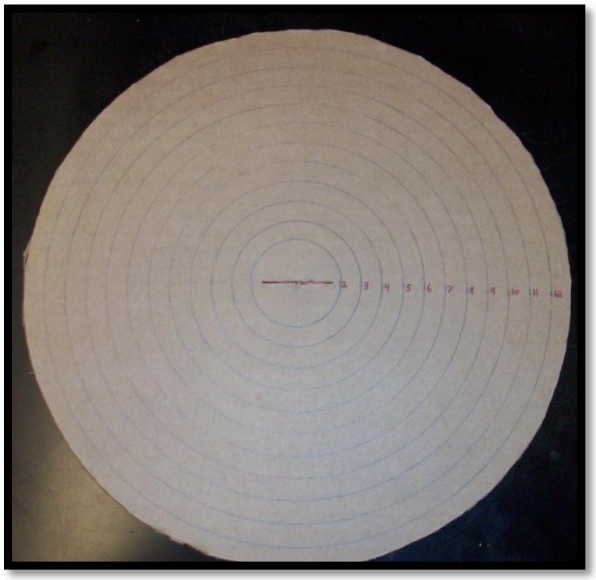

Figure 8-4: Concentric Circles and Slit Drawn on Corrugated Cardboard

Figure 8-5: Circle with 12cm Radius on Ruler Placed inside Filter

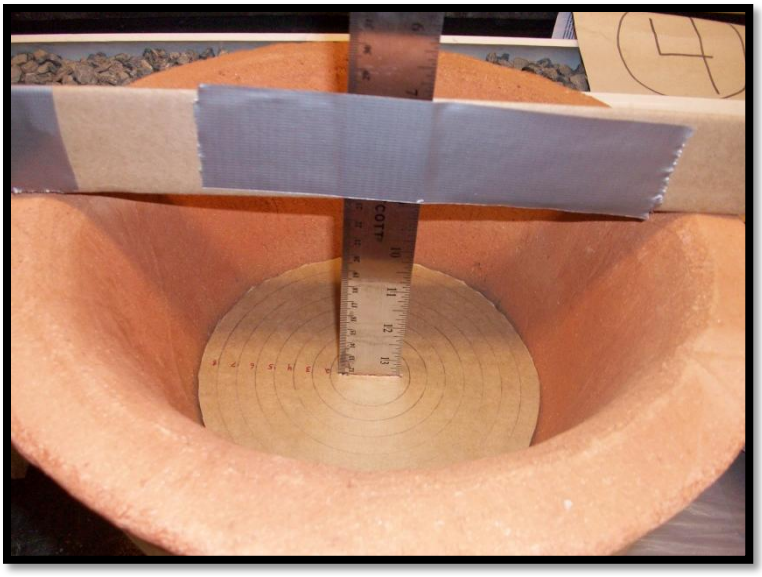

Figure 8-6: Circle with 9cm Radius on Ruler Placed inside Filter

Figure 8-7: Rings of Circle Remainders Placed Inside Filter

8.1.3.3 Determination of Radius Change with Height and Thickness Using Filter Slices

Initially, the thickness of the filter was assumed to be constant. Therefore, the thickness of the filter walls were thought to be equal to the thickness of the filter lips, which are more readily measurable. The filter was cut into slices in later experiments (Section 8.4.3), which provided an opportunity to measure the inner and outer radii and determine the change in thickness with radius and height.

8.2 Measurement of Flow through Paraboloid Filter

To observe how flowrate through the paraboloid filter changes with the height of the water, a trial was run. The filter was first saturated in a bucket of water for 24 hours. A clear flowrate container (Figure 4-33), the same type used to measure flowrate in Ghana, was placed

inside a clear 5 gal bucket. The filter was set on the edges of the clear bucket, and a ruler was positioned vertically inside the fitler, as was done during the determination of the change of radius with height. Water was added up to 21cm, the approximate height aligned with the bottom of the exterior filter lips; flow through the filter lips would have distorted results. The volume of water accumulated in the flowrate container was measured at every 1cm decrease in the height of the water inside the filter. When only a few centimeters of water remained, a clear plastic 1L beaker replaced the flowrate container to capture the remaining volume of water more accurately. Three drops from the bottom of the filter were lost during the change of containers, which was considered negligible. The test was stopped at around 4cm of water remaining because of the excessive time to filter the remaining water with such low head.

Figure 8-8: Left: Filter Set Inside Clear Bucket with Vertical Ruler Above Flowrate Container Right: Filter Set Inside Clear Bucket with Vertical Ruler Above 1L Beaker

8.3 Model of Flow through Paraboloid Filter

The first goal of developing the model is to determine the initial flowrate of the filter for a given starting height of water as a function of height. Filter factories typically report the flowrate of the filter based upon the volume of water collected during the first hour of flow, so this model is of practical significance. The second goal is to determine a representative hydraulic conductivity of the filter. Finally, the third goal is to determine if the hydraulic conductivity is constant throughout the filter.

8.3.1 Applying Darcy's Law to Paraboloid Filter

Previous work has modeled flow through ceramic filters according to Darcy's Law, which describes flow through a porous medium of a given thickness subject to a head. It is most simply applied to downward flow through a horizontal medium with a constant head. Darcy's Law will also be used to describe flow through the Paraboloid Filter, though it is subject to different geometry.

As a first approximation, it is reasonable to assume that the hydraulic conductivity is constant throughout the height of the filter. Comparisons to flowrate measurements with height can also help determine if the hydraulic conductivity is constant. Other factors may complicate the modeling of flow through filter walls, and likewise determination of hydraulic conductivity.

One such factor is the volume of water stored in the filter walls. Using equation (8-6) to determine the total volume of the filter walls excluding the lips, and considering the filter has average porosity of 45% (Section 9.4), there is roughly 0.98L of storage in the walls. This is significant, considering that the interior of the filter can hold roughly 6L of water. As the height of the water in the filter goes down, increasing amounts of filter wall become exposed. It is possible that water contained in the filter walls above the height of the water leaves the filter walls. During a test, this amount of water is added to the total volume of water assumed to be produced by the submerged portions of the filter wall, leading to an overestimate of the actual flowrate.

Another factor is the flow path of the water drops. The water will flow from high to low head, or from the inside of the filter to the exterior, where it coheres with other water drops and drips off the bottom of the filter. While water may not flow exactly perpendicular to the wall, and hence through the thickness, t, the assumption seems appropriate.

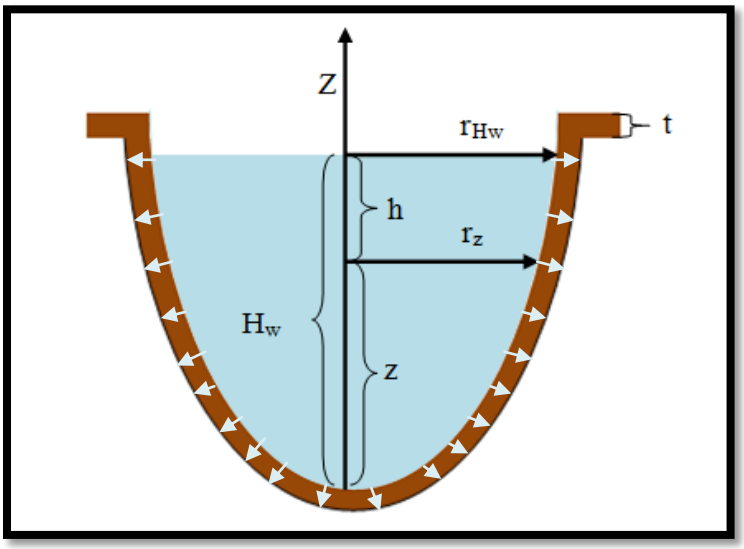

Figure 8-9: Paraboloid Filter with Relevant Dimensions and Modeled Flow Path

Darcy's Law for Paraboloid Filter with Constant Hydraulic Conductivity and Thickness

$$Q = \frac{K}{t}\int_0^{H_w} dA(z)\, h(z) \qquad (8\text{-}8)$$

where:

Q	is the flowrate
K	is the hydraulic conductivity
t	is the thickness
H_w	is the height of the water
dA	is the differential cross-sectional area through which water flows at height z
h(z)	is the head above height z

The head, h(z), above the height z is given simply by the difference between the height of water and height.

Head above Height Z

$$h(z) = H_w - z \tag{8-9}$$

The differential cross-sectional area through which water flows at height z, A(z), is the circumference of the circle at that height multiplied by an infinitesimally small slant height, dl. However, it is useful to perform the integral in terms of a differential height, dz, shown below.

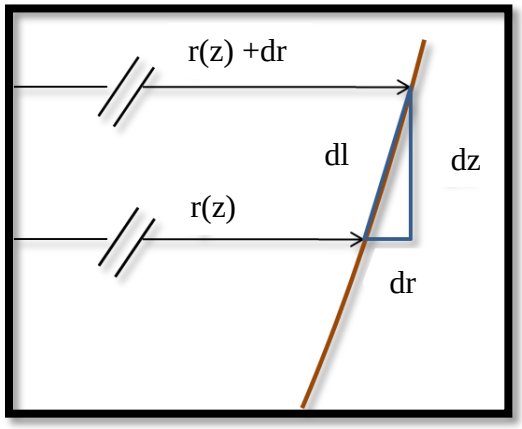

Figure 8-10: Close-Up View of Filter Side Wall

Differential Cross-Sectional Area

$$dA = 2\pi r(z) dl \tag{8-10}$$

Slant Height

$$dl = \sqrt{\left(\frac{dr}{dz}\right)^2 + 1}\, dz \tag{8-11}$$

First Derivative of Radius (Equation 8-4) with Respect to Height

$$\frac{dr}{dz} = \frac{c/2}{\sqrt{z}} \tag{8-12}$$

Differential Cross-Sectional Area, Expanded

$$dA = 2\pi c\sqrt{c^2/4 + z}\, dz \tag{8-13}$$

Darcy's Law for Paraboloid Filter with Constant Hydraulic Conductivity and Thickness, Expanded

$$Q = \frac{2\pi cK}{t} \int_0^{H_w} \sqrt{c^2/4 + z}\, (H_w - z) dz \tag{8-14}$$

The integral was solved using integration by parts.

$$Q = \frac{4\pi cK}{3t}\left[-H_w (c^2/4)^{\frac{3}{2}} + \frac{2}{5}\left((c^2/4 + H_w)^{\frac{5}{2}} - (c^2/4)^{\frac{5}{2}}\right)\right] \tag{8-15}$$

8.3.2 Comparison of Modeled Flow Through Paraboloid Filter and Flower Pot Filter

A comparison was made between the initial flowrate of a paraboloid filter and flower pot filter. The interior volume, height, thickness and hydraulic conductivity were kept constant between the two filters. The angle θ representing the divergence of the flower pot filter wall from normal was held constant when adjusting the dimensions of the flower pot filters used in Part II to agree with the constraints listed above for this comparison. The flow through the paraboloid filter was modeled using (8-15), and the flow through the flower pot filter was modeled using (7-6).

8.4 Determining the Hydraulic Conductivity with Height

Three approaches were used in order to determine if and how the hydraulic conductivity of the paraboloid filter changes over its height. Ideally, mercury porosimetry would have been used, but the machine was out of service.

8.4.1 Determining the Weighted Average Hydraulic Conductivity with Height

First, results from the laboratory test described in Section 8.2 were compared with results predicted by the model developed in Section 8.3. Still, in that test set-up, the volume of the water stored in the walls of the filter could complicate the results. The best fit hydraulic conductivity was found using Excel Solver so that the modeled flowrate matched the measured flowrate at a given height interval. In this way, the change in the weighted hydraulic conductivity over height can be observed. After cutting the filter into slices as described in Section 8.4.3, the thickness of the filter was found to decrease slightly from 2.0cm at the bottom to 1.5 cm at the top. Modeled hydraulic conductivity was found assuming both constant and linearly decreasing thickness with height.

8.4.2 Determining the Hydraulic Conductivity of Three Segments

The second approach also used the results from the laboratory test described in Section 8.2, but divided the filter into three segments of equal height.

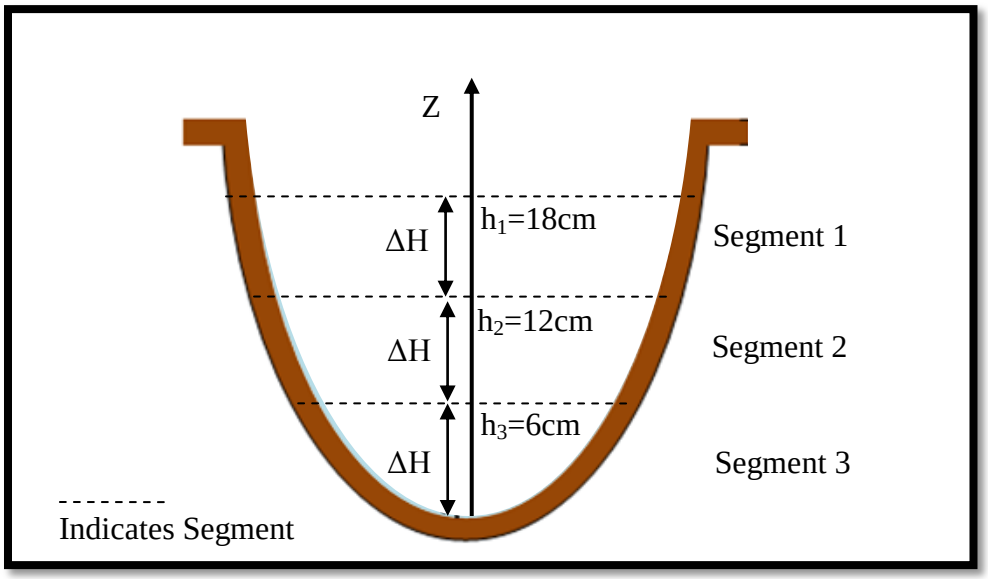

Figure 8-11: Paraboloid Filter Slices

This approach considers that during the first time interval, ΔT_1, when the water is at height h_1, water filters through segments 1, 2 and 3, and the volume that filters through is equal to the volume of segment 1. The second time interval, ΔT_2, begins when the water height reaches h_2 and water filters only through segments 2 and 3; again the volume that filters through is equal to the volume of segment 2. The third time interval, ΔT_3, begins when the water height reaches h_3 and water filters only through segment 3. As before, the volume the filters through is equal to the volume of segment 3.

The head, H_{ave}, experienced by each segment during each time interval is taken to be the average of the head at four positions: the head at the top and bottom of the segment at the beginning of the time interval, and the head at the top and bottom of the segment at the end of the time interval. The head at each position is a multiple of height between each segment, ΔH, which is 6cm for this filter. Darcy's law is applied to each segment for each time interval.

Flowrate for first time interval, ΔT_1.

$$\frac{V_{3,1}}{\Delta T_1} = \frac{K_3 A_3}{t} \frac{(3\Delta H + 2\Delta H + 2\Delta H + \Delta H)}{4} \tag{8-16}$$

$$\frac{V_{2,1}}{\Delta T_1} = \frac{K_2 A_2}{t} \frac{(2\Delta H + \Delta H + \Delta H + 0)}{4} \tag{8-17}$$

$$\frac{V_{1,1}}{\Delta T_1} = \frac{K_1 A_1}{t} \frac{(\Delta H + 0 + 0 + 0)}{4} \tag{8-18}$$

$$V_1 = V_{3,1} + V_{2,1} + V_{1,1} = \frac{\Delta H \Delta T_1}{t}\left(2K_3 A_3 + K_2 A_2 + \frac{K_1 A_1}{4}\right) \tag{8-19}$$

Flowrate for second time interval, ΔT_2.

$$\frac{V_{3,2}}{\Delta T_2} = \frac{K_3 A_3}{t} \frac{(2\Delta H + \Delta H + \Delta H + 0)}{4} \tag{8-20}$$

$$\frac{V_{2,2}}{\Delta T_2} = \frac{K_2 A_2}{t} \frac{(\Delta H + 0 + 0 + 0)}{4} \tag{8-21}$$

$$V_2 = V_{3,2} + V_{2,2} = \frac{\Delta H \Delta T_2}{t}\left(K_3 A_3 + \frac{K_2 A_2}{4}\right) \tag{8-22}$$

Flowrate for third time interval, ΔT_3.

$$\frac{V_{3,3}}{\Delta T_3} = \frac{K_3 A_3}{t}\left(\frac{\Delta H}{4}\right) \tag{8-23}$$

$$V_3 = V_{3,3} = \frac{\Delta H \Delta T_3}{t}(K_3 A_3) \tag{8-24}$$

The above equations are combined and solved for hydraulic conductivity, K, for each of the three segments.

$$K_3 = \frac{t}{A_3 \Delta H}\left(\frac{4V_3}{\Delta T_3}\right) \tag{8-25}$$

$$K_2 = \frac{t}{A_2 \Delta \mathrm{H}} \left(\frac{4V_2}{\Delta T_2} - \frac{16V_3}{\Delta T_3} \right) \quad (8\text{-}26)$$

$$K_1 = \frac{t}{A_1 \Delta \mathrm{H}} \left(\frac{4V_1}{\Delta T_1} - \frac{16V_2}{\Delta T_2} + \frac{32V_3}{\Delta T_3} \right) \quad (8\text{-}27)$$

The volume of each segment was determined using Equation 8-6 and subtraction. The surface area of each segment was found by integrating Equation 8-13, as shown below (8-28). The surface area calculated using (8-28) was found to be the same surface area calculated using equation (8-5).

$$A = \frac{4\pi c}{3} \left[\left(\frac{c^2}{4} + h_U \right)^{3/2} - \left(\frac{c^2}{4} + h_L \right)^{3/2} \right] \quad (8\text{-}28)$$

where:

A	is the area
c	is the coefficient
h_U	is the upper height
h_L	is the lower height

8.4.3 Determining the Hydraulic Conductivity of Filter Slices

The third approach attempted to measure the hydraulic conductivity of several sections of the filter directly. The filter was cut into horizontal slices, and the flow was measured for one hour with a constant head of water. In this way, the results were not affected by water stored in unsubmerged, exposed portions of the filter wall above the filter slice.

To calculate the flow through a slice of the filter, the same model is used as for an intact filter, but the bounds of the integral are changed to reflect the upper height, H_U, and lower height, H_L, of the section from which the slice of the filter came. Also, the height of the water H_W needs to be adjusted to reflect the head of water experienced by the slice, h, which is the height of the water in the bucket. The average thickness of each slice was used for t, thickness.

$$Q = \frac{2\pi c K}{t} \left[(H_w - z) \left(\frac{2}{3} (c^2/4 + z)^{\frac{3}{2}} \right) \Big|_{H_L}^{H_U} + \left(\frac{4}{15} (c^2/4 + z)^{\frac{5}{2}} \right) \Big|_{H_L}^{H_U} \right] \quad (8\text{-}29)$$

$$Q = \frac{4\pi c K}{3t} \left[\left((H_w - H_U)(c^2/4 + H_U)^{\frac{3}{2}} - (H_w - H_L)(c^2/4 + H_L)^{\frac{3}{2}} \right) + \frac{2}{5} \left((c^2/4 + H_U)^{\frac{5}{2}} - (c^2/4 + H_L)^{\frac{5}{2}} \right) \right] \quad (8\text{-}30)$$

$$H_W = H_U + h \quad (8\text{-}31)$$

The same paraboloid filter used in the previous flowrate study was sectioned into slices. Each slice was cut to a height of 3cm using a hacksaw; though the prior study had a maximum water height of 21cm, the top slice was not used due to interference with the filter lip, as shown in Figure 8-11. The inner and outer radii of the slices were measured. Flexible, hard plastic

from the casing of an office binder were used to close off the bottom of the filter. Large amounts of Gorilla Brand glue were used to attach the wetted filter slice first to the bottom of the bucket, and then to the binder closure. Gorilla Brand glue was used because it activates when wet, as opposed to other glues which require dry surfaces. This allowed for quick repair if a leak was spotted during the study because the glue cured in less than 2 hours. A caulk that bonds, seals and caulks to was also attempted, but it did not remain adhered when submerged. The best option would have been to use a ceramic "bucket" for a very tight seal. While the slices were unsaturated, the seals between the bottom binder material, filter slice and bucket were tested.

Each bucket with the attached filter slice was set on top of a Styrofoam support in a clear container during the test. The Styrofoam support was required to elevate the filter slice from the filtered water accumulating the in container. The interior of the buckets were 36cm tall; the water height was kept constant at 34cm. After 1 hour, the bucket was carefully removed, and the water that accumulated in the container was carefully measured in a 500mL graduated cylinder. If any leaks in the seals were detected, the seals were patched and test restarted.

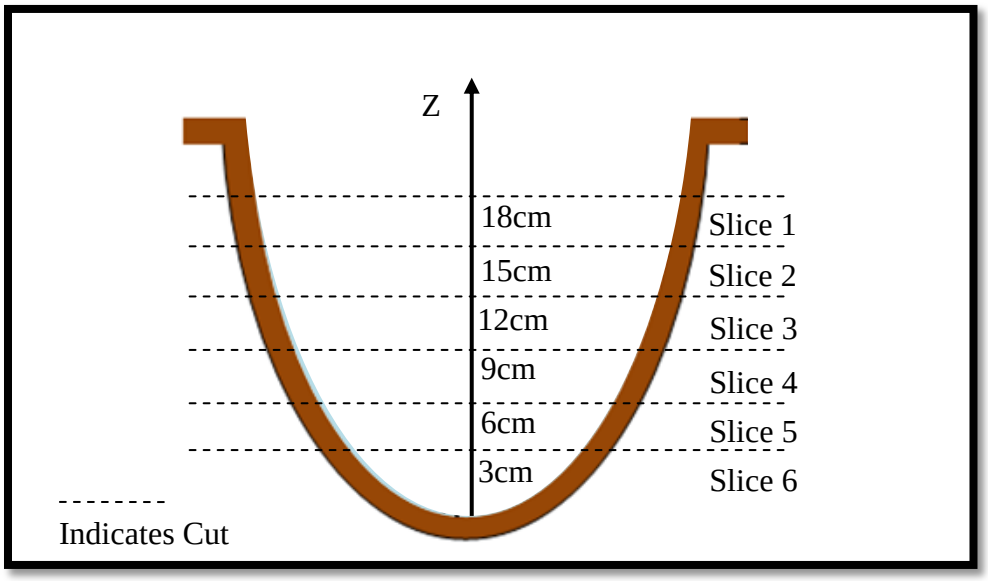

Figure 8-11: Paraboloid Filter Slices

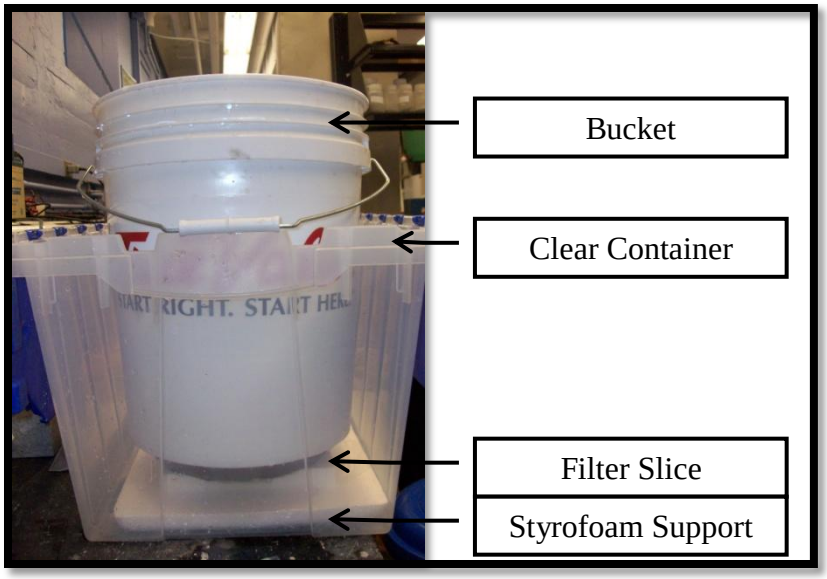

Figure 8-12: Hydraulic Conductivity with Height Test Set-Up

Figure 8-13: Left: Inside of Bucket with Filter Slice, Right: Bottom of Bucket with Filter Slice

8.5 Determining Total Porosity with Height

It is also useful to determine the total porosity of the filter, to see if it changes with height. The total porosity of the filter slices was found using the same techniques described in Section 4.5.2.2. Equation 4-3 is repeated here for convenience. The total porosity of each filter slice was compared to its hydraulic conductivity to see if there is a correlation.

$$Total\ Porosity = \frac{V_W}{V_{SS}} = \frac{M_{SS} - M_{DS}}{M_{SS} - M_{US}} \quad (4\text{-}3)$$

where:

V_W	is volume of water in saturated solid
V_{SS}	is volume of saturated solid
M_{SS}	is mass of saturated solid
M_{DS}	is mass of dry solid
M_{US}	is the mass of saturated solid when underwater

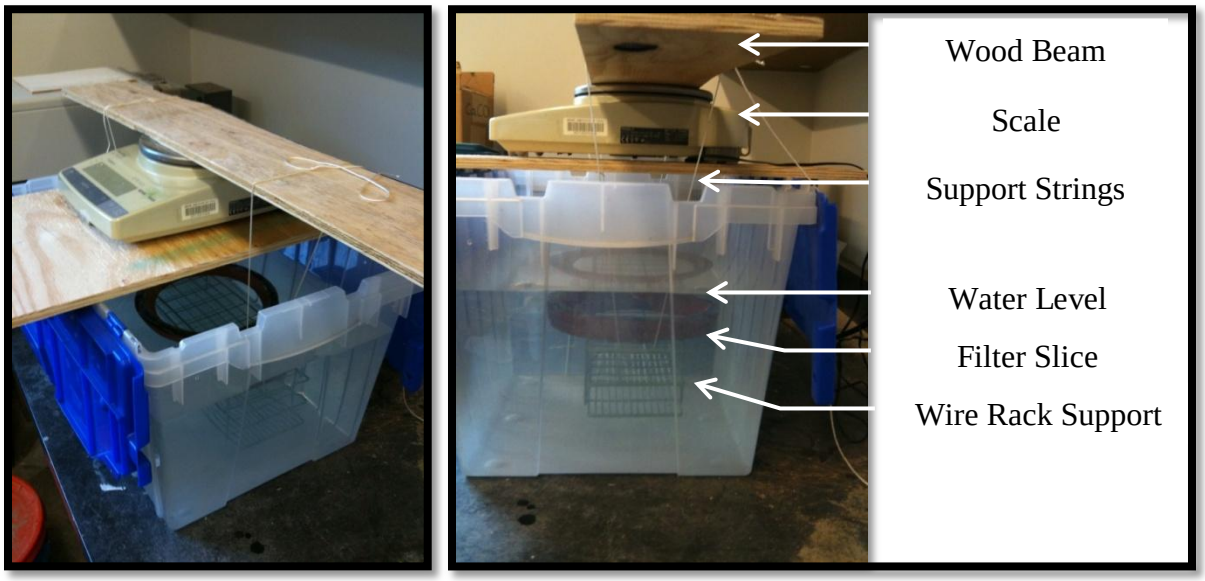

Figure 8-14: Filter Piece Volume Measurement Set-Up

9.0 Model and Testing of Flow through Paraboloid Filter Results

9.1 Geometry of Paraboloid Filter

Figure 9-1 compares the fit of the modeled radii with height found using Equation 8-4 to the radii determined using the three methods described in Section 8.1.3. Figure 9-2 demonstrates the fit of the modeled radii with coefficient c, found to be 2.685 $cm^{1/2}$, with those found using the method described in Section 8.1.3.1.

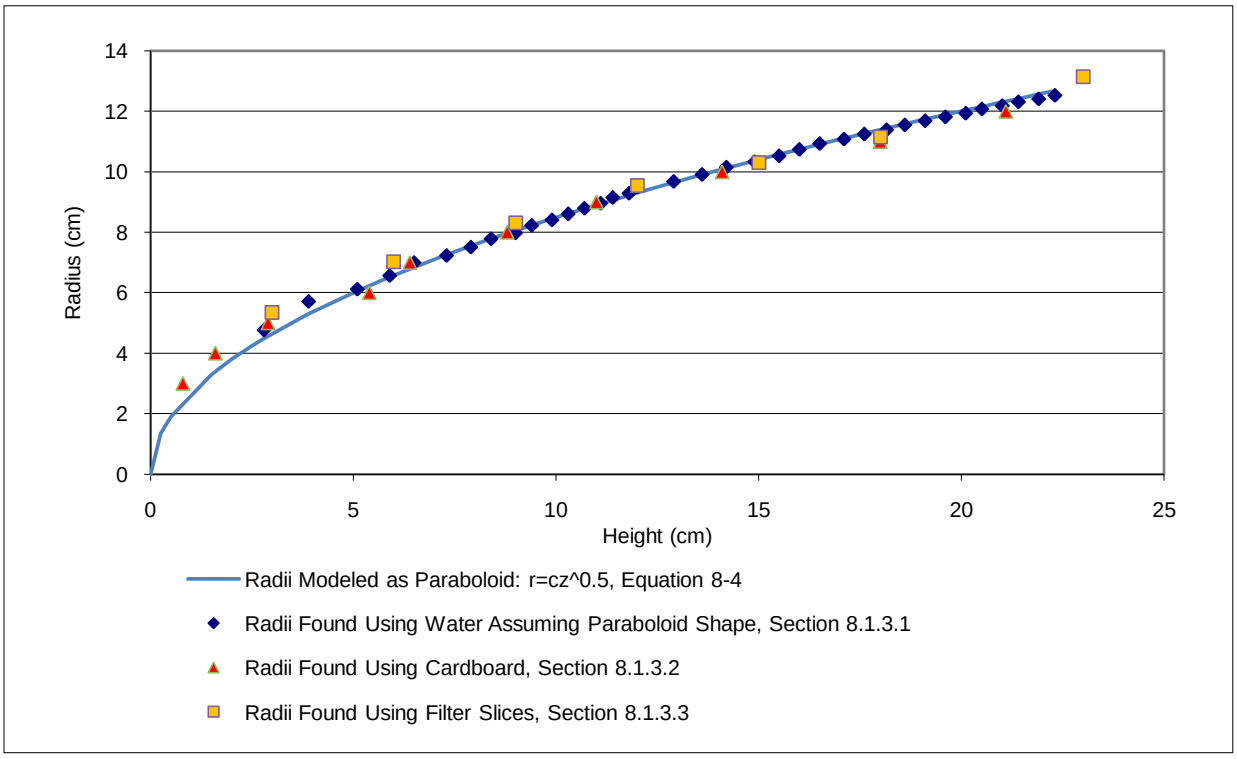

Figure 9-1: Change of Radius with Height, Measured Radii Compared to Model $r(z) = 2.685\sqrt{z}$

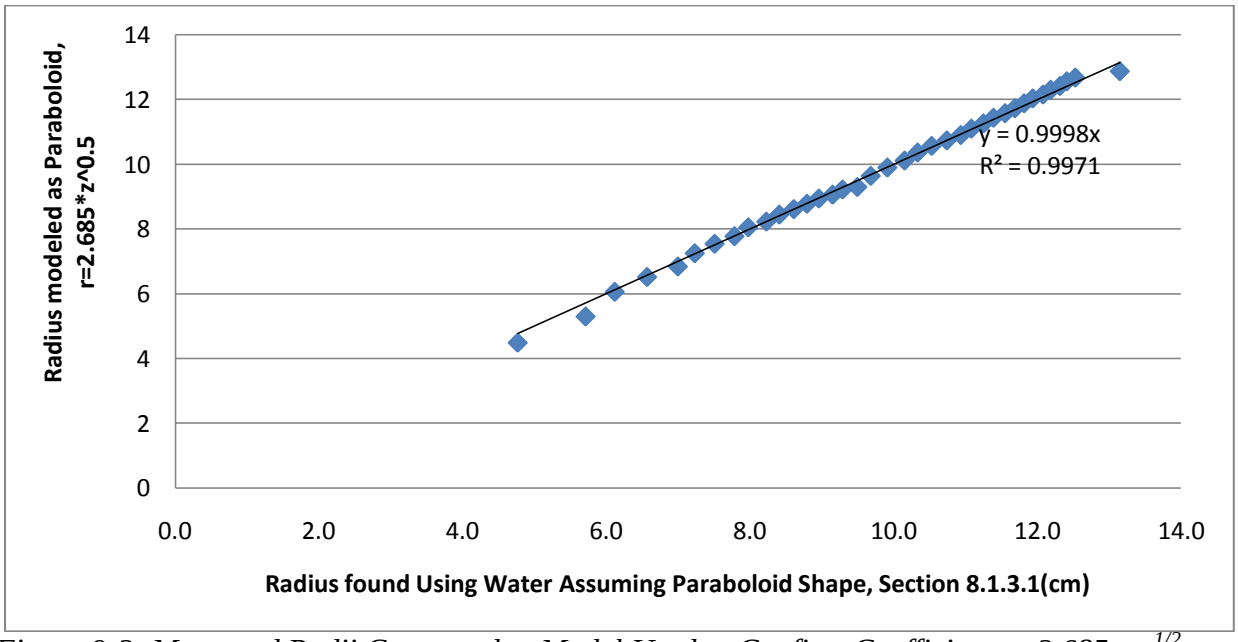

Figure 9-2: Measured Radii Compared to Model Used to Confirm Coefficient c=2.685 $cm^{1/2}$

9.2 Results of Measurement of Flow through Paraboloid Filter

Figure 9-3 presents the flowrate calculated from measurements described in Section 8.2.

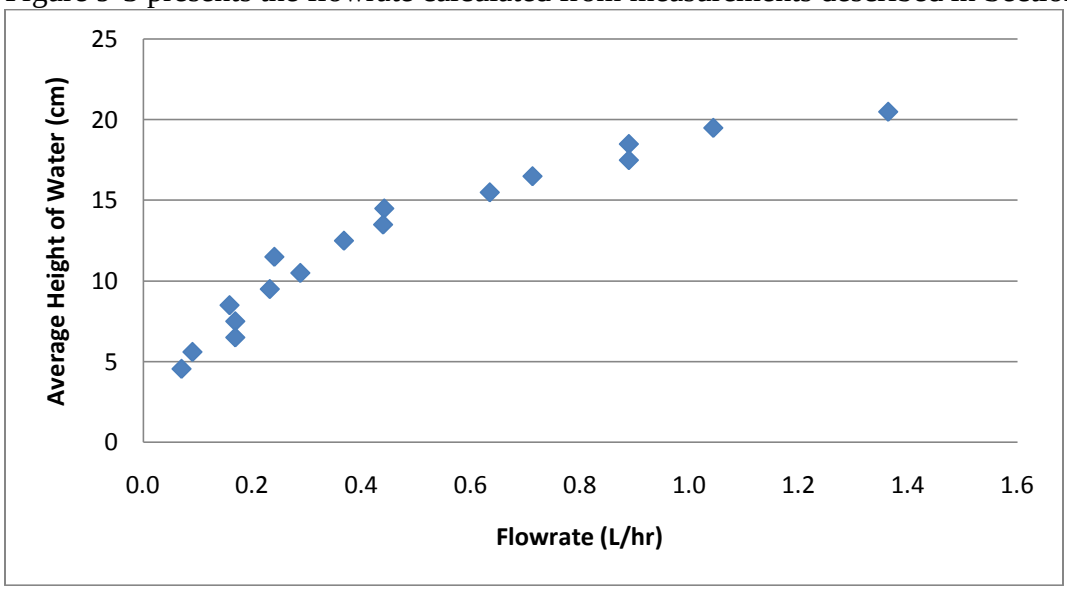

Figure 9-3: Flowrate Compared to Average Height of Water for Time Interval

9.3 Results of Comparison of Modeled Flow through Paraboloid Filter and Flower Pot Filter

Section 8.3.2 describes the methods of the comparison. Table 9-1 presents the results measured flowrate for the paraboloid filter and modeled hydraulic conductivity with a water height, H_W, of 19.5cm and radius at the top of the water, r_T, of 11.9cm. The modeled flowrate of a flower pot filter with the same volume, V, water height, and thickness, t, is presented.

Table 9-1 Comparison of Flowrate by Filter Shape

Shape	Q (L/hr)	K (cm/hr)	H_w (cm)	V (L)	r_T (cm)	r_B (cm)	t (cm)
Paraboloid	1.04	0.234	19.5	4.34	11.9	0	2
Flower Pot	1.38	0.234	19.5	4.34	10.2	6.5	2

9.4 Results of Methods to Determine Hydraulic Conductivity with Height

9.4.1 Weighted Average Hydraulic Conductivity with Height Results

Section 8.4.1 describes the methods used to determine weighted average hydraulic with height, presented in Table 9-2. Figure 9-4 compares the modeled hydraulic conductivities assuming constant and variable thickness.

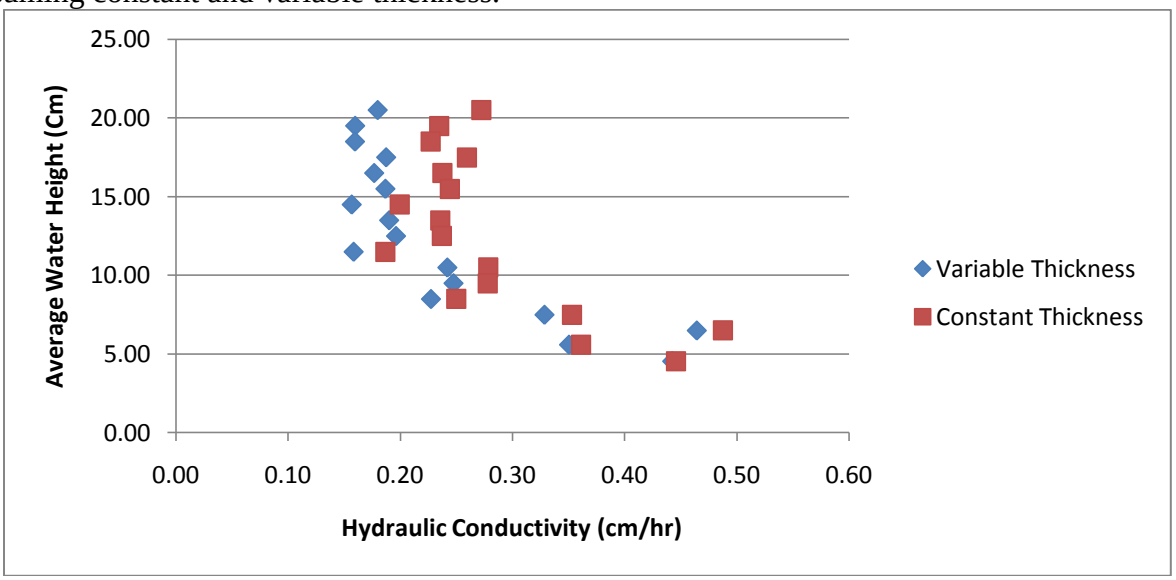

Figure 9-4: Weighted Average Hydraulic Conductivity Compared to Average Height of Water for Time Interval

Table 9-2: Results of Flowrate Test and Modeled Weighted Average Hydraulic Conductivity

Average Water Height for Δt (cm)	Measured Flowrate, Q (L/hr)	Modeled Hydraulic Conductivity, K (cm/hr) Constant Thickness	Modeled Hydraulic Conductivity, K (cm/hr) Variable Thickness
20.50	1.36	0.272	0.180
19.50	1.04	0.234	0.160
18.50	0.89	0.227	0.159
17.50	0.89	0.259	0.187
16.50	0.71	0.238	0.177
15.50	0.63	0.244	0.187
14.50	0.44	0.199	0.157
13.50	0.44	0.236	0.190
12.50	0.37	0.237	0.196
11.50	0.24	0.187	0.158
10.50	0.29	0.278	0.242
9.50	0.23	0.278	0.247
8.50	0.16	0.250	0.227
7.50	0.17	0.353	0.329
6.50	0.17	0.488	0.464
5.60	0.09	0.361	0.350
4.55	0.07	0.446	0.442

9.4.2 Hydraulic Conductivity of Three Segments Results

Section 8.4.2 describes the methods used to determine the hydraulic conductivity for each segment, as presented in Table 9-3. Figure 9-5 displays the modeled hydraulic conductivities as a function of the final time interval, ΔT_3, to demonstrate the sensitivity to that value.

Table 9-3: Hydraulic Conductivity Calculated for Each Segment

Segment	Height Interval	Hydraulic Conductivity* (cm/hr)
1	12cm - 18cm	0.188
2	6cm - 12cm	0.208
3	0cm - 6cm	0.175

*These values were calculated for ΔT_3=22 hours

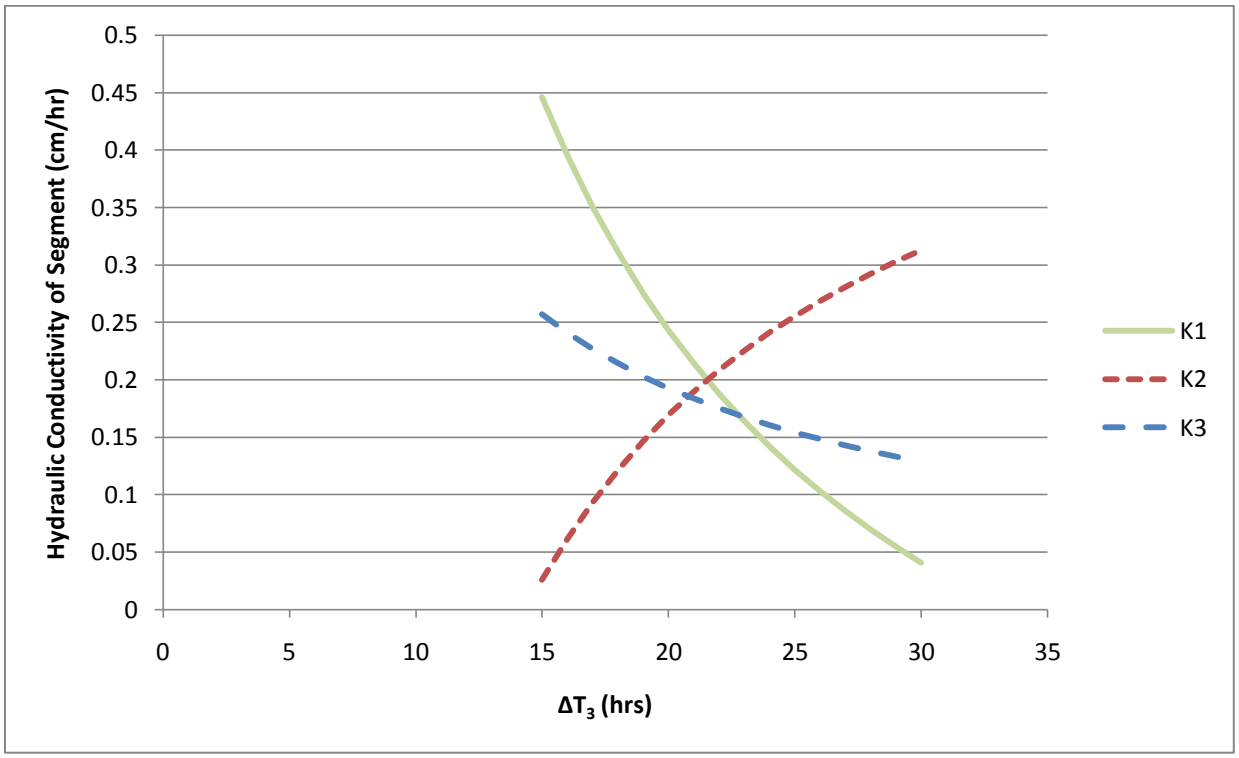

Figure 9-5: Hydraulic Conductivity of Segments, Sensitive to Final Time Interval, ΔT_3
ΔT_3=22 hours is the Best Guess Measurement

9.4.3 Hydraulic Conductivity of Filter Slices Results

Section 8.4.3 describes the methods used to determine the hydraulic conductivity of the filter slices. The results are presented in Figure 9-6.

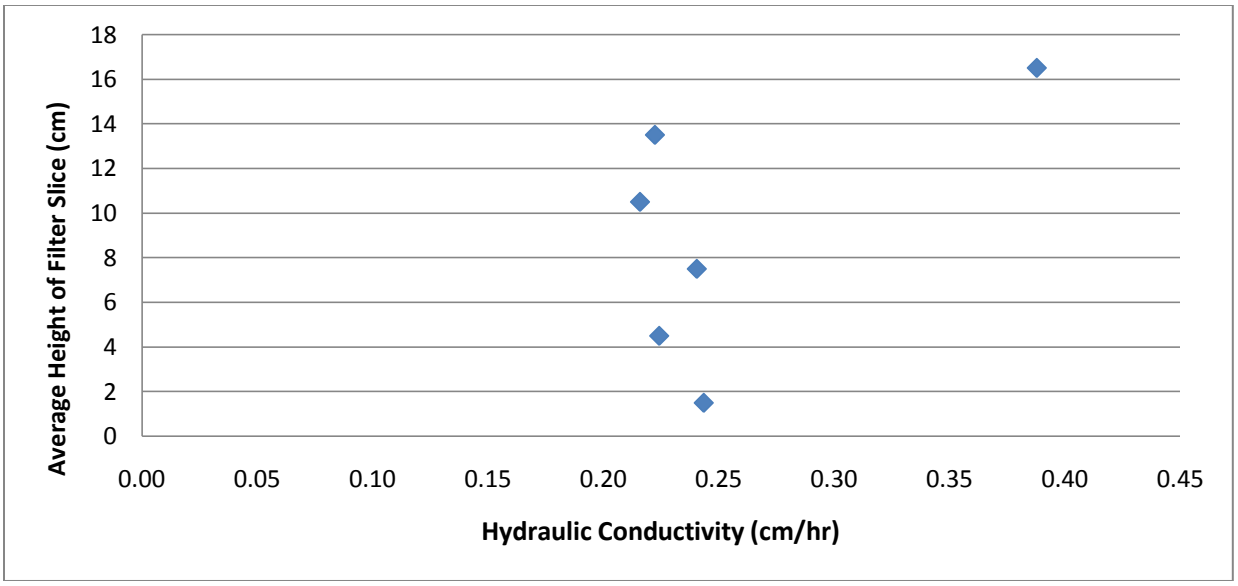

Figure 9-6: Hydraulic Conductivity of Each Filter Slice

9.4.4 Summary of Hydraulic Conductivity Results

Figure 9-7 summarizes the mean hydraulic conductivities for three height intervals of the filter found by methods described in section 8.4.

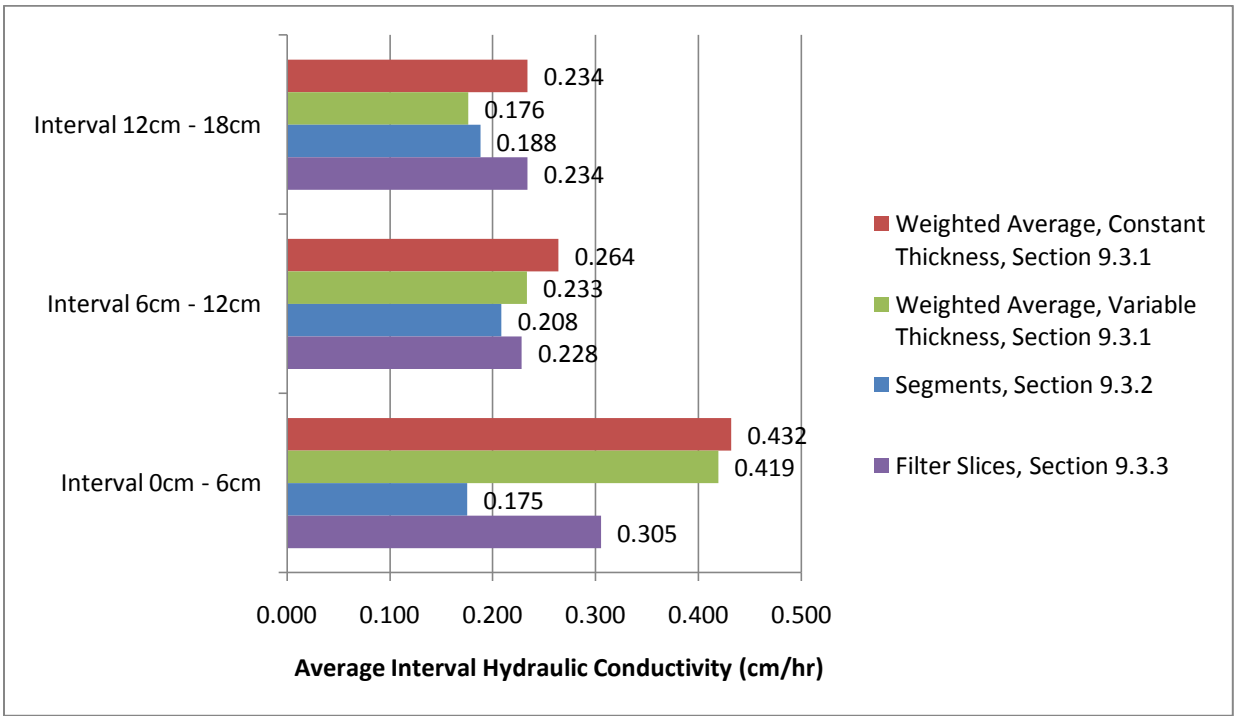

Figure 9-7: Summary of Average Hydraulic Conductivities Determined by Three Methods

9.5 Total Porosity of Filter Slices Results

Section 8.5 describes the methods used to determine the total porosity of the filter slices, presented in Figure 9-8.

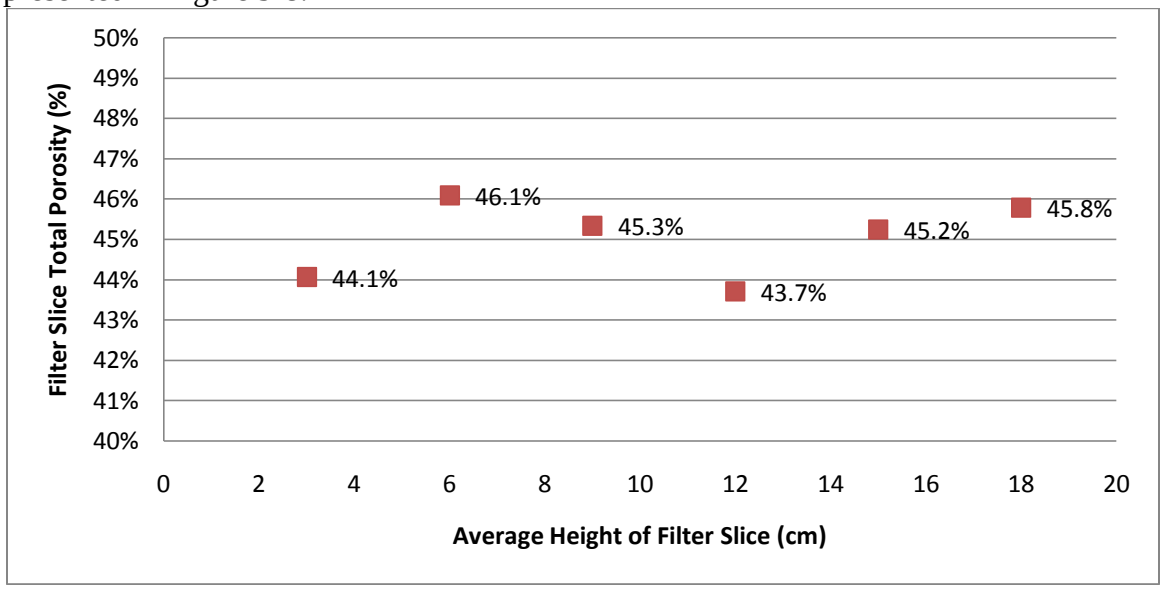

Figure 9-8: Total Porosity of Each Filter Slice

10.0 Model and Testing of Flow through Paraboloid Filter Discussion

10.1 Geometry of Paraboloid Filter

Both methods of determining radius with height, using water in Section 8.1.3.1 and cardboard in Section 8.1.3.2, match the results directly measured from filter slices, Section 8.1.3.3, well. For practical purposes, a factory wishing to model its paraboloid filter can arrive at the coefficient c by measuring the interior height and radius at the top of the filter.

$$\frac{r_{top}}{\sqrt{z_{top}}} = c \tag{8-32}$$

10.2 Measurement of Flow through Paraboloid Filter

There is a clear trend in the flowrate through the filter compared to the average height of water: the flowrate decreases non-linearly with decreasing water height. Deviations from that trend can be explained by experimental error and water draining from the filter walls.

10.3 Model of Flow through Paraboloid Filter

The model of flow through the paraboloid filter derived from Darcy's Law seems to accurately represent the flow, and can easily be applied to any paraboloid filter whose geometric coefficient, c, is known.

10.3.1 Comparison of Modeled Flow through Paraboloid Filter and Flower Pot Filter

Comparing a paraboloid filter and flower pot filter with the same height of water, volume and wall thickness, the flower pot filter has a slightly higher flowrate, 1.32 times greater. The flower pot filter has a larger surface area on the bottom than the paraboloid filter does towards the bottom, meaning that more surface area experiences higher head, leading to a higher flowrate. The difference in flowrates is not significant enough to deter a factory from producing paraboloid filters if desired for other reasons.

10.4 Methods to Determine Hydraulic Conductivity with Height

The three methods used to determine the change of hydraulic conductivity with height produced similar values; however the weighted average method indicated that the bottom of the paraboloid filter had higher hydraulic conductivities. The assumption that the filter has a constant hydraulic is confirmed because other factors likely explain the higher hydraulic conductivities at the bottom of the filter.

All of these methods resulted in mean hydraulic conductivities several times greater than the mean of those reported by van Halem (2006) for filters in Ghana, Nicaragua and Cambodia, 0.09 cm/hr, found using mercury intrusion porosimetry. It is unclear, however, if the mercury intrusion porosimetry measurements were taken from filters which had never been loaded with turbid water, or from filters that had been loaded repeatedly with turbid water. If the former is the case, then differences in production materials and techniques explain the differences; if the latter is the case, then a lower hydraulic conductivity would be expected because of particles clogging the pores.

10.4.1 Weighted Hydraulic Conductivity with Height

Determining weighted hydraulic conductivity with height resulted in similar values to those calculated by other methods. The hydraulic conductivities determined assuming a constant

thickness of 2cm, which had a mean of 0.282 cm/hr and standard deviation of 0.083 cm/hr, were overall greater than those determined using a smaller, variable thickness, which has a mean of 0.238 cm/hr and standard deviation of 0.099 cm/hr. This is logical because hydraulic conductivity is directly related to thickness in Darcy's Law. The latter method provides more realistic results because the thickness actually varies and is not constant. This is a product of the relationship between the female and male mold of the filter, and the extent to which the filters were completely pressed. Adjustments can be made to the mold and the press if need be. However, if all paraboloid filters are found to have variable thickness despite changes to the mold and press, it would be useful to derive a model for flow considering t(z), allowing thickness to vary with height.

Higher hydraulic conductivities toward the bottom of the filter can be explained by exaggerated flowrate measurements due to draining from water stored in the filter walls. When the water height in the filter is low, much of the upper portion of the filter is not submerged; any water that drains out of the filter wall and is collected is falsely attributed to flow out of the bottom portion. This effect is greater when the water height is lower. Because hydraulic conductivity and flowrate are directly related, increased flowrate results in an increased hydraulic conductivity calculation.

10.4.2 Hydraulic Conductivity of Three Segments

This method involved the most approximation and least amount of precision. The length of the third time interval, ΔT_3, is very difficult to measure because it takes much longer for the final height of water to reach zero than for the other intervals due to decreased head. The results, unfortunately, are very sensitive to this value. Results produced a range of hydraulic conductivities from 0.026 cm/hr to 0.446 cm/hr varying ΔT_3 from 15 hours to 30 hours. At 22 hours, however, the values converge and range from 0.175 cm/hr to 0.208 cm/hr. These values are similar to those determined using a weighted average hydraulic conductivity assuming variable thickness.

Using a series expansion of the formulas for hydraulic conductivity (8-25), (8-26), and (8-27), it is also possible to extend this method to include more segments. By dividing the filter into more segments, the relative importance of the final time interval is reduced, leading to less sensitive results.

10.4.3 Hydraulic Conductivity of Filter Slices

This method was the most direct approach to determining hydraulic conductivity. The range of modeled hydraulic conductivities was from 0.216 cm/hr to 0.388 cm/hr; there is no trend relating hydraulic conductivity to height. Visible leaks were not detected in slices 2 through 5, but some leaks from slice 1 were difficult to patch; leaks may have artificially increased the flowrate, and the modeled hydraulic conductivity along with it. Therefore, the highest hydraulic conductivity value, 0.388 cm/hr is considered an outlier. The remaining values are fairly consistent throughout the height of the filter, with a mean value of 0.229 cm/hr and standard deviation of 0.012 cm/hr. These values are consistent with those determined by the other methods.

10.5 Total Porosity of Filter Slices

The average total porosity of the filter slices, 45.0% with 1.0% standard deviation, is consistent with the average total porosity of the filter lip pieces for filter 15, 45.7% with 3.3%

standard deviation presented in Section 5.2 determined by methods described in Section 4.5.2.2. There was no clear trend in change in total porosity of the filter slices with filter height, and it did not correlate with the hydraulic conductivities of the filter slices. The small standard deviation in the total porosities and lack of trend in the hydraulic conductivity explains these observations.

11.0 Optimal Removal and Flowrate Study Conclusions and Recommendations

11.1 Recommendations for Pure Home Water

11.1.1 Recommended Filter Design

The 12-week study of the performance of the ceramic water filters enabled conclusions to be drawn about the impact of several design variables on several performance categories. Watters (2010) completed a study on the relative strength of the design variables on the strength of the fired filters; his results are shown. This is useful information because a weak filter prone to breakage is less able to consistently deliver quality drinking water.

Table 11-1: Summary of Findings for Design Variable Impact on Performance Category

Key:

Empty cells indicate no statistical effect of design variable on performance category

"Better" indicates that the design variable outperforms the other design variable(s) for the performance category

"Worse" indicates that the other design variable(s) outperforms the design variable for the performance category

"In Between" indicates that the performance of the design variable lies in between that of the other design variables for the performance category

Design Variable / Performance Category		*E. coli* Removal	Total Coliform Removal	Flowrate	Turbidity Removal	Strength (Watters, 2010)
Combustible Type	Rice Husk	Worse	Better	Better	Worse	More, Stronger
	Sawdust	Better	Worse	Worse	Better	Less, Stronger
Addition of Grog	Grog					
	No Grog					
Percentage Combustible by mass	Low			Worse		Better
	Medium			In Between		In Between
	High			Better		Worse
Additional Variables	Sifting Combustible			Worse		Better
	Paraboloid Shape			Worse		

From this summary, it is difficult to make conclusions about which design variables to select if all performance categories are weighted equally. Since none of the filters had satisfactory turbidity removal, that performance category is removed from the ranking scheme. Neglecting turbidity removal, rice husk filters overall perform better than sawdust filters. The addition of a low proportion of grog had no effect on any of the performance categories. Since filters with more combustible have more void space, it makes sense that they would be weaker than a less porous filter as confirmed by Watters (2010). The summary of results suggest that choosing to sift the combustible or not is an even trade-off between flowrate and strength, there are additional factors to consider. Sifting the combustible adds an extra step in the production process; it is not very onerous to sift the sawdust, but sifting rice husk is tedious and difficult. It is surprising that the flowrate of the paraboloid filter is statistically lower than the flower pot filter made of the same recipe because the model would predict the reverse for very low turbidity water. The difference in flowrates is not great, and may be explained by other factors.

Given these considerations and trusting in the validity of the results, the optimal filter design type seems to be flower pot or paraboloid filters made with a medium percentage unsifted rice husk by mass 26.7% of the total mass excluding grog or 25.0% including grog, with grog added at the potter's discretion. This description represents filter recipes 3 and 4.

To confirm the anticipated best overall performance of filters 3 and 4, each filter pair was compared based on all performance categories excluding turbidity removal. A score based on the statistical tiered ranking of each filter pair based on performance category was assigned, and a combined scoring system was created where a lower score represents better performance, and the lowest score possible is 4. The lowest possible score is 4 if a filter ranked 1 in each category.

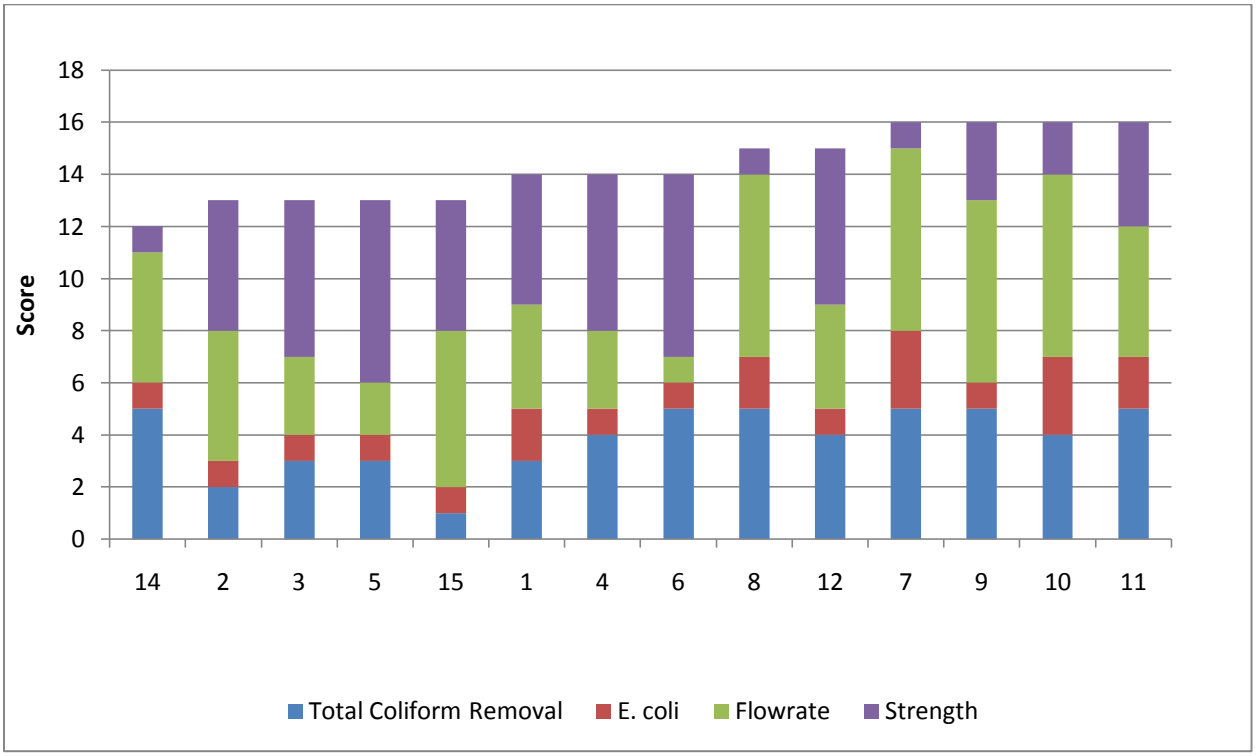

Figure 11-1: Combined Statistical Tier Ranking by Performance Categories except Turbidity

All of the filter pairs scored between 12 and 16, filters scoring above 15 should not be considered for production. An explanation for the close range of scores for all the filters is that the statistical ranking did not result in many tiers, and few filters performed consistently better in all categories. Filters 3 and 4 score 13 and 14, respectively, and are within the acceptable score range.

11.1.2 Recommendations for Coagulation

Due to the inability of any of the filter designs to remove influent turbidity satisfactorily, even at very low flowrates, additional methods to reduce turbidity should be pursued. According to a drinking water consumer choice survey in Northern Ghana completed by Green (2008), both urban and rural consumers prefer clear water to turbid water. Coagulation is an effective method for reducing turbidity, and several products exist to effectively at the household level in Northern Ghana, most notably alum. Although the water may appear clear after coagulation with alum, it is important that households also filter their water to remove any microorganisms that were not settled out during coagulation.

11.1.3 Recommended Further Research

That the turbidity removal results in this study are poor and do not directly relate to total coliform removal results is a troubling phenomena. Johnson (2007) reported that ceramic water filters manufactured in Accra and sold by Pure Home Water in Northern Ghana from 2005-2007 were capable of reducing on average 92% of turbidity, with a resulting average filtered water turbidity of 11NTU. The filters studied by Johnson (2007) greatly outperform the turbidity removal of filters in this study, though they have similar total coliform removal. At worst, the mismatch in total coliform removal and turbidity removal in this study could mean that indeed the performance of rice husk filters at removing total coliform is over-estimated, which would change the recommended filter design. To test if the higher turbidity of filtered water does not impact the total coliform removal results, filters with recipes 3 and 4 should be tested for additional months using the Quanti-Tray®[11] method of coliform analysis. The Quanti-Tray® method used by Klarman (2009) is a most probable number method that is available at the Pure Home Water Laboratory in Northern Ghana and does not require filtration. Thus it would likely have reduced interference by turbid water. Some of the Quanti-Tray® results should be compared to membrane filtration results in an attempt to detect differences in counts as a result of the testing method.

It would also be useful to determine the particle size distribution of the suspended solids in the influent water using a hydrometer. The analysis could be done according to ASTM D422 - 63 Standard Test Method for Particle-Size Analysis of Soils. This way, the necessary filter pore size to screen suspended solids causing turbidity could be determined. Alternatively, sequential filtration, described by Losleben (2008) could be used.

As part of the further research, filters made in Accra, paraboloid filters, and filters made with different clay types should be studied. A flaw of this study is the lack of a control. To remedy that for future studies, testing filters made in Accra concurrently with filters made in Tamale could provide useful comparisons. It would be useful to compare input combustible material in Accra-made filters to those used in this study to determine if that can account for differences in turbidity removal performance. Differences in clay may also be a factor.

---

[11]Quanti-Tray® is a product of Idexx Laboratories, Inc. http://www.idexx.com/view/xhtml/en_us/water/quanti-tray.jsf?selectedTab=Overview

The Pure Home Water factory will likely produce more paraboloid filters than flower pot filters as a result of the easier production process with the permanent press. Thus, before marketing the filters, triplicates of paraboloid filters made with recipes 3 and 4 should be tested using Quanti-Tray®. For comparison, paraboloid filters made with recipes 9 and 10 should be tested concurrently.

The total amount of clay available from the current source of Gbalhai clay is unknown, and other clay sources are available. Given that, the clay from each source should be characterized using Atterberg limits and particle size distribution techniques and classified. If a clay source seems suitable based on its plasticity, the performance filters made with that source of clay should be tested.

11.2 Flow through Paraboloid Shaped Filters Conclusions and Recommendations

11.2.1 Model of Flow through Paraboloid Shaped Filters

A model was developed to determine the flow through paraboloid shaped filter for a given height of water.

$$Q = \frac{4\pi cK}{3t}\left[-H_w(c^2/4)^{\frac{3}{2}} + \frac{2}{5}\left((c^2/4 + H_w)^{\frac{5}{2}} - (c^2/4)^{\frac{5}{2}}\right)\right] \quad (8\text{-}15)$$

where:

Q	is the flowrate
c	is the coefficient relating the change in radius with height
K	is the hydraulic conductivity
t	is the thickness
H_w	is the height of the water

This model is found to represent flow through the paraboloid filter assuming constant hydraulic conductivity and filter wall thickness. The filter actually has a slightly variable wall thickness, which may need to be incorporated into the model in the future if changes to the mold and press are not made.

11.2.1 Determination of Hydraulic Conductivity with Height

Three methods were used to determine the hydraulic conductivity of the filter with height; one determined the weighted average hydraulic conductivity and two determined the actual hydraulic conductivity. Both methods that determined the actual hydraulic conductivity produced results that imply that the hydraulic conductivity is constant throughout the filter wall. The method that determined the weighted average hydraulic conductivity implied that the hydraulic conductivity increased toward the bottom of the filter, but that result can be explained by water draining from the upper portion of the filter walls, exaggerating the flowrate and modeled hydraulic conductivities.

12.0 References

ASTM. *ASTM C 373-88: Standard Test Method for Water Absorption, Bulk Density, Apparent Porosity, and Apparent Specific Gravity of Fired Whiteware Products.* American Society for Testing and Materials.

ASTM. *ASTM D 6913 – 04 (2009): Standard Test Methods for Particle-Size Distribution (Gradation) of Soils Using Sieve Analysis.* American Society for Testing and Materials.

ASTM. *ASTM D2487 – 10 Standard Practice for Classification of Soils for Engineering Purposes (Unified Soil Classification System).* American Society for Testing and Materials.

ASTM. *ASTM D4318 - 10 Standard Test Methods for Liquid Limit, Plastic Limit, and Plasticity Index of Soils.* American Society for Testing and Materials.

ASTM. *ASTM D854 - 10 Standard Test Methods for Specific Gravity of Soil Solids by Water Pycnometer.* American Society for Testing and Materials.

Bloem, S. (2008). Silver Impregnated Ceramic Water Filter: Flowrate versus the removal efficiency of pathogens. *(Masters Thesis)* . Delft, Netherlands: Delft University of Technology.

Caldwell, L. (2009, June 25). Guinea Worm Eradication Program Gets Results in Ghana. *America.gov* .

CIA. (2010). *Ghana*. Retrieved May 10, 2010, from CIA World Factbook: https://www.cia.gov/library/publications/the-world-factbook/geos/gh.html

Desmyter, D. A. (2008). Monitoring and Evaluation of 1,000 Households receiving ceramic Pot (Kosim) Filters after an Emergency Flood Mass Distribution in Northern Ghana. *Water Environment Federation Disinfection 2009: International Ceramic Pot Filter Workshop.*

Fahlin, C. J. (2003). *Hydraulic Properties Investigation of the Potters for Peace Colloidal Silver Impregnated, Ceramic Filter.* Boulder, Colorado: University of Colorado at Boulder.

Green, V. (2008). *Household Water Treatment and Safe Storage Options For Northern Region Ghana: Consumer Preference And Relative Cost.* MIT.

Johnson, S. (2007). *Health and Water Quality Monitoring of Pure Home Water's Ceramic Filter Dissemination in the Northern Region of Ghana (Masters Thesis).* MIT.

Klarman, M. (2009). *Investigation of Ceramic Pot Filter Design Variables.* Atlanta, Georgia: Emory University.

Lantagne, D. S. (2001). *Investigation of the Potters for Peace Colloidal Silver Impregnated Ceramic Water Filter: Report 1: Intrinsic Effectiveness.* USAID.

Leftwich, M. e. (2009). *Understanding the Filtron Ceramic Water Filter.* Princeton, NJ: Princeton University.

Losleben, T. R. (2008). *Pilot Study of Horizontal Roughing Filtration in Northern Ghana as Pretreatment for Highly Turbid Dugout Water. Master's Thesis.* Massachusetts Institute of Technology.

Mathworld, W. (n.d.). *Parabola*. Retrieved May 10, 2010, from Wolfram Mathworld: http://mathworld.wolfram.com/Parabola.html

Mathworld, W. (n.d.). *Paraboloid.* Retrieved May 10, 2010, from Wolfram Mathworld: http://mathworld.wolfram.com/Paraboloid.html

Mendenhall, W. a. (2006). *Statistics for Engineering and the Sciences, 5th Edition.* Upper Saddle Riveer: Pearson Prentice Hall.

Oyandel-Craver, V. a. (2008). Sustainable Colloidal-Silver-Impregnated Ceramic Filter for Point-of-Use Water Treatment. *Environ. SCi. Technol.* , 927-933.

Sanitation, W. J. (2010). *Estimates for the Use of Improved Drinking-Water Sources: Ghana.*

van Halem, D. (2006). *Ceramic silver impregnated pot filters for household drinking water treatment in developing countries.* Delft, Netherlands: Delft University of Technology.

van Halem, D. e. (2009). Assessing the sustainability of the silver-impregnated ceramic pot filter for low-cost household drinking water treatement. *Physics and Chemistry of the Earth* , 36-42.

Watters, T. (2010). *The Effect of Compositional and Geometric Changes to the Bending Strength of the Ghanaian Ceramic Pot Filter. Master's thesis.* Massachusetts Institute of Technology.

WHO. (2004). *Guidelines for Drinking-water Quality: Third Edition.* Geneva: World Health Organization.

WHO. (2010). *Ghana: Health Profile*. Retrieved May 10, 2010, from World Health Organization: Global Health Observatory: Country Profiles: http://www.who.int/gho/countries/gha.pdf

APPENDICES

APPENDIX A: Pictures of Filters

Figure A-1: Views of Filter 1A

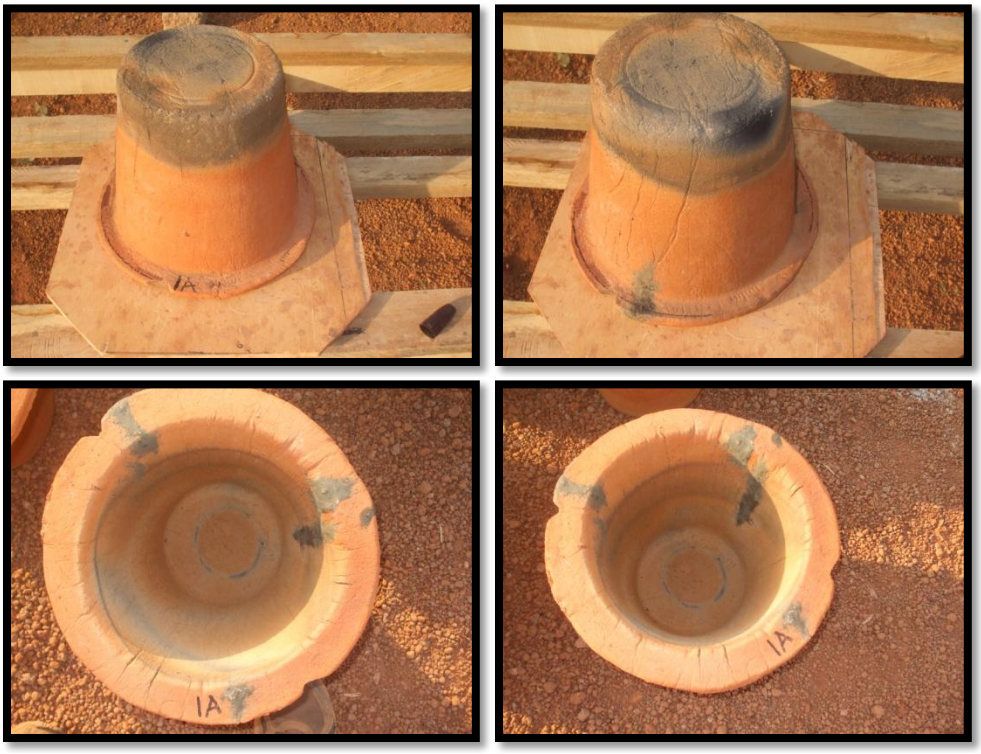

Figure A-2: Views of Filter 1B

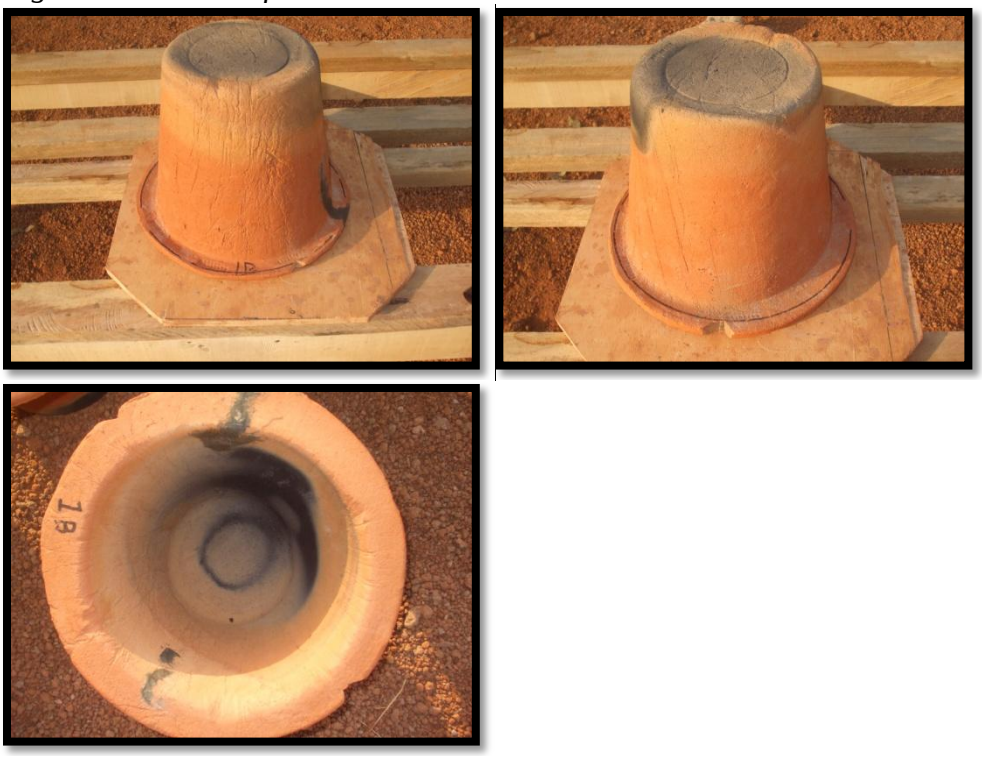

Figure A-3: Views of Filter 2A

Figure 4: Views of Filter 2B

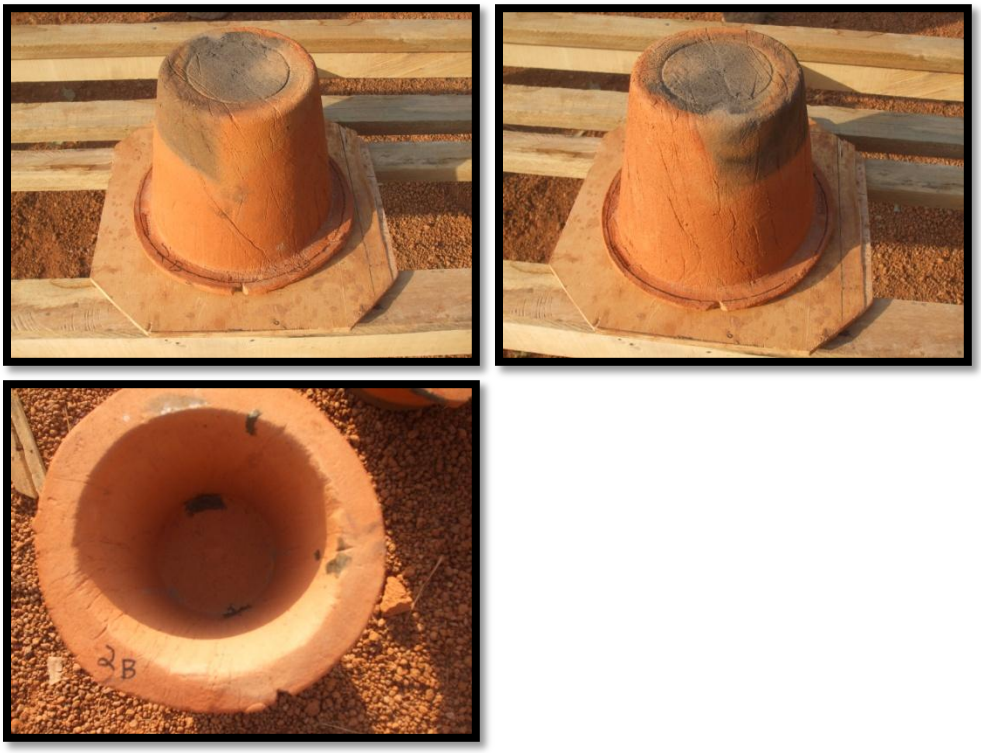

Figure 5: Views of Filter 3A

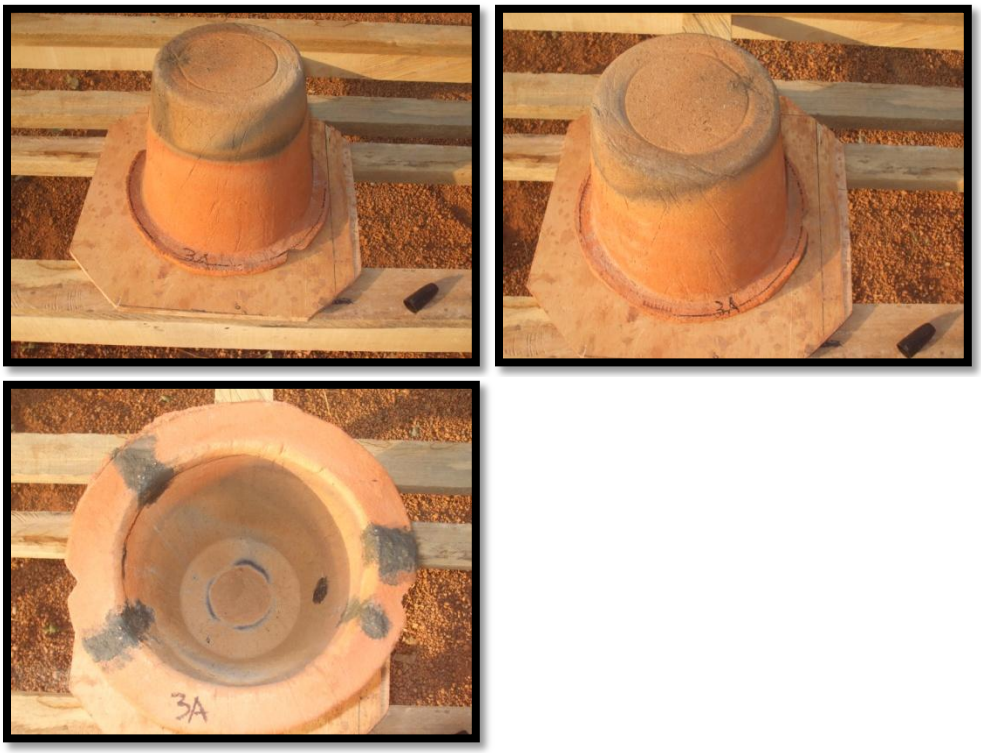

Figure 6: Views of Filter 3B

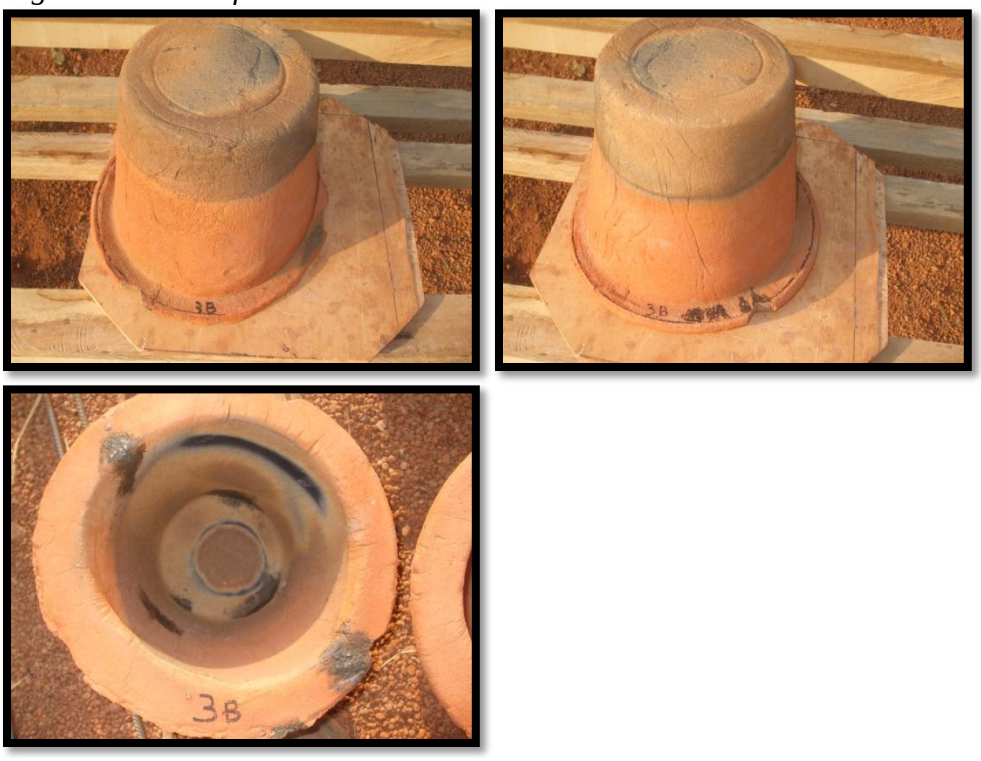

Figure 7: Views of Filter 4A

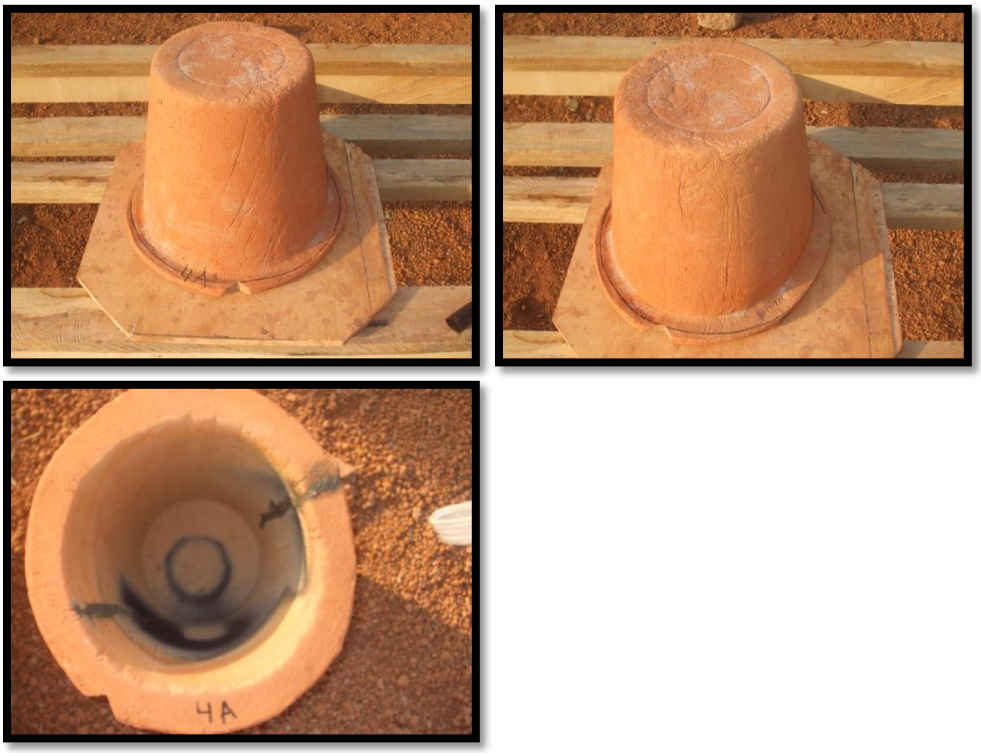

Figure 8: Views of Filter 4B

Figure 9: Views of Filter 5A

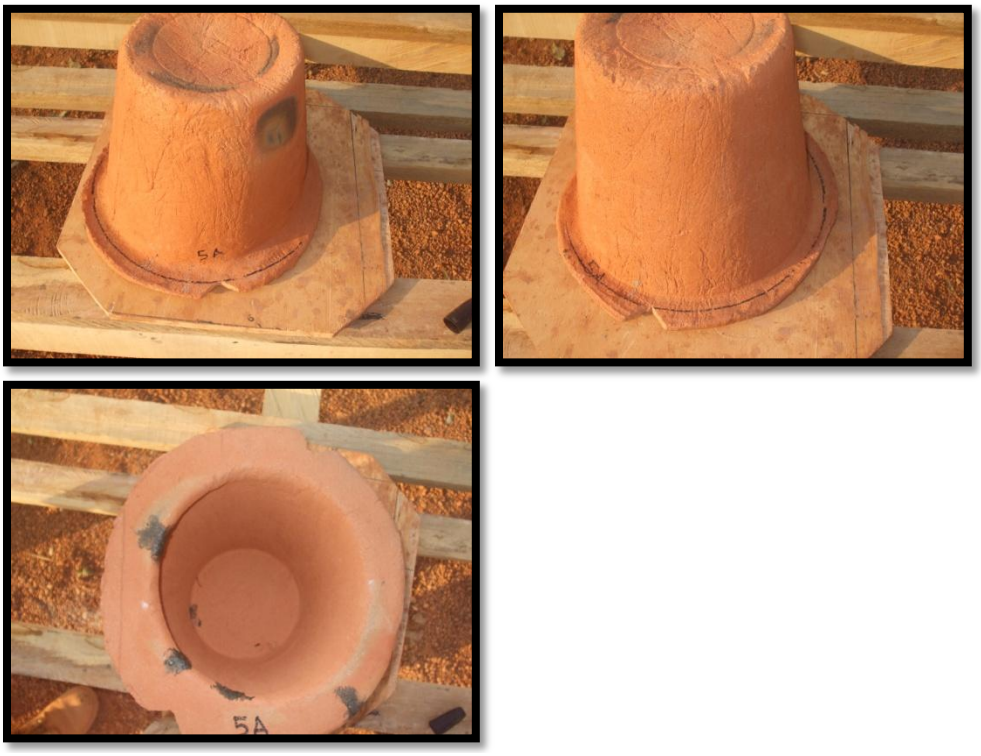

Figure 10: Views of Filter 5B

Filter 11: Views of Filter 6A

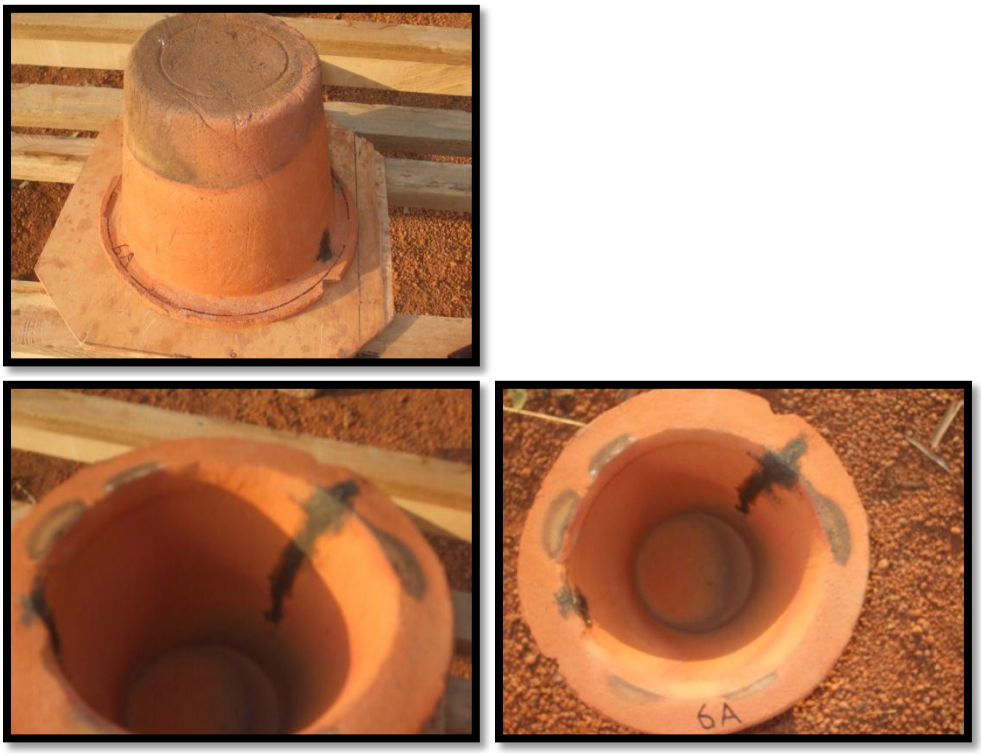

Figure 12: Views of Filter 6B

Figure 13: Views of Filter 7A

Figure 14: Views of Filter 7B

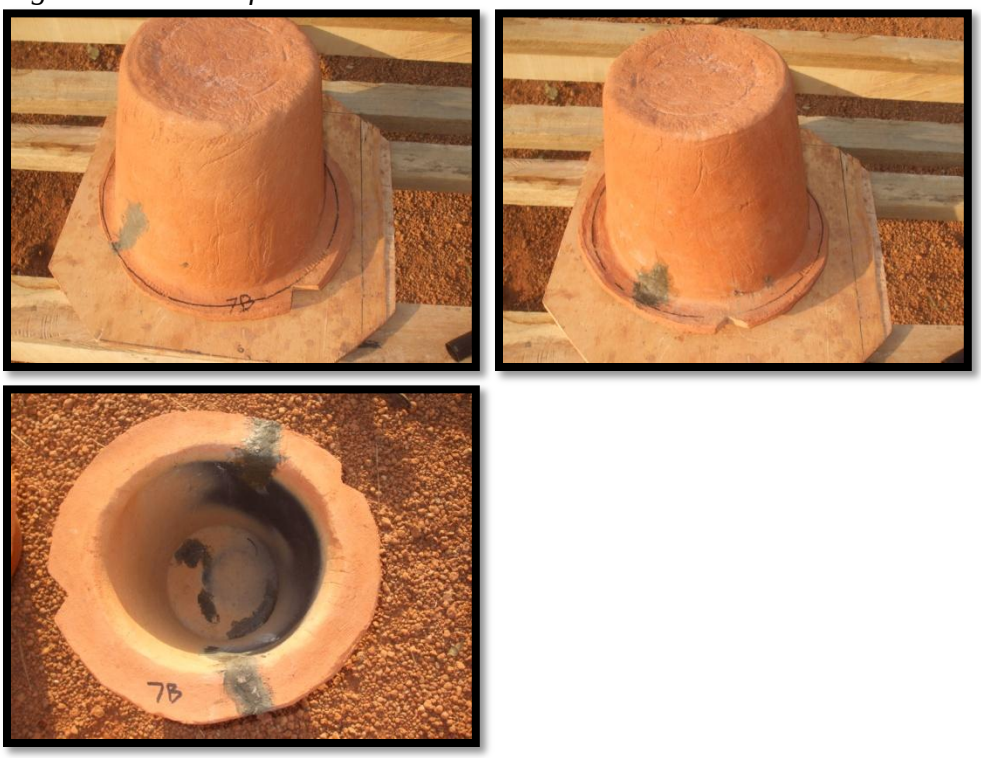

Figure 15: Views of Filter 8A

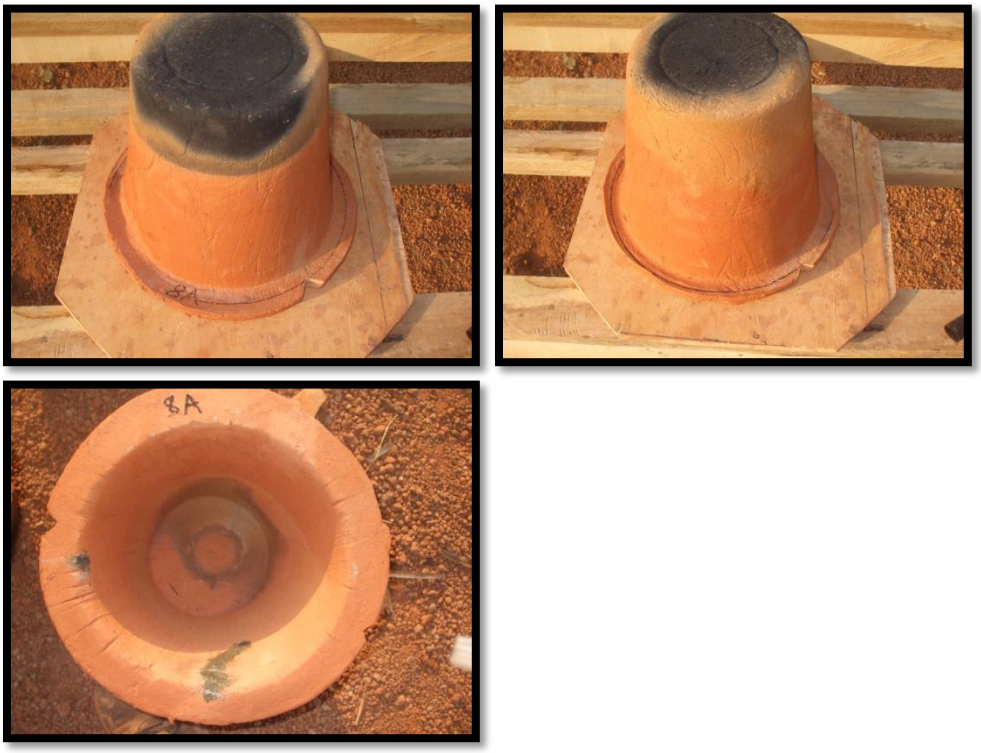

Figure 16: Views of Filter 8B

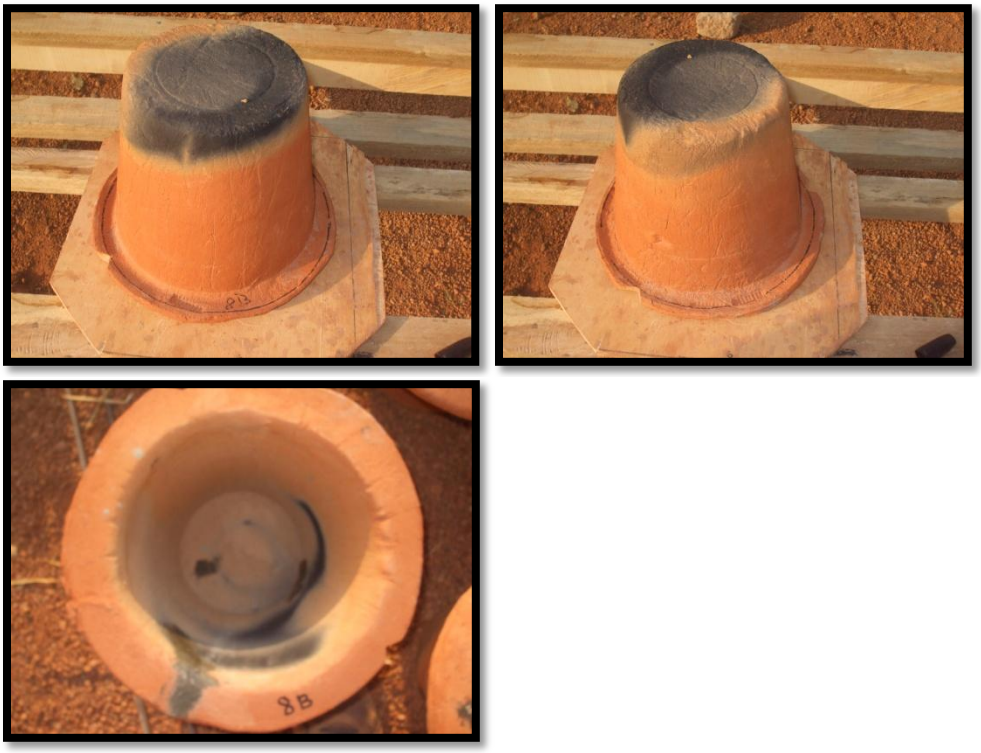

Figure 17: Views of Filter 9A

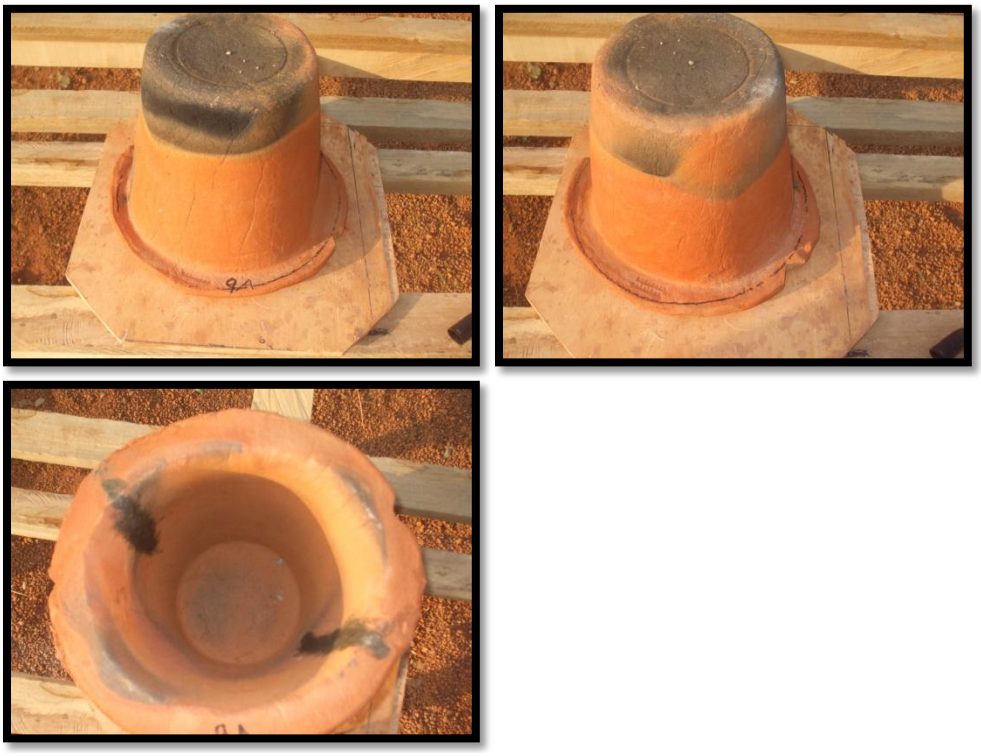

Figure 18: Views of Filter 9B

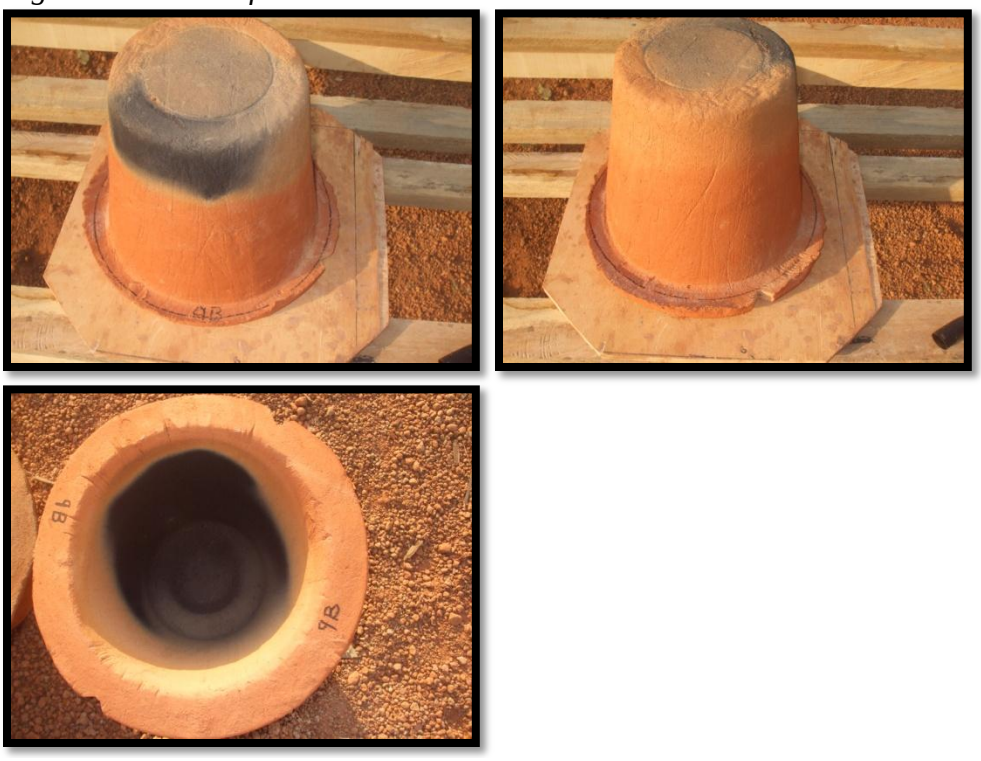

Figure 19: Views of Filter 10A

Figure 20: Views of Filter 10B

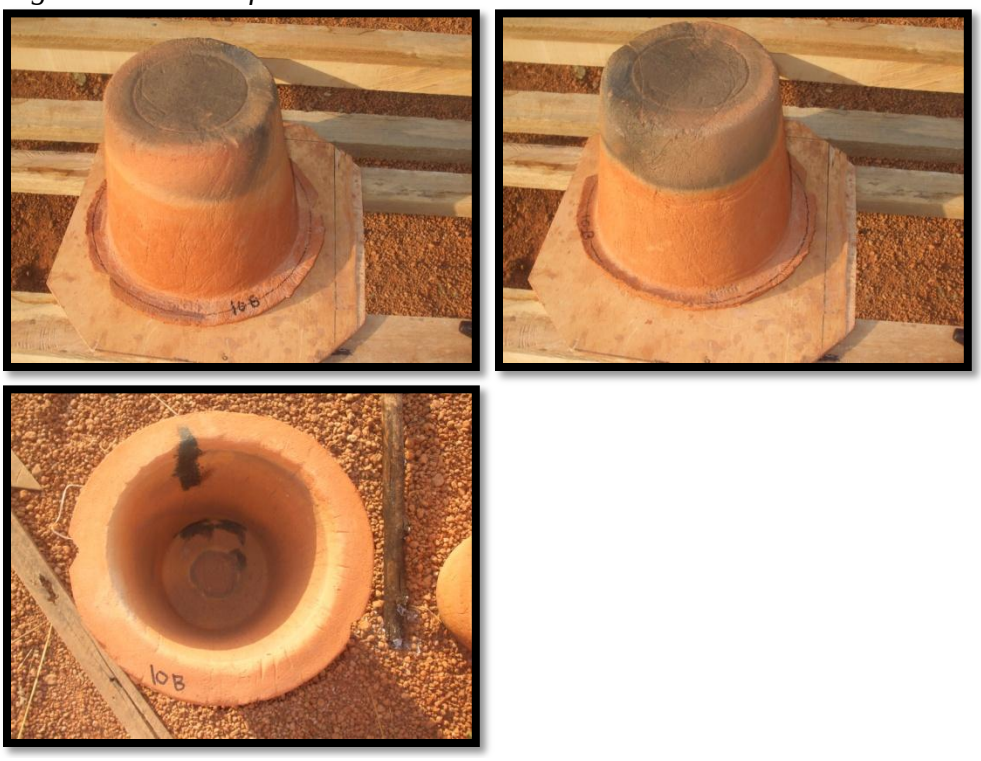

Figure 21: Views of Filter 11A

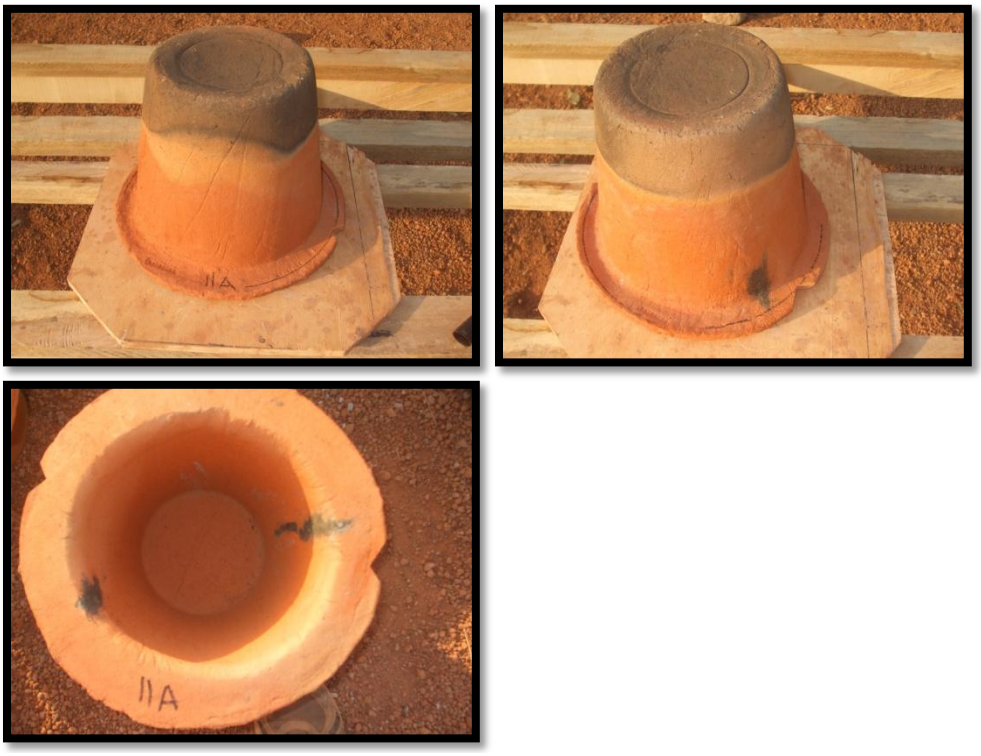

Figure 22: Views of Figure 11B

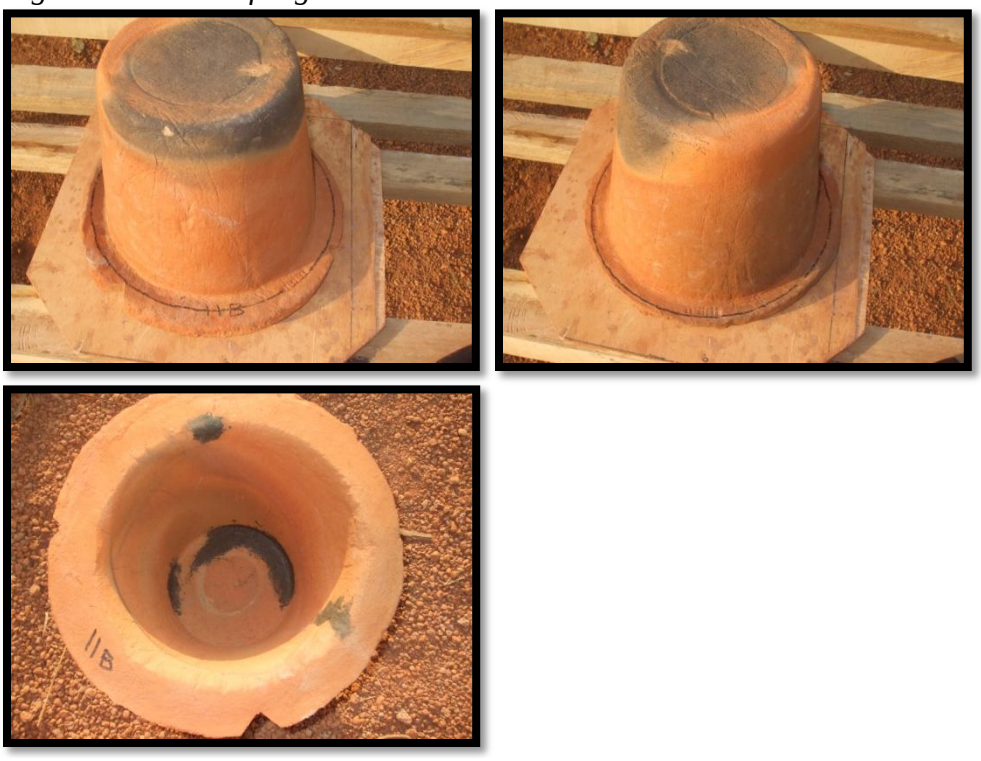

Figure 23: Views of Filter 12A

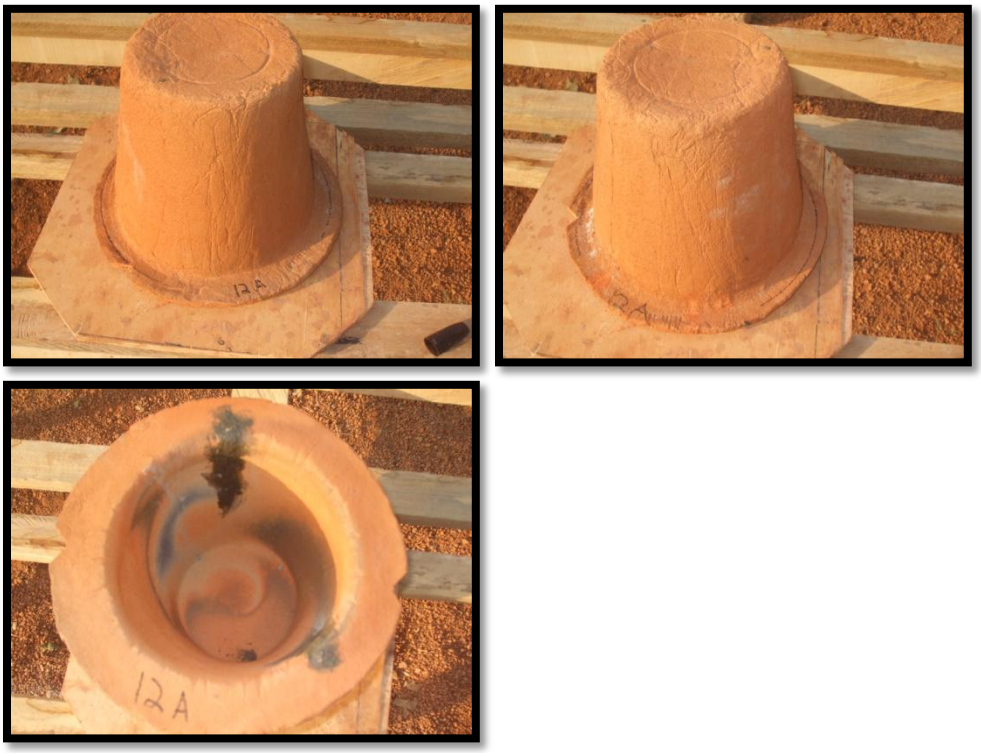

Figure 24: Views of Figure 12B

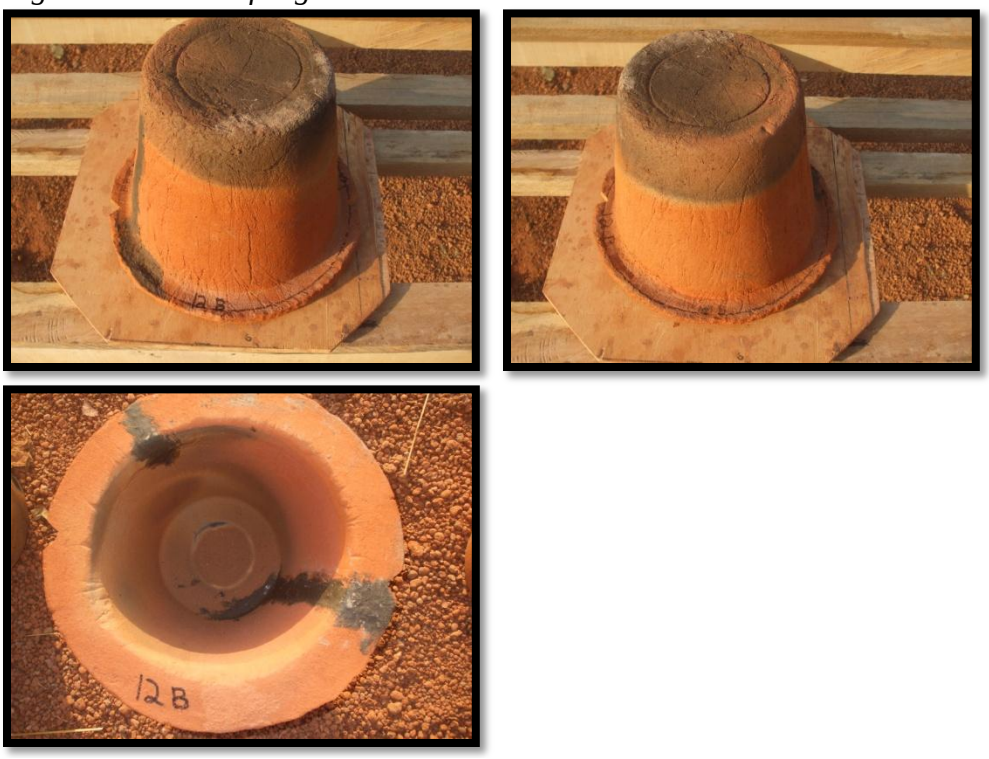

Figure 25: Views of Filter 13A

Figure 26: Views of Filter 13B

Figure 27: Views of Filter 14A

Figure 28: Views of Filter 14B

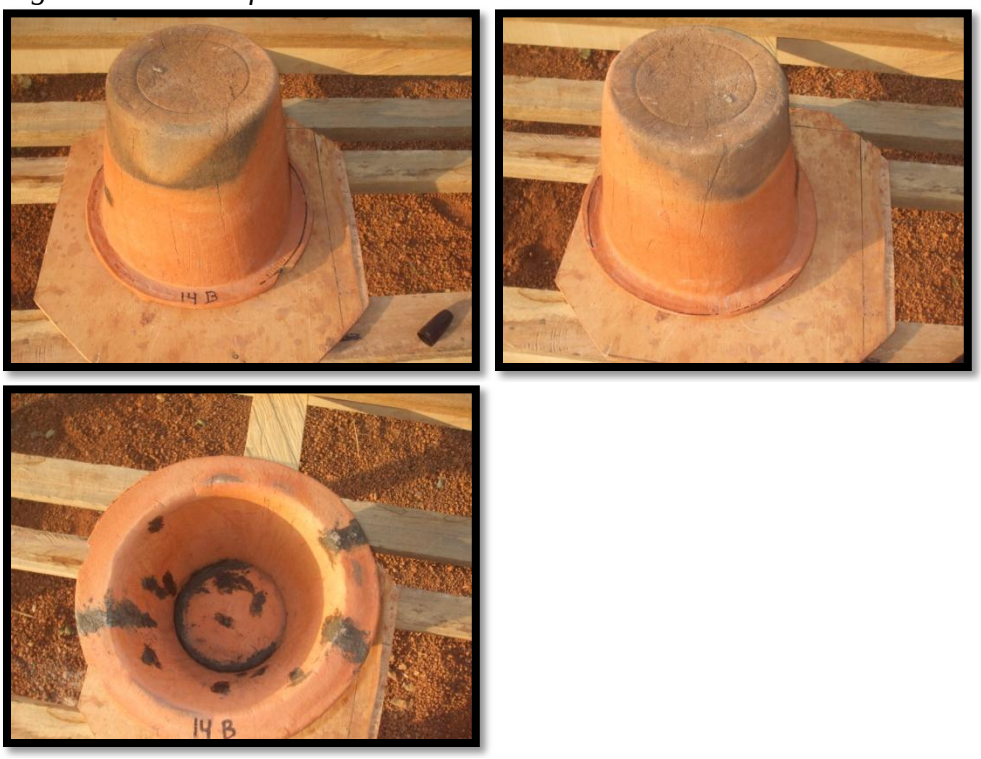

Figure 29: Views of Filter 15A

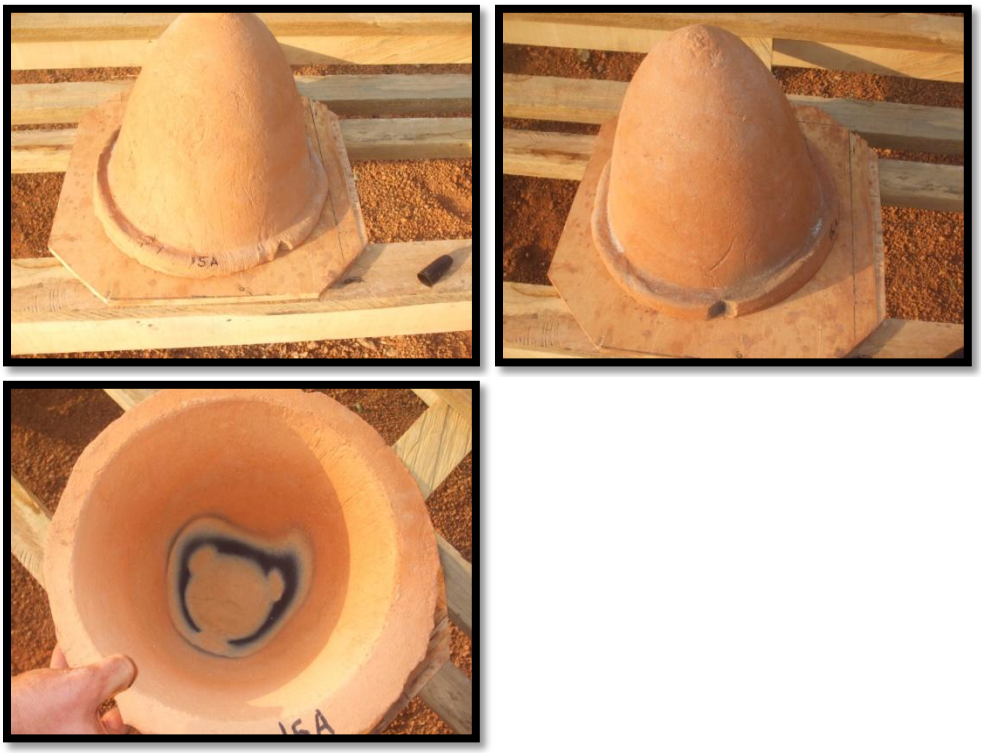

Figure 30: Views of Filter 15B

APPENDIX B: Filter Input Material Recipes

Table B-1 presents the mass of material added to create each clay mix for a pair of filters and some excess. Note that it does not represent the mass of material added to create each filter, but the mass:mass ratio of inputs.

Table B-1: Mass of Material Added to Each Clay Mix

Filter	Combustible Type	Total Combustible (kg)	Fine Combustible (kg)	Waste Combustible (kg)	Clay (kg)	Grog (kg)
1	Rice Husk	3.00	1.50	1.50	11	0
2	Rice Husk	3.00	1.50	1.50	11	1
3	Rice Husk	4.00	2.00	2.00	11	0
4	Rice Husk	4.00	2.00	2.00	11	1
5	Rice Husk	5.00	2.50	2.50	11	0
6	Rice Husk	5.00	2.50	2.50	11	1
7	Sawdust	2.19	1.09	1.09	11	0
8	Sawdust	2.19	1.09	1.09	11	1
9	Sawdust	2.91	1.46	1.46	11	0
10	Sawdust	2.91	1.46	1.46	11	1
11	Sawdust	3.64	1.82	1.82	11	0
12	Sawdust	3.64	1.82	1.82	11	1
13	Sawdust, sifted	1.82	1.82	0.00	11	0
14	Rice Husk, sifted	2.55	2.55	0.00	11	0
15	Rice Husk	3.00	1.50	1.50	11	1

APPENDIX C: Total Coliform Data

Table C-1: Total Coliforms (CFU /100 mL: Hose/Influent Water and Filtered Water*

** Values are based on the larger of two sample volumes tested*

Week	1	2	3	4	5	6	7	8	9	10	11	12
Hose 1-3	510	TNTC	TNTC	TNTC	1500	1600	TNTC	7500	6500	3300	3400	2700
1A	0	0	0	190	20	0	0	0	0	0	4	0
1B	4	0	0	0	0	0	0	0	0	10	0	0
2A	0	0	0	0	10	0	0	0	4	0	10	0
2B	0	0	0	0	0	0	0	0	0	2	6	4
3A	10	0	0	0	0	0	0	0	0	0	4	0
3B	0	0	0	0	0	30	0	15	32	0	2	8
Hose 4-6	TNTC	350	TNTC	TNTC	2500	2500	TNTC	7200	5700	5100	2300	3100
4A	0	20	0	10	10	20	0	0	4	0	0	0
4B	0	0	0	0	0	30	0	0	0	0	4	0
5A	0	0	50	0	0	0	0	0	0	0	0	4
5B	0	10	0	0	0	30	0	0	0	20	0	0
6A	0	20	0	0	0	50	0	0	0	0	4	0
6B	0	10	TNTC	0	0	20	0	0	24	0	0	0
Hose 7-9	TNTC	200	3900	TNTC	3500	2700	6700	TNTC	2800	3500	2700	2500
7A	10	0	TNTC	10	0		0	0	0	0	0	0
7B	80	130	190	90	0	40	0	20	25	32	4	0
8A	0	40	6	0	0	10	0	10	0	0	2	0
8B	10	0	TNTC	2			0	4	0	0	0	0
9A	10	0	100	0	0	10	0	TNTC	4	8	4	0
9B	0	0	TNTC	0	0	0	0	0	0	0	0	0
Hose 10-12	TNTC	490	4200	2600	1500	4500	5300	TNTC	3700	5200	2100	2800
10A	20	16	0	5	0	10	16	0	0	0	0	0
10B	0	0	0	0	0	20	0	0	1	0	0	0
11A	0	80	0	10	4	30	0	0	37	0	1	0
11B	10	120	0	40	20	20	0	0	0	2	2	0
12A	0	60	0	40	0	0	0	0	0	0	0	0
12B	0	0	0	20	0	10	10	0	0	0	0	0
Hose 13-15		TNTC	TNTC	4700	1200	TNTC	TNTC	TNTC	3700	4800	2900	2400
13A												
13B				0	0	0						
14A		0	110	0	0	0	0	100	TNTC	6	10	0
14B			0	0								
15A		0	30	0	0	0	0	0	2	0	0	0
15B			0	0	0	0	0	0	0	TNTC	0	0

In order to calculate the Log Removal Values (LRVs) of Total Coliform performed by the filters, it was necessary to make a conservative adjustment to the data. Results from membrane filtration testing were Too Numerous To Count (26 events, 8%) were adjusted by assuming the count was the maximum in the acceptable counting range, 200. Results from membrane filtration testing that were zero (184 events, 58%) were adjusted to be equal to one.

Table C-2: Total Coliform Log Removal Data

Week	1	2	3	4	5	6	7	8	9	10	11	12
1A	2.71	3.30	4.30	2.02	1.88	3.20	4.30	3.88	3.81	3.52	2.93	3.43
1B	2.11	3.30	4.30	4.30	3.18	3.20	4.30	3.88	3.81	2.52	3.53	3.43
2A	2.71	3.30	4.30	4.30	2.18	3.20	4.30	3.88	3.21	3.52	2.53	3.43
2B	2.71	3.30	4.30	4.30	3.18	3.20	4.30	3.88	3.81	3.22	2.75	2.83
3A	1.71	3.30	4.30	4.30	3.18	3.20	4.30	3.88	3.81	3.52	2.93	3.43
3B	2.71	3.30	4.30	4.30	3.18	1.73	4.30	2.70	2.31	3.52	3.23	2.53
4A	2.60	1.24	4.30	3.30	2.40	2.10	4.30	3.86	3.15	3.71	3.36	3.49
4B	2.60	2.54	4.30	4.30	3.40	1.92	4.30	3.86	3.76	3.71	2.76	3.49
5A	2.60	2.54	2.60	4.30	3.40	3.40	4.30	3.86	3.76	3.71	3.36	2.89
5B	2.60	1.54	4.30	4.30	3.40	1.92	4.30	3.86	3.76	2.41	3.36	3.49
6A	2.60	1.24	4.30	4.30	3.40	1.70	4.30	3.86	3.76	3.71	2.76	3.49
6B	2.60	1.54	1.00	4.30	3.40	2.10	4.30	3.86	2.38	3.71	3.36	3.49
7A	2.30	2.30	0.59	3.30	3.54		3.83	4.30	3.45	3.54	3.43	3.40
7B	1.40	0.19	1.31	2.35	3.54	1.83	3.83	3.00	2.05	2.04	2.83	3.40
8A	3.30	0.70	2.81	4.30	3.54	2.43	3.83	3.30	3.45	3.54	3.13	3.40
8B	2.30	2.30	0.69	4.00			3.83	3.70	3.45	3.54	3.43	3.40
9A	2.30	2.30	1.59	4.30	3.54	2.43	3.83	1.30	2.85	2.64	2.83	3.40
9B	3.30	2.30	0.99	4.30	3.54	3.43	3.83	4.30	3.45	3.54	3.43	3.40
10A	2.00	1.49	3.62	2.72	3.18	2.65	2.52	4.30	3.57	3.72	3.32	3.45
10B	3.30	2.69	3.62	3.41	3.18	2.35	3.72	4.30	3.57	3.72	3.32	3.45
11A	3.30	0.79	3.62	2.41	2.57	2.18	3.72	4.30	2.00	3.72	3.32	3.45
11B	2.30	0.61	3.62	1.81	1.88	2.35	3.72	4.30	3.57	3.41	3.02	3.45
12A	3.30	0.91	3.62	1.81	3.18	3.65	3.72	4.30	3.57	3.72	3.32	3.45
12B	3.30	2.69	3.62	2.11	3.18	2.65	2.72	4.30	3.57	3.72	3.32	3.45
13A												
13B				3.67	3.08	4.30						
14A		3.30	2.26	3.67	3.08	4.30	4.30	2.30	0.57	2.90	2.46	3.38
14B		0.70	4.30	3.67								
15A		3.30	2.82	3.67	3.08	4.30	4.30	4.30	3.27	3.68	3.46	3.38
15B			4.30	3.67	3.08	4.30	4.30	4.30	3.57	1.08	3.46	3.38

Table C-3: Total Coliform Log Removal Tiered Ranking of Filter Pairs based on Series of Two-Sample T-Tests assuming Unequal Variances with 95% Confidence by Excel Data Analysis

Key:

No	No evidence that filter in left column has greater mean than filter in the right column. $\|T\|<t$ and $p>\alpha$
Greater	Filter in left column has greater mean than filter in the right column. $\|T\|>t$ and $T>0$
Lesser	Filter in left column has lesser mean than filter in the right column. $\|T\|>t$ and $T<0$
T	Test statistic; if $\|T\|>t$, then $p<\alpha$ also.
p	Population proportion; if $p<\alpha=.05$, evidence of difference in means
t	Student's t value
>?	Denotes test of whether filter in left column has a greater mean than filter in right column

		15	2	1	5	3	4	12	10	6	8	9	14	11	7	TIER
15	T		0.612324	0.861948	1.048326	1.049705	1.220489	1.574627	1.669292	1.606345	1.802675	2.117696	1.747173	2.595948	3.165048	**1**
	p		0.271894	0.196806	0.150173	0.149859	0.114465	0.061423	0.051339	0.057846	0.039489	0.020011	0.047973	0.006471	0.001502	
	t		1.683851	1.681952	1.681071	1.681071	1.681071	1.681952	1.682878	1.681952	1.683851	1.681071	1.724718	1.681952	1.684875	
	>?		No	No	No	No	No	No	No	No	Greater	Greater	Greater	Greater	Greater	
2	T									1.20544	1.405679	1.736165	1.442551	2.264407	2.883175	**2**
	p									0.117648	0.084081	0.045022	0.083161	0.014593	0.003345	
	t									1.684875	1.687094	1.682878	1.734064	1.684875	1.689572	
	>?									No	No	Greater	No	Greater	Greater	
1	T											1.396742	1.236799	1.926813	2.55477	**3**
	p											0.084749	0.115616	0.030393	0.007377	
	t											1.68023	1.729133	1.681952	1.685954	
	>?											No	No	Greater	Greater	
5	T											1.157674	1.083561	1.688898	2.322614	**3**
	p											0.126552	0.145725	0.049157	0.012686	
	t											1.679427	1.724718	1.68023	1.683851	
	>?											No	No	Greater	Greater	
3	T											1.158715	1.083985	1.690312	2.324335	**3**
	p											0.126342	0.145633	0.049021	0.012635	
	t											1.679427	1.724718	1.68023	1.683851	
	>?											No	No	Greater	Greater	
4	T												0.929056	1.452166	2.08825	**4**
	p												0.181708	0.076696	0.021438	
	t												1.720743	1.679427	1.681952	
	>?												No	No	Greater	
12	T												0.767244	1.260196	1.929265	**4**
	p												0.226183	0.107197	0.030499	
	t												1.729133	1.681071	1.684875	
	>?												No	No	Greater	
10	T												0.780503	1.309828	1.996256	**4**
	p												0.222619	0.098864	0.026756	
	t												1.734064	1.683851	1.688298	
	>?												No	No	Greater	
6	T												0.523992	0.855613	1.482225	**5**
	p												0.302545	0.198323	0.072625	
	t												1.710882	1.67866	1.679427	
	>?												No	No	No	
8	T														1.400615	**5**
	p														0.084337	
	t														1.681952	
	>?														No	
9	T														1.23206	**5**
	p														0.112311	
	t														1.681071	
	>?														No	
14	T														0.656985	**5**
	p														0.258482	
	t														1.705618	
	>?														No	
11	T														0.683273	**5**
	p														0.249008	
	t														1.68023	
	>?														No	

Table C-4: Total Coliform Log Removal, Series of Two-Sample T-Tests assuming Unequal Variances with 95% Confidence, Rice Husk Filters Sorted in Order of Increasing Percent combustible by mass and Combustible Type by Excel Data Analysis

Key:

No	No evidence that filter in left column has greater mean than filter in the right column. $\|T\|<t$ and $p>\alpha$
Greater	Filter in left column has greater mean than filter in the right column. $\|T\|>t$ and $T>0$
Lesser	Filter in left column has lesser mean than filter in the right column. $\|T\|>t$ and $T<0$
T	Test statistic; if $\|T\|>t$, then $p<\alpha$ also.
p	Population proportion; if $p<\alpha=.05$, evidence of difference in means
t	Student's t value
>?	Denotes test of whether filter in left column has a greater mean than filter in right column

		2	1	4	3	6	5
2	T		0.3129561	0.7438227	0.5378803	1.2054397	0.5369484
	p		0.3778799	0.2305145	0.296685	0.1176484	0.2970041
	t		1.6794274	1.6810707	1.68023	1.6848751	1.68023
	>?		No	No	No	No	No
1	T			0.434091	0.224184	0.917177	0.2237409
	p			0.333148	0.411804	0.182143	0.4119748
	t			1.679427	1.67866	1.681952	1.6786604
	>?			No	No	No	No
4	T				-0.21266	0.50516	-0.2125688
	p				0.416267	0.307984	0.4163013
	t				1.67866	1.68023	1.6786604
	>?				No	No	No
3	T					-0.21257	-0.0001517
	p					0.416301	0.4999398
	t					1.67866	1.6786604
	>?					No	No
6	T						-0.7092538
	p						0.2409976
	t						1.6810707
	>?						No
5	T						
	p						
	t						
	>?						

Table C-5: Total Coliform Log Removal, Series of Two-Sample T-Tests assuming Unequal Variances with 95% Confidence, Sawdust Filters Sorted in Order of Increasing Percent Combustible by mass and Combustible Type by Excel Data Analysis

Key:

No	No evidence that filter in left column has greater mean than filter in the right column. $\|T\|<t$ and $p>\alpha$
Greater	Filter in left column has greater mean than filter in the right column. $\|T\|>t$ and $T>0$
Lesser	Filter in left column has lesser mean than filter in the right column. $\|T\|>t$ and $T<0$
T	Test statistic; if $\|T\|>t$, then $p<\alpha$ also.
p	Population proportion; if $p<\alpha=.05$, evidence of difference in means
t	Student's t value
>?	Denotes test of whether filter in left column has a greater mean than filter in right column

		8	7	10	9	12	11
8	T		1.4006148	-0.4446948	0.2236426	-0.4303262	0.7533902
	p		0.0843372	0.3295315	0.4120473	0.334606	0.227614
	t		1.6819524	1.6859545	1.6810707	1.682878	1.68023
	>?		No	No	No	No	No
7	T			-1.99626	-1.23206	-1.92926	-0.6832733
	p			0.026756	0.112311	0.030499	0.2490083
	t			1.688298	1.681071	1.684875	1.68023
	>?			Lesser	No	Lesser	No
10	T				0.727559	-0.00563	1.3098282
	p				0.23546	0.497767	0.0988635
	t				1.681952	1.679427	1.683851
	>?				No	No	No
9	T					-0.69868	0.5562516
	p					0.244173	0.2903674
	t					1.679427	1.6786604
	>?					No	No
12	T						1.2601958
	p						0.1071975
	t						1.6810707
	>?						No
11	T						
	p						
	t						
	>?						

APPENDIX D: *E. coli* Data

Table D-1: E. coli (CFU /100 mL): Hose/Influent Water and Filtered Water*

* Values are based on the larger of two sample volumes tested

Week	1	2	3	4	5	6	7	8	9	10	11	12
Hose 1-3	40	0	800	100	0	0	0	0	0	0	0	0
1A	0	0	0	0	0	0	0	0	0	0	0	0
1B	4	0	0	0	0	0	0	0	0	0	0	0
2A	0	0	0	0	0	0	0	0	0	0	0	0
2B	0	0	0	0	0	0	0	0	0	0	0	0
3A	0	0	0	0	0	0	0	0	0	0	0	0
3B	0	0	0	0	0	0	0	0	0	0	0	0
Hose 4-6	40	0	400	200	0	0	0	0	0	0	0	0
4A	0	0	0	0	0	0	0	0	0	0	0	0
4B	0	0	0	0	0	0	0	0	0	0	0	0
5A	0	0	0	0	0	0	0	0	0	0	0	0
5B	0	0	0	0	0	0	0	0	0	0	0	0
6A	0	0	0	0	0	0	0	0	0	0	0	0
6B	0	0	0	0	0	0	0	0	0	0	0	0
Hose 7-9	80	0	200	700	0	0	0	0	0	0	0	0
7A	10	0	0	0	0		0	0	0	0	0	0
7B	0	0	10	20	0	0	0	0	0	0	0	0
8A	0	0	0	0	0	0	0	0	0	0	0	0
8B	0	0	8	0			0	0	0	0	0	0
9A	0	0	0	0	0	0	0	0	0	0	0	0
9B	0	0	0	0	0	0	0	0	0	0	0	0
Hose 10-12	20	0	0	100	0	0	0	0	0	0	0	0
10A	20	0	0	0	0	0	0	0	0	0	0	0
10B	0	0	0	0	0	0	0	0	0	0	0	0
11A	0	0	0	0	0	0	0	0	0	0	0	0
11B	10	0	0	0	0	0	0	0	0	0	0	0
12A	0	0	0	0	0	0	0	0	0	0	0	0
12B	0	0	0	0	0	0	0	0	0	0	0	0
Hose 13-15		0	400	100	0	0	0	0	0	0	0	0
13A												
13B				0	0	0						
14A		0	0	0	0	0	0	0	0	0	0	0
14B		0	0	0								
15A		0	0	0	0	0	0	0	0	0	0	0
15B			0	0	0	0	0	0	0	0	0	0

APPENDIX E: Comparison between Sampling Methods

Table E-1: Total Coliform and E. coli counts in Filtered Water in Both the Standard Container Used in the Study, and Sterile Whirl-Pak® Bags

Week	Filter	Container Total Coliform, CFU/100mL	Whirl-Pak® Total Coliform, CFU/100mL	Difference Total Coliform, CFU/100mL	Container *E. coli*, CFU/100mL	Whirl-Pak® *E. coli*, CFU/100mL	Difference *E. coli*, CFU/100mL
8	1A	0	0	0	0	0	0
8	1B	0	0	0	0	0	0
8	2A	0	0	0	0	0	0
8	2B	0	0	0	0	0	0
8	3A	0	0	0	0	0	0
8	3B	15	60	-45	0	0	0
8	4A	0	0	0	0	0	0
8	4B	0	0	0	0	0	0
8	5A	0	0	0	0	0	0
8	5B	0	0	0	0	0	0
8	6A	0	0	0	0	0	0
8	6B	0	0	0	0	0	0
7	7A	0	0	0	0	0	0
7	7B	0	0	0	0	0	0
7	8A	0	0	0	0	0	0
7	8B	0	0	0	0	0	0
7	9A	0	0	0	0	0	0
7	9B	0	0	0	0	0	0
7	10A	16	32	-16	0	0	0
7	10B	0	0	0	0	0	0
7	11A	0	0	0	0	0	0
7	11B	0	0	0	0	0	0
7	12A	0	0	0	0	0	0
7	12B	10	0	10	0	0	0
7	13A						
7	13B						
7	14A	0	0	0	0	0	0
7	14B						
7	15A	0	0	0	0	0	0
7	15B	0	0	0	0	0	0

Table E-2: Results of Statistical Test

Test: Total Coliform		Test: *E. coli*
Mean	-0.40741	All values are 0.
StDev	9.954741	
Sample, n	27	
t .025, n-1	2.056	
|T|	0.212658	

|T|<t.025	Not enough evidence to reject that means are equal

APPENDIX F: Turbidity Data

Table F-1: Turbidity (NTU) for Hose/Influent Water and Filtered Water

Week	1	2	3	4	5	6	7	8	9	10	11	12
Hose 1-3	161	119	157	113	105	142	165	166	226	195	153	131
1A	143	105	114	12	94	133	140	129	127	97	96	79
1B	149	114	130	107	102	107	113	107	121	138	133	93
2A	146	88	99	135	101	130	153	140	103	128	126	107
2B	125	82	90	114	102	147	141	115	115	112	97	99
3A	138	88	108	120	90	117	122	115	104	133	128	15
3B	110	94	110	98	97	103	107	102	100	134	126	120
Hose 4-6	239	102	145	115	108	144	157	122	177	153	165	152
4A	110	79	108	113	103	121	103	97	105	63	66	93
4B	120	58	120	113	105	106	107	101	97	127	137	105
5A	139	89	122	114	101	106	107	94	93	91	92	85
5B	145	79	124	110	98	99	97	93	100	115	122	76
6A	142	45	123	96	101	102	102	99	101	128	126	127
6B	131	90	117	111	106	106	107	106	104	123	130	132
Hose 7-9	152	167	153	121	117	135	167	175	251	155	160	146
7A	110	2	18	8	107		87	10	10	13	63	47
7B	144	118	142	99	109	111	132	140	201	145	139	99
8A	143	163	139	114	104	108	104	125	12	10	93	51
8B	75	2	9	4			15	11	15	15	57	77
9A	109	81	63	6	14	65	67	82	125	63	54	139
9B	81	31	6	62	72	11	7	3	17	15	67	92
Hose 10-12	156	207	150	110	102	127	160	215	198	162	158	151
10A	37	28	9	20	26	17	7	12	3	5	6	10
10B	43	25	13	22	24	19	12	12	3	8	9	10
11A	65	60	38	48	37	37	31	47	15	16	27	32
11B	50	52	14	35	35	20	9	12	8	16	19	18
12A	82	81	58	65	52	47	53	45	11	22	47	39
12B	62	68	39	48	46	37	38	49	6	39	36	29
Hose 13-15	132	222	151	115	141	120	170	327	198	159	149	152
13A												
13B				93	124	110						
14A	134	213	141	115	124	114	115	314	215	126	118	110
14B	110	108	105	51								
15A		100	92	81	115	112	84	162	126	96	116	121
15B			91	138	121	115	137	230	85	75	85	97

Table F-2: Turbidity Removal (%) for Each Filter

Week	1	2	3	4	5	6	7	8	9	10	11	12
1A	11%	12%	27%	89%	10%	6%	15%	22%	44%	50%	37%	40%
1B	7%	4%	17%	5%	3%	25%	32%	36%	46%	29%	13%	29%
2A	9%	26%	37%	-19%	4%	8%	7%	16%	54%	34%	18%	18%
2B	22%	31%	43%	-1%	3%	-4%	15%	31%	49%	43%	37%	24%
3A	14%	26%	31%	-6%	14%	18%	26%	31%	54%	32%	16%	89%
3B	32%	21%	30%	13%	8%	27%	35%	39%	56%	31%	18%	8%
4A	54%	23%	26%	2%	5%	16%	34%	20%	41%	59%	60%	39%
4B	50%	43%	17%	2%	3%	26%	32%	17%	45%	17%	17%	31%
5A	42%	13%	16%	1%	6%	26%	32%	23%	47%	41%	44%	44%
5B	39%	23%	14%	4%	9%	31%	38%	24%	44%	25%	26%	50%
6A	41%	56%	15%	17%	6%	29%	35%	19%	43%	16%	24%	16%
6B	45%	12%	19%	3%	2%	26%	32%	13%	41%	20%	21%	13%
7A	28%	99%	88%	93%	9%		48%	94%	96%	92%	61%	68%
7B	5%	29%	7%	18%	7%	18%	21%	20%	20%	6%	13%	32%
8A	6%	2%	9%	6%	11%	20%	38%	29%	95%	94%	42%	65%
8B	51%	99%	94%	97%			91%	94%	94%	90%	64%	47%
9A	28%	51%	59%	95%	88%	52%	60%	53%	50%	59%	66%	5%
9B	47%	81%	96%	49%	38%	92%	96%	98%	93%	90%	58%	37%
10A	76%	86%	94%	82%	75%	87%	96%	94%	98%	97%	96%	93%
10B	72%	88%	91%	80%	76%	85%	93%	94%	98%	95%	94%	93%
11A	58%	71%	75%	56%	64%	71%	81%	78%	92%	90%	83%	79%
11B	68%	75%	91%	68%	66%	84%	94%	94%	96%	90%	88%	88%
12A	47%	61%	61%	41%	49%	63%	67%	79%	94%	86%	70%	74%
12B	60%	67%	74%	56%	55%	71%	76%	77%	97%	76%	77%	81%
13A												
13B				19%	12%	8%						
14A	-2%	4%	7%	0%	12%	5%	32%	4%	-9%	21%	21%	28%
14B	17%	51%	30%	56%								
15A		55%	39%	30%	18%	7%	51%	50%	36%	40%	22%	20%
15B			40%	-20%	14%	4%	19%	30%	57%	53%	43%	36%

Table F-3: Turbidity Removal, Series of Two-Sample T-Tests assuming Unequal Variances with 95% Confidence, Rice Husk Filters Sorted in Order of Increasing Percent combustible by mass and Combustible Type by Excel Data Analysis

Key:

No	No evidence that filter in left column has greater mean than filter in the right column. $\|T\|<t$ and $p>\alpha$
Greater	Filter in left column has greater mean than filter in the right column. $\|T\|>t$ and $T>0$
Lesser	Filter in left column has lesser mean than filter in the right column. $\|T\|>t$ and $T<0$
T	Test statistic; if $\|T\|>t$, then $p<\alpha$ also.
p	Population proportion; if $p<\alpha=.05$, evidence of difference in means
t	Student's t value
>?	Denotes test of whether filter in left column has a greater mean than filter in right column

		2	1	4	3	6	5
2	T		-0.80471	-1.38159	-1.21717	-0.5306	-1.37088
	p		0.212563	0.086886	0.114875	0.299213	0.088682
	t		1.67866	1.67866	1.67866	1.681071	1.68023
	>?		No	No	No	No	No
1	T			-0.5091	-0.37942	0.389145	-0.42553
	p			0.306586	0.353061	0.349591	0.336285
	t			1.679427	1.67866	1.682878	1.681071
	>?			No	No	No	No
4	T				0.120417	1.014498	0.13184
	p				0.452339	0.157946	0.447856
	t				1.67866	1.68023	1.68023
	>?				No	No	No
3	T					0.840136	-0.00371
	p					0.202795	0.498527
	t					1.681952	1.681071
	>?					No	No
6	T						-0.9796
	p						0.166203
	t						1.67866
	>?						No
5	T						
	p						
	t						
	>?						

Table F-4: Turbidity Removal, Series of Two-Sample T-Tests assuming Unequal Variances with 95% Confidence, Sawdust Filters Sorted in Order of Increasing Percent combustible by mass and Combustible Type by Excel Data Analysis

Key:

No	No evidence that filter in left column has greater mean than filter in the right column. $\|T\|<t$ and $p>\alpha$
Greater	Filter in left column has greater mean than filter in the right column. $\|T\|>t$ and $T>0$
Lesser	Filter in left column has lesser mean than filter in the right column. $\|T\|>t$ and $T<0$
T	Test statistic; if $\|T\|>t$, then $p<\alpha$ also.
p	Population proportion; if $p<\alpha=.05$, evidence of difference in means
t	Student's t value
>?	Denotes test of whether filter in left column has a greater mean than filter in right column

		8	7	10	9	12	11
8	T		1.305641	-4.10843	-0.86062	-1.56383	-2.80735
	p		0.099309	0.000215	0.197496	0.064752	0.004772
	t		1.681071	1.713872	1.687094	1.703288	1.708141
	>?		No	Lesser	No	No	Lesser
7	T			-6.21764	-2.45488	-3.42645	-4.7776
	p			1E-06	0.009269	0.000924	2.77E-05
	t			1.710882	1.683851	1.699127	1.703288
	>?			Lesser	Lesser	Lesser	Lesser
10	T				4.545744	5.980641	3.329132
	p				4.8E-05	3.33E-07	0.00094
	t				1.701131	1.687094	1.683851
	>?				Greater	Greater	Greater
9	T					-0.83458	-2.60141
	p					0.204729	0.006896
	t					1.688298	1.69236
	>?					No	Greater
12	T						-2.64571
	p						0.005595
	t						1.679427
	>?						Greater
11	T						
	p						
	t						
	>?						

APPENDIX G: Flowrate Data

Table G-1: Flowrate (L/hour) for each filter

Week	1	2	3	4	5	6	7	8	9	10	11	12
1A	1.2	1	0.6	1	1.4	1	0.6	1.2	0.1	0.1	0.6	0.4
1B	3	2.6	2.6	2	2.8	2.2	1.4	1.2	0.4	0.5	1.2	1
2A	1.4	0.8	1.2	1	0.8	0.8	0.8	1	0.2	0.3	0.6	0.6
2B	0.8	1	1.2	0.6	0.8	1	0.6	0.8	0.2	0.2	0.8	0.6
3A	2	1.4	2.2	2.4	2	1.8	1.8	2	0.3	0.5	1.6	1.2
3B	3	2.2	4	3.4	3.6	3.8	3.6	3.2	0.8	0.8	2	1.6
4A	1.4	1.4	2	1.6	2.8	2	1.6	1.6	0.3	0.4	0.6	0.4
4B	2.2	1.8	3.6	3.2	3.2	2.6	2.2	2.8	1	0.8	1.6	1.6
5A	3	3.2	3.2		5	4.2	3.4	1.4	0.8	0.7	1.2	0.8
5B	4.6		5.4		5.8	6	5	4	1	1.8	2.4	2
6A	5.8	7.8	8.8	7	8.8	8.6	8.8	7	1.8	2.4	4.2	3.8
6B	3.4	4	5.4	3.6	6	5.4	4.6	3.6	1.2	1.4	1.6	1.6
7A	0.4	0.4	0.4	0.1	0.1		0.02	0.02	0.01	0.01	0.02	0.02
7B	0.6	0.4	0.6	0.1	0.8	0.8	0.8	1	0.4	0.3	0.6	0.4
8A	1	0.6	0.4	0.4	0.4	0.6	0.4	0.6	0.1	0.05	0.1	0.1
8B	0.4	0.4	0.4	0.02			0.02	0.02	0.01	0.01	0.02	0.02
9A	1	0.4	1	0.6	0.8	0.8	0.8	0.6	0.1	0.1	0.2	0.2
9B	0.4		0.4	0.6	0.2	0.1	0.02	0.02	0.01	0.01	0.02	0.02
10A	0.6	0.4	0.4	0.6	0.6	0.4	0.2	0.1	0.1	0.05	0.2	0.2
10B	0.6	0.4	0.2	0.4	0.4	0.4	0.2	0.1	0.05	0.1	0.2	0.2
11A	1.4	0.8	0.8	1	1.2	1	0.8	0.4	0.2	0.2	0.6	0.6
11B	1	0.4	0.6	0.6	1.6	0.8	0.6	0.2	0.1	0.3	0.4	0.4
12A	2.4	1.6	1.4		2.8	2.2	1	0.1	0.3	0.5	0.8	0.8
12B	1.4	1	1	1.4	3	2	1.2	0.4	0.4	0.5	1	1
13A	0.4	0.4										
13B	0.4	0.4		0.1	2	2						
14A	0.6	0.4	0.4	0.4	2	2.2	2	0.8	0.7	0.9	2.2	2
14B	0.4	0.4	0.1	0.1			0	0				
15A	0.4	0.4	0.6	0.2	0.6	0.8	0.6	0.4	0.2	0.3	0.8	0.8
15B	0.4	0.4	0.1	0.2	0.6	0.6	0.6	0.1	0.05	0.1	0.8	0.8

Table G-2: Flowrate Tiered Ranking of Filter Pairs based on Series of Two-Sample T-Tests assuming Unequal Variances with 95% Confidence by Excel Data Analysis

Key:

No	No evidence that filter in left column has greater mean than filter in the right column. $\|T\|<t$ and $p>\alpha$
Greater	Filter in left column has greater mean than filter in the right column. $\|T\|>t$ and $T>0$
Lesser	Filter in left column has lesser mean than filter in the right column. $\|T\|>t$ and $T<0$
T	Test statistic; if $\|T\|>t$, then $p<\alpha$ also.
p	Population proportion; if $p<\alpha=.05$, evidence of difference in means
t	Student's t value
>?	Denotes test of whether filter in left column has a greater mean than filter in right column

		6	5	3	4	1	12	2	14	11	15	9	7	10	8	TIER
6	T		2.715526	4.814554												1
	p		0.004821	1.83E-05												
	t		1.682878	1.695519												
	>?		Greater	Greater												
5	T			2.152888	3.034613											2
	p			0.019485	0.002522											
	t			1.693889	1.699127											
	>?			Greater	Greater											
3	T				1.227498	3.157583	3.320611									3
	p				0.113009	0.001436	0.000919									
	t				1.679427	1.68023	1.681071									
	>?				No	Greater	Greater									
4	T					2.034445	2.191095	5.102041	3.376819							3
	p					0.023848	0.016892	1.05E-05	0.000836							
	t					1.67866	1.68023	1.701131	1.684875							
	>?					Greater	Greater	Greater	Greater							
1	T						0.116603	2.686613	1.493739	3.062607	4.405542					4
	p						0.453847	0.005911	0.071751	0.002212	7.51E-05					
	t						1.679427	1.699127	1.685954	1.693889	1.703288					
	>?						No	Greater	No	Greater	Greater					
12	T							2.648058	1.416086	3.037336	4.448688					4
	p							0.006479	0.082672	0.002361	7.2E-05					
	t							1.699127	1.688298	1.693889	1.705618					
	>?							Greater	No	Greater	Greater					
2	T								-0.55516	0.851206	3.632758	4.039893				5
	p								0.292326	0.199632	0.000364	0.000106				
	t								1.720743	1.68023	1.68023	1.68023				
	>?								No	No	Greater	Greater				
14	T									0.961945	2.084007	2.448867				5
	p									0.173041	0.025098	0.011382				
	t									1.713872	1.724718	1.717144				
	>?									No	Greater	Greater				
11	T										2.252242	2.819392				5
	p										0.014932	0.003564				
	t										1.683851	1.679427				
	>?										Greater	Greater				
15	T											0.984838	1.103184	2.430154	2.257689	6
	p											0.16524	0.138041	0.009723	0.014549	
	t											1.682878	1.681071	1.681952	1.681071	
	>?											No	No	Greater	Greater	
9	T													0.861366	0.971913	7
	p													0.197535	0.168329	
	t													1.690924	1.681952	
	>?													No	No	
7	T													0.873381	0.981029	7
	p													0.194122	0.166033	
	t													1.688298	1.681071	
	>?													No	No	
10	T														0.287647	7
	p														0.387633	
	t														1.688298	
	>?														No	

Table G-3: Flowrate, Series of Two-Sample T-Tests assuming Unequal Variances with 95% Confidence, Rice Husk Filters Sorted in Order of Increasing Percent combustible by mass and Combustible Type by Excel Data Analysis

Key:

No	No evidence that filter in left column has greater mean than filter in the right column. $\|T\|<t$ and $p>\alpha$
Greater	Filter in left column has greater mean than filter in the right column. $\|T\|>t$ and $T>0$
Lesser	Filter in left column has lesser mean than filter in the right column. $\|T\|>t$ and $T<0$
T	Test statistic; if $\|T\|>t$, then $p<\alpha$ also.
p	Population proportion; if $p<\alpha=.05$, evidence of difference in means
t	Student's t value
>?	Denotes test of whether filter in left column has a greater mean than filter in right column

		5	6	3	4	1	2
5	T		-2.71553	2.152888	3.034613	4.316239	5.938658
	p		0.004821	0.019485	0.002522	8.95E-05	3.4E-06
	t		1.682878	1.693889	1.699127	1.701131	1.720743
	>?		Lesser	Greater	Greater	Greater	Greater
6	T			4.814554	5.535559	6.540159	7.791567
	p			1.83E-05	2.87E-06	2.17E-07	2.51E-08
	t			1.695519	1.699127	1.701131	1.710882
	>?			Greater	Greater	Greater	Greater
3	T				1.227498	3.157583	6.089673
	p				0.113009	0.001436	8.35E-07
	t				1.679427	1.68023	1.703288
	>?				No	Greater	Greater
4	T					2.034445	5.102041
	p					0.023848	1.05E-05
	t					1.67866	1.701131
	>?					Greater	Greater
1	T						2.686613
	p						0.005911
	t						1.699127
	>?						Greater
2	T						
	p						
	t						
	>?						

Table G-4: Flowrate, Series of Two-Sample T-Tests assuming Unequal Variances with 95% Confidence, Sawdust Filters Sorted in Order of Increasing Percent combustible by mass and Combustible Type by Excel Data Analysis

Key:

No	No evidence that filter in left column has greater mean than filter in the right column. |T|<t and p>α
Greater	Filter in left column has greater mean than filter in the right column. |T|>t and T>0
Lesser	Filter in left column has lesser mean than filter in the right column. |T|>t and T<0
T	Test statistic; if |T|>t, then p<α also.
p	Population proportion; if p<α=.05, evidence of difference in means
t	Student's t value
>?	Denotes test of whether filter in left column has a greater mean than filter in right column

		11	12	9	10	7	8
11	T		-2.08827	2.819392	4.202612	2.985922	3.959141
	p		0.023779	0.003564	9.43E-05	0.002326	0.000146
	t		1.710882	1.679427	1.69236	1.681071	1.682878
	>?		Lesser	Greater	Greater	Greater	Greater
12	T			4.766078	5.464584	4.86095	5.40236
	p			2.25E-05	6.44E-06	2.03E-05	5.18E-06
	t			1.697261	1.710882	1.701131	1.703288
	>?			Greater	Greater	Greater	Greater
9	T				0.861366	0.045352	0.971913
	p				0.197535	0.482016	0.168329
	t				1.690924	1.68023	1.681952
	>?				No	No	No
10	T					-0.87338	0.287647
	p					0.194122	0.387633
	t					1.688298	1.688298
	>?					No	No
7	T						0.981029
	p						0.166033
	t						1.681071
	>?						No
8	T						
	p						
	t						
	>?						

APPENDIX H: Filter Pair Comparison Tests

"Equal Means" demonstrates that there is not enough evidence to reject the null hypothesis that the population means are equal. "Unequal Means" demonstrates that there is enough evidence to reject the null hypothesis that the population means are equal.

Table H-1: Total Coliform Log Removal, Two-tailed tests of the differences between the population means of matched events of filters A and B in a pair with a 95% confidence interval.

	Differences	Differences	Differences				
Filter Pair	Mean	Standard Deviation	Sample Size	T	|T|	t.025	|T|> t?
1	-0.198	0.934	10	-0.669	0.669	2.262	Equal Means
2	-0.130	0.378	10	-1.089	1.089	2.262	Equal Means
3	0.316	0.805	10	1.241	1.241	2.262	Equal Means
4	-0.373	0.547	10	-2.153	2.153	2.262	Equal Means
5	0.208	0.902	10	0.729	0.729	2.262	Equal Means
6	0.298	0.854	10	1.105	1.105	2.262	Equal Means
7	0.906	0.768	9	3.537	3.537	2.306	Unequal Means
8	0.103	0.930	8	0.313	0.313	2.365	Equal Means
9	-0.551	0.784	10	-2.220	2.220	2.262	Equal Means
10	-0.411	0.622	10	-2.087	2.087	2.262	Equal Means
11	0.103	0.696	10	0.470	0.470	2.262	Equal Means
12	-0.008	0.764	10	-0.033	0.033	2.262	Equal Means
14	0.065	1.774	4	0.073	0.073	3.182	Equal Means
15	0.282	1.158	10	0.771	0.771	2.262	Equal Means

Table H-2: E. coli count, Two-tailed tests of the differences between the population means of matched events of filters A and B in a pair with a 95% confidence interval.

	Differences	Differences	Differences				
Filter Pair	Mean	Standard Deviation	Sample Size	T	|T|	t.025	|T|> t?
1	-0.400	1.265	10	-1	1	2.262	Equal Means
2	0.000	0.000	10	#DIV/0!	#DIV/0!	2.262	Equal Means
3	0.000	0.000	10	#DIV/0!	#DIV/0!	2.262	Equal Means
4	0.000	0.000	10	#DIV/0!	#DIV/0!	2.262	Equal Means
5	0.000	0.000	10	#DIV/0!	#DIV/0!	2.262	Equal Means
6	0.000	0.000	10	#DIV/0!	#DIV/0!	2.262	Equal Means
7	-2.222	8.333	9	-0.8	0.8	2.306	Equal Means
8	-1.000	2.828	8	-1	1	2.365	Equal Means
9	0.000	0.000	10	#DIV/0!	#DIV/0!	2.262	Equal Means
10	2.000	6.325	10	1	1	2.262	Equal Means
11	-1.000	3.162	10	-1	1	2.262	Equal Means
12	0.000	0.000	10	#DIV/0!	#DIV/0!	2.262	Equal Means
15	0.000	0.000	8	#DIV/0!	#DIV/0!	2.365	Equal Means

Table H-3: Turbidity Removal, Two-tailed tests of the differences between the population means of matched events of filters A and B in a pair with a 95% confidence interval.

	Differences	Differences	Differences				
Filter Pair	Mean	Standard Deviation	Sample Size	T	|T|	t.025	|T|> t?
1	8%	29%	10	0.896	0.896	2.262	Equal Means
2	-5%	9%	10	-1.842	1.842	2.262	Equal Means
3	-5%	9%	10	-1.825	1.825	2.262	Equal Means
4	3%	16%	10	0.519	0.519	2.262	Equal Means
5	0%	7%	10	-0.205	0.205	2.262	Equal Means
6	6%	14%	10	1.397	1.397	2.262	Equal Means
7	57%	31%	9	5.511	5.511	2.306	Unequal Means
8	-54%	39%	8	-3.907	3.907	2.365	Unequal Means
9	-18%	36%	10	-1.632	1.632	2.262	Equal Means
10	1%	2%	10	1.876	1.876	2.262	Equal Means
11	-9%	6%	10	-4.649	4.649	2.262	Unequal Means
12	-6%	8%	10	-2.468	2.468	2.262	Unequal Means
14	-36%	18%	4	-4.013	4.013	3.182	Unequal Means
15	9%	23%	8	1.117	1.117	2.365	Equal Means

Table H-4: Flowrate, Two-tailed tests of the differences between the population means of matched events of filters A and B in a pair with a 95% confidence interval.

	Differences	Differences	Differences				
Filter Pair	Mean	Standard Deviation	Sample Size	T	|T|	t.025	|T|> t?
1	-1.050	0.672	10	-4.941	4.941	2.262	Unequal Means
2	0.110	0.251	10	1.383	1.383	2.262	Equal Means
3	-1.200	0.583	10	-6.508	6.508	2.262	Unequal Means
4	-0.830	0.472	10	-5.566	5.566	2.262	Unequal Means
5	-1.488	0.770	8	-5.465	5.465	2.365	Unequal Means
6	2.820	1.175	10	7.586	7.586	2.262	Unequal Means
7	-0.393	0.350	9	-3.367	3.367	2.306	Unequal Means
8	0.284	0.236	8	3.397	3.397	2.365	Unequal Means
9	0.449	0.299	9	4.497	4.497	2.306	Unequal Means
10	0.060	0.099	10	1.908	1.908	2.262	Equal Means
11	0.160	0.250	10	2.021	2.021	2.262	Equal Means
12	0.156	0.436	9	1.070	1.070	2.306	Equal Means
14	0.600	0.735	6	2.000	2.000	2.571	Equal Means
15	0.135	0.170	10	2.510	2.510	2.262	Unequal Means

APPENDIX I: Total Porosity of Filter Lip Data

Table I-1: Measurements of Filter Lip Pieces for Total Porosity; Direct Volume Method

	Dry Mass (g)	Dry Mass (g)	Wet Mass (g)	Wet Mass (g)	Vol. Disp. (cc)	Vol. Disp. (cc)	Total Poro-sity	Total Poro-sity	Total Poro-sity	Total Poro-sity
	Piece A	Piece B	Piece A	Piece B	Piece A	Piece B	Piece A	Piece B	Average A & B	St. Dev. A & B
1A	2.1	1.68	2.91	2.34	1.7	1.5	48%	44%	46%	3%
1B	3.94	0.84	5.47	1.23	3.7	0.7	41%	56%	49%	10%
2A	2.11	3.4	2.99	4.76	1.8	3	49%	45%	47%	3%
2B	1.55	1.22	2.24	1.74	1.9	1	36%	52%	44%	11%
3A	2.44	1.4	3.52	2.18	2.3	1.4	47%	56%	51%	6%
3B	2.68	2.47	3.91	3.48	2.6	2.1	47%	48%	48%	1%
4A	2.53	2.5	3.79	3.68	2.5	2.2	51%	54%	52%	2%
4B	1.59	1.52	2.45	2.27	1.7	1.4	51%	54%	52%	2%
5A	2.35	3.78	3.82	6	2.5	4.3	59%	52%	55%	5%
5B	1.47	1.07	2.39	1.74	1.5	1.2	61%	56%	59%	4%
6A	1.52	1.34	2.39	2.09	1.7	1.3	51%	58%	55%	5%
6B	2.64	1.42	4.03	2.28	2.6	1.6	54%	54%	54%	0%
7A	4.56	3.92	6.22	5.24	4	3.2	42%	41%	41%	0%
7B	3.82	2.7	5.2	3.68	3.5	2.3	40%	43%	41%	2%
8A	3.01	1.61	4.06	2.24	2.5	1.4	42%	45%	44%	2%
8B	1.96	2.16	2.72	3.01	1.8	3	42%	28%	35%	10%
9A	4.16	2.31	6.16	3.26	4.1	2	49%	48%	48%	1%
9B	3.01	2.66	4.4	2.97	2.8	2	50%	16%	48%	4%
10A	3.09	1.41	4.54	2.13	3.1	1.4	47%	52%	49%	3%
10B	3.35	1.55	4.88	2.25	3.2	1.6	48%	44%	46%	3%
11A	2.22	1.73	3.63	2.76	2.5	2	57%	52%	54%	3%
11B	3.43	0.9	5.2	1.46	3.7	1	48%	56%	52%	6%
12A	2.05	1.72	3.27	2.79	2.3	1.7	53%	63%	58%	7%
12B	2.28	1.43	3.69	2.26	2.7	1.5	52%	55%	54%	2%
13A	2.78	1.96	3.63	2.46	2.5	1.5	34%	33%	34%	0%
13B	2.19	1.19	2.79	1.48	1.7	0.8	35%	36%	36%	1%
14A	1.96	1.58	2.54	2.12	1.3	1.2	45%	45%	45%	0%
14B	2.11	2.22	2.86	2.98	1.6	1.7	47%	45%	46%	2%
15A	4.45	0.66	5.86	0.96	3.3	0.7	43%	43%	43%	0%
15B	3.06	2.54	4.5	3.61	2.6	2.4	56%	45%	50%	8%

Table I-2: Measurements of Filter Lip Pieces for Total Porosity; Indirect Volume Method

	Dry Mass (g)	Dry Mass (g)	Wet Mass (g)	Wet Mass (g)	Underwater Mass (g)	Underwater Mass (g)	Total Porosity	Total Porosity	Total Porosity	Total Porosity
	Piece A	Piece B	Piece A	Piece B	Piece A	Piece B	Piece A	Piece B	Average A & B	St. Dev. A & B
1A	2.09	1.67	2.82	2.26	1.09	0.86	42%	42%	42%	0%
1B	3.91	0.83	5.29	1.17	2.01	0.43	42%	46%	44%	3%
2A	2.1	3.33	2.89	4.68	1.09	1.75	44%	46%	45%	2%
2B	1.53	1.21	2.14	1.7	0.81	0.66	46%	47%	47%	1%
3A	2.42	1.39	3.41	2.06	1.25	0.7	46%	49%	48%	2%
3B	2.65	2.46	3.77	3.34	1.34	1.23	46%	42%	44%	3%
4A	2.51	2.47	3.67	3.6	1.28	1.26	49%	48%	49%	0%
4B	1.57	1.5	2.35	2.24	0.79	0.77	50%	50%	50%	0%
5A*	3.39		5.27		1.71		53%			
5B	1.45	0.89	2.26	1.43	0.66	0.44	51%	55%	53%	3%
6A	1.47	1.33	2.31	2.07	0.75	0.67	54%	53%	53%	1%
6B	2.61	1.41	3.9	2.22	1.28	0.71	49%	54%	52%	3%
7A	4.52	3.9	6.04	5.14	2.03	1.76	38%	37%	37%	1%
7B	3.81	2.69	5.05	3.6	1.74	1.26	38%	39%	38%	1%
8A	2.99	1.59	4.05	2.16	1.44	0.76	41%	41%	41%	0%
8B	1.96	2.14	2.66	2.97	0.89	1.01	40%	42%	41%	2%
9A	4.13	2.3	5.86	3.2	1.77	1.01	42%	41%	42%	1%
9B	3	2.03	4.25	2.89	1.32	0.92	43%	44%	43%	1%
10A	3.08	1.41	4.42	2.06	1.34	0.64	44%	46%	45%	2%
10B	3.32	1.53	4.69	2.16	1.53	0.71	43%	44%	44%	0%
11A	2.25	1.72	3.45	2.61	0.93	0.72	48%	47%	47%	0%
11B	3.4	0.9	5	1.43	1.41	0.36	45%	50%	47%	4%
12A	2.04	1.7	3.12	2.64	0.87	0.76	48%	50%	49%	1%
12B	2.26	1.42	3.53	2.18	0.97	0.61	50%	49%	49%	1%
13A	2.78	1.95	3.55	2.42	1.34	0.94	35%	32%	33%	2%
13B	2.17	1.2	2.7	1.56	1.09	0.59	33%	37%	35%	3%
14A	1.29	1.56	1.66	2.08	0.71	0.85	39%	42%	41%	2%
14B	2.09	2.2	2.81	2.94	1.13	1.21	43%	43%	43%	0%
15A	3.4	1.64	4.48	2.26	1.86	0.9	41%	46%	44%	3%
15B	3.04	2.52	4.39	3.55	1.63	1.35	49%	47%	48%	1%

*Filter lip pieces for 5A crumbled; pieces A and B were indistinguishable, so taken as a group. Note that filter 5A was in the coldest spot in the kiln during firing, which could partly explain its weaknes compared to 5B.

APPENDIX J: Radii with Height

Table J-1: Radii Found Using Volume of Water, Assuming Paraboloid Shape

Height (cm)	Volume of Water Added (L)	Cumulative Volume of Water Added (L)	Radius, Modeled as Paraboloid (cm)
2.8	0.1	0.1	4.8
3.9	0.1	0.2	5.7
5.1	0.1	0.3	6.1
5.9	0.1	0.4	6.6
6.5	0.1	0.5	7.0
7.3	0.1	0.6	7.2
7.9	0.1	0.7	7.5
8.4	0.1	0.8	7.8
9	0.1	0.9	8.0
9.4	0.1	1	8.2
9.9	0.1	1.1	8.4
10.3	0.1	1.2	8.6
10.7	0.1	1.3	8.8
11.1	0.1	1.4	9.0
11.4	0.1	1.5	9.2
11.8	0.1	1.6	9.3
12	0.1	1.7	9.5
12.9	0.2	1.9	9.7
13.6	0.2	2.1	9.9
14.2	0.2	2.3	10.2
14.9	0.2	2.5	10.3
15.5	0.2	2.7	10.5
16	0.2	2.9	10.7
16.5	0.2	3.1	10.9
17.1	0.2	3.3	11.1
17.6	0.2	3.5	11.3
18.15	0.2	3.7	11.4
18.6	0.2	3.9	11.6
19.1	0.2	4.1	11.7
19.6	0.2	4.3	11.8
20.1	0.2	4.5	11.9
20.5	0.2	4.7	12.1
21	0.2	4.9	12.2
21.4	0.2	5.1	12.3
21.9	0.2	5.3	12.4
22.3	0.2	5.5	12.5

Table J-2: Radii Found Using Circular Cardboard

Radius of Cardboard (cm)	Height on Ruler (cm)	Height Adjusted for Cardboard Thickness (cm)
3	1.2	0.8
4	2	1.6
5	3.3	2.9
6	5.8	5.4
7	6.8	6.4
8	9.2	8.8
9	11.4	11
10	14.5	14.1
11	18.4	18
12	21.5	21.1

Table J-3: Radii Found Using Filter Slices

	Lower Height (cm)	**Lower Inner Radius (cm)**	**Upper Height (cm)**	**Upper Inner Radius (cm)**
Slice 1	0	0.0	3	5.2
Slice 2	3	5.5	6	6.95
Slice 3	6	7.1	9	8.25
Slice 4	9	8.4	12	9.45
Slice 5	12	9.6	15	10.25
Slice 6	15	10.4	18	11.15

APPENDIX K: Flowrate Test

Table K-1: Data from Drawdown Test to Determine Flowrate

Height of Water in Filter (cm)	Volume of Water Collected (L)	Cumulative Time (Hours)	Flowrate (L/Hour)
21	0		
20	0.5	0.37	1.36
19	0.9	0.75	1.04
18	1.3	1.20	0.89
17	1.7	1.65	0.89
16	2.08	2.18	0.71
15	2.45	2.77	0.63
14	2.7	3.33	0.44
13	3	4.02	0.44
12	3.3	4.83	0.37
11	3.5	5.67	0.24
10	3.73	6.47	0.29
9	3.95	7.42	0.23
8	4.1	8.37	0.16
7	4.26	9.32	0.17
6	4.42	10.27	0.17
5.2	4.56	11.85	0.09
3.9	4.69	13.67	0.07

APPENDIX L: Hydraulic Conductivity with Height

Table L-1: Hydraulic Conductivity of Three Segments

Segment	1	2	3
H_U (cm)	18	12	6
ΔT (hrs)	3.63	6.38	22*
V (cm^3)	2000	1120	630
A (cm^2)	414.4	331.6	217.9
t (cm)	1.5	1.7	2
K (cm/hr)	0.187906	0.208495	0.175226

*The final time interval, ΔT_3, was difficult to measure accurately. 22 hours is the best guess.

Table L-2: Hydraulic Conductivity of Filter Slices

Filter Slice	Upper Height (cm)	Water Height (cm)	Flowrate (L/hour): Trial 1	Flowrate (L/hour): Trial 2	Flowrate (L/hour): Trial 3	Flowrate (L/hour): Average	Hydraulic Conductivity (cm/hr)
1	3	37	0.385	0.380		0.383	0.243
2	6	39	0.350	0.460	0.450	0.420	0.224
3	9	42	0.660	0.595		0.628	0.240
4	12	46	0.790			0.790	0.216
5	15	49	1.00	0.780	1.150	0.977	0.222
6	18	52	2.07	1.70		1.885	0.388

APPENDIX M: Total Porosity of Filter Slices

Table M-1: Total Porosity of Filter Slices

Slice	Mass Underwater (g)	Mass Saturated (g)	Mass Dry (g)	Volume Slice (cm^3)	Mass Water Voids (g)	Total Porosity
1	253.74	659.61	480.77	405.87	178.84	44.1%
2	181.37	449.48	325.91	268.11	123.57	46.1%
3	197.11	492.75	358.71	295.64	134.04	45.3%
4	209.37	524.36	386.68	314.99	137.68	43.7%
5	198.48	494.16	360.39	295.68	133.77	45.2%
6	231.36	573.94	417.08	342.58	156.86	45.8%